ABSTRACT

LIU, MENGRAN. Tailoring Synthetic Chlorophylls and Bacteriochlorophylls with Features for Wavelength Tuning, Solubility, and Bioconjugation (Under the direction of Professor Jonathan S. Lindsey).

Chlorophylls and bacteriochlorophylls are Nature's chosen chromophores for capturing light in the red and near infrared (NIR) spectral regions. Synthetic chlorins or bacteriochlorins contain the core of natural chlorophylls and bacteriochlorophylls, respectively. An understanding of the effects of substituents on the spectral properties of these chromophores greatly benefits from sythetic methodologies that can afford unsubstituted or sparsely substituted chlorins or bacteriochlorins with placement of desired substituents at designated positions. In this work, all synthetic chlorins and bacteriochlorins have been synthesized based on *de novo* routes, and resulting chlorins or bacteriochlorins are stabilized by one or two gem-dimethyl groups located in the reduced rings of macrocycles, respectively.

The first part of this work involves the synthesis of formylchlorins to provide initial models for understanding the strong red absorption of native 2- or 3-formylchlorophylls (*f* and *d*). Access to a 2-formylchlorin relied on bromination of a tetrahydrodipyrrin–dibutylboron complex, whereas a 3-formylchlorin was prepared by installation of the bromo group in the earliest precursor, pyrrole-2-carboxaldehyde. Complexation of the tetrahydrodipyrrin with a dialkylboron motif caused electrophilic substitution (bromination, formylation) to proceed predominantly at the β^7- rather than α-position of the pyrrole ring. The 7-position of the hydrodipyrrin ultimately gives rise to substituents at the chlorin 2-

position (ring A), which has heretofore been little accessed. Two isomeric formylchlorins were prepared by Pd-mediated carbonylation of the corresponding bromochlorins. The two formylchlorins differ in absorption spectral properties: the Q_y absorption maximum is 654 or 664 nm for the 2- or 3-formylchlorin, respectively.

In the part of tuning polarity of tetrapyrrole macrocycles, stable synthetic chlorins and bacteriochlorins have been tailored with PEG groups for use in aqueous solution. For chlorins, three molecular designs have been developed which differ with regard to order of the installation (pre/post-formation of the chlorin macrocycle) and position of the PEG groups. Six PEGylated synthetic chlorins (three free bases, three zinc chelates) have been prepared, of which four are equipped with a bioconjugatable (carboxylic acid) tether. The most effective design for aqueous solubilization entails facial encumbrance where PEG groups project above and below the plane of the hydrophobic disk-like chlorin macrocycle. The chlorins possess strong absorption at ~400 nm (B band) and in the red region (Q_y band); regardless of wavelength of excitation, emission occurs in the red region. The spectral properties are essentially unchanged in DMF and water for the facially encumbered chlorins, which also exhibited narrow Q_y absorption and emission bands (full-width-at-half maximum of each <25 nm). The water-solubility was assessed by absorption spectroscopy over the concentration range 0.4 mM – 0.4 mM.

For bacteriochlorins, the synthesis have been achieved, from two common bacteriochlorin building blocks, of five wavelength-tunable, bioconjugatable and water-soluble bacteriochlorins along with two non-bioconjugatable benchmarks. The use of 3,5-disubstituted aryl groups at the pyrrolic β-positions places the PEG chains above and below

the macrocycle to suppress aggregation in aqueous media. A handle containing a single carboxylic acid is incorporated to allow bioconjugation. The seven hydrophilic bacteriochlorins in water display a range of NIR Q_y absorption (679–819 nm), sharp emission (21–36 nm fwfm) and modest fluorescence quantum yield (0.017–0.13). Each bacteriochlorin is neutral (non-ionic) yet soluble in organic (e.g., CH_2Cl_2, DMF) and aqueous solutions. Water solubility was assessed using absorption spectroscopy by changing the concentration ~1000-fold (190–690 μM to 0.19–0.69 μM).

In the last part, we report the synthesis and characterization of several oxobacteriochlorins. The absorption spectra have been characterized to gain a deeper understanding of the energetic effects of the oxo group in the pyrroline motif. The work advances capabilities for tailoring the properties of bacteriochlorins by straightforward synthetic means.

Tailoring Synthetic Chlorophylls and Bacteriochlorophylls with Features for Wavelength Tuning, Solubility, and Bioconjugation

by
Mengran Liu

A dissertation submitted to the Graduate Faculty of
North Carolina State University
in partial fulfillment of the
requirements for the degree of
Doctor of Philosophy

Chemistry

Raleigh, North Carolina
2016

APPROVED BY:

_____	_____
Jonathan S. Lindsey Committee Chair	Christian Melander
_____	_____
Reza A. Ghiladi	Joshua G. Pierce

DEDICATION

This work is dedicated to my parents.

BIOGRAPHY

Mengran Liu (b. 1988) grew up in Tianjin, China and did her undergraduate studies at Nankai University in Tianjin (2007–2011) where she earned her Bachelor's degree in Chemistry. After graduation, she joined the Lindsey group in North Carolina State University (2011–2016) working on the synthesis of chlorophyll and bacteriochlorophyll analogues.

ACKNOWLEDGMENTS

First of all, I would like to thank my advisor Dr. Jonathan S. Lindsey. It is a great honor for me to be his student. I appreciate his ideas, advice, time, patience and support which made my research in graduate school fruitful. He is an example for our graduate students, his genuine passion for science and his devotion to career were contagious and inspiring, which are always motivations for my life.

I would like to thank my committee members Dr. Ghiladi, Dr. Melander, and Dr. Pierce who reviewed my work and provided great suggestions.

I would like to thank our collaborators from the Holten lab at Washington University in St. Louis, the Bocian lab at University of California at Riverside, our NMR supervisor Dr. Xiaoyan Sun, our X-ray structural facility director Dr. Roger Sommer, and our mass spectrometry lab supervisor Danielle Lehman at North Carolina State University. Without their assistance, this work would not be successful.

It has been a great pleasure to work with all past and present group members. The coworkers for this work Dr. Jiangbin Jiang, Dr. Nuonuo Zhang, Dr. Chih-Yuan Chen, I appreciate their wisdom and efforts to the PEGylated hydroporphyrins, they are the best scientists. I would like to thank Dr. Pothiappan Vairaprakash, his guidance and advice helped me get through the difficulties in my research. I am grateful to Dr. Masahiko Taniguchi for his support and friendship during the beginning of my graduae studies. His personality and life philosophy provided me differenct aspects to think and solve problems. Together with Dr. Lindsey, Dr. Taniguchi taught me what high standard research is. I thank our group administrator, Ms. Ann Norcross, she makes our group more like a family.

At last to my parents Jie Liu and Fengying Chen, there are no words to express how thankful I am for you love and support. Thank you.

My deepest gratitude to those great peoples in my life who help me be a better person.

TABLE OF CONTENTS

LIST OF TABLES

LIST OF FIGURES

LIST OF SCHEMES

LIST OF CHARTS

CHAPTER 1

General Introduction: Chlorins and Bacteriochlorins

Introduction

Porphyrins, chlorins and bacteriochlorins are three basic pigments in nature. Chlorins and bacteriochlorins respect the fundamental chromophores of chlorophylls and bacteriochlorophylls, respectively (Chart 1.1). Each of these three macrocycles is a tetrapyrrole with an alternating double-bond pathway. Compared with the π-system of a porphyrin, a chlorin has one reduced pyrrole ring and a bacteriochlorin has two reduced pyrrole rings on the opposite sides of the macrocycle. The different conjugation pathway and symmetry cause porphyrins, chorins and bacteriochlorins to absorb different colors of sunlight (Figure 1.1). Porphyrins absorb strongly in the blue spectral region (B or Soret band), and moderately in the visible region. Chlorins have less intense B band in the violet-blue spectral region, meanwhile the characteristic long-wavelength absorption band (Q_y band) are located in the red spectral region (600–700 nm). Bacteriochlorins further stretch their B bands into the near ultraviolet and Q_y bands into the near infrared (NIR) spectral region (800–1000 nm).

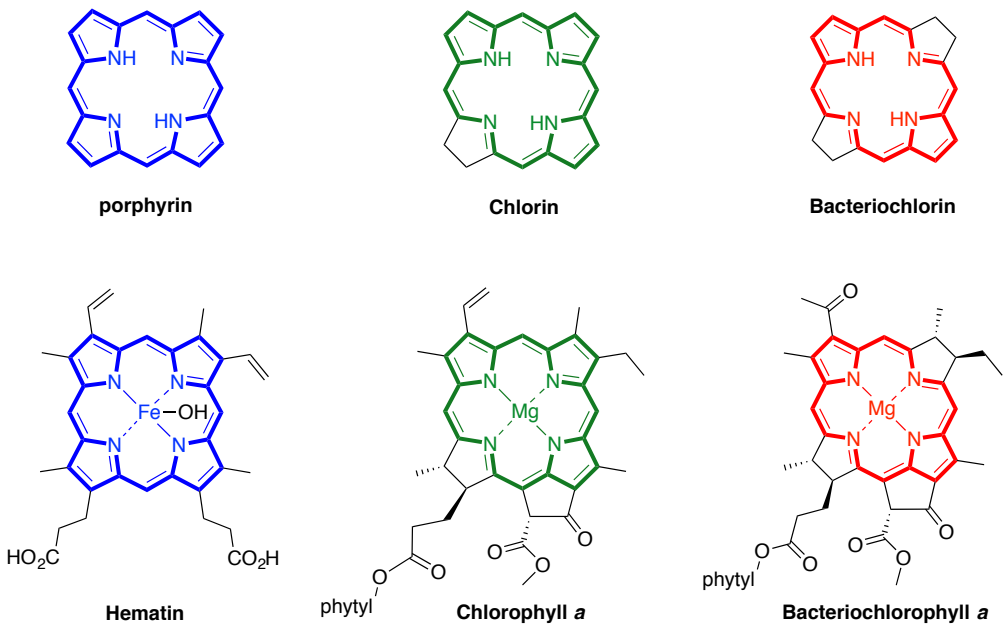

Chart 1.1. Three π-systems in tetrapyrrole pigments (top), and representative examples in nature (bottom).

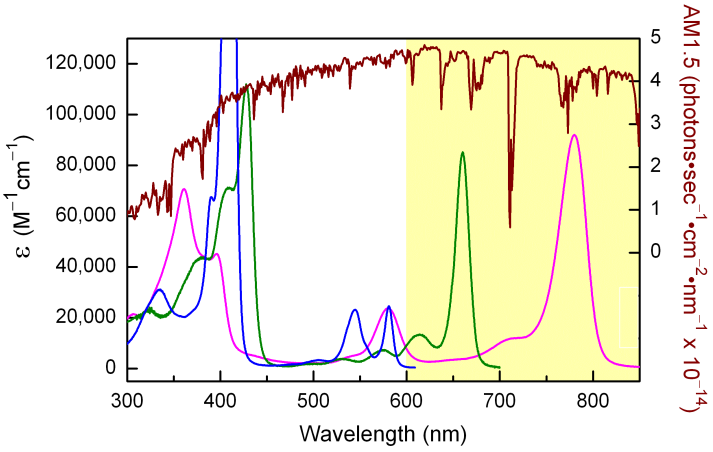

Figure 1.1. Representative absorption spectra of a porphyrin (hematin, blue line), chlorin (chlorophyll *a*, green line), and bacteriochlorin (bacteriochlorophyll *a*, pink line) under solar spectrum (brown line).

Chlorins and bacteriochlorins are powerful chromophores for photochemistry studies

in the red and NIR spectral regions. For solar energy science, nearly half of the photons are above 600 nm,[1] hence the ability to capture light in red and NIR spectral regions is essential to increase the overall solar photoconversion. For flow cytometry,[2-4] spectrally distinct chlorins and bacteriochlorins featured with narrow emission bands (15–20 nm full-width-at-half-maximum, fwhm) can be needed in the red and NIR regions to increase the range of multicolor applications. For optical imaging in medicine,[5] light in the NIR spectral region affords the deepest penetration in soft tissue, because light in NIR region gives less scattering than shorter wavelengths and minimal absorption by natural pigments.

In our group, we focus on the fundamental study of effects of substituents on the spectral properties of chlorophylls and bacteriochlorophylls, which would be greatly benefited from the methodologies which can afford stable unsubstituted or sparsely substituted chlorins or bacteriochlorins with desired substituents at the assigned positions. One source of chlorins and bacteriochlorins stem from the derivatization of naturally occurring chlorophylls and bacteriochlorophylls. However, the resulting chromophores encountered limited stability and lack of synthetic malleability due to nearly fully substituted β positions about the perimeter of the macrocycle. In our group, the preparation of chlorins and bacteriochlorins follows *de novo* synthesis routes, where the stable chlorin or bacteriochlorin contains one or two gem-dimethyl, groups respectively, to lock the structure of the tetrapyrrole macrocycle, otherwise adventitious dehydrogenation might occur. Over the years, versatile stable chlorins and bacteriochlorins with the ability to control over the introduction of different and specific substituents for different molecular designs and purposes have been prepared under the *de novo* synthesis route. In this work, formylchlorins

were synthesized from *de novo* route to provide initial models for understanding the strong red absorption of native 2- or 3-formylchlorophylls (chlorophyll *f* and *d*, see Chapter 2).

For wavelength tuning purposes, auxochromes installed at the β-positions of the macrocycles of hydroporphyrins were able to cause hyperchromic and bathochromic effects of the longest-wavelength absorption band,[6,7] which stems from a transition that is polarized along the axis that bisects rings A and C,[8] as shown in Chart 1.2. Perhaps the most straightforward yet powerful synthetic building blocks of hydroporphyrins are 3,13-dibromochlorins and 3,13-dibromobacteriochlorins (Chart 1.2). Bromo groups were introduced at the 3- and 13-positions to further Pd-mediated coupling derivatization reactions. The chlorin synthesis entailed acidic condensation of two halves of the chlorin, Western half and Eastern half, followed by metal- mediated oxidative cyclization. The Western half is a tetrahydrodipyrrin whereas the Eastern half is a 9-bromo-1-formyldipyrromethane. The synthetic bacteriochlorin came from acidic self-condensation of a dihydrodipyrrin precursor. In total, a 5-step concise synthesis afforded bacteriochlorin from a pyrrole aldehyde. The bromo group introduced at the 3- or 13-position of the hydroporphyrin originated from a 4-bromopyrrole-2-carboxaldehyde via the intermediacy of the 8-brominated hydrodipyrrins or dipyrromethane precursor. The electrophilic aromatic bromination of pyrrole-2-carboxaldehyde extensively goes to the 4-position.[9]

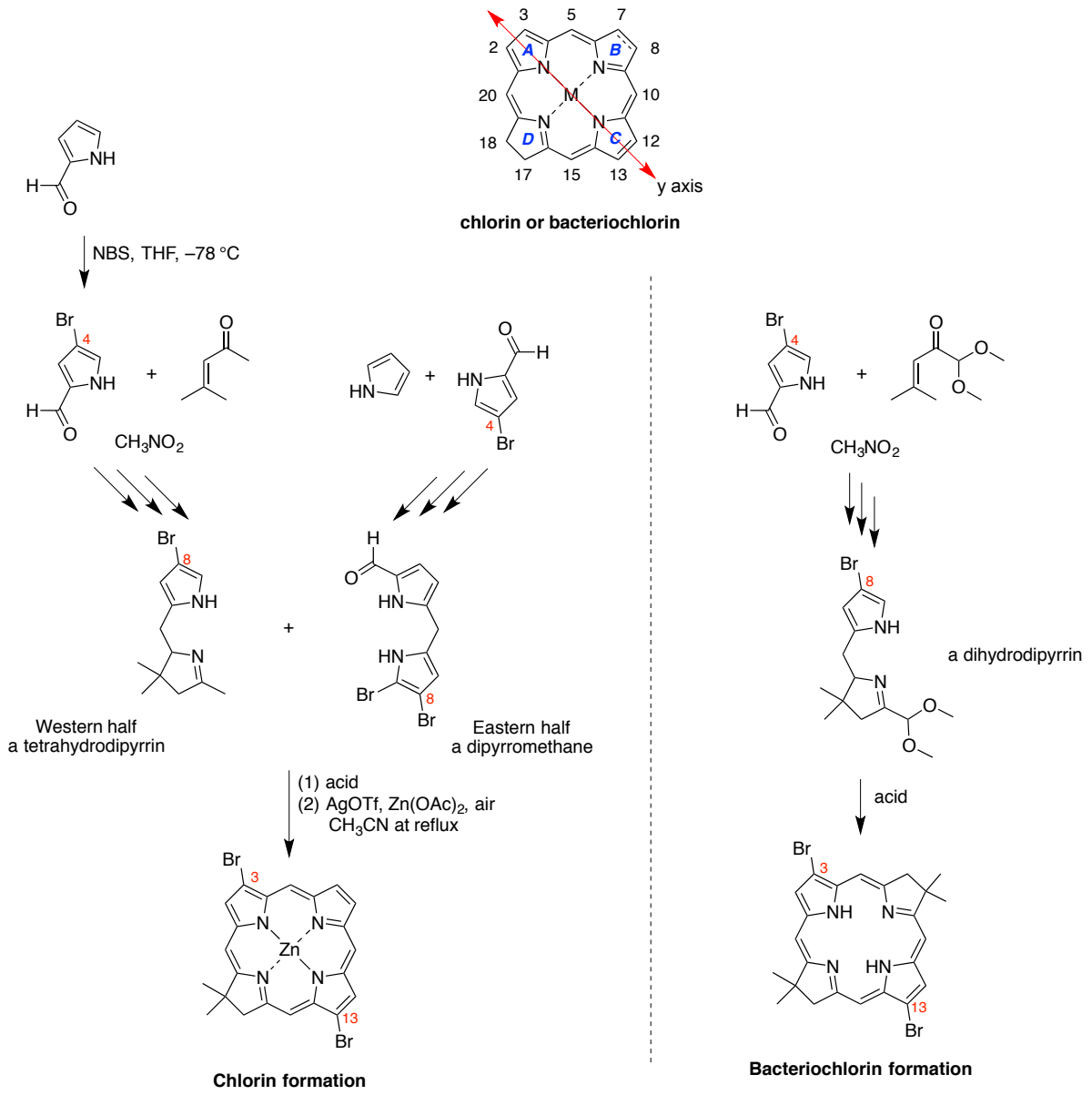

Chart 1.2. Chlorin and bacteriochlorin nomenclature (top); *de novo* synthesis of 3,13-dibrominated chlorin (left) and bacteriochlorin (right).

Expanding the applications of these red-NIR-functional chromophores in energy sciences and photomedicine requires the ability to tailor their physicochemical properties in

aqueous media. An objective of our work has been to gain access to a palette of hydroporphyrins with features not only wavelength-tunable, but also water-soluble and bioconjugatable. Achieving this aim has required development of new methodology as well as examination of various molecular designs. Indeed, a palette of lipophilic bacteriochlorins bearing diverse tethers was recently prepared for bioorthogonal labeling.[10] Achieving water-solubility proved quite challenging as a singular goal and was even more daunting to consider in the context of maintaining the other desired features.

For molecular design of tuning the polarity of hydroporphyrins, we aimed to incorporate motif(s) to change the overall polarity of the compounds. A classic idea to avoid hydrophobic aggregation of hydroporphyrins macrocycles entails facial encumbrance to place polar groups above and below the plane of the macrocycle (Chart 1.3). To date, a systematic study of a collection of polar motifs to tune the polarity of porphyrins,[11-14] chlorins,[15] and bacteriochlorins[16,17] have been conducted, which identified PEG groups as very attractive candidates for aqueous solubilization relative to ionic groups such as phosphates, phosphonates, alkyl ammonium and carboxylates. A challenging aspect of the architectures that ionic groups for aqueous solubilization (a pH-dependent phenomenon) with regards to synthetic manipulations was simultaneously employing an *N*-hydroxysuccinimide (NHS) motif for bioconjugation.[16] However, these deleterious cross-reactions can be avoid by the highly polar but nonionic PEG group for water solubility. Moreover, the PEG group is commercially available in various lengths[18] (monodisperse or polydisperse) with a single derivatizable handle,[18-21] and is soluble in water as well as a variety of organic solvents.[22]

Accordingly, workup of PEGylated compounds can be achieved by partitioning crude reaction mixtures between an aqueous phase and dichloromethane.

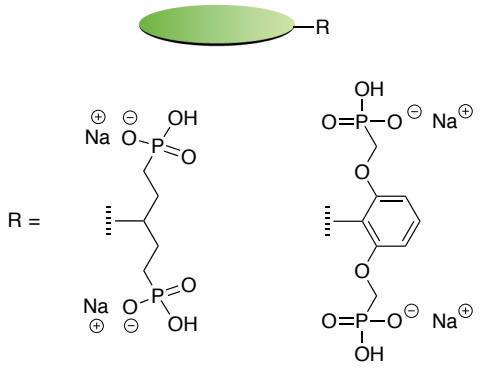

Chart 1.3. Facially encumbering motifs for aqueous solubilization of a chlorin (green disk).

Here, water-soluble chlorins and bacteriochlorins have been prepared via *de novo* synthesis as tailorable analogues of chlorophylls and bacteriochlorophylls. Each hydroporphyrin incorporates PEG groups for aqueous solubilization. Diverse architectures were examined that vary in structure and in strategy for installation of the PEG groups (see Chapters 3 and 4).

In the last, we report the synthesis and characterization of several oxobacteriochlorins. The fundamental core of naturally occurring tolyporphins[23–29] is a dioxobacteriochlorin (Chart 1.4). The most intriguing feature for oxobacteriochlorins is the hypsochromic effect of the oxo group on the Q_y band of bacteriochlorins, the spectral region of oxobacteriochlorins otherwise is less accessible due to the elaboration of synthesis. In

addition, the pyrroline oxo group would provide another site for further functionalization, with perhaps interesting features for such derivatives in wavelength tuning (see Chapter 5).

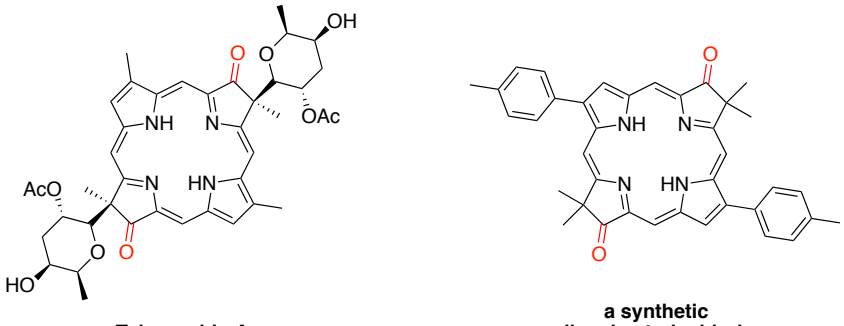

Chart 1.4. Naturally occurring (left) and synthetic (right) oxobacteriochloirns.

References:

1 N. Y. Kiang, J. Siefert, Govindjee and R. E. Blankenship, *Astrobiol.*, 2007, **7**, 222–251.

2 P. K. Chattopadhyay, C.-M. Hogerkorp and M. Roederer, *Immunology*, 2008, **125**, 441–449.

3 P. K. Chattopadhyay and M. Roederer, *Methods*, 2012, **57**, 251–258.

4 S. C. Bendall, G. P. Nolan, M. Roederer and P. K. Chattopadhyay, *Trends Immunol.*, 2012, **33**, 323–332.

5 K. Licha, *Top. Curr. Chem.,* 2002, **222**, 1–29.

6 J. K. Laha, C. Muthiah, M. Taniguchi, B. E. McDowell, M. Ptaszek and J. S. Lindsey, *J. Org. Chem.*, 2006, **71**, 4092–4102. Additions and Corrections: J. K. Laha, C. Muthiah, M. Taniguchi, B. E. McDowell, M. Ptaszek and J. S. Lindsey, *J. Org. Chem.*, 2009, **74**, 5122.

7 M. Taniguchi, D. L. Cramer, A. D. Bhise, oH. L. Kee, D. F. Bocian, D. Holten and J. S. Lindsey, *New J. Chem.*, 2008, **32**, 947–958.

8 O. Mass, M. Taniguchi, M. Ptaszek, J. W. Springer, K. M. Faries, J. R. Diers, D. F. Bocian, D. Holten and J. S. Lindsey, *New J. Chem*., 2011, **35**, 76–88.

9 H. J. Anderson and S.-F. Lee, *Can*. *J*. *Chem*., 1965, **43**, 409–414.

10 J. Jiang, M. Taniguchi and J. S. Lindsey, *J. New J. Chem.*, 2015, **39**, 4534–4550.

11 K. E. Borbas, P. Mroz, M. R. Hamblin and J. S. Lindsey, *Bioconjugate Chem*., 2006, **17**, 638–653.

12 Z. Yao, K. E. Borbas and J. S. Lindsey, *New J. Chem.*, 2008, **32**, 436–451.

13 K. E. Borbas, H. L. Kee, D. Holten and J. S. Lindsey, *Org. Biomol. Chem.*, 2008, **6**, 187–194.

14 A. Z. Muresan and J. S. Lindsey, *Tetrahedron*, 2008, **64**, 11440–11448.

15 K. E. Borbas, V. Chandrashaker, C. Muthiah, H. L. Kee, D. Holten and J. S. Lindsey, *J. Org. Chem*., 2008, **73**, 3145–3158.

16 J. Jiang, C.-Y. Chen, N. Zhang, P. Vairaprakash and J. S. Lindsey, *New J. Chem.*, 2015, **39**, 403–419.

17 J. Jiang, E. Yang, K. R. Reddy, D. M. Niedzwiedzki, C. Kirmaier, D. F. Bocian, D. Holten and J. S. Lindsey, *New J. Chem.*, 2015, **39**, 5694–5714.

18 J. Herzberger, K. Niederer, H. Pohlit, J. Seiwert, M. Worm, F. R. Wurm and H. Frey, *Chem. Rev.*, 2016, **116**, 2170–2243.

19 S. Zalipsky and J. M. Harris, in *Poly(ethylene glycol) Chemistry and Biological Applications*, ed. J. M. Harris and S. Zalipsky, American Chemical Society:

Washington, DC, 1997, pp. 1–13.

20 M. S. Thompson, T. P. Vadala, M. L. Vadala, Y. Lin and J. S. Riffle, *Polymer*, 2008, **49**, 345–373.

21 N. Larson and H. Ghandehari, *Chem. Mater.*, 2012, **24**, 840–853.

22 J. M. Harris, in *Poly(ethylene glycol) Chemistry – Biotechnical and Biomedical Applications*, ed. J. M. Harris, Plenum Press: New York, 1992, pp. 1–14.

23 M. R. Prinsep, F. R. Caplan, R. E. Moore, G. M. L. Patterson and C. D Smith, *J. Am. Chem. Soc.*, 1992, **114**, 385–387.

24 C. D. Smith, M. R. Prinsep, F. R. Caplan, R. E. Moore and G. M. L Patterson, *Oncol. Res.*, 1994, **6**, 211–218.

25 M. R. Prinsep, G. M. L. Patterson, L. K. Larsen and C. D. Smith, *Tetrahedron*, 1995, **51**, 10523–10530.

26 P. Morliere, J.-C. Maziere, R. Santus, C. D. Smith, M. R. Prinsep, C. C. Stobbe, M. C. Fenning, J. L. Golberg and J. D. Chapman, *Cancer Res.*, 1998, **58**, 3571–3578.

27 M. R. Prinsep, G. M. L. Patterson, L. K. Larsen, and C. D. Smith, *J. Nat. Prod.*, 1998, **61**, 1133–1136.

28 T. G. Minehan, L. Cook-Blumberg, Y. Kishi, M. R. Prinsep and R. E. Moore, *Angew. Chem. Int. Ed.*, 1999, **38**, 926–928.

29 M. R. Prinsep and J. Puddick, *Phytochem. Anal.*, 2011, **22**, 285–290.

CHAPTER 2

Regioselective β-Pyrrolic Electrophilic Substitution of Hydrodipyrrin–Dialkylboron Complexes Facilitates Access to Synthetic Models for Chlorophyll *f*

Preamble. The contents in this chapter have been published[86] with contributions from the following individuals. Marcin Ptaszek: synthesis of tetrahydrodipyrrin–dialkylboron complexes. Olga Mass: derivatization of tetradiypyrrin–dibutylboron complexes. Roger D. Sommer: X-ray structure analyses.

Introduction

Native chlorophylls are distinguished by the presence of auxochromes at specific sites about the perimeter of the macrocycle. Chlorophyll *a* and *b* both bear a vinyl group at the 3-position, for example, whereas chlorophyll *d* contains a 3-formyl group (Chart 2.1).[1] The location of auxochromes at the 3-position causes a hyperchromic and bathochromic effect on the long-wavelength absorption band (Q_y band), which stems from a transition that is polarized along the axis that bisects rings A and C.[2] The presence of a methyl group at the 2-position was long considered a universal feature of chlorophylls. However, the recently discovered chlorophyll *f* contains a formyl group at the 2-position in addition to a 3-vinyl substituent.[3,4] The synthesis of model chlorins that contain diverse auxochromes at the 3-position has proved incisive for probing the effects of auxochromes on spectral, electronic, and photophysical features.[5-8] We sought similar access to synthetic 2-substituted chlorins

for fundamental comparisons of the effects of substituents at the 2- versus 3-positions.

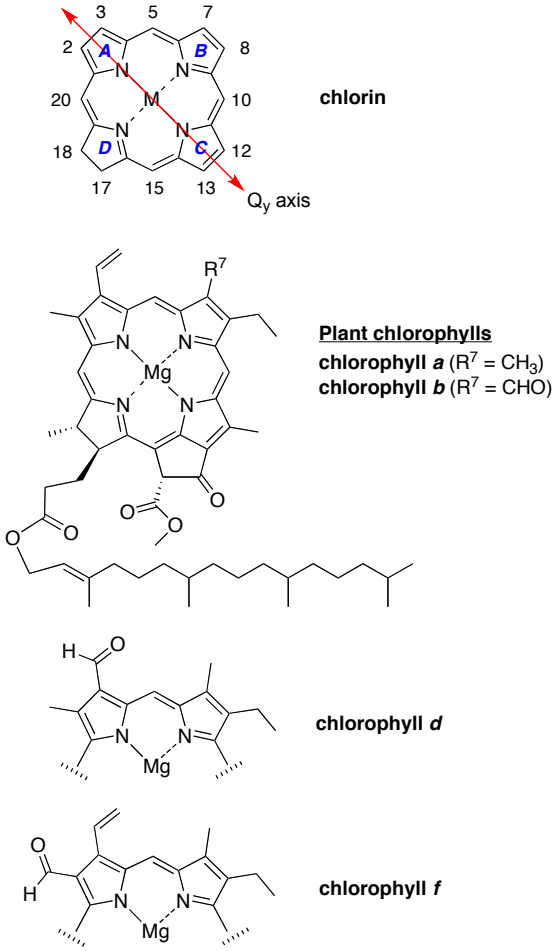

Chart 2.1. Chlorin nomenclature and natural chlorophylls.

The synthetic chemistry of chlorins has been a topic of widespread interest and has advanced considerably over the years.[9-23] A *de novo* route that we have developed to gain access to chlorins is shown in Scheme 2.1.[24] A Western half and an Eastern half are reacted in a two-step procedure to afford the corresponding chlorin. The Western half is a 1,3,3-

trimethyl-2,3,4,5-tetrahydrodipyrrin (or a corresponding dihydrodipyrrin,[25] not shown) whereas the Eastern half is a dipyrromethane. The chlorin bears a geminal dimethyl group in the pyrroline ring thereby precluding adventitious dehydrogenation leading to the porphyrin.

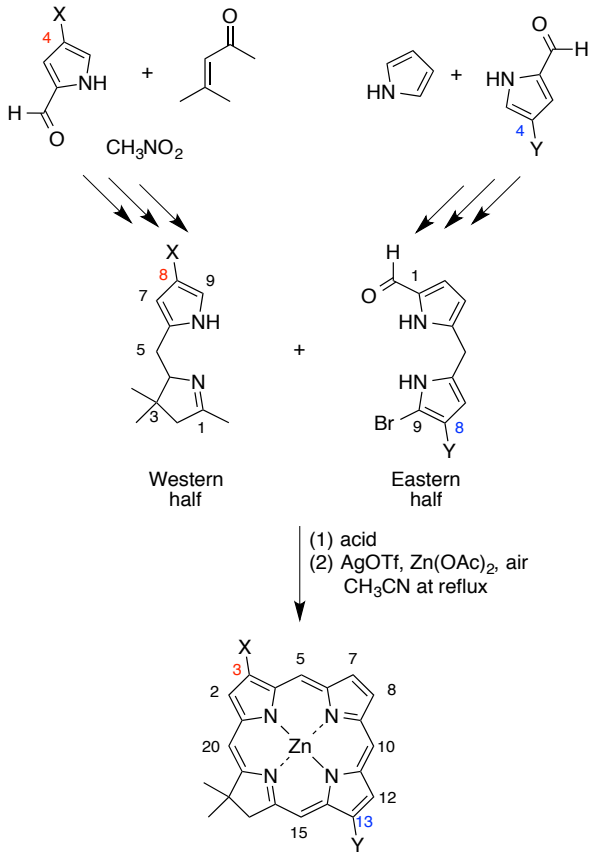

Scheme 2.1. *De novo* route to 3,13-disubstituted chlorins.

The synthesis of the Western half begins with a pyrrole-2-carboxaldehyde. A substituent can be incorporated at the 3-position of the chlorin by beginning with a 4-bromopyrrole-2-carboxaldehyde (via the intermediacy of the 8-substituted Western half).[5] Pyrrole-2-carboxaldehyde readily undergoes electrophilic bromination at the 4-position.[26]

Similarly, a 13-substituted chlorin can be prepared by beginning with a 4-bromopyrrole-2-carboxaldehyde via the intermediacy of the 8-substituted Eastern half.[5,27] By means of these and related approaches, all sites have been accessed (*vide infra*) to date with the sole exception of the chlorin 2-position (a 2-arylchlorin has been prepared[28] but the route employed is not compatible with the introduction of a 2-formyl group). The synthesis of a 2-bromochlorin building block could begin with the corresponding 3-substituted pyrrole-2-carboxaldehyde, but the synthesis of such pyrroles is lengthy.[29] During the course of this work, Fukuda *et al*. reported a method for the directed lithiation at the 2-position of a 3-bromo-*N*-benzensulfonylpyrrole, which also could be employed as an early point of departure to access 2-substituted pyrroles.[30,31] Regardless, the motivation here was to investigate complementary approaches for elaborating advanced precursors (i.e., hydrodipyrrins) of chlorins. While this work began as an effort in pure synthesis, the subsequent discovery,[3,32] structure determination,[4] and spectroscopic investigation[33,34] of chlorophyll *f*; the growing appreciation of the rich ecological variety of photosynthesis including use of the strong-red absorbing chlorophylls *d* and *f*;[35-39] and consideration of the expanded (and possibly expandable) spectral range of photosynthesis[40,41] together have heightened our focus on routes to chlorins that could accommodate diverse substituents in ring A.

As part of a program to improve tetrapyrrole synthetic methodology, complexation aides were found to facilitate the isolation, handling, and derivatization of acyldipyrromethanes, the precursors to tetrapyrroles. The complexation aides include a dibutyltin complex of a 1,9-diacyldipyrromethane (**A**)[42] and a dialkylboron complex of a 1-

acyldipyrromethane (**B**)[43] (Chart 2.2). The coordination complex of each of these ligands was hydrophobic and could be easily purified by silica pad filtration and/or crystallization, whereas the uncomplexed species streaked upon chromatography and/or were poorly crystalline. Such dialkylboron complexation aides were applied to imidazole–dipyrromethanes (**C**, **D**),[44] whereupon the isolated complex contained a covalent pyrrolic N–B bond and a dative imidazolyl N–B bond.

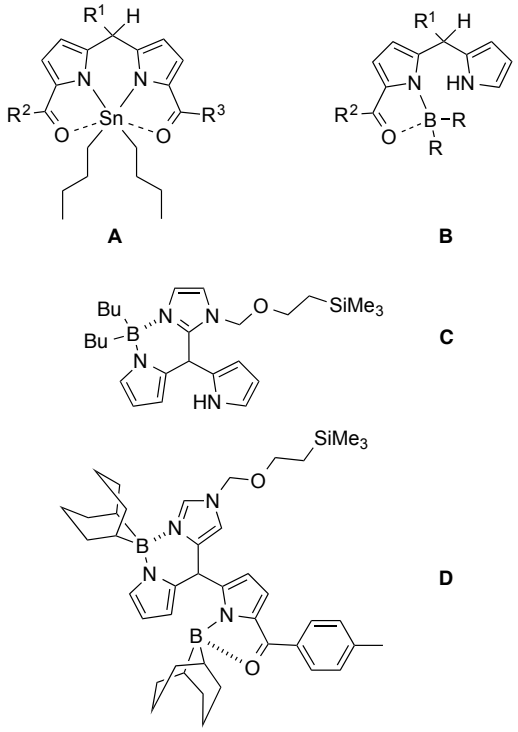

Chart 2.2. Complexes of pyrrolic compounds.

Here, we sought to explore analogous complexation aides for tetrahydrodipyrrins and dihydrodipyrrins, the precursors to hydroporphyrins, wherein the bonding was expected to

resemble that in the dialkylboron–imidazole–dipyrromethanes **C** and **D**. Tetrahydrodipyrrins typically are highly polar, streak on chromatographic media, and do not readily crystallize. Moreover, the presence of two heterocyclic rings with far different reactivity (pyrrole and pyrroline) can lead to unexpected reactions and synthetic difficulties.[45] Dihydrodipyrrins are less polar but also less stable than tetrahydrodipyrrins.[24] Initially, our goal was to facilitate purification and handling of the tetrahydrodipyrrin, but in the course of our work we realized that boron complexation alters the usual selectivity of the pyrrole upon electrophilic aromatic substitution.

In this paper, we report the investigation of dialkylboron complexation of hydrodipyrrins. The dialkylboron unit masks both the pyrrolic and pyrrolenic nitrogen atoms of the hydrodipyrrin. The derivatization processes of interest include pyrrolic bromination and formylation for potential synthetic elaboration of the corresponding ring A of the chlorins. The dialkylboron unit directs substitution chiefly to a pyrrolic β-position rather than the α-position (as occurs in the unprotected pyrrole). One application of the dialkylboron complexation method entails the *de novo* synthesis of 2-substituted free base chlorins bearing bromo or formyl groups. An in-depth study of the spectroscopic properties of the free base chlorins and metal chelates will be described elsewhere. While our chief interests are in spectroscopic properties, we note the work of Balaban and Tamiaki, who have showed that placement of carbonyl groups at distinct locations enables control over the nature of assemblies of tetrapyrrole macrocycles akin to chlorosome-like architectures.[19,46-49] Taken together, the results reported provide an initial step toward partial mimics of chlorophyll *f*, and should broaden the scope of synthetic chlorin chemistry.

Results and discussion

(I) Dialkylboron complexation of hydrodipyrrins

(A) Synthesis of tetrahydrodipyrrin–dialkylboron complexes. Tetrahydrodipyrrin **1**[45] is a crucial building block in a rational synthesis of chlorins.[24,25,50] Reaction of **1** with dibutylboron triflate in CH_2Cl_2 containing triethylamine (TEA) afforded the crude tetrahydrodipyrrin–dialkylboron complex, which upon washing with saturated aqueous $NaHCO_3$, silica-pad filtration and recrystallization (aqueous ethanol) afforded **1-BBu$_2$** in pure form (62% yield). The **1-BBu$_2$** complex is stable to routine handling. Crystals of **1-BBu$_2$** suitable for X-ray analysis were obtained by slow evaporation of a solution of Et_2O/MeOH.

Table 2.1. Synthesis of dialkylboron complexes of tetrahydrodipyrrins.

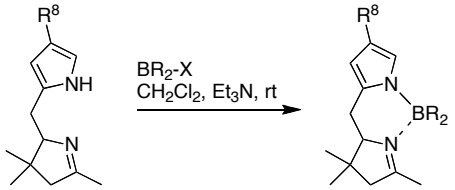

1 (R^8 = H)
1-Br^8 (R^8 = Br)

Entry	BR_2-X	Product	R	R^8	Yield, %
1	BBu_2-OTf	**1-BBu$_2$**	Bu	H	62
2	BMe_2-Br	**1-BMe$_2$**	Me	H	67
3	BBu_2-OTf	**1-Br^{8}BBu$_2$**	Bu	Br	70

Reaction of **1** with dimethylboron bromide under nitrogen at 0 °C afforded the

corresponding dimethylboron complex **1-BMe$_2$** in 67% yield (entry 2, Table 2.1). Compound **1-BMe$_2$** was less stable than **1-BBu$_2$**, decomposed on silica (thus purification was performed by filtration through neutral alumina), and darkened quickly when kept at room temperature. Because of instability, compound **1-BMe$_2$** was not fully characterized. Instability issues with **1-BMe$_2$** and problems with handling dimethylboron bromide (highly pyrophoric, not available commercially as a solution) makes application of **1-BMe$_2$** less attractive than **1-BBu$_2$**. The dibutylboron complex **1-Br^{8}BBu$_2$** was prepared in analogous fashion from 8-bromotetrahydrodipyrrin[5,51] **1-Br^8** in 70% yield (entry 3). A crystal of **1-Br^{8}BBu$_2$** suitable for X-ray analysis was obtained from $CHCl_3$/hexanes by slow evaporation at 4 °C.

(B) A Dihydrodipyrrin-Boron Complex. Treatment of *p*-tolyldihydrodipyrrin **2**[52] with BBu_2OTf in the presence of Et_3N in CH_2Cl_2 afforded dihydrodipyrrin complex **2-BBu$_2$** in 87% yield (Scheme 2.2). A crystal of **2-BBu$_2$** suitable for X-ray analysis was obtained from Et_2O/MeOH by slow evaporation at 1 °C. The unsubstituted dibutylboron complex **3-BBu$_2$** was prepared in the analogous fashion from dihydrodipyrrin **3**[53] in 27% yield.

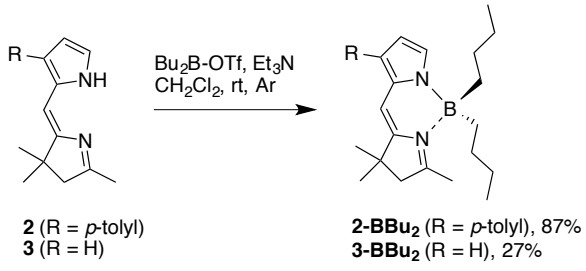

2 (R = *p*-tolyl)
3 (R = H)

2-BBu$_2$ (R = *p*-tolyl), 87%
3-BBu$_2$ (R = H), 27%

Scheme 2.2. Synthesis of a dihydrodipyrrin–boron complex.

(II) Derivatization of hydrodiypyrrin–dibutylboron complexes

(A) Reconnaissance. Electrophilic aromatic substitution of unsubstituted pyrrole proceeds first at the pyrrole α-positions.[54] On the other hand, the regioselective bromination or acylation of pyrroles at the β-positions presents a challenge.[55] In general, electrophilic aromatic substitution at the β-positions can be directed (1) by an electron-withdrawing group present at the α-position,[5] (2) by a bulky protecting group on the pyrrole nitrogen,[56,57] or in some cases (3) by rearrangement of the α-substituted pyrrole to a β-substituted pyrrole.[58-60] In accord with the expected reactivity of pyrrole, the bromination of tetrahydrodipyrrin **1** proceeded at the 9-position[53] (i.e., the free α-pyrrole position) to afford **1-Br^9** (Scheme 2.3).

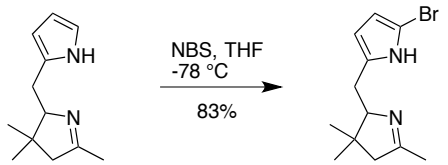

1 **1-Br^9**

Scheme 2.3. Pyrrolic α-bromination.

Here, we describe studies of electrophilic substitution of the dialkylboron–hydrodipyrrin complexes. The motivation for developing chemistry for selective β-substitution stems from the desire to introduce diverse substituents at the corresponding positions of the pyrroles in the chlorin macrocycle, in particular those in ring A.

(B) Bromination or formylation. Bromination of tetrahydrodipyrrin **1-BBu$_2$** with 1

molar equiv of NBS at –78 °C afforded three brominated products, namely **1-Br^{7}BBu$_2$**, **1-Br^{7}Br^{8}BBu$_2$** and **1-Br^{8}BBu$_2$** in the ratio 10:2:1 on the basis of ^{1}H NMR spectroscopy of the crude reaction mixture. A small amount of unreacted starting material also was observed; regardless, no α-pyrrole substituted products were detected. The main product, **1-Br^{7}BBu$_2$**, was isolated in 53% yield upon recrystallization three times from methanol (Scheme 2.4). (Note that chromatography failed to separate **1-Br^{7}BBu$_2$** and **1-Br^{7}Br^{8}BBu$_2$**.) The boron complex of bromohydrodipyrrin **1-Br^{7}BBu$_2$** is less stable than that of the parent **1-BBu$_2$**.

A Vilsmeier formylation of tetrahydrodipyrrin **1-BBu$_2$** with $POCl_3$/DMF in CH_2Cl_2 afforded 7-formyltetrahydrodipyrrin **1-F^{7}BBu$_2$** as a major product with small amounts of regioisomers **1-F^{8}BBu$_2$** and **1-F^{9}BBu$_2$** (Scheme 2.4). Column chromatography afforded pure **1-F^{7}BBu$_2$** in 70% yield. The position of the formyl group in **1-F^{7}BBu$_2$** was established by ^{1}H NMR spectroscopy (see Supplimentary information).

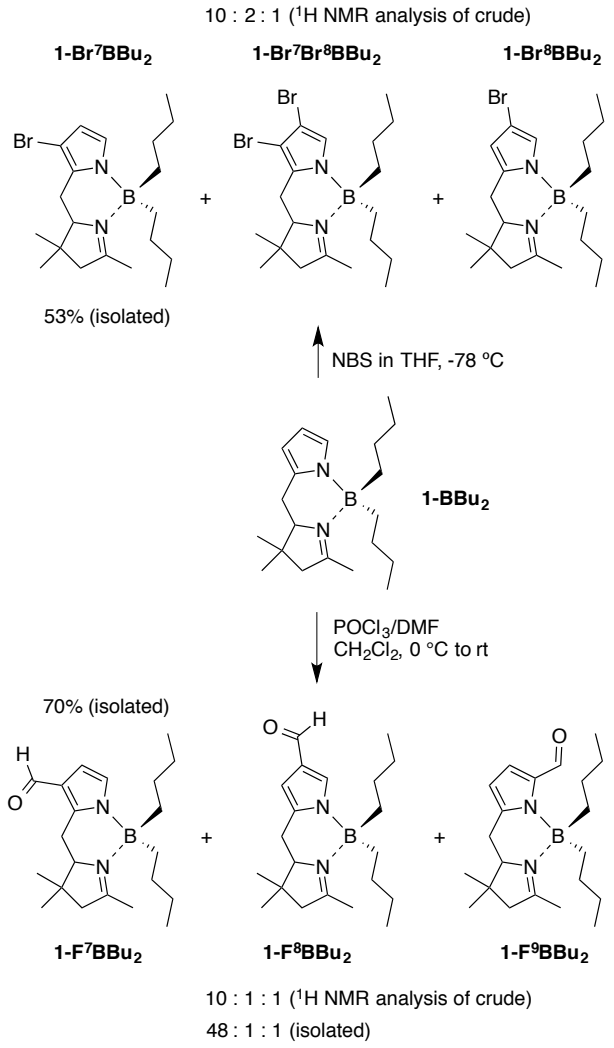

Scheme 2.4. Electrophilic substitution of a dialkylboron–tetrahydrodipyrrin.

(C) Formylation following bromination. The target **1-Br^{8}F^{7}BBu$_2$** obtained after formylation is a potentially valuable building block for chlorin synthesis, given that the 8-position of a tetrahydrodipyrrin will become the 3-position of a chlorin. Accordingly, formylation of **1-Br^{8}BBu$_2$** was pursued. Application of the same conditions ($POCl_3$/DMF) employed for **1-BBu$_2$**, however, resulted in a mixture of products including chloro/bromo

exchange. Upon replacement of $POCl_3$ with $POBr_3$,[61] several products were formed and isolated and yields determined via chromatography (Scheme 2.5). The fractions in order of elution include an unknown, isomer **1-Br^{8}F^{9}BBu$_2$** (9% yield), the desired compound **1-Br^{8}F^{7}BBu$_2$** (46% yield), and **1-BBu$_2$** (21% yield).

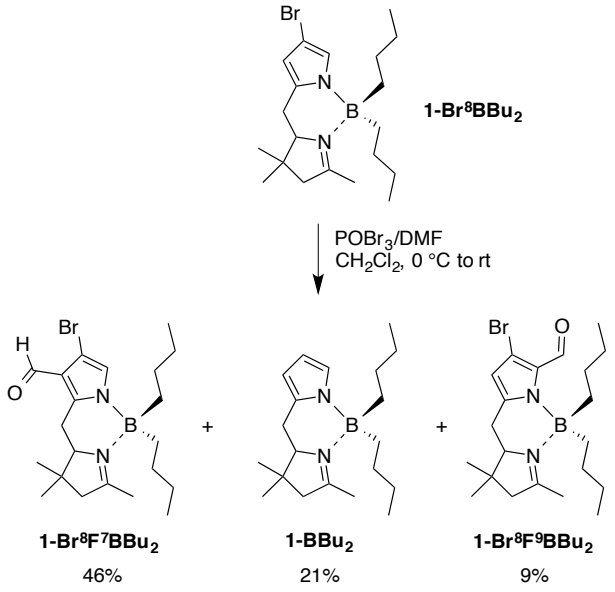

Scheme 2.5. Formylation of **1-Br^{8}BBu$_2$**.

(D) Bromination following formylation. We also synthesized **1-Br^{8}F^{7}BBu$_2$** via another route, in which **1-F^{7}BBu$_2$** served as the starting material. Thus, treatment of **1-F^{7}BBu$_2$** with NBS at –78 °C under argon afforded **1-Br^{8}F^{7}BBu$_2$** in 69% yield along with isomer **1-Br^{9}F^{7}BBu$_2$** in 23% yield (Scheme 2.6). A crystal of **1-Br^{8}F^{7}BBu$_2$** suitable for X-ray analysis was obtained from CH_2Cl_2/hexanes by slow evaporation at 4 °C. In summary, the ability to gain access to the 8-bromo-7-formyl substitution pattern is quite attractive for

eventual preparation of chlorophyll *f* model compounds.

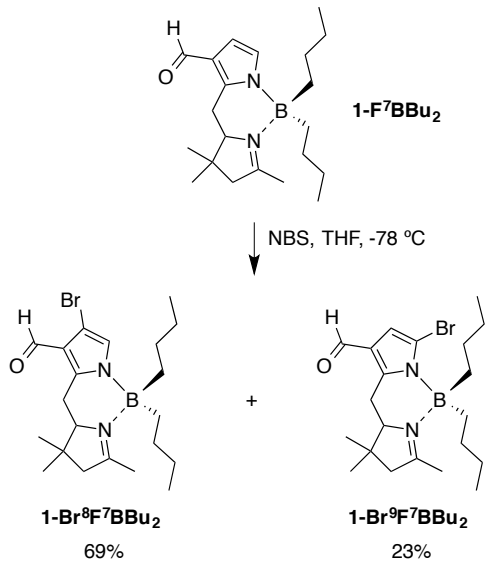

Scheme 2.6. Bromination of **1-F^{7}BBu$_2$**.

(E) Bromination of dihydrodipyrrin–boron complexes. Bromination of dihydrodipyrrin **3-BBu$_2$** with 1 molar equiv of NBS at –78 °C afforded three brominated products (Scheme 2.7), which upon chromatography were identified as **3-Br^{7}Br^{8}BBu$_2$** (28% yield), **3-Br^{8}BBu$_2$** (11% yield) and **3-Br^{7}BBu$_2$** (10% yield). A small amount of unreacted starting material also was observed; however, α-pyrrole substituted products were not detected. The boron complexes of the bromodihydrodipyrrin darkened and decomposed upon standing overnight in NMR tubes at room temperature, reflecting the lesser stability versus the corresponding bromotetrahydrodipyrrin complexes.

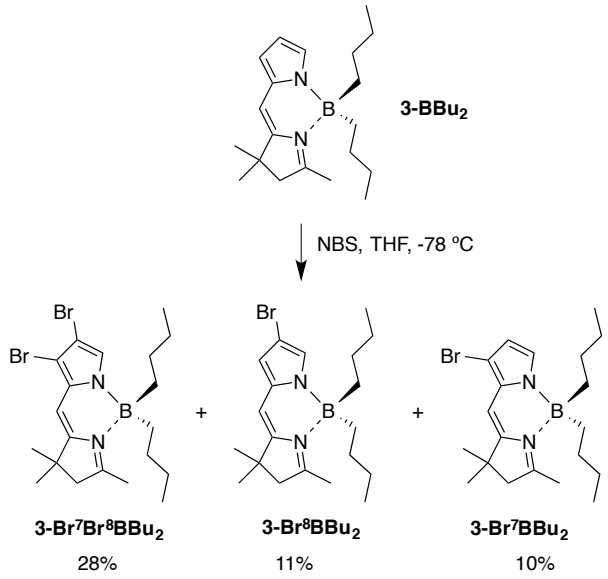

Scheme 2.7. Bromination of a dihydrodipyrrin–boron complex.

(F) Limitations of hydrodipyrrin–boron complexes. Dialkylboron complexation of the tetrahydrodipyrrin proved very beneficial in directing electrophilic substitution to the β- rather than α-pyrrolic positions. On the other hand, a number of other transformations were unsuccessful: (1) attempts to dehydrogenate tetrahydrodipyrrin **1-BBu$_2$** using a variety of reagents (DDQ, *p*-chloranil, SeO_2, $Pb(OAc)_4$/AcOH, CuO) to give dihydrodipyrrin **3-BBu$_2$** failed (as does the reaction with **1**); (2) attempts to oxidize the 1-methyl group of tetrahydrodipyrrin **1-BBu$_2$** with SeO_2 to give the 1-formyl group failed (yet the reaction succeeds with diverse dihydrodipyrrins[62,63]); (3) the dibutylboron complex of a dihydrodipyrrin–acetal (analogue of **1** bearing a 1,1-dimethoxymethyl group), used in bacteriochlorin chemistry,[64] failed to form; (4) Pd-mediated coupling of bromotetrahydrodipyrrin–dialkylboron complexes (e.g., **1-Br^{8}BBu$_2$**) such as carbonylation

failed (as do such reactions in general with uncomplexed hydrodipyrrins); and (5) treatment of **1-F^{7}BBu$_2$** with *tert*-butylamine gave the aldimine but ruthenium-mediated attempts to install an alkyl group at the adjacent 8-position failed (yet the reaction works well with arenes).[65] In summary, the benefits of dialkylboron complexation, while significant, appear limited to regioselective electrophilic substitution of tetrahydrodipyrrins.

(III) Characterization

(A) NMR spectroscopy. The most pronounced changes in the ^{1}H NMR spectrum upon complexation of tetrahydrodipyrrin **1** to give **1-BBu$_2$** are as follows: (1) a downfield chemical shift of the resonance from the 1-methyl group from 2.05 ppm to 2.41 ppm; and (2) a downfield chemical shift of the resonances of H^{2} (protons at the pyrroline 2-position). For dihydrodipyrrin **2-BBu$_2$** versus **2**, the most significant chemical shift was observed for H^{5} (from 5.97 ppm to 6.30 ppm). The resonances observed for protons in selected tetrahydrodipyrrins were assigned by NOESY and are provided in the Experimental Section.

Each dialkylboron complex was examined by ^{11}B NMR spectroscopy using the ^{11}B standard, B(OH)$_3$, at 19.8 ppm in DMF[66] as a standard. Each dialkylboron complex exhibited a broad singlet in the range 0.89–2.72, to be compared with that of similar compounds such as *N*-(9-borabicyclo[3.3.1]non-9-yl)pyrrole (59.9 ppm)[67] and the 9-BBN complex of monoacyldipyrromethanes (~13 ppm).[43] The relative upfield shift of **1-BBu$_2$** is characteristic for species in which boron is coordinated with an N_{imino} nitrogen.[68]

(B) X-ray characterization. X-ray structural analysis was performed of the dibutylboron complexes of three tetrahydrodipyrrins (**1-BBu$_2$**, **1-Br^{8}BBu$_2$**, and **1-Br^{8}F^{7}BBu$_2$**) and dihydrodipyrrin **2-BBu$_2$** (Figure 2.1). The tetrahydrodipyrrins each contain

a stereogenic center (C4) and are expected to form as racemic mixtures. In this regard, **1-Br^{8}F^{7}BBu$_2$** crystallizes in a chiral space group *Pna*2$_1$, with the asymmetric unit (Z' = 2) containing one molecule of each enantiomer (see Supplimentary information). The other materials with stereogenic centers, **1-BBu$_2$** and **1-Br^{8}BBu$_2$**, crystallize in the centrosymmetric space groups *P*2$_1$/*n* or *P*2$_1$/*c* respectively, containing both enantiomers in the unit cell. Electron density peaks in the difference map of **1-Br^{8}F^{7}BBu$_2$** revealed disorder in the position of Br on both of the molecules in the asymmetric unit at the respective β-pyrrolic positions. Modeling this disorder favored (97:3) the Br on the 8- versus 9-position of the tetrahydrodipyrrin system. The 9-position is the pyrrole α-position, indicating a small amount of α-bromo substituted product (**1-Br^{9}F^{7}BBu$_2$**) in the isolated sample of **1-Br^{8}F^{7}BBu$_2$**.

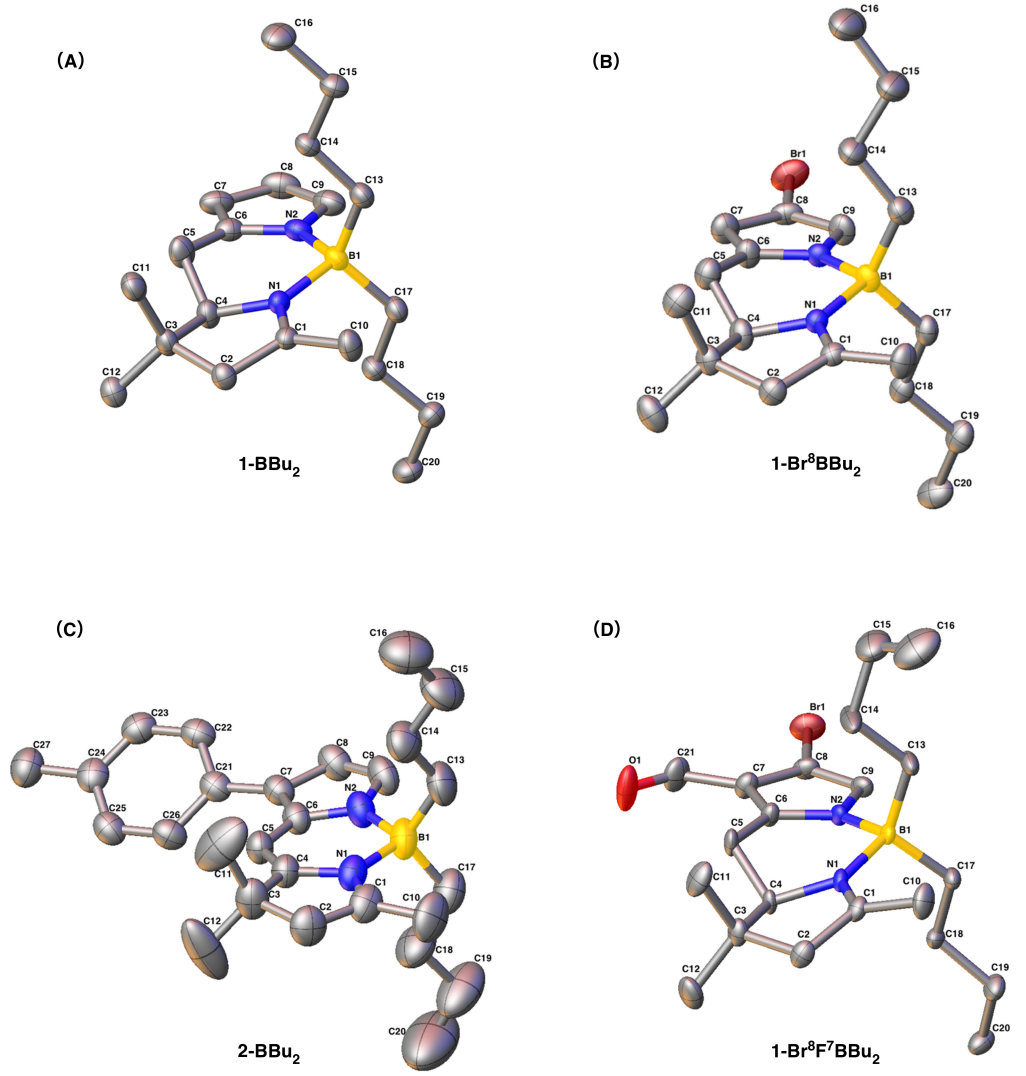

Figure 2.1. ORTEP drawing of (A) tetrahydrodipyrrin **1-BBu$_2$**, (B) tetrahydrodipyrrin **1-Br^{8}BBu$_2$**, (C) dihydrodipyrrin **2-BBu$_2$**, and (D) tetrahydrodipyrrin **1-Br^{8}F^{7}BBu$_2$**. Ellipsoids are displayed at the 50% probability level and hydrogen atoms are omitted for clarity. The large spherical ellipsoids of **2-BBu$_2$** result from high thermal motion.

A key difference between the two types of compounds is the greater coplanarity of the pyrrole and pyrroline rings of dihydrodipyrrin **2-BBu$_2$** versus that of the tetrahydrodipyrrins due to the unsaturated versus saturated C4–C5 bond, respectively.

Regardless, the butyl chains attached to the boron center are thrust above and below the ligand plane in each case, as expected. The B–N (pyrrolic) bond length in **1-BBu$_2$** (1.570 Å), **1-Br^{8}BBu$_2$**, (1.567 Å), **2-BBu$_2$** (1.568 Å) and **1-Br^{8}F^{7}BBu$_2$** (1.571 Å) is slightly shorter than for that of a monoacyldipyrromethane (**B**, Chart 2.2, 1.588 Å).[43] The B–N (pyrrolinyl) bond length in **1-BBu$_2$** (1.631 Å), **1-Br^{8}BBu$_2$**, (1.637 Å), **1-Br^{8}F^{7}BBu$_2$** (1.623 Å) and **2-BBu$_2$** (1.640 Å) is longer than that of the B–N (pyrrolic). The bromo and formyl group in **1-Br^{8}F^{7}BBu$_2$** are introduced via successive derivatization of **1-BBu$_2$**; thus, the single-crystal X-ray structure of **1-Br^{8}F^{7}BBu$_2$** provides proof of the regioselectivity of the electrophilic aromatic processes (bromination, formylation) in the presence of the dibutylboron unit.

(IV) Decomplexation of dibutylboron–tetrahydrodipyrrins

The decomplexation of **1-BBu$_2$** was examined under several conditions, drawing on experience with conditions developed for dialkylboron complexes of 1-acyldipyrromethanes (e.g., **B**, Chart 2.2).[43] The use of 1-pentanol at reflux[43] caused decomplexation but the liberated **1** did not precipitate from hexanes, which prompted examination of other conditions. Refluxing solutions containing phenoxide anion, hydrazine monohydrate, or KOH were successful with **1-BBu$_2$** but upon application to the formyl compound **1-F^{7}BBu$_2$** gave only starting material. Attempts to use KOH (50 equiv) or TBAF also did not afford **1-F^7**. The milder base K_2CO_3 in methanol led to the desired compound, but with a large amount of starting material. K_3PO_4 afforded better solubility in methanol and increased the yield to 60% yield for **1-F^7**. The same conditions with **1-Br^{8}F^{7}BBu$_2$** or **1-Br^{7}BBu$_2$** gave the free tetrahydrodipyrrin **1-Br^{8}F^7** or **1-Br^7** in 63% or 66% yield, respectively (Scheme 2.8).

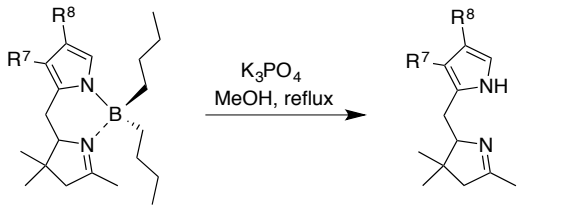

1-F^{7}BBu$_2$
1-Br^{8}F^{7}BBu$_2$
1-Br^{7}BBu$_2$

1-F^7 (60%)
1-Br^{8}F^7 (63%)
1-Br^7 (66%)

Scheme 2.8. Decomplexation of β-pyrrolic substituted dibutylboron–tetrahydrodipyrrins.

(V) Isomeric formylchlorins

(A) Synthesis. Two isomeric formylchlorins were prepared in a continuation of our studies of the effects of auxochromes on the spectral properties of chlorins. Prior theoretical studies have "walked the formyl group around the ring" but no experimental studies have yet made available the 2-formylchlorin and 3-formylchlorin (a 3-formyl-10-mesitylchlorin has been prepared previously[5]). Formylchlorins can be prepared by Pd-mediated carbonylation of the corresponding bromochlorins.[69] Access to the 2-bromochlorin was achieved by bromination of the dibutylboron-complexed Western half (**1-BBu$_2$**), whereas a 3-bromochlorin was prepared by installation of the bromo group in the earliest precursor, pyrrole-2-carboxaldehyde. Thus, the reaction of Eastern half **4**[50] and Western half **1-Br^7** or **1-Br^8** was employed to synthesize 2-bromochlorin **FbC-Br^2** or 3-bromochlorin **FbC-Br^3**, respectively, as shown in Scheme 2.9. Compound **1-Br^7** was obtained by bromination of **1-BBu$_2$** followed by decomplexation and chromatographic purification, whereas **1-Br^8** is a known compound[5,51] obtained from 4-bromopyrrole-2-carboxaldehyde. The chlorin-forming reaction was carried out under standard conditions of acid-catalyzed condensation (*p*-

$TsOH \cdot H_2O$ in $MeOH/CH_2Cl_2$ under argon for 50 min) followed by zinc(II)-mediated oxidative cyclization [$Zn(OAc)_2$, 2,2,6,6-tetramethylpiperidine (TMPi), and AgOTf in CH_3CN at reflux exposed to air for 22 h]. The resulting zinc chlorins were then demetalated upon treatment with trifluoroacetic acid. This route provided access to the free base 2-bromochlorin or 3-bromochlorin in yield of 5% or 14%, respectively. The yields, while low, are typical of those for sparsely substituted chlorins.[50]

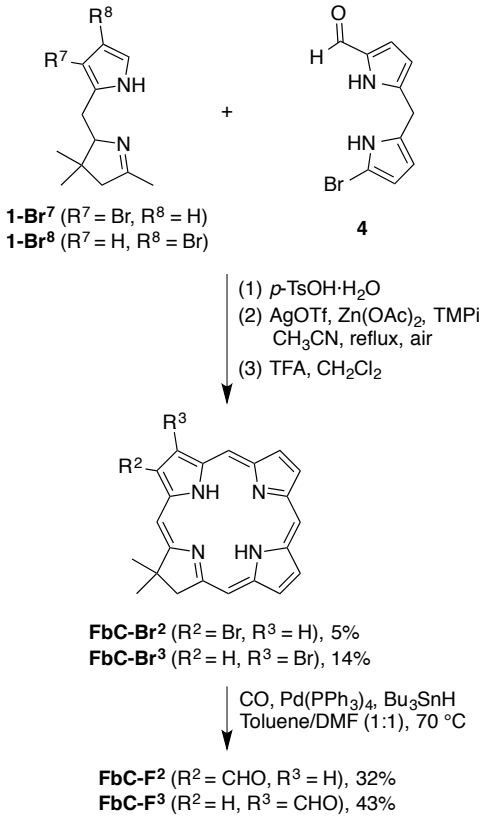

Scheme 2.9. Synthesis of formylchlorins.

Treatment of the bromochlorin **FbC-Br^2** or **FbC-Br^3** with Bu_3SnH and a

stoichiometric amount of $Pd(PPh_3)_4$ in toluene/DMF (1:1) at 70 °C under an atmosphere of CO gave the corresponding 2-formylchlorin **FbC-F^2** or 3-formylchlorin **FbC-F^3** in 32% or 43% yield, respectively. Each target chlorin was characterized by absorption spectroscopy, ^{1}H NMR spectroscopy, ^{13}C NMR spectroscopy and high-resolution mass spectrometry.

(B) Absorption spectral properties. The formylchlorin **FbC-F^2** or **FbC-F^3** exhibits an intense B (Soret) band and a characteristic strong Q_y band (Figure 2.2). The B band of **FbC-F^3** exhibited a short-wavelength shoulder of significant intensity, resulting in a slightly larger full-width-at-half-maximum (fwhm, 38 nm) than that of **FbC-F^2** (34 nm). Significant differences in Q_y absorption maximum and absorption intensity occurred depending on the site of formyl substitution. The Q_y absorption maximum of the two formylchlorins shifted from 654 to 664 nm and paralleled the bathochromic shift of the B band from 404 to 416 nm for **FbC-F^2** versus **FbC-F^3**, respectively. In addition, a slight hyperchromic effect of the Q_y band was observed accompanying the bathochromic shift.

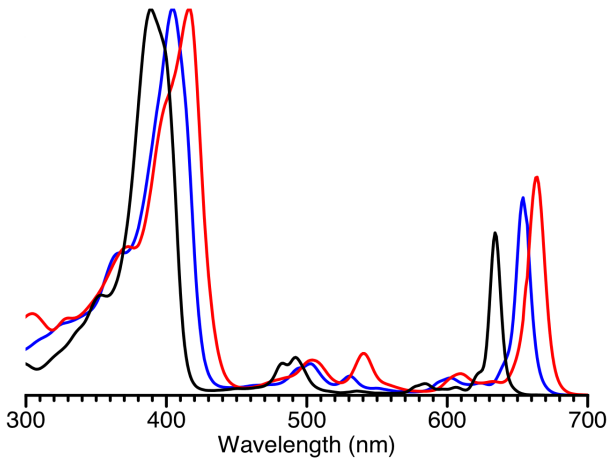

Figure 2.2. Absorption spectra in toluene at room temperature (normalized at the B bands) of **FbC** (black), **FbC-F^2** (blue) and **FbC-F^3** (red).

The spectra of the two formylchlorins can be contrasted with that of the fully unsubstituted chlorin **FbC** (Chart 2.3),[70] which exhibits B and Q_y absorption at 389 and 634 nm. Although the accurate determination of molar absorption coefficients can be difficult especially with small samples, the ratio of the Q_y and B bands provides a relative measure of the changing band intensities. The B/Q_y band ratio is 2.4 (**FbC**), 2.0 (**FbC-F^2**), or 1.8 (**FbC-F^3**). Thus, the formyl group introduces a pronounced bathochromic and hyperchromic shift on the Q_y band, with the effect larger at the 3- versus 2-position.

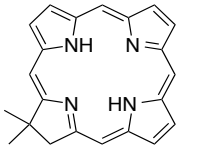

FbC

Chart 2.3. Benchmark chlorin.

Outlook

Directed routes to stable hydroporphyrins rely extensively on hydrodipyrrin chemistry, a domain of chemistry where much methodology development remains to be done. In general, the synthetic methods available for manipulating hydrodipyrrins are incommensurate with the architectural challenges and scientific opportunities presented by the target macrocycles. The work described herein has established a new route to 2-substituted chlorins. The route relies on the formation of a dibutylboron complex of a tetrahydrodipyrrin, the Western half precursor to the chlorin. The introduction of dialkylboron unit directs electrophilic aromatic substitution (bromination, formylation) chiefly to the β-pyrrolic 7-position, which ultimately gives rise to the chlorin 2-position. The

role of steric versus electronic factors that underpin the unusual substitution pattern in the tetrahydrodipyrrin–dialkylboron complex remains unknown. Regardless, in combination with literature data, a clear trend has emerged for electrophilic substitution of increasingly unsaturated substrates, as shown in Figure 2.3. Substitution of the tetrahydrodipyrrin–dialkylboron complex proceeds chiefly at the 7-position (adjacent to the alkyl substituent); for the dihydrodipyrrin–dialkylboron complex, reaction proceeds equivalently at the 7- and 8-positions; and for the dipyrrin–difluoroboron complex (i.e., a BODIPY dye), bromination (Br_2),[71] chlorination (NCS),[72] or formylation (Vilsmeier, 80 °C)[73] proceeds selectively at the 8-position. The steric effects of the 5-aryl group in these substitution processes remains unknown.

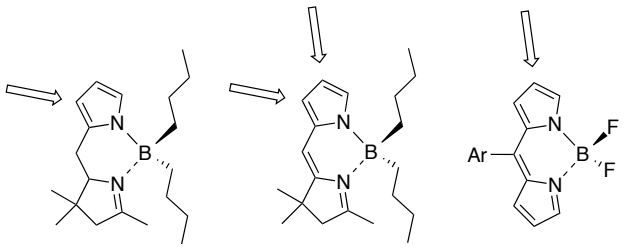

Figure 2.3. Preferred site(s) of electrophilic substitution in hydrodipyrrin–boron complexes.

The availability of the 2-formyl and 3-formylchlorins lacking any other substituents enables fundamental studies to assess the origin of the spectral and photophysical properties of the more highly substituted natural chlorophylls.[40,74] The *de novo* route complements semisynthesis approaches that begin with natural chlorophylls.[75] The access to 2-substituted

chlorins now completes our circumambulation of the ring, as access to the 3,[5,76] 5,[24,25,50] 7,[69,76,77] 8,[77] 10,[24,25,50] 12,[27,28] 13,[2,5,78] 15,[70,76,78,79] 17,[70,80] 18,[80] and 20[69,79] positions has already been achieved, as has installation of the isocyclic ring[2,81] (and 6-membered imide analogues[78] thereof) characteristic of the native chlorophyll structures. More generally, the availability of 2-substituted chlorins provides an initial approach toward sparsely substituted chlorophyll *f* analogues.

Experimental section

(I) General

^{1}H (400 MHz) and ^{13}C (100 MHz) NMR spectra were recorded in $CDCl_3$ unless noted otherwise. ^{11}B NMR spectroscopy (160 MHz) was performed at room temperature using a boron-free NMR tube, $CDCl_3$ as solvent and $B(OH)_3$ in DMF as external standard (referenced to 19.8 ppm).[66] Absorption spectra were collected in toluene. Melting points are uncorrected. Silica gel (40 μm average particle size) was used for column chromatography. Compounds **1**,[45] **1-Br**[8],[5,51] **2**,[52] **3**,[53] and **4**[50] were prepared as described in the literature.

(II) Synthesis

10-(Dibutylboryl)-2,3,4,5-tetrahydro-1,3,3-trimethyldipyrrin (1-BBu$_2$). A solution of **1** (380 mg, 2.00 mmol) in CH_2Cl_2 (4.0 mL) was treated with TEA (1.0 mL) and dibutylboron triflate (4.00 mL of 1 M solution in CH_2Cl_2, 2 mmol). The reaction mixture was stirred at room temperature. After 1 h, CH_2Cl_2 was added. TLC analysis [silica, hexanes/CH_2Cl_2 (2:1)] showed the presence of a yellow, highly fluorescent, non-polar product (trace amount, R_f = 0.57), in addition to the title compound (R_f = 0.50). The yellow impurity could not be removed by chromatography or crystallization. The organic phase was washed three times with $NaHCO_3$, which did remove the yellow impurity. The organic phase was concentrated. The resulting oil was filtered through a pad of silica (CH_2Cl_2). The filtrate was concentrated. Crystallization from hot EtOH/water afforded pale yellow crystals that gave a single spot upon TLC analysis (389 mg, 62%): mp 135–136 °C; ^{11}B δ 0.98; ^{1}H NMR δ 0.42–0.55 (m, 2H), 0.62–0.66 (m, 2H), 0.79–0.82 (m, 6H), 1.11 (s, 3H), 1.14–1.19

(m, 4H) 1.21 (s, 3H), 1.20–1.22 (m, 4H), 2.38–2.39 (m, 3H), 2.60–2.65 (m, 1H), 2.77–2.81 (m, 1H) 2.82–2.85 (m, 2H), 3.82–3.86 (m, 1H), 5.90–5.91 (m, 1H), 6.09–6.10 (m, 1H), 6.66–6.67 (m, 1H); ^{13}C NMR δ 14.29, 14.38, 19.1, 23.0, 23.5, 25.2, 26.2, 26.6, 26.7, 28.1, 28.4, 38.8, 56.1, 80.0, 102.8, 106.1, 121.1, 130.1, 180.4; ESI-MS obsd 315.2970, calcd 315.2966 [$(M + H)^+$, M = $C_{20}H_{35}BN_2$].

10-(Dimethylboryl)-2,3,4,5-tetrahydro-1,3,3-trimethyldipyrrin (1-BMe$_2$). A solution of **1** (0.190 g, 1.00 mmol) in CH_2Cl_2 (4.0 mL) was treated with TEA (0.5 mL) and dimethylboron bromide (0.195 mL, 2.00 mmol) at 0 °C. After 5 min, the cooling bath was removed and the mixture was stirred at room temperature for 1 h. Then the mixture was concentrated and the resulting material was filtered through neutral alumina (CH_2Cl_2), affording an off-white solid (0.154 g, 67%). Due to instability, the characterization of the title compound was incomplete. ^{1}H NMR δ 0.00 (s, 3H), 0.20 (s, 3H), 1.03 (s, 3H), 1.21 (s, 3H), 2.39–2.40 (m, 3H), 2.58–2.63 (m, 1H), 2.73–2.78 (m, 1H), 2.82–2.85 (m, 1H), 2.87–2.91 (m, 1H), 3.96–4.00 (m, 1H), 5.90–5.91 (m, 1H), 6.12–6.13 (m, 1H), 6.70–6.71 (m, 1H); ^{13}C NMR 19.4, 23.3, 25.5, 26.3, 38.7, 56.2, 78.8, 103.5, 106.8, 129.2.

10-(Dibutylboryl)-2,3-dihydro-1,3,3-trimethyl-7-(4-methylphenyl)dipyrrin (2-BBu$_2$). A solution of **2** (0.100 g, 0.359 mmol) and TEA (0.18 mL, 1.3 mmol) in CH_2Cl_2 (5.1 mL) was treated with dibutylboron triflate (0.72 mL, 1 M in CH_2Cl_2, 0.72 mmol) under argon at room temperature. The reaction mixture was stirred for 1 h under argon. The reaction mixture was quenched with water. The organic phase was dried (Na_2SO_4), concentrated, and chromatographed [silica, hexanes/CH_2Cl_2 (1:1)] to afford a light yellow solid (0.13 g, 87%): mp 87–88 °C; ^{1}H NMR δ 0.70–0.89 (m, 12H), 0.96–1.04 (m, 2H), 1.17–1.22 (m, 7H), 1.27

(s, 3H), 2.35 (s, 3H), 2.42 (s, 3H), 2.74 (s, 3H), 6.32–6.34 (m, 1H), 6.83–6.84 (m, 1H), 7.20 (d, J = 8.1 Hz, 2H), 7.38 (d, J = 8.1 Hz, 2H); ^{13}C NMR δ 8.9, 14.4, 19.1, 21.3, 26.3, 28.0, 29.2, 37.6, 46.8, 54.6, 108.7, 124.0, 125.3, 128.1, 129.3, 134.5, 135.0, 147.9, 174.7; ESI-MS obsd 402.3320, calcd 402.3315 [$(M + H)^+$, M = $C_{27}H_{39}BN_2$].

10-(Dibutylboryl)-2,3-dihydro-1,3,3-trimethyldipyrrin (3-BBu$_2$). A solution of **3** (45 mg, 0.24 mmol) and TEA (0.10 mL, 0.72 mmol) in CH_2Cl_2 (0.5 mL) was treated with dibutylboron triflate (0.48 mL, 1 M in CH_2Cl_2, 0.48 mmol) under argon at room temperature. The reaction mixture was stirred for 1 h under argon. The reaction mixture was quenched with water. The organic phase was washed (brine), dried (Na_2SO_4), concentrated, and chromatographed [silica, hexanes/CH_2Cl_2 (1:1)] to afford a light yellow solid (20 mg, 27%): mp 98–100 °C; ^{1}H NMR δ 0.60–0.72 (m, 2H), 0.73–0.78 (m, 10H), 0.84–0.92 (m, 2H), 1.11–1.20 (m, 4H), 1.25 (s, 6H), 2.44 (s, 3H), 2.77 (s, 2H), 6.07 (s, 1H), 6.09–6.13 (m, 1H), 6.16–6.20 (m, 1H), 6.78–6.82 (m, 1H); ^{13}C NMR δ 14.3, 18.9, 25.9, 26.3, 27.9, 29.1, 29.8, 37.2, 54.5, 107.5, 108.5, 109.6, 125.5, 128.3, 147.4, 175.0; ESI-MS obsd 313.2720, calcd 313.2813 [$(M + H)^+$, M = $C_{20}H_{33}BN_2$].

7,8-Dibromo-10-(dibutylboryl)-2,3-dihydro-1,3,3-trimethyldipyrrin (3-Br^{7}Br^{8}BBu$_2$). A solution of **3-BBu$_2$** (18 mg, 0.058 mmol) in THF (1.2 mL) was chilled in a dry ice/acetone bath for 10 min under argon. Then, the solution was treated with one portion of NBS (10.3 mg, 0.058 mmol). After stirring for 1 h at –78 °C, hexanes was added, and the mixture was allowed to warm by removal of the dry ice/acetone bath. Water was added when the internal reaction temperature reached 0 °C. The organic phase was washed (water), dried (Na_2SO_4), concentrated and chromatographed [silica, CH_2Cl_2/hexanes (1:4)]. Four

bands were observed in the following order of elution: unreacted starting material, **3-Br^{7}BBu$_2$** (2.0 mg, 10%), **3-Br^{8}BBu$_2$** (2.4 mg, 11%), and the title compound (7.6 mg, 28%). The title compound was a yellow solid with fluorescence under long-wavelength UV illumination. Each of the isolated compounds is somewhat unstable, hence the assignments are provisional on the basis of limited characterization data. Data for the title compound: ^{1}H NMR δ 0.60–0.72 (m, 2H), 0.73–0.78 (m, 10H), 0.84–0.92 (m, 2H), 1.11–1.20 (m, 4H), 1.25 (s, 6H), 2.42 (s, 3H), 2.80 (s, 2H), 6.05 (s, 1H), 6.74 (s, 1H); ESI-MS obsd 468.1055, calcd 468.1056 [$(M + H)^+$, M = $C_{20}H_{31}BBr_2N_2$].

Data for 8-bromo-10-(dibutylboryl)-2,3-dihydro-1,3,3-trimethyldipyrrin (**3-Br^{8}BBu$_2$**): ^{1}H NMR δ 0.60–0.72 (m, 2H), 0.73–0.78 (m, 10H), 0.84–0.92 (m, 2H), 1.11–1.20 (m, 4H), 1.25 (s, 6H), 2.44 (s, 3H), 2.80 (s, 2H), 6.10 (s, 1H), 6.12 (d, J = 2.8 Hz, 1H), 6.71 (d, J = 2.8 Hz, 1H).

Data for 7-bromo-10-(dibutylboryl)-2,3-dihydro-1,3,3-trimethyldipyrrin (**3-Br^{7}BBu$_2$**): ^{1}H NMR δ 0.60–0.72 (m, 2H), 0.73–0.78 (m, 10H), 0.84–0.92 (m, 2H), 1.11–1.20 (m, 4H), 1.25 (s, 6H), 2.42 (s, 3H), 2.80 (s, 2H), 6.05 (s, 1H), 6.12 (s, 1H), 6.74 (s, 1H); ESI-MS obsd 390.1959, calcd 390.1951 [$(M + H)^+$, M = $C_{20}H_{32}BBrN_2$].

7-Bromo-10-(dibutylboryl)-2,3,4,5-tetrahydro-1,3,3-trimethyldipyrrin (1-Br^{7}BBu$_2$). A solution of **1-BBu$_2$** (200 mg, 0.636 mmol) in THF (12.8 mL) at –78 °C under argon was treated with NBS (112 mg, 0.636 mmol). The reaction mixture was stirred for 1 h at –78 °C under argon. Hexanes was added. Water was added when the internal reaction temperature reached 0 °C. The organic phase was separated, dried (Na_2SO_4), and concentrated. Recrystallization three times from methanol afforded the title compound (100

mg, 40%). The mother liquor was collected and recrystallized three times from methanol to afford an additional 32 mg, giving a total yield of 53% (132 mg): mp 105–107 °C; ^{11}B δ 1.19; ^{1}H NMR δ 0.35–0.55 (m, 2H), 0.58–0.85 (m, 8H), 0.89–1.27 (m, 8H), 1.03 (s, 3H), 1.24 (s, 3H), 3.38 (d, *J* = 1.9 Hz, 3H), 2.59–2.69 (m, 2H), 2.78–2.93 (m, 2H), 3.77–3.83 (m, 1H), 6.12 (d, *J* = 2.8 Hz, 1H), 6.61 (d, *J* = 2.8 Hz, 1H); ^{13}C NMR δ 14.33, 14.39, 19.1, 23.0, 23.3, 23.6, 26.3, 26.47, 26.62, 27.9, 28.2, 38.8, 56.1, 79.3, 90.5, 108.6, 120.7, 127.3, 181.1; ESI-MS obsd 392.2111, calcd 392.2108 [$(M + H)^+$, M = $C_{20}H_{34}BBrN_2$]. The same procedure at the 50 mg (0.16 mmol) scale with chromatography [silica, hexanes/CH_2Cl_2 (4:1)] afforded the title product (28 mg, 45%) containing 10% of dibromo impurity (**1-Br^{7}Br^{8}BBu$_2$**). Also, no increase in selectivity was achieved upon treatment of a 5-fold less concentrated solution of **1-BBu$_2$** (10 mM) with NBS solution (20 mM) via cannula (dropwise) over 1 h.

8-Bromo-10-(dibutylboryl)-2,3,4,5-tetrahydro-1,3,3-trimethyldipyrrin (1-Br^{8}BBu$_2$). A solution of **1-Br^8** (600 mg, 2.23 mmol) in anhydrous CH_2Cl_2 (15 mL) was treated with TEA (1.1 mL, 8.00 mmol) and dibutylboron triflate (4.5 mL, 1M in CH_2Cl_2, 0.45 mmol). The reaction mixture was stirred at room temperature for 1 h. Water was added. The organic extract was washed (brine), dried (Na_2SO_4), concentrated and chromatographed [silica, hexanes/CH_2Cl_2 (2:1)] to afford white crystals (612 mg, 70%): mp 118–120 °C (dec.); ^{11}B δ 0.97; ^{1}H NMR δ 0.39–0.54 (m, 2H), 0.55–0.91 (m, 10H), 1.01 (s, 3H), 1.07–1.18 (m, 4H), 1.19–1.30 (m, 2H), 1.22 (s, 3H), 2.38 (d, *J* = 2.2 Hz, 3H), 2.64 (dd, *J* = 18 Hz, *J* = 1.5 Hz, 1H), 2.76–2.83 (m, 3H), 3.78–3.82 (m, 1H), 5.89 (d, *J* = 1.8 Hz, 1H), 6.58 (d, *J* = 1.8 Hz, 1H); ^{13}C NMR δ 14.0, 14.1, 18.8, 23.2, 24.7, 25.9, 26.23, 26.29, 27.6, 27.9, 38.5, 55.7, 79.1,

93.1, 105.3, 120.2, 130.3, 180.8; ^{11}B δ 0.97; ESI-MS obsd 392.2097, calcd 392.2108 [(M + H)$^+$, M = $C_{20}H_{34}BBrN_2$].

10-(Dibutylboryl)-7-formyl-2,3,4,5-tetrahydro-1,3,3-trimethyldipyrrin (1-F^{7}BBu$_2$). A solution of **1-BBu$_2$** (568 mg, 1.81 mmol) and DMF (1.00 mL, 13.0 mmol) in CH_2Cl_2 (13.9 mL) was treated with $POCl_3$ (0.185 mL, 1.99 mmol) at 0 °C under argon. After stirring for 3 h at 0 °C, the reaction mixture was treated with 2M aqueous NaOH (10 mL) at 0 °C, and the reaction mixture was vigorously stirred for 20 min at 0 °C. The organic phase was washed (water, brine), dried (Na_2SO_4), concentrated and chromatographed [silica, hexanes/ethyl acetate (1:1)]. Three products were isolated in the following order: **1-F^{9}BBu$_2$** (yellow solid, 9 mg, 1%), **1-F^{8}BBu$_2$** (yellow solid, 9 mg, 1%), and the title compound **1-F^{7}BBu$_2$** (yellow solid, 435 mg, 70% yield). (Note that thorough removal of DMF prior to chromatography is crucial for the separation.) Data for **1-F^{7}BBu$_2$**: TLC R_f = 0.40 [silica, hexanes/ethyl acetate (1:1)]; mp 114–116 °C; ^{11}B δ 0.89; ^{1}H NMR δ 0.44–0.55 (m, 2H), 0.58–0.83 (m, 10H), 0.87–0.99 (m, 2H), 1.08 (s, 3H), 1.10–1.18 (m, 2H), 1.19–1.26 (m, 2H), 1.27 (s, 3H), 2.41 (d, J = 5.0 Hz, 3H), 2.69–2.87 (m, 3H), 3.57–3.63 (m, 1H), 3.81–3.86 (m, 1H), 6.53 (d, J = 2.7 Hz, 1H), 6.61 (d, J = 2.7 Hz, 1H), 9.77 (s, 1H); ^{13}C NMR δ 13.46, 13.50, 18.3, 22.2, 22.8, 23.2, 25.46, 25.52, 25.6, 27.1, 27.4, 38.1, 55.3, 77.2, 109.7, 120.0, 121.9, 137.9, 181.2, 184.8; ESI-MS obsd 343.2945, calcd 343.2952 [(M + H)$^+$, M = $C_{21}H_{35}BN_2O$].

Data for 10-(dibutylboryl)-8-formyl-2,3,4,5-tetrahydro-1,3,3-trimethyldipyrrin (**1-F^{8}BBu$_2$**): TLC R_f = 0.50 [silica, hexanes/ethyl acetate (1:1)]; mp 104.5–106.5 °C; ^{11}B δ 1.09;

^{1}H NMR δ 0.44–0.55 (m, 2H), 0.58–0.83 (m, 10H), 0.87–0.99 (m, 2H), 1.08 (s, 3H), 1.10–1.18 (m, 2H), 1.19–1.26 (m, 2H), 1.25 (s, 3H), 2.41 (d, *J* = 5.0 Hz, 3H), 2.70–2.74 (m, 1H), 2.79–2.87 (m, 3H), 3.79–3.81 (m, 1H), 6.36–6.38 (m, 1H), 7.29 (s, 1H), 9.68 (s, 1H); ^{13}C NMR δ 14.4, 19.2, 23.5, 25.1, 26.1, 26.43, 26.52, 27.8, 28.1, 39.0, 56.1, 79.5, 102.9, 126.6, 132.7, 133.6, 181.8, 185.7; ESI-MS obsd 343.2924, calcd 343.2919 [$(M + H)^+$, M = $C_{21}H_{35}BN_2O$].

Data for 10-(dibutylboryl)-9-formyl-2,3,4,5-tetrahydro-1,3,3-trimethyldipyrrin (**1-F^{9}BBu$_2$**): TLC R_f = 0.65 [silica, hexanes/ethyl acetate (1:1)]; mp 94–95 °C; ^{11}B δ 2.44;^{1}H NMR δ 0.44–0.55 (m, 2H), 0.58–0.83 (m, 10H), 0.87–0.99 (m, 2H), 1.08 (s, 3H), 1.10–1.18 (m, 2H), 1.19–1.26 (m, 2H), 1.26 (s, 3H), 2.46 (d, *J* = 5.0 Hz, 3H), 2.70–2.91 (m, 3H), 2.95 (dd, *J* = 3.6 Hz, *J* = 15.4 Hz, 1H), 3.93–3.97 (m, 1H), 6.02 (d, *J* = 3.9 Hz, 1H), 7.14 (d, *J* = 3.9 Hz, 1H), 9.81 (s, 1H); ^{13}C NMR δ 14.3, 19.5, 23.7, 26.23, 26.34, 26.43, 27.2, 28.54, 28.64, 29.9, 38.0, 56.4, 78.2, 107.9, 120.9, 136.4, 140.3, 180.9, 181.6; ESI-MS obsd 343.2925, calcd 343.2919 [$(M + H)^+$, M = $C_{21}H_{35}BN_2O$].

8-Bromo-10-(dibutylboryl)-7-formyl-2,3,4,5-tetrahydro-1,3,3-trimethyldipyrrin (1-Br^{8}F^{7}BBu$_2$). Bromination following formylation: A solution of **1-Br^{8}BBu$_2$** (100 mg, 0.255 mmol) and DMF (0.078 mL) in CH_2Cl_2 (2.5 mL) was treated with $POBr_3$ (80.2 mg, 0.280 mmol) at 0 °C under argon. After stirring for 2.5 h at 0 °C, a 2 M aqueous solution of NaOH (10 mL) was added at 0 °C, and the reaction mixture was vigorously stirred for 20 min at 0 °C. The organic phase was washed (water, brine), dried (Na_2SO_4), concentrated and chromatographed [silica, hexanes/ethyl acetate (2:1)] to give the title compound as a dark red

solid. Data for **1- $Br^8F^7BBu_2$**: mp 90–92 °C; ^{11}B δ 0.98; ^{1}H NMR δ 0.41–0.46 (m, 2H), 0.57–0.84 (m, 10H), 0.87–0.99 (m, 2H), 1.07 (s, 3H), 1.10–1.18 (m, 2H), 1.19–1.24 (m, 2H), 1.26 (s, 3H), 2.41 (d, *J* = 1.8 Hz, 3H), 2.66–2.88 (m, 3H), 3.68–3.84 (m, 2H), 6.57 (s, 1H), 9.76 (s, 1H); ^{13}C NMR δ 14.31, 14.32, 19.2, 22.9, 23.6, 24.1, 26.28, 26.31, 26.36, 27.9, 28.1, 39.0, 56.0, 77.6, 99.5, 117.0, 122.0, 138.5, 182.5, 186.6; ESI-MS obsd 421.2032, calcd 421.2024 [$(M + H)^+$, M = $C_{21}H_{34}BBrN_2O$].

Data for 8-bromo-10-(dibutylboryl)-9-formyl-2,3,4,5-tetrahydro-1,3,3-trimethyldipyrrin (**1-$Br^8F^9BBu_2$**): ^{11}B δ 1.45; ^{1}H NMR δ 0.41–0.46 (m, 2H), 0.57–0.84 (m, 10H), 0.87–0.99 (m, 2H), 1.07 (s, 3H), 1.10–1.18 (m, 2H), 1.19–1.24 (m, 2H), 1.26 (s, 3H), 2.41 (d, *J* = 2.0 Hz, 3H), 2.56–2.86 (m, 3H), 3.74–3.82 (m, 2H), 7.33 (s, 1H), 9.73 (s, 1H); ^{13}C NMR δ 14.19, 14.23, 19.1, 22.3, 23.6, 24.5, 26.03, 26.07, 26.2, 27.6, 27.8, 38.9, 56.0, 78.7, 122.7, 129.7 130.8, 182.4, 185.3; ESI-MS obsd 421.2020, calcd 421.2024 [$(M + H)^+$, M = $C_{21}H_{34}BBrN_2O$].

The title compound was also synthesized by formylation following bromination: A solution of **1-F^7BBu_2** (200 mg, 0.583 mmol) in THF (11.6 mL) was chilled in an acetone/dry ice bath for 10 min under argon. Then the solution was treated with one portion of NBS (104 mg, 0.583 mmol). After stirring for 1 h at –78 °C, hexanes was added. Water was added when the internal reaction temperature reached 0 °C. The organic phase was washed (water), dried (Na_2SO_4), concentrated and chromatographed [silica, hexanes/ethyl acetate (2:1)] to give the title compound as a dark red solid (168 mg, 69%) as well as isomer **1-$Br^9F^7BBu_2$** (56 mg, 23%). Data for **1-$Br^8F^7BBu_2$** are the same as above. Data for 9-bromo-10-(dibutylboryl)-7-formyl-2,3,4,5-tetrahydro-1,3,3-trimethyldipyrrin (**1-$Br^9F^7BBu_2$**): mp 159–

161 °C; ^{11}B δ 2.72; ^{1}H NMR (300 MHz) δ 0.41–0.46 (m, 2H), 0.57–0.83 (m, 10H), 0.87–0.99 (m, 2H), 1.08 (s, 3H), 1.10–1.18 (m, 2H), 1.19–1.26 (m, 2H), 1.27 (s, 3H), 2.41 (d, J = 1.8 Hz, 3H), 2.65–2.89 (m, 3H), 3.69 (dd, J = 16.2 and 3.6 Hz, 1H), 3.88–4.00 (m, 1H), 6.59 (s, 1H), 9.70 (s, 1H); ^{13}C NMR δ 14.2, 14.3, 19.3, 23.3, 23.5, 23.7, 25.2, 26.0, 26.2, 27.4, 28.0, 28.5, 37.9, 56.3, 77.5, 104.1, 114.7, 121.3, 139.8, 181.7, 184.9; ESI-MS obsd 421.2038, calcd 421.2024 [$(M + H)^+$, M = $C_{21}H_{34}BBrN_2O$].

7-Formyl-2,3,4,5-tetrahydro-1,3,3-trimethyldipyrrin (1-F^7). A sample of **1-F^{7}BBu$_2$** (343 mg, 1.00 mmol) in CH_3OH (40 mL) was treated with K_3PO_4 (10.6 g, 50.0 mmol) and refluxed for 20 h. Upon cooling to room temperature, the mixture was washed with water and brine. The organic layer was dried ($NaSO_4$) and concentrated. The crude product was chromatographed (silica, ethyl acetate) to afford a light yellow oil (130 mg, 60%) and recovered starting material (21 mg, 6%). Data for the title compound: ^{1}H NMR (300 MHz) δ 0.98 (s, 3H), 1.16 (s, 3H), 2.05 (d, J = 1.6 Hz, 3H), 2.34 (AB, ^{2}J = 16.8 Hz, 1H), 2.42 (AB, ^{2}J = 16.8 Hz, 1H), 2.61 (ABX, ^{2}J = 15.6 Hz, ^{3}J = 12.0 Hz, 1H), 3.41 (ABX, ^{2}J = 15.6 Hz, ^{3}J = 2.8 Hz, 1H), 3.63–3.69 (m, 1H), 6.54–6.57 (m, 1H), 6.66–6.69 (m, 1H), 9.90 (s, 1H), 10.73–10.89 (br s, 1H); ^{13}C NMR δ 20.7, 23.1, 26.0, 27.2, 42.3, 54.5, 79.4, 109.0, 118.2, 121.6, 141.2, 175.6, 186.0; ESI-MS obsd 219.1500, calcd 219.1492 [$(M + H)^+$, M = $C_{13}H_{18}N_2O$].

8-Bromo-7-formyl-2,3,4,5-tetrahydro-1,3,3-trimethyldipyrrin (1-Br^{8}F^7). A sample of **1-Br^{8}F^{7}BBu$_2$** (120 mg, 0.286 mmol) in CH_3OH (11 mL) was treated with K_3PO_4 (3.00 g, 14.3 mmol) and refluxed for 20 h. Upon cooling to room temperature, the mixture was washed with water and brine. The organic layer was dried ($NaSO_4$) and concentrated.

The crude product was chromatographed (silica, ethyl acetate) to afford a yellow oil (54 mg, 63%) and recovered starting material (7 mg, 6%). Data for the title compound: ^{1}H NMR (300 MHz) δ 0.96 (s, 3H), 1.18 (s, 3H), 2.03 (d, J = 1.6 Hz, 3H), 2.35 (AB, ^2J = 12.6 Hz, 1H), 2.40 (AB, ^2J = 12.6 Hz, 1H), 2.54 (ABX, ^2J = 11.8 Hz, ^3J = 9.0 Hz, 1H), 3.54 (ABX, ^2J = 11.8, ^3J = 2.6 Hz, 1H), 3.65–3.68 (m, 1H), 6.59 (s, 1H), 9.89 (s, 1H), 11.28–11.50 (br s, 1H); ^{13}C NMR δ 20.4, 23.0, 26.3, 26.9, 42.2, 54.4, 79.0, 99.4, 117.4, 122.0, 140.4, 175.8, 187.2; ESI-MS obsd 297.0600, calcd 297.0597 [$(M + H)^+$, M = $C_{13}H_{17}BrN_2O$].

8-Bromo-2,3,4,5-tetrahydro-1,3,3-trimethyldipyrrin (1-Br^7). A sample of **1-Br^{7}BBu$_2$** (250 mg, 0.633 mmol) in CH_3OH (25.0 mL) was treated with K_3PO_4 (6.67 g, 31.3 mmol) and refluxed for 14 h. Upon cooling to room temperature, the mixture was washed with water and brine. The organic layer was dried ($NaSO_4$) and concentrated. The crude product was chromatographed (silica, ethyl acetate) to afford a red oil (112 mg, 66%): ^{1}H NMR (300 MHz) δ 0.96 (s, 3H), 1.14 (s, 3H), 2.04 (d, J = 1.8 Hz, 3H), 2.331 (AB, ^2J = 16.8 Hz, 1H), 2.335 (AB, ^2J = 16.8 Hz, 1H), 2.41 (ABX, ^2J = 16.0 Hz, ^3J = 11.4 Hz, 1H), 2.84 (ABX, ^2J = 16.0 Hz, ^3J = 4.0 Hz, 1H), 3.56–3.62 (m, 1H), 6.10 (t, J = 3.0 Hz, 1H), 6.60 (t, J = 3.0 Hz, 1H), 10.00–10.26 (br s, 1H); ^{13}C NMR (75 MHz) δ 20.4, 22.8, 26.0, 27.0, 42.0, 54.3, 79.5, 93.8, 109.9, 116.5, 129.0, 175.1; ESI-MS obsd 269.0652, calcd 269.0648 [$(M + H)^+$, M = $C_{12}H_{17}BrN_2$].

2-Bromo-17,18-dihydro-18,18-dimethylporphyrin (FbC-Br^2). Following a general procedure,[24] a solution of **1-Br^7** (300 mg, 1.12 mmol) and **4** (282 mg, 1.12 mmol) in anhydrous CH_2Cl_2 (26.4 mL) was treated with a solution of p-TsOH·H_2O (1.05 g, 5.54 mmol) in anhydrous methanol (5.28 mL) under argon. The reaction mixture immediately

turned red. The mixture was stirred for 50 min under argon, then treated with 2,2,6,6-tetramethylpiperidine (2.03 mL, 11.9 mmol) and concentrated to dryness. The resulting brown solid was suspended in acetonitrile (110 mL) followed by the successive addition of 2,2,6,6-tetramethylpiperidine (5.28 mL, 30.8 mmol), $Zn(OAc)_2$ (3.04 g, 16.6 mmol) and AgOTf (854 mg, 3.32 mmol). The resulting suspension was refluxed for 22 h exposed to air. The crude mixture was filtered through a silica pad with CH_2Cl_2. The filtrate was concentrated and dissolved in anhydrous CH_2Cl_2 (66 mL). TFA (880 μL) was added dropwise to the resulting mixture. After 5 min, saturated aqueous $NaHCO_3$ was added slowly. The organic layer was extracted, dried ($NaSO_4$) and concentrated. The crude product was chromatographed [silica, CH_2Cl_2/hexanes (1:2)] to afford a green solid (23 mg, 5%): ^{1}H NMR δ –2.48 (br s, 2H), 2.10 (s, 6H), 4.63 (s, 2H), 8.94 (d, J = 4.4 Hz, 1H), 9.06–9.07 (m, 3H), 9.10 (s, 1H), 9.25 (d, J = 4.4 Hz, 1H), 9.29 (s, 1H), 9.80 (s, 1H), 9.85 (s, 1H); ^{13}C NMR δ 31.6, 47.0, 52.2, 92.8, 97.3, 105.0, 106.52, 106.62, 124.4, 128.1, 128.6, 132.8, 133.2; ESI-MS obsd 419.0874, calcd 419.0866 [$(M + H)^+$, M = $C_{22}H_{19}BrN_4$]; λ_{abs} 391, 641 nm.

3-Bromo-17,18-dihydro-18,18-dimethylporphyrin (FbC-Br^3). Following a general procedure,[24] a solution of **1-Br^8** (534 mg, 1.98 mmol) and **4** (498 mg, 1.98 mmol) in anhydrous CH_2Cl_2 (52 mL) was treated with a solution of *p*-TsOH·H_2O (1.88 g, 9.90 mmol) in anhydrous methanol (13 mL) under argon. The reaction mixture immediately turned red. The mixture was stirred for 50 min under argon, then treated with 2,2,6,6-tetramethylpiperidine (2.5 mL, 15 mmol) and concentrated to dryness. The resulting brown solid was suspended in acetonitrile (200 mL) followed by the successive addition of 2,2,6,6-

tetramethylpiperidine (6.6 mL, 40 mmol), $Zn(OAc)_2$ (5.45 g, 29.4 mmol) and AgOTf (1.53 g, 5.94 mmol). The resulting suspension was refluxed for 22 h exposed to air. The crude mixture was filtered through a silica pad with CH_2Cl_2. The filtrate was concentrated and dissolved in anhydrous CH_2Cl_2 (100 mL). TFA (1.5 mL) was added dropwise to the resulting mixture. After 5 min, saturated aqueous $NaHCO_3$ was added slowly. The organic layer was extracted, dried ($NaSO_4$) and concentrated. The crude product was chromatographed [silica, CH_2Cl_2/hexanes (1:2)] to afford a green solid (116 mg, 14%): ^{1}H NMR δ –2.49 (s, 2H), 2.03 (s, 6H), 4.60 (s, 2H), 8.84 (s, 1H), 8.90 (d, *J* = 4.0 Hz, 1H), 9.00 (s, 1H), 9.01–9.03 (m, 2H), 9.08 (d, *J* = 4 Hz, 1H), 9.19 (d, *J* = 4.8 Hz, 1H), 9.78 (s, 1H), 9.92 (s, 1H); ^{13}C NMR δ 31.4, 46.7, 52.0, 94.2, 97.0, 105.0, 106.6, 124.2, 128.6, 132.7, 133.2; ESI-MS obsd 419.0875, calcd 419.0866 [$(M + H)^+$, M = $C_{22}H_{19}BrN_4$]; λ_{abs} 391, 640 nm.

2-Formyl-17,18-dihydro-18,18-dimethylporphyrin (FbC-F^2). Following a procedure for reductive carbonylation,[69] a mixture of **FbC-Br^2** (30.0 mg, 0.0715 mmol) and $Pd(PPh_3)_4$ (82.6 mg, 0.0715 mmol) was dried under vacuum for 1 h. The reaction flask was filled with CO gas and anhydrous toluene/DMF [3.6 mL, (1:1)]. CO gas was bubbled through the stirred reaction mixture for 2 h at 70 °C. After 2 h, the reaction mixture was treated with Bu_3SnH (20.0 μL, 0.0715 mmol), and then stirred for 10 min. The reaction mixture was then cooled to room temperature, concentrated and subjected to column chromatography [silica, CH_2Cl_2/hexanes (1:1)] to afford a green solid (8.5 mg, 32%): ^{1}H NMR δ –1.58 (br s, 2H), 2.05 (s, 6H), 4.54 (s, 2H), 8.32 (d, *J* = 5 Hz, 1H), 8.85–8.87 (m,

2H), 8.97 (d, J = 4 Hz, 1H), 9.08 (d, J = 4.0 Hz, 1H), 9.53 (s, 1H), 9.54 (s, 1H), 9.69 (s, 1H), 9.76 (s, 1H), 11.25 (s, 1H); ^{13}C NMR δ 31.6, 46.4, 52.7, 94.5, 97.1, 105.6, 110.6, 126.2, 129.9, 131.4, 132.6, 134.7, 137.6, 141.9, 151.5, 155.1, 167.0, 176.6, 188.6; ESI-MS obsd 369.1706, calcd 369.1710 [$(M + H)^+$, M = $C_{23}H_{20}N_4O$]; λ_{abs} 404, 654 nm.

3-Formyl-17,18-dihydro-18,18-dimethylporphyrin (FbC-F^3). Following a procedure for reductive carbonylation,[69] a mixture of **FbC-Br^3** (0.100 g, 0.238 mmol) and $Pd(PPh_3)_4$ (0.275 g, 0.238 mmol) was dried under vacuum for 1 h. The reaction flask was filled with CO gas and anhydrous toluene/DMF [12.0 mL, (1:1)]. CO gas was bubbled through the stirred reaction mixture for 2 h at 70 °C. After 2 h, the reaction mixture was treated with Bu_3SnH (63.7 μL, 0.238 mmol), and then stirred for 10 min. The reaction mixture was then cooled to room temperature, concentrated and subjected to column chromatography [silica, CH_2Cl_2/hexanes (1:1)] to afford a brown solid (38.0 mg, 43%): ^{1}H NMR δ −2.16 (br s, 2H), 2.04 (s, 6H), 4.60 (s, 2H), 8.91 (d, J = 4.0 Hz, 1H), 8.93−8.95 (m, 2H), 9.00 (s, 1H), 9.08 (d, J = 4.0 Hz, 1H), 9.15 (d, J = 4 Hz, 1H), 9.35 (s, 1H), 9.65 (s, 1H), 10.52 (s, 1H), 11.4 (s, 1H); ^{13}C NMR δ 31.6, 46.2, 52.7, 96.9, 98.0, 105.1, 106.9, 126.0, 126.2, 129.3, 133.3, 135.3, 136.4, 137.6, 140.7, 153.2, 155.0, 165.3, 173.7, 188.9; ESI-MS obsd 369.1718, calcd 369.1710 [$(M + H)^+$, M = $C_{23}H_{20}N_4O$]; λ_{abs} 416, 664 nm.

(III) X-ray structural determinations

(A) Data collection and processing. All X-ray measurements were made on a Bruker-Nonius X8 Apex2 CCD system. The frame integration was performed using SAINT+ or SAINT.[82]

(B) Structure solution and refinement. The structures were solved by direct

methods using XS. Additional positions for disordered atoms were found in subsequent difference maps during multiple rounds of refinement. The hydrogen atom positions were placed at idealized positions and were allowed to ride on the parent atom with isotropic displacement parameters of 1.2 or 1.5 times the parent. The calculated structure factors included corrections for polarization, and an absorption correction using SADABS.[83] The structure was refined using the SHELXL program from the SHELX2013[84] package, and graphic plots were produced using OLEX2[85] crystallographic package.

Acknowledgment

This work was supported by a grant from the Chemical Sciences, Geosciences and Biosciences Division, Office of Basic Energy Sciences, of the U. S. Department of Energy (DE-FG02-96ER14632). ^{11}B NMR spectra were collected at the National Institutes of Environmental and Health Sciences in Research Triangle Park with the assistance of Dr. Xiaoyan Sun. Mass spectra were obtained at the Mass Spectrometry Laboratory for Biotechnology at North Carolina State University. Partial funding for the facility was obtained from the North Carolina Biotechnology Center and the National Science Foundation.

Electronic supplementary information (ESI) available: Summary of NMR characterization of selected formyltetrahydrodipyrrins; X-ray data table for four compounds (**1-BBu$_2$**, CCDC 974409; **1-Br^{8}BBu$_2$**, CCDC 974410; **1-Br^{8}F^{7}BBu$_2$**, CCDC 974411; **2-BBu$_2$**, CCDC 974412); display of the enantiomers of compound **1-Br^{8}F^{7}BBu$_2$**; exploratory results for decomplexation of **1-BR$_2$**; characterization data for all new compounds. For ESI and crystallographic data in CIF or other electronic format, see DOI: 10.1039/XX.

References

1 H. Scheer, In *Chlorophylls and Bacteriochlorophylls. Biochemistry, Biophysics, Functions and Applications,* ed. B. Grimm, R. J. Porra, W. Rüdiger and H. Scheer, Springer, Dordrecht, The Netherlands, 2006, pp. 1–26.

2 O. Mass, M. Taniguchi, M. Ptaszek, J. W. Springer, K. M. Faries, J. R. Diers, D. F. Bocian, D. Holten and J. S. Lindsey, *New J. Chem*., 2011, **35**, 76–88.

3 M. Chen, M. Schliep, R. D. Willows, Z.-L. Cai, B. A. Neilan and H. Scheer, *Science*, 2010, **329**, 1318–1319.

4 R. D. Willows, Y. Li, H. Scheer and M. Chen, *Org. Lett.*, 2013, **15**, 1588–1590.

5 J. K. Laha, C. Muthiah, M. Taniguchi, B. E. McDowell, M. Ptaszek and J. S. Lindsey, *J. Org. Chem.*, 2006, **71**, 4092–4102. *Erratum*, *J. Org. Chem.*, 2009, **74**, 5122.

6 H. L. Kee, C. Kirmaier, Q. Tang, J. R. Diers, C. Muthiah, M. Taniguchi, J. K. Laha, M. Ptaszek J. S. Lindsey, D. F. Bocian and D. Holten, *Photochem. Photobiol*., 2007, **83**, 1110–1124.

7 H. L. Kee, C. Kirmaier, Q. Tang, J. R. Diers, C. Muthiah, M. Taniguchi, J. K. Laha, M. Ptaszek, J. S. Lindsey, D. F. Bocian and D. Holten, *Photochem. Photobiol*., 2007, **83**, 1125–1143.

8 J. W. Springer, K. M. Faries, H. L. Kee, J. R. Diers, C. Muthiah, O. Mass, C. Kirmaier, J. S. Lindsey, D. F. Bocian and D. Holten, *Photochem. Photobiol.,* 2012, **88**, 651–674.

9 W. Flitsch, *Adv. Heterocyclic Chem*., 1988, **43**, 73–126.

10 K. M. Smith, In *Chlorophylls*, ed. H. Scheer, CRC Press: Boca Raton, FL, USA, 1991, pp. 115–143.

11 P. H. Hynninen, In *Chlorophylls*, ed. H. Scheer, CRC Press: Boca Raton, FL, USA, 1991, pp. 145–209.

12 F.-P. Montforts, B. Gerlach and F. Höper, *Chem. Rev.*, 1994, **94**, 327–347.

13 F.-P. Montforts and M. Glasenapp-Breiling, *Prog. Heterocyclic Chem.*, 1998, **10**, 1–24.

14 M. G. H. Vicente, In *The Porphyrin Handbook*, ed. K. M. Kadish, K. M. Smith, R.Guilard, Academic Press, San Diego, CA 2000, Vol. 1, pp. 149–199.

15 L. Jaquinod, In *The Porphyrin Handbook*, ed. K. M. Kadish, K. M. Smith and R. Guilard, Academic Press, San Diego, CA 2000, Vol. 1, pp. 201–237.

16 R. K. Pandey and G. Zheng, In *The Porphyrin Handbook*, ed. K. M. Kadish, K. M. Smith and R. Guilard, Academic Press, San Diego, CA 2000, Vol. 6, pp. 157–230.

17 F.-P. Montforts and M. Glasenapp-Breiling, *Fortschr. Chem. Org. Naturst*., 2002, **84**, 1–51.

18 V. Y. Pavlov and G. V. Ponomarev, *Chem. Heterocycl. Compd.*, 2004, **40**, 393–425.

19 T. S. Balaban, H. Tamiaki and A. R. Holzwarth, *Top. Curr. Chem.*, 2005, **258**, 1–38.

20 M. O. Senge, A. Wiehe and C. Ryppa, In *Chlorophylls and Bacteriochlorophylls. Biochemistry, Biophysics, Functions and Applications*, ed. B. Grimm, R. J. Porra, W. Rüdiger and H. Scheer, Springer, Dordrecht, The Netherlands, 2006, pp. 27–37.

21 S. Fox and R. W. Boyle, *Tetrahedron*, 2006, **62**, 10039–10054.

22 M. Galezowski and D. T. Gryko, *Curr. Org. Chem*., 2007, **11**, 1310–1338.

23 A. M. G. Silva and J. A. S. Cavaleiro, In *Progress in Heterocyclic Chemistry*, ed. G. W. Gribble and J. A. Joule, Elsevier, Amsterdam, 2008, Vol. 19, ch. 2, pp. 44–69.

24 M. Taniguchi, D. Ra, G. Mo, T. Balasubramanian and J. S. Lindsey, *J. Org. Chem.*, 2001, **66**, 7342–7354.

25 J.-P. Strachan, D. F. O'Shea, T. Balasubramanian and J. S. Lindsey, *J. Org. Chem.*, 2000, **65**, 3160–3172.

26 H. J. Anderson and S.-F. Lee, *Can. J. Chem*., 1965, **43**, 409–414.

27 O. Mass, M. Ptaszek, M. Taniguchi, J. R. Diers, H. L. Kee, D. F. Bocian, D. Holten, and J. S. Lindsey, *J. Org. Chem*., 2009, **74**, 5276–5289.

28 T. Balasubramanian, J.-P. Strachan, P. D. Boyle and J. S. Lindsey, *J. Org. Chem.*, 2000, **65**, 7919–7929.

29 L. Ghosez, C. Franc, F. Denonne, C. Cuisinier and R. Touillaux, *Can. J. Chem*., 2001, **79**, 1827–1839.

30 T. Fukuda, T. Ohta, E.-I. Sudo and M. Iwao, *Org. Lett*., 2010, **12**, 2734–2737.

31 T. Fukuda and M. Iwao, *Heterocycles*, 2012, **86**, 1261–1273.

32 M. Chen, Y. Li, D. Birch and R. D. Willows, *FEBS Lett.*, 2012, **586**, 3249–3254.

33 Y. Li, N. Scales, R. E. Blankenship, R. D. Willows and M. Chen, *Biochim. Biophys. Acta.*, 2012, **1817**, 1292–1298.

34 Y. Li, Z.-L. Cai and M. Chen, *J. Phys. Chem. B*, 2013, **117**, 11309–11317.

35 S. Ohashi, H. Miyashita, N. Okada, T. Iemura, T. Watanabe and M. Kobayashi, *Photosyn. Res.*, 2008, **98**, 141–149.

36 B. Kraütler, *Angew. Chem. Int. Ed.*, 2011, **50**, 2439–2441.

37 A. M. Wood, *J. Phycol.,* 2012, **48**, 1317–1319.

38 A. W. D. Larkum, M. Chen, Y. Li, M. Schliep, E. Trampe, J. West, A. Salih and M. Kühl, *J. Phycol.,* 2012, **48**, 1320–1327.

39 M. Schliep, G. Cavigliasso, R. G. Quinnell, R. Stranger and A. W. D. Larkum, *Plant Cell Env.*, 2013, **36**, 521–527.

40 M. Chen and R. E. Blankenship, *Trends Plant Sci.*, 2011, **16**, 427–431.

41 M. Chen and H. Scheer *J. Porphyrins Phthalocyanines*, 2013, **17**, 1–15.

42 S.-I. Tamaru, L. Yu, W. J. Youngblood, K. Muthukumaran, M. Taniguchi and J. S. Lindsey, *J. Org. Chem*., 2004, **69**, 765–777.

43 K. Muthukumaran, M. Ptaszek, B. Noll, W. R. Scheidt and J. S. Lindsey, *J. Org. Chem*., 2004, **69**, 5354–5364.

44 J. Bhaumik, Z. Yao, K. E. Borbas, M. Taniguchi and J. S. Lindsey, *J. Org. Chem.*, 2006, **71**, 8807–8817.

45 M. Ptaszek, J. Bhaumik, H.-J. Kim, M. Taniguchi and J. S. Lindsey, *Org. Process Res. Dev.*, 2005, **9**, 651–659.

46 T. S. Balaban, M. Linke-Schaetzel, A. D. Bhise, N. Vanthuyne and C. Roussel, *Eur. J. Org. Chem.*, 2004, 3919–3930.

47 T. S. Balaban, *Acc. Chem. Res.* 2005, **38**, 612–623.

48 T. Jochum, C. M. Reddy, A. Eichhöfer, G. Buth, J. Szmytkowski, H. Kalt, D. Moss and T. S. Balaban, *Proc. Natl. Acad. Sci. U.S.A.*, 2008, **105**, 12736–12741.

49 T. S. Balaban, A. D. Bhise, G. Bringmann, J. Bürck, C. Chappaz-Gillot, A. Eichhöfer, D. Fenske, D. C. G. Götz, M. Knauer, T. Mizoguchi, D. Mössinger, H. Rösner, C.

Roussel, M. Schraut, H. Tamiaki and N. Vanthuyne, *J. Am. Chem. Soc.*, 2009, **131**, 14480–14492.

50 M. Ptaszek, B. E. McDowell, M. Taniguchi, H.-J. Kim and J. S. Lindsey, *Tetrahedron*, 2007, **63**, 3826–3839.

51 M. Krayer, T. Balasubramanian, C. Ruzié, M. Ptaszek, D. L. Cramer, M. Taniguchi and J. S. Lindsey, *J. Porphyrins Phthalocyanines*, 2009, **13**, 1098–1110.

52 H.-J. Kim and J. S. Lindsey, WO 2006089122.

53 H.-J. Kim, D. K. Dogutan, M. Ptaszek and J. S. Lindsey, *Tetrahedron*, 2007, **63**, 37–55.

54 A. H. Jackson, In *Pyrroles. Part One. The Synthesis and the Physical and Chemical Aspects of the Pyrrole Ring*, ed. R. A. Jones, John Wiley & Sons, New York, 1990, pp. 295–303.

55 C. Schmuck and D. Rupprecht, *Synthesis*, 2007, 3095–3110.

56 J. M. Muchowski and D. R. Solas, *Tetrahedron Lett.*, 1983, **24***,* 3455–3456.

57 B. L. Bray, P. H. Mathies, R. Naef, D. R. Solas, T. T. Tidwell, D. R. Artis and J. M. Muchowski, *J. Org. Chem.*, 1990, **55**, 6317–6328.

58 M. Kakushima, P. Hamel, R. Frenette and J. Rokach, *J. Org. Chem.*, 1983, **48**, 3214–3219.

59 R. Settambolo, R. Lazzaroni, T. Messeri, M. Mazzetti and P. Salvadori, *J. Org. Chem.*, 1993, **58**, 7899–7902.

60 C. Zonta, F. Fabris and O. De Lucchi, *Org. Lett.*, 2005, **7**, 1003–1006.

61 K. R. Reddy, J. Jiang, M. Krayer, M. A. Harris, J. W. Springer, E. Yang, J. Jiao, D.

M. Niedzwiedzki, D. Pandithavidana, P. S. Parkes-Loach, C. Kirmaier, P. A. Loach, D. F. Bocian, D. Holten and J. S. Lindsey, *Chem. Sci.*, 2013, **4**, 2036–2053.

62 P. A. Jacobi, S. Lanz, I. Ghosh, S. H. Leung, F. Löwer and D. Pippin, *Org. Lett.*, 2001, **3**, 831–834.

63 K. R. Reddy, E. Lubian, M. P. Pavan, H.-J. Kim, E. Yang, D. Holten and J. S. Lindsey, *New J. Chem.*, 2013, **37***,* 1157–1173.

64 H.-J. Kim and J. S. Lindsey, *J. Org. Chem.*, 2005, **70**, 5475–5486.

65 F. Kakiuchi, M. Yamauchi, N. Chatani and S. Murai, *Chem. Lett.*, 1996, 111–112.

66 M. J. S. Dewar and R. Jones, *J. Am. Chem. Soc.*, 1967, **89**, 2408–2410.

67 B. Wrackmeyer and B. Schwarze, *J. Organomet. Chem.,* 1997, **534**, 207–211.

68 B. Wrackmeyer, *Annu. Rep. NMR Spectrosc.*, 1988, **20**, 61–203.

69 C. Muthiah, D. Lahaye, M. Taniguchi, M. Ptaszek and J. S. Lindsey, *J. Org. Chem*., 2009, **74**, 3237–3247.

70 M. Taniguchi, M. Ptaszek, B. E. McDowell and J. S. Lindsey, *Tetrahedron*, 2007, **63**, 3840–3849.

71 L. Jiao, W. Pang, J. Zhou, Y. Wei, X. Mu, G. Bai and E. Hao, *J. Org. Chem*., 2011, **76**, 9988–9996.

72 G. Duran-Sampedro, A. R. Agarrabeitia, I. Garcia-Moreno, A. Costela, J. Bañuelos, T. Arbeloa, I. Lopez Arbeloa, J. L. Chiara and M. J. Ortiz, *Eur. J. Org. Chem*., 2012, 6335–6350.

73 C. Yu, L. Jiao, H. Yin, J. Zhou, W. Pang, Y. Wu, Z. Wang, G. Yang and E. Hao, *Eur. J. Org. Chem*., 2011, 5460–5468.

74 W. M. Manning and H. H. Strain, *J. Biol. Chem.*, 1943, **151**, 1–19.

75 H. Tamiaki and M. Kunieda, In *Handbook of Porphyrin Science*, ed. K. M. Kadish, K. M. Smith and R. Guilard, World Scientific Co., Singapore, 2011, Vol. 11, ch. 51, pp. 223–290.

76 O. Mass, D. R. Pandithavidana, M. Ptaszek, K. Santiago, J. W. Springer, J. Jiao, Q. Tang, C. Kirmaier, D. F. Bocian, D. Holten and J. S. Lindsey, *New J. Chem.*, 2011, **35**, 2671–2690.

77 C. Muthiah, M. Ptaszek, T. M. Nguyen, K. M. Flack and J. S. Lindsey, *J. Org. Chem*., 2007, **72**, 7736–7749.

78 M. Ptaszek, D. Lahaye, M. Krayer, C. Muthiah and J. S. Lindsey, *J. Org. Chem*., 2010, **75**, 1659–1673.

79 M. Taniguchi, M. N. Kim, D. Ra and J. S. Lindsey, *J. Org. Chem*., 2005, **70**, 275–285.

80 M. Taniguchi, H.-J. Kim, D. Ra, J. K. Schwartz, C. Kirmaier, E. Hindin, J. R. Diers, S. Prathapan, D. F. Bocian, D. Holten and J. S. Lindsey, *J. Org. Chem.*, 2002, **67**, 7329–7342.

81 J. K. Laha, C. Muthiah, M. Taniguchi and J. S. Lindsey, *J. Org. Chem.*, 2006, **71**, 7049–7052.

82 (a) Bruker-Nonius, SAINT+ version 7.07B, 2004, Bruker-Nonius, Madison, WI 53711, USA; (b) Bruker-Nonius, SAINT version 2009.9, 2009, Bruker-Nonius, Madison, WI 53711, USA; (c) Bruker-Nonius, SAINT version 7.78A, 2009, Bruker-

Nonius, Madison, WI 53711, USA; (d) Bruker-Nonius, SAINT version 8.32B, 2013, Bruker-Nonius, Madison, WI 53711, USA.

83 (a) Bruker-Nonius, SADABS version 2.10, 2004, Bruker-Nonius, Madison, WI 53711, USA; (b) Bruker-Nonius, SADABS version 2009.9, 2009, Bruker-Nonius, Madison, WI 53711, USA; (c) Bruker-Nonius, SADABS version 2008/1, 2008, Bruker-Nonius, Madison, WI 53711, USA; (d) Bruker-Nonius, SADABS version 2012/1, 2012, Bruker-Nonius, Madison, WI 53711, USA.

84 G. M. Sheldrick, *Acta Cryst.*, 2008, **A64**, 112–122.

85 O. V. Dolomanov, L. J. Bourhis, R. J. Gildea, J. A. K. Howard and H. Puschmann, *J. Appl. Cryst.*, 2009, **42**, 339–341.

86 M. Liu, M. Ptaszek, O. Mass, D. J. Minkler, R. D. Sommer, J. Bhaumik and J. S. Lindsey, *New J. Chem.*, 2014, **38**, 1717–1730.

CHAPTER 3

Bioconjugatable, PEGylated Hydroporphyrins for Photochemistry and Photomedicine. Narrow-Band, Red-Emitting Chlorins

Preamble. This contents in this chapter have been submitted[67] with contributions from the following individuals. Chih-Yuan Chen: synthesis of **FbC2**, **ZnC2** and corresponding precursors. Amit Kumar Mandal (Holten group, Washington University, St. Louis): photophysical property studies on PEGylated chlorins. Rosemary B. Evans-Storms and J. Bruce Pitner (NIRvana Sciences, Research Triangle Park): flow cytometry study.

Introduction

Photochemistry in the red (600–700 nm) and near infrared (NIR, 700–1400 nm) spectral regions has been less investigated than in the shorter wavelength visible or ultraviolet regions, yet holds powerful attractions. For solar photoconversion, nearly half of the solar photons are at wavelengths >600 nm.[1] For optical imaging in medicine,[2] the deepest penetration in soft tissue occurs in the NIR spectral region wherein light exhibits significantly less scattering than at shorter wavelengths and minimal absorption by natural pigments and the vibrational overtones of water.[3] For flow cytometry and related analytical methods in clinical diagnostics, an objective is to squeeze as many spectrally distinct fluorophores into the ultraviolet–visible–NIR region as possible thereby enabling multiplex analyses (i.e., polychromatic flow cytometry[4-6]). Nonetheless, far fewer chromophores are

available for photochemical studies in the red and NIR spectral regions than at wavelengths of 200–600 nm, and most NIR absorbers that are available have quite broad spectral features.[7,8]

Nature's chosen chromophores for the red and NIR spectral regions are chlorophylls and bacteriochlorophylls, respectively.[9] The fundamental chromophore of a chlorophyll or bacteriochlorophyll is a chlorin or bacteriochlorin, respectively, wherein one or two β,β′-double bonds has been reduced relative to the π-system of a porphyrin (Chart 3.1). Synthetic methodology for preparing such tetrapyrrole macrocycles has advanced enormously over the years, with the ability now in hand to create reasonably diverse macrocycles and tailor the structure of the immediate environment.[10-21] Yet, suitable molecular designs for the aforementioned photochemical applications typically must satisfy multiple criteria. The criteria encompass wavelength tunability, features for bioconjugation, strong absorption, good fluorescence quantum yield (a proxy for a reasonably long-lived singlet excited state), and tailorable polarity for solubility in diverse media.[22] Meeting all such criteria simultaneously often poses design challenges and can stretch the limits of synthetic capabilities. Moreover, many of the applications of red- and NIR-functional chromophores require solubilization in water. In this regard, the development of general strategies for aqueous solubilization of tetrapyrrole macrocycles has remained a stubborn unsolved challenge.

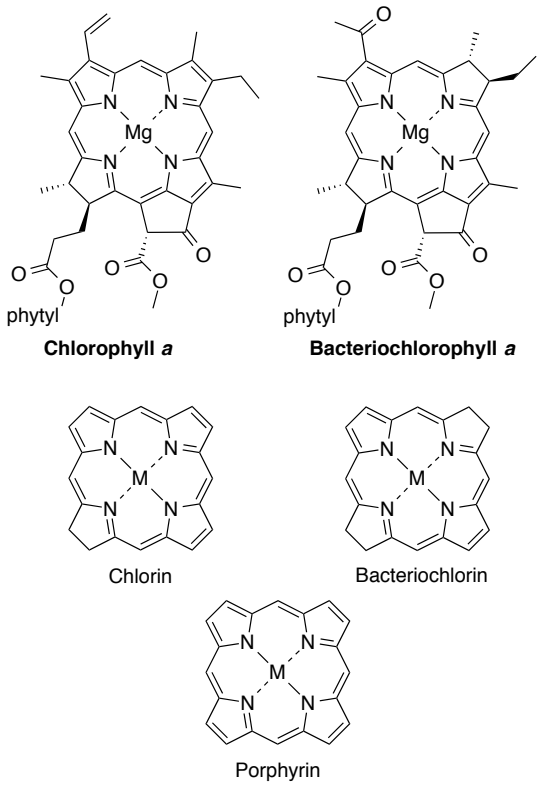

Chart 3.1. Natural pigments and core chromophores.

A classic design for aqueous solubilization of porphyrins relies on appending polar groups at the perimeter of the macrocycle, exemplified by pyridyl and sulfonato porphyrins.[23,24] A more recent example entails similar appendages of oligoethylenoxy (i.e., PEG) groups, which have found extensive application and success across organic chemistry for aqueous solubilization.[25-27] The mere introduction of PEG groups is not necessarily a panacea, however, as illustrated by the tetra(*p*-PEG_{10})phenylporphyrin, T(*p*-PEG_{10})PP (Chart 3.2), which exhibited significant aggregation in water at a concentration as low as 0.1 μM.[28]

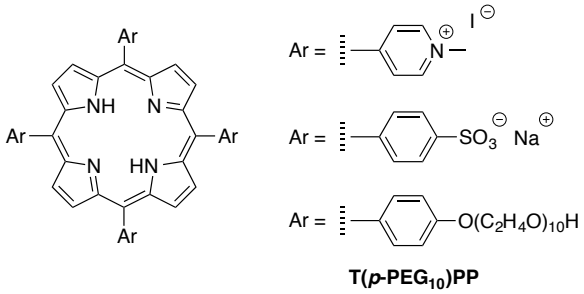

T(*p*-PEG$_{10}$)PP

Chart 3.2. Synthetic porphyrins designed for aqueous solubility.

One strategy implemented to mitigate aggregation has been to place polar groups above and below the plane of the macrocycle, thereby shielding the intrinsically hydrophobic disk-like macrocycle by facial encumbrance. Such groups that have been employed with chlorins[29] contain phosphonates (Chart 3.3), whereas a broader selection of ionic groups have been employed with porphyrins[30-33] and to some extent with bacteriochlorins.[34,35] Because the ionic groups impart solubility in water but not (typically) in non-aqueous solvents, the polar group typically must be installed or unveiled in the last synthetic step, whereupon purification often entails merely washing the product with solvents. Moreover, the preparation of an activated ester (for bioconjugation) in the presence of ionic groups such as phosphates, phosphonates, and carboxylates can result in deleterious cross-reaction.[34] The PEG group is an attractive alternative to these ionic species.[36] The PEG group is nonionic, is commercially available in various lengths[27] (monodisperse or polydisperse) with a single derivatizable handle,[25,27,37,38] and is soluble in water as well as a variety of organic solvents.[36] Accordingly, workup of PEGylated compounds can be achieved by partitioning crude reaction mixtures between an aqueous phase and dichloromethane.

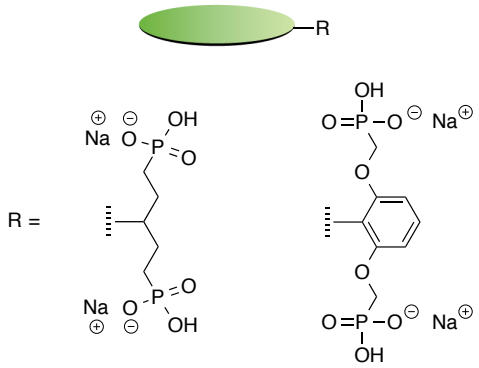

Chart 3.3. Facially encumbering motifs for aqueous solubilization of a chlorin (green disk).

In this paper we report the design and synthesis of a handful of chlorins bearing PEG groups and a bioconjugatable handle. A companion paper reports the development of corresponding bacteriochlorins.[39] Our specific motivations for preparing bioconjugatable, PEGylated (bacterio)chlorins stemmed from a desire to pursue two research areas. One area entails utilization of the PEGylated molecules as light-harvesting constituents in biohybrid antenna complexes via attachment at hydrophilic terminal regions of membrane-spanning photosynthetic peptides.[40] A second research area focuses on the utilization of the PEGylated (bacterio)chlorins as fluorophores in clinical diagnostics, particularly flow cytometry, where antibodies are to be multiply labeled. While diverse porphyrins have been used in bioconjugation studies,[24,41] few PEGylated synthetic chlorins have heretofore been reported,[42-45] and only one was equipped (but not tested) with a bioconjugatable tether.[45] The chlorins described herein have been characterized for solubility in dilute aqueous solution. The photophysical properties, including rate constants and yields for fluorescence emission,

have been measured. One chlorin was attached to an antibody and examined via flow cytometry. Taken together, the advances reported herein broaden the scope of synthetically accessible chromophores for use in the red spectral region, particularly where sharp absorption and emission bands are advantageous.

Results and discussion

(I) Molecular design and synthesis strategy

The *de novo* synthesis of chlorins developed in our laboratory provides the foundation for the creation of stable chlorin macrocycles that contain diverse substituents about the perimeter.[15] Each synthetic chlorin bears a geminal dimethyl group in the reduced, pyrroline ring to block adventitious dehydrogenation (Chart 3.4). Tuning the position of the long-wavelength (Q_y) absorption band can be accomplished chiefly by (1) introduction of auxochromes at positions along the y-axis (i.e., the β-pyrrole positions 2, 3, 12 and 13 in rings A and C), and (2) metalation, and to lesser extent by (3) introduction of auxochromes at positions along the x-axis (i.e., the β-pyrrole positions 7 and 8, and the β-pyrroline position 17) in rings B and D. Given the desire to exploit the β-pyrrole positions for wavelength tuning, a water-solubilization motif and a bioconjugatable tether are ideally installed at positions 5 and 15.

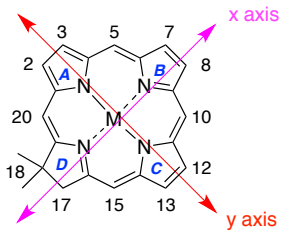

Chart 3.4. Synthetic route to chlorins.

Exploration of a number of designs has led to the synthesis of the target compounds shown in Chart 3.5. The synthesis relies on conversion of an aldehyde (compound **1** series) to a dipyrromethane (**2** series), a 1-acyldipyrromethane (**3** series), and a 1-acyl-9-bromodipyrromethane (**3-Br** series) to give the Eastern half, which is reacted with a tetrahydrodipyrrin Western half (**4** series) to form the chlorin. In the first design, the PEG groups are installed via click chemistry with a PEG-azide following construction of a trialkynyl-substituted chlorin macrocycle. The chlorin is prepared from a 2,4,6-tris(propargyloxy)phenyl-substituted Eastern half and an unsubstituted Western half. The resulting zinc chlorin **ZnC1** and free base chlorin **FbC1** were examined for water solubility but lack a bioconjugatable tether. Click chemistry has found growing use in tetrapyrrole chemistry but only occasionally applied with chlorins.[46] In the second design, the PEG groups and a bioconjugatable tether were pre-installed in the Eastern half to give chlorins **ZnC2** and **FbC2**. The first two designs rely on a 2,6-disubstituted meso-aryl group to impart facial encumbrance and achieve water solubility. In the third design, a 3,13-diacetylchlorin bearing a bioconjugatable group was converted to the corresponding chalcone thereby affording chlorins **ZnC3** and **FbC3**. This third design lacks the facial encumbrance of the first two designs but, as in the first design, is attractive in the installation of the PEG groups

in the final step of the synthesis. As part of this work, a number of other designs were investigated and abandoned owing to synthetic limitations (see Supplimentary information).

(1) PEG Post-Installation (chlorin-triazole by click reaction)

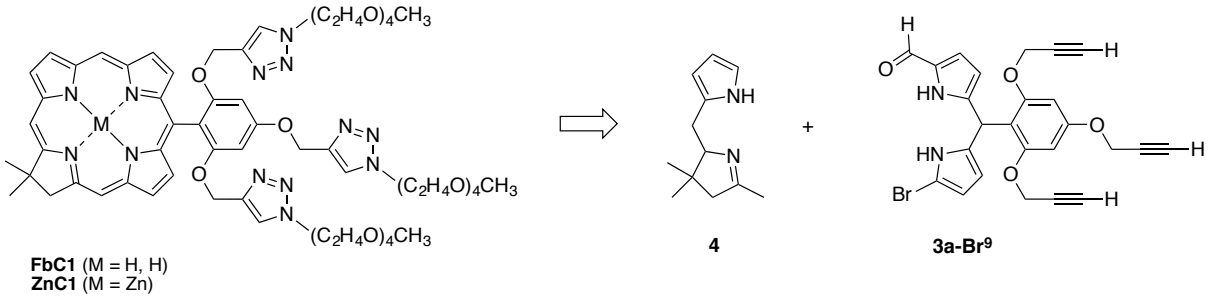

(2) PEG Pre-Installation

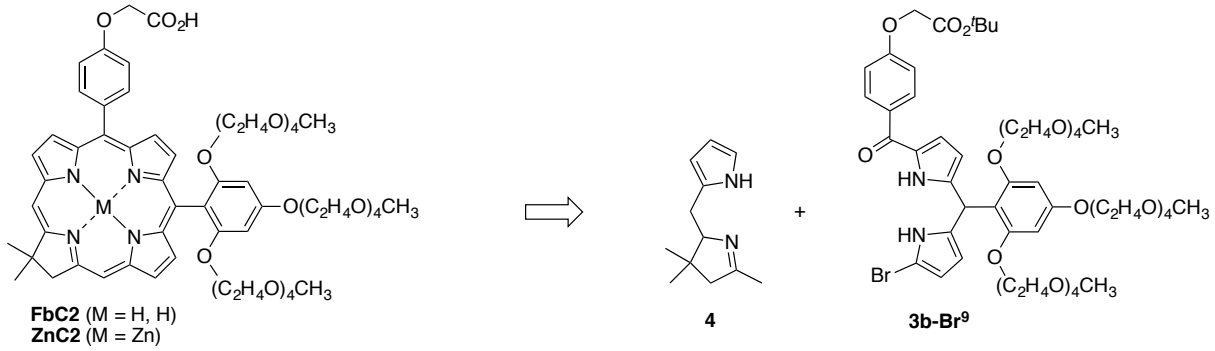

(3) PEG Post-Installation (chlorin-chalcone by aldol condensation)

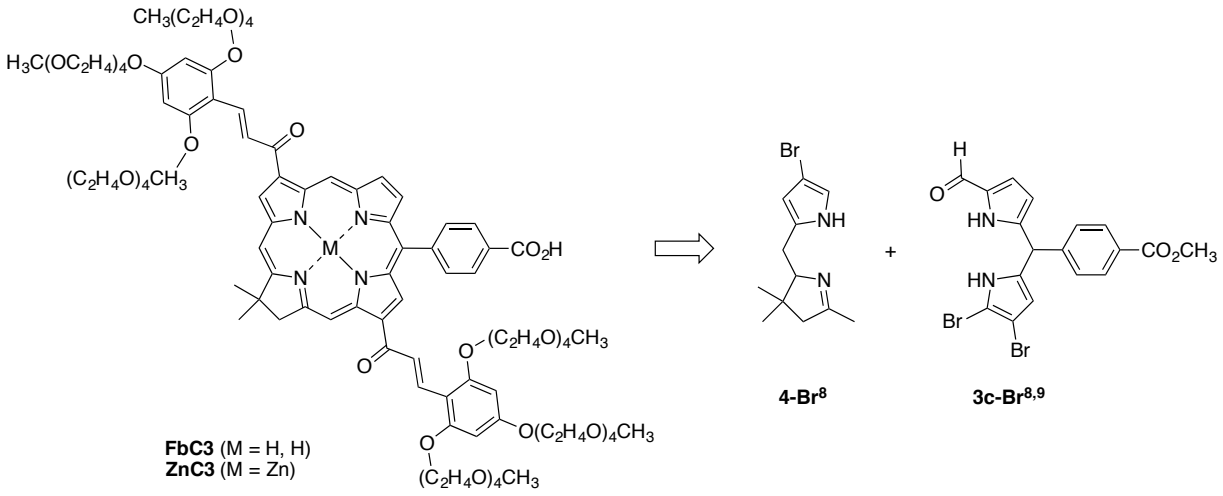

Chart 3.5. Molecular design and key precursors of synthetic chlorins.

(II) Synthesis

(A) Dipyrromethanes. The synthesis of an Eastern half begins with an aldehyde and pyrrole. Two aldehydes (**1a** and **1b**) required herein have been made from 2,4,6-trihydroxybenzaldehyde (phloroglucinol carboxaldehyde), whereas the other aldehyde **1c**[47] is a known compound. The reaction of 2,4,6-trihydroxybenzaldehyde and propargyl bromide in the presence of K_2CO_3 at 80 °C afforded 2,4,6-tris(propargyloxy)benzaldehyde **1a** in 87% yield without chromatographic purification (Scheme 3.1). The *O*-alkylation of 2,4,6-trihydroxybenzaldehyde with 1-bromo-3,6,9,12-tetraoxatridecane [$CH_3(OC_2H_4)_4Br$] in the presence of K_2CO_3 for 1.5 h[33] gave PEGylated benzaldehyde **1b** in a yield of 36%. Partially PEGylated product **1b′** was also isolated in 20% yield.

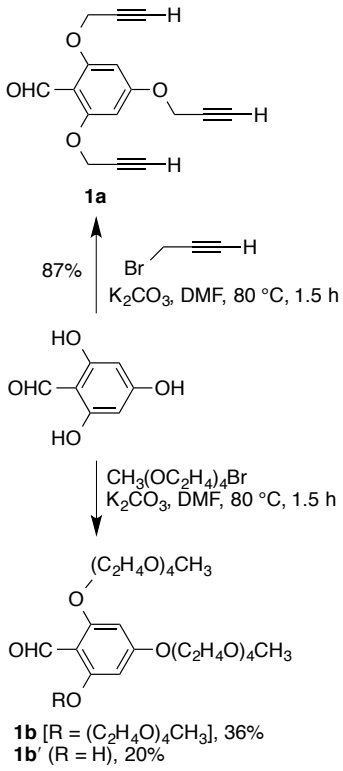

Scheme 3.1. Synthesis of aldehydes.

Dipyrromethanes were readily synthesized in a solventless process from the corresponding aldehyde in a solution of excess pyrrole containing $InCl_3$ or TFA as catalyst[47] (Scheme 3.2). Thus, reaction of aldehyde **1a** or **1b** with pyrrole in the presence of $InCl_3$ gave dipyrromethane **2a** or **2b** in 52% or 74%, respectively. Alternatively, a streamlined route to dipyrromethane **2b** entailed the following: (a) the *O*-alkylation of 2,4,6-trihydroxybenzaldehyde was prolonged to 16 h; (2) the crude product **1b** (containing a trace amount of **1b′**) was directly used in condensation with pyrrole and ~1 equiv of $InCl_3$; and (3) flash chromatography afforded dipyrromethane **2b** in a total yield of 54% (Scheme 3.1). Dipyrromethane **2c**[47] was synthesized as described in the literature.

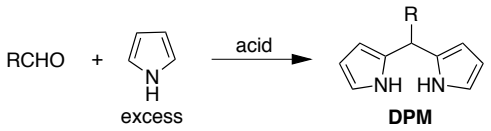

RCHO	R	acid yield	DPM
1a	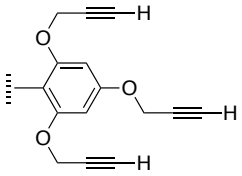	$InCl_3$ 52% (here)	**2a**
1b	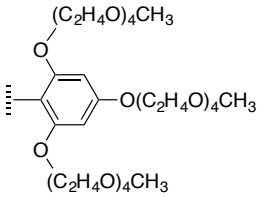	$InCl_3$ 74% (here)	**2b**
1c	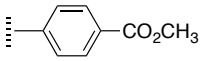	$InCl_3$ 75% (ref 150)	**2c**

Scheme 3.2. Synthesis of dipyrromethanes from the corresponding aldehydes.

(B) Chlorins. (1) Design I – Chlorins without a bioconjugatable tether. Design I relies on a tris(propargyloxy)phenyl motif at the chlorin 10-position, whereupon click chemistry can be employed with the three alkynes and the PEG-azide $CH_3(OC_2H_4)_6N_3$ (**PEG_6-N_3**). The synthesis of the Eastern half proceeded by Vilsmeier formylation[48] of **2a** with $POCl_3$/DMF, which afforded 1-formyldipyrromethane **3a** as the major product in 51% yield along with 1,9-diformylated byproduct **3a′** (not shown) in 20% yield (Scheme 3.3). Bromination of **3a** with 1 equiv of NBS at –78 °C afforded **3a-Br**[9] in 68% yield. Because **3a-Br**[9] decomposed quickly at room temperature, the chlorin synthesis was initiated

immediately. The chlorin-forming reaction[49] of **3a-Br**[9] and Western half **4**[50] entailed acid-catalyzed condensation (*p*-TsOH·H_2O in MeOH/CH_2Cl_2 under argon for 30 min) followed by zinc (II)-mediated oxidative cyclization [$Zn(OAc)_2$, 2,2,6,6-tetramethylpiperdine (TMPi), and AgOTf in CH_3CN at reflux exposed to air for 22 h]. In this manner, trispropargyl zinc chlorin **pro-ZnC1** was obtained in 15% yield.

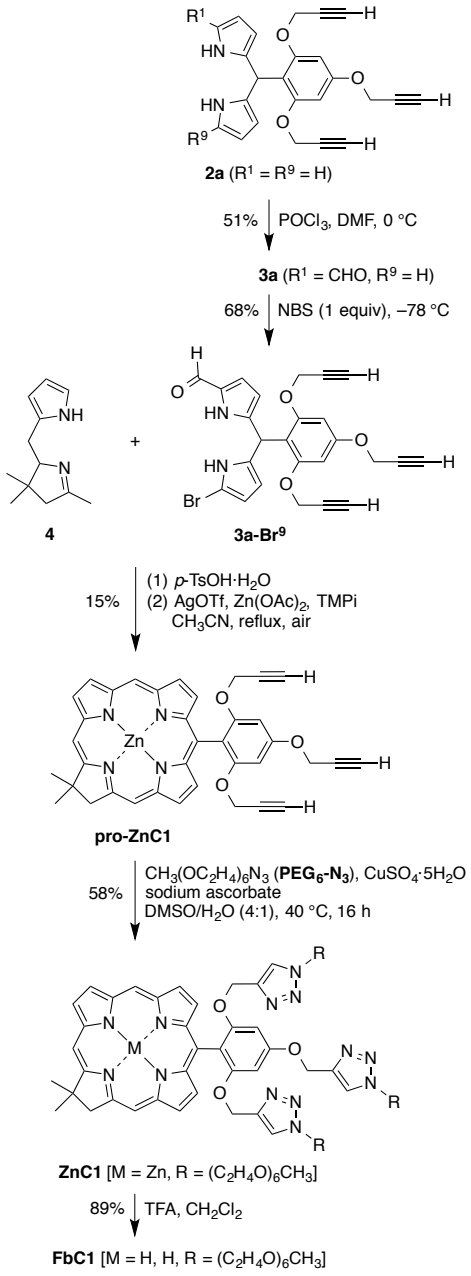

Scheme 3.3. Synthesis of PEGylated chlorins **FbC1** and **ZnC1** via click chemistry.

The click reaction of **pro-ZnC1** with **PEG_6-N_3** was examined under several conditions concerning the solvent and amount of copper (see Table 3.3). Ultimately,

treatment of **pro-ZnC1** and **PEG_6-N_3** in DMSO with a stoichiometric amount of Cu(I) catalyst (freshly prepared from $CuSO_4 \cdot 5H_2O$ and sodium ascorbate) in H_2O at 40 °C gave the zinc triazole-PEG-chlorin **ZnC1** in 58% yield. Demetalation with TFA gave the corresponding free base chlorin **FbC1** in 89% yield (Scheme 3.3). Performing the click reaction with the zinc rather than the free base chlorin was essential to avoid undesired copper insertion, given that (1) copper(II) chlorins are unsuitable for many photochemical applications due to the short excited–state lifetime,[51] and (2) demetalation of a copper chlorin requires strong acid and often proceeds in low yield.[52] Still, a zinc chlorin can potentially transmetalate with copper. Two tests proved the absence of any copper chlorin in the target chlorins: (1) upon demetalation of zinc chlorin **ZnC1** with TFA, the expected bathochromic shift of the Q_y band was observed for the neutralized sample; and (2) no copper chlorin peak was observed upon MALDI-MS analysis.

PEGylated chlorins **FbC1** and **ZnC1** were examined by UV-Vis spectroscopy in water and exhibited good water solubility (see Supplimentary information). Successful installation of the PEG moiety by click reaction and resulting water solubility prompted examination of routes to analogous chlorins equipped with a bioconjugatable tether. Several synthetic problems were encountered, however, that limited the viability of this approach (see Supplimentary information).

(2) Design II – Chlorins with a bioconjugatable tether at the 5-position. Incorporation of the bioconjugatable tether at the 5-position of chlorin can be achieved via acylation of the corresponding dipyrromethane.[49,53] The acylation reagent was prepared by selective alkylation of 4-hydroxybenzoic acid. Thus, 4-hydroxybenzoic acid was treated with

n-Bu_4POH in THF at 0 °C under argon, followed by the addition of *tert*-butyl bromoacetate[54] to form the phenolic ether **5** in 87% yield (Scheme 3.4). Benzoic acid **5** was prepared previously via a 3-step procedure.[55] Reaction of **5** with oxalyl chloride under argon in anhydrous CH_2Cl_2 afforded the acid chloride, which was treated with 2-mercaptopyridine in anhydrous THF to give pyridyl thioester **6** in 45% yield. Alternatively, streamlined procedures beginning with 4-hydroxybenzoic acid and use of recrystallization in lieu of chromatography afforded **6** in 32% yield.

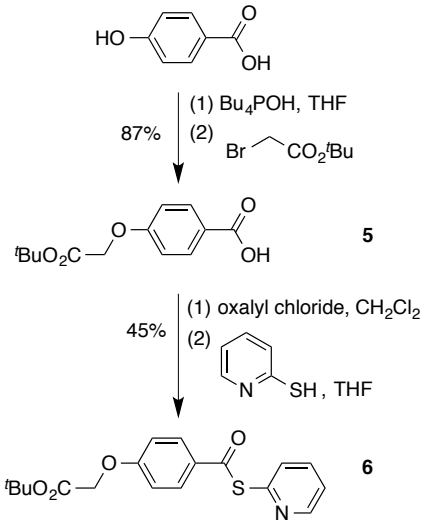

Scheme 3.4. Synthesis of Mukaiyama acylation reagent.

Treatment of PEGylated dipyrromethane **2b** with **6** afforded acyldipyrromethane **3b** in 41% yield (Scheme 3.5). Bromination[56] of acyldipyrromethane **3b** with 1 equivalent of NBS at –78 °C followed by reduction with $NaBH_4$ in THF/MeOH at room temperature afforded the 9-bromodipyrromethane-1-carbinol. Condensation of the latter with Western

half **4** in the presence of TFA followed by zinc-mediated oxidative cyclization gave zinc chlorin **pro-ZnC2** in 11% yield. Treatment of **pro-ZnC2** with 20% TFA in CH_2Cl_2 to hydrolyze the *tert*-butyl ester afforded PEGylated free base chlorin **FbC2**. Subsequently, **FbC2** was treated with $Zn(OAc)_2$ in CH_2Cl_2 to give zinc chlorin **ZnC2** in 95% yield. Chlorins **FbC2** and **ZnC2** constitute water-soluble, bioconjugatable, spectrally distinct chromophores with absorption and emission in the red spectral region. Examination of **pro-ZnC2** by ^{1}H NMR spectroscopy validated the geometric design, showing the projection of the 2,6-substituted PEG groups in the vicinity of the π-electron cloud of the chlorin macrocycle, but the 4-substituted PEG group not in the ring current (see Supplimentary information). Attempts to extend this synthetic approach to a broader palette of chlorins, which required incorporation of auxochromes in rings A and C, were not successful (see Supplimentary information); hence, we turned to an alternative design.

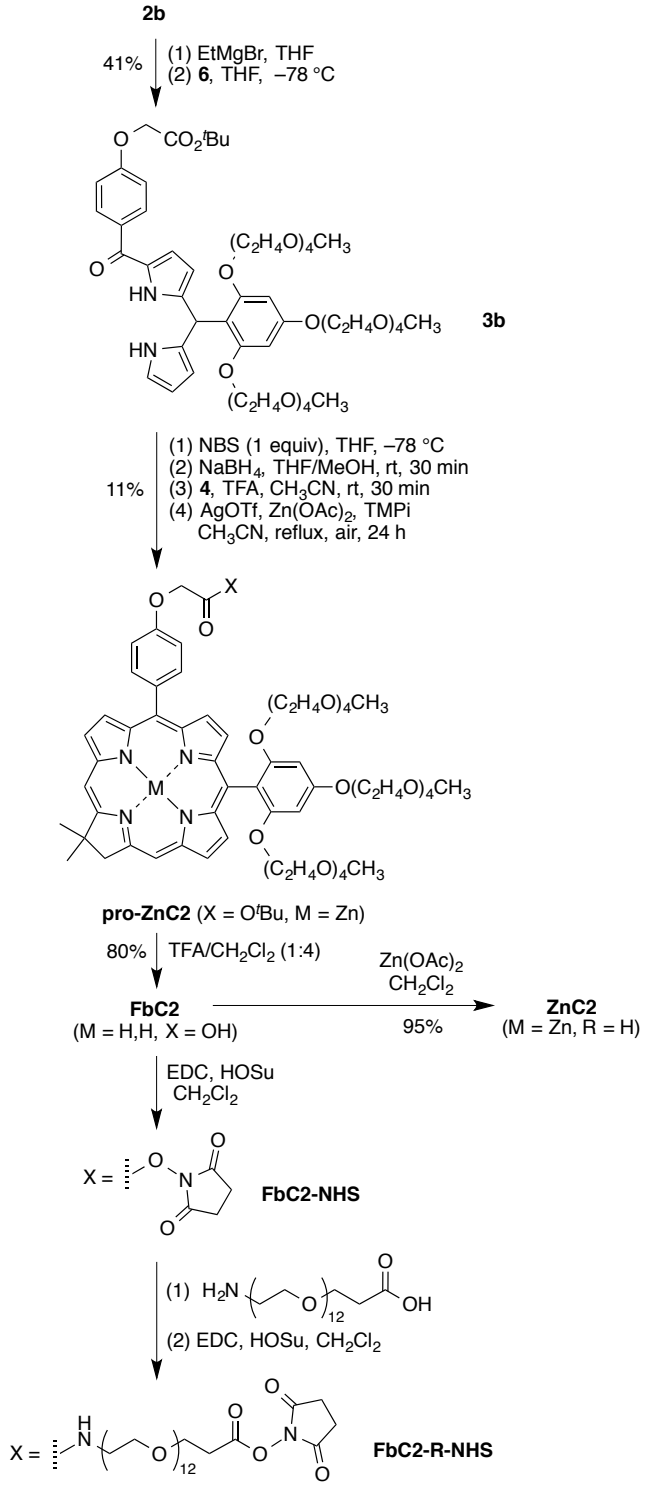

Scheme 3.5. Synthesis of PEGylated, bioconjugatable chlorins.

Chlorin **FbC2** was converted to the *N*-hydroxysuccinimide (NHS) active ester by reaction with EDC as shown in Scheme 3.5. The resulting active ester **FbC2-NHS** could be used for protein derivatization, but also was amidated with a longer PEG-azide followed by NHS activation with EDC to give chlorin **FbC2-R-NHS**, which contains 24 PEG (i.e., –OCH_2CH_2O–) units. The two chlorin NHS esters were prepared for use in flow cytometry studies (*vide infra*). As is customary in bioconjugate chemistry, the active esters were not purified to homogeneity given that the chlorin–protein conjugate can be readily freed of unbound chlorin prior to use in biological applications. The chlorin NHS esters were characterized by absorption ^{1}H NMR spectroscopy and MALDI mass spectrometry and were estimated to be ~80% pure.

(3) Design III – Chlorins with a bioconjugatable tether at the 10-position. Chlorins with chalcones at the 3,13-positions are known to have a bathochromically shifted Q_y band, but this design had not previously been adapted for water solubility and bioconjugation. While the PEGylated porphyrin shown in Chart 3.1 had very poor water solubility, we sought to examine whether the presence of multiple PEG groups on each arene as well as the nonplanar configuration of the chlorin–chalcone architecture would impart aqueous solubility. Thus, vicinal dibromination of known 1-formyldipyrromethane **3c** gave Eastern half **3c-Br**[8,9] (structure not shown),[18] which was used directly without further purification (Scheme 3.6). Condensation of **3c-Br**[8,9] with bromo-Western half[57] **4-Br**[8] gave 3,13-dibromochlorin **pro-FbC3-Br**[3,13] in 10% yield from **3c**. Stille coupling[58] with tributyl(1-ethoxyvinyl)tin and a catalytic amount of $(Ph_3P)_2PdCl_2$ in CH_3CN/DMF (3:2) followed by acidic hydrolysis gave 3,13-diacetylchlorin **pro-FbC3-A**[3,13] in 90% yield. The

aldol condensation[59] of **pro-FbC3-A**[3,13] with excess aldehyde **1b** in ethanolic NaOH under microwave (MW) irradiation afforded chlorin–chalcone **FbC3**. Metalation of **FbC3** with $Zn(OAc)_2$ in $CHCl_3/CH_3OH$ gave **ZnC3** in 84% yield. This chlorin–chalcone strategy provides a concise and efficient route, particularly given the ease of purification afforded by installation of the PEG moieties in the last step of the process.

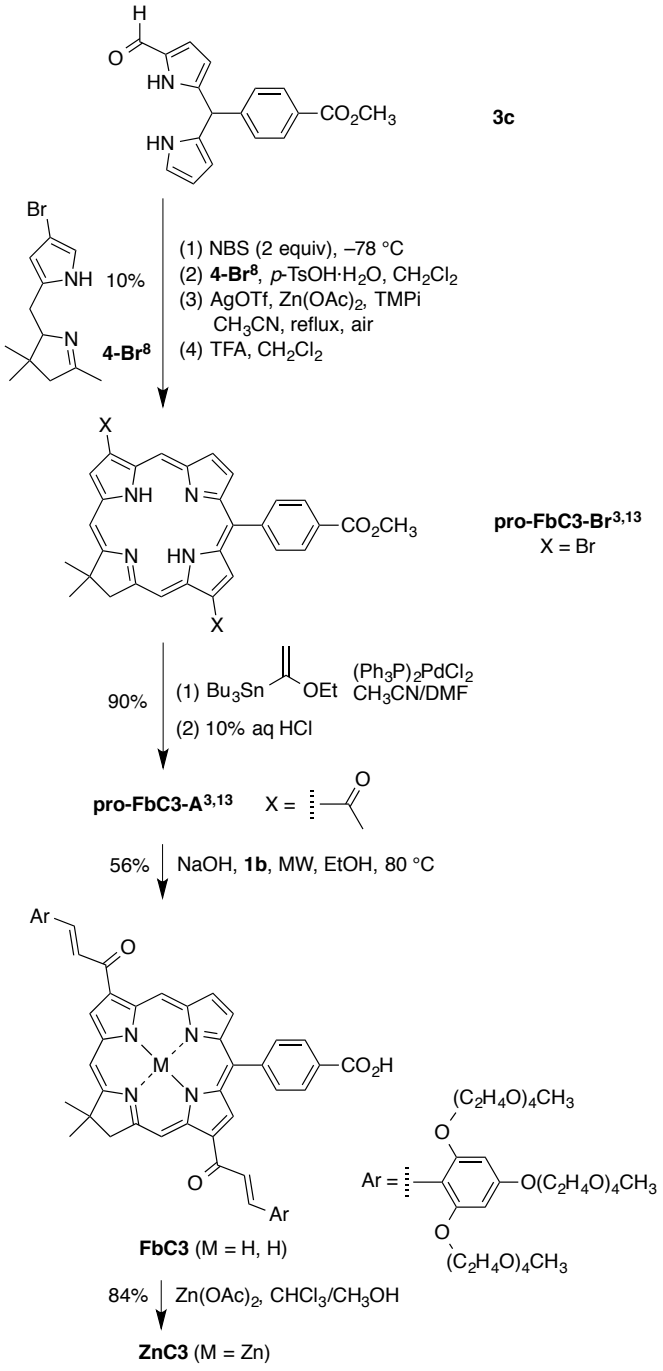

Scheme 3.6. Synthesis of PEGylated chlorins **ZnC3** and **FbC3**.

(4) Handling of PEGylated compounds. The PEG groups are distinct from many other groups used to impart water solubility in two regards: (1) PEG groups are non-ionic, and (2) PEGylated compounds can be partitioned preferentially into organic solvents from an aqueous medium.[36] Thus, the PEGylated chlorins were quite soluble in CH_2Cl_2 or ethyl acetate, and could be extracted from aqueous solution to CH_2Cl_2 or ethyl acetate without significant loss. The purification of PEGylated compounds entailed gradient elution chromatography. For some of the PEGylated tetrapyrrole macrocycles, the improved purification involved a sequence of three chromatography procedures:[60] (1) removal of common impurities by silica chromatography; (2) separation of PEG-containing impurities by gravity-flow size-exclusion chromatography (SEC); and (3) final silica chromatography to remove residual impurities (see the Supplimentary information).

(III) Photophysical characterization

(A) Static spectral properties. Figure 3.1A shows the absorption spectra of chlorins **ZnC2**, **FbC2**, **ZnC3**, and **FbC3** in DMF at room temperature normalized to the B band maximum (416–455 nm). Figure 3.1B focuses on the NIR region with spectra normalized to the characteristic sharp Q_y band (610–687 nm). The corresponding fluorescence emission bands are in the range 613–692 nm.

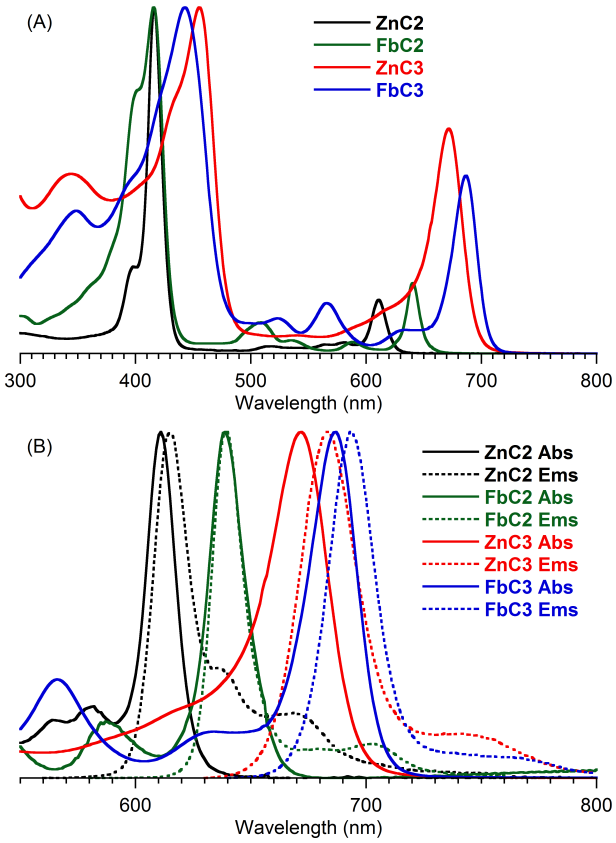

Figure 3.1. (A) Absorption spectra of PEGylated chlorins in DMF; (B) normalized Q_y absorption and emission spectra of chlorins in DMF.

The absorption and fluorescence spectra of the same four chlorins in DMF are shown in Figure 3.2A along with those for **FbC1** and **FbC1**. The spectra of all six chlorins in water are shown in Figure 3.2B. The absorption spectra in Figure 3.2 are normalized to the total (300–900 nm) absorption intensity obtained upon integration of the spectra plotted against wavenumbers (cm^{-1}). This approach is useful for comparing relative peak-intensity changes for related tetrapyrroles, and overcomes some of the drawbacks with other normalization methods or using (uncertain) extinction coefficients.[61] Each absorption spectrum contains

three main features: the strong near-ultraviolet (NUV) Soret bands (B_x and B_y, 410–445 nm), a very weak green-orange Q_x band (520–560 nm) and a red or NIR Q_y band (609–706 nm). The Soret and Q_y band positions are listed in Table 3.1. Several general spectral characteristics are as follows: (1) The NUV B_y and B_x bands overlap completely with each other for the zinc chlorins but only partially overlap for the free base chlorins. (2) The weak Q_x bands of free base chlorins are further weakened in the case of zinc chlorins. (3) The Q_y bands for the two chlorin–chalcones (**ZnC3** and **FbC3**) are moderately strong whereas the Q_y bands for the other four chlorins (**ZnC1**, **FbC1**, **ZnC2** and **FbC2**) are relatively weak. (4) All the origin bands are typically accompanied by one weaker vibronic satellite band to higher energy by roughly 1000 cm^{-1}.

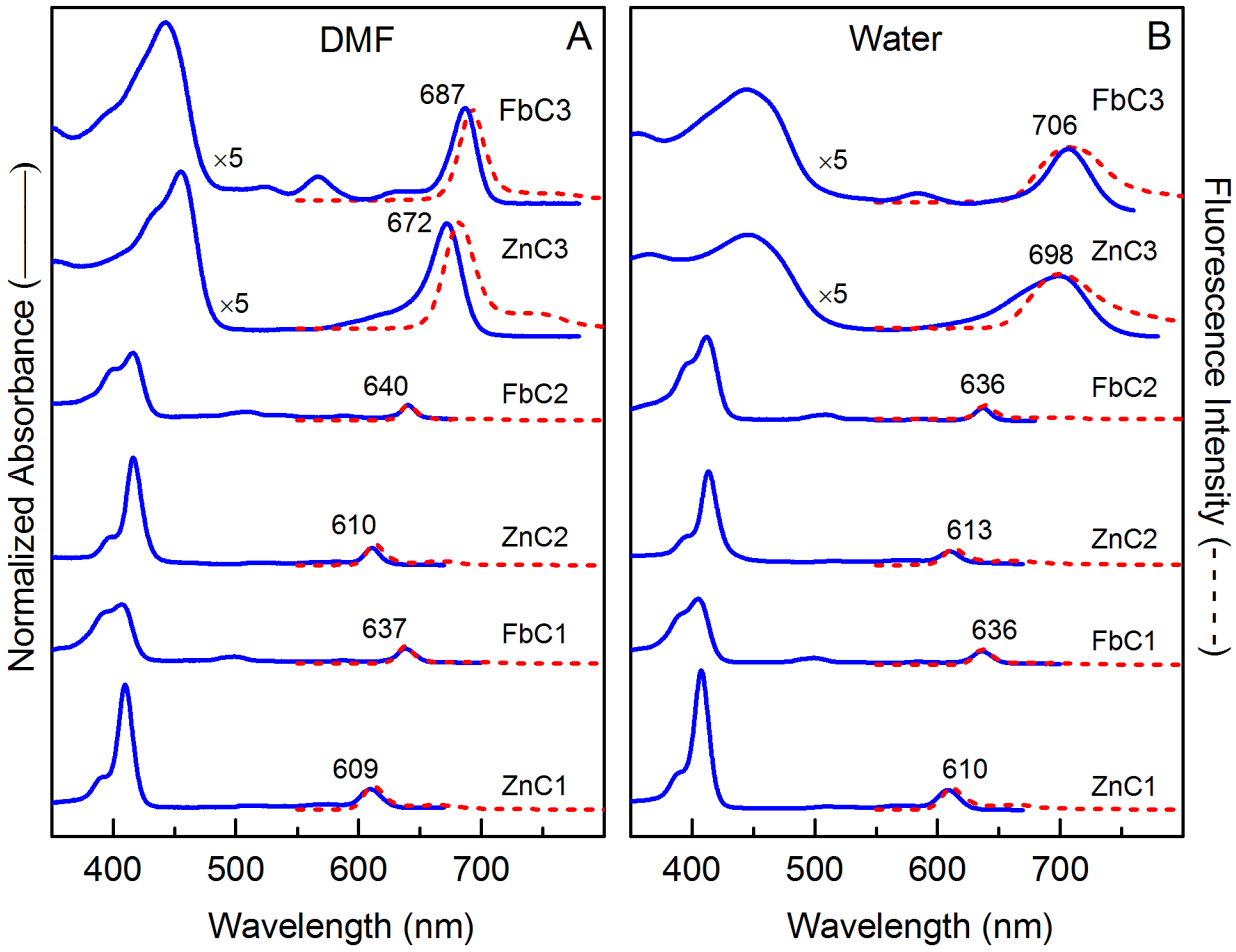

Figure 3.2. Absorption (blue solid) and fluorescence (red dashed) spectra of PEGylated chlorins in (A) DMF and (B) water. The emission intensities are normalized to the Q_y absorption for ease of presentation.

For chlorins, **ZnC1**, **FbC1**, **ZnC2** and **FbC2**, the Q_y absorption bands have a full-width-at-half-maximum (FWHM) in the range 12–18 nm (14 nm average) in DMF and 14–19 nm (17 nm average) in water (Table 3.1). The greater FWHM in water versus DMF is paralleled by a decrease in Q_y-band peak intensity (relative to the Soret maximum) in water versus DMF. The compensating effects of bandwidth with peak height indicate that the

integrated intensity (oscillator strength) of the Q_y band generally does not change appreciably with solvent. For the two chlorin–chalcones (**ZnC3** and **FbC3**), the peak intensity of Q_y band (relative to the Soret maximum) is much higher than that of other four chlorins and the FWHM again increases in water versus DMF.

Table 3.1. Spectral properties of PEGylated chlorins in DMF and in water.

Chlorin	Solvent[a]	B_{max} abs (nm)	Q_y abs (nm)	Q_y abs fwhm	I_{Qy}/I_{By}	$\sum Q_y/\sum B_y$	Q_y em (nm)	Q_y em fwhm
ZnC1	DMF	410	609	18	0.16	0.20	612	20
	water	408	610	19	0.14	0.15	611	22
FbC1	DMF	406	637	15	0.25	0.12	639	16
	water	404	636	17	0.20	0.12	637	18
ZnC2	DMF	416	610	14	0.15	0.16	613	17
	water	414	613	16	0.15	0.15	614	24
FbC2	DMF	416	640	12	0.25	0.15	640	15
	water	412	636	14	0.14	0.06	638	17
ZnC3	DMF	455	672	28	0.68	0.38	682	30
	water	445	698	71	0.57	0.38	700	60
FbC3	DMF	443	687	25	0.52	0.19	692	26
	water	445	706	42	0.52	0.22	710	58

[a]The samples in water contained 5% DMF as a cosolvent.

The spectra in Figure 3.2 and Q_y band data in Table 3.1 reveal that the addition of a bioconjugatable tether at 5-position in chlorins **ZnC2** and **FbC2** gives a small (~2 nm) bathochromic shift in the Q_y bands with respect to **ZnC1** and **FbC1** in DMF. A small diminution of intensity of the Q_y band is also observed in the case of **FbC1** with respect to that of **FbC2** in water for incorporation of the bioconjugatable tether at the 5-position (Table

3.1). For chlorin–chalcone **FbC3**, the Q_y band shows a ~15 nm bathochromic shift with respect to the corresponding zinc chlorin **ZnC3**.

The fluorescence spectra of all PEGylated chlorins are dominated by the $Q_y(0,0)$ emission band, with a weaker (0,1) band to longer wavelength (Figure 3.2A and 3.2B). For chlorins **ZnC1**, **FbC1**, **ZnC2** and **FbC2**, the fluorescence maximum shifts within 3 nm from the $Q_y(0,0)$ absorption maximum in both DMF and water, indicating a very small Stokes shift. On the other hand, in DMF the Stokes shift for chlorin–chalcones **ZnC3** and **FbC3** are 5 nm and 10 nm, respectively. In water, the shift is smaller, 2 nm for **ZnC3** or 4 nm for **FbC3.** For chlorins **ZnC1**, **FbC1** and **FbC2**, the solvent effect causes a hypsochromic shift of 1–2 nm in the Q_y fluorescence maximum in water versus DMF. Contrarily, the Q_y fluorescence maximum shifts bathochromically for **ZnC2** (1 nm), **ZnC3** (18 nm) and **FbC3** (8 nm).

(B) Excited-state properties. The measured photophysical properties of the chlorins are the lifetime (τ_S) of the lowest singlet excited state (S_1, Q_y), the fluorescence quantum yield (Φ_f), i.e. the yield of S_1 to S_0, and the triplet yield (Φ_{isc}), i.e. the yield of S_1 to T_1 intersystem crossing. The yield of S_1 to S_0 internal conversion is obtained by the difference: $\Phi_{ic} = 1 - \Phi_f - \Phi_{isc}$. The fluorescence ($k_f$), internal conversion ($k_{ic}$), and intersystem crossing (k_{isc}) decay rate constants of the lowest singlet excited state are related via the expressions $\tau_S = (k_f + k_{ic} + k_{isc})^{-1}$ and $\Phi_x = k_x \cdot \tau_S$, where x = f, isc or ic. Thus, all three excited-state rate constants can be calculated from the lifetime and yields (Table 3.2).

The Φ_f values range from 0.013 to 0.080 and the τ_S values range from 1.8 ns to 2.1 ns for the zinc chlorins **ZnC1** and **ZnC2** (Table 3.2) in both DMF and water. For the

corresponding free base analogues, the Φ_f values are higher (0.14–0.25) and the τ_S values are much longer (8.2–10.2 ns). For the chlorin–chalcones, **ZnC3** and **FbC3**, the Φ_f values are relatively higher (0.34 and 0.33, respectively) than for the other chlorins in DMF (Table 3.2).

Table 3.2. Photophysical properties of PEGylated chlorins in DMF and water.[a]

Chlorin	Solvent[b]	Q_y em (nm)	τ_S (ns)	Φ_f	Φ_{isc}	Φ_{ic}	k_f^{-1} (ns)	k_{isc}^{-1} (ns)	k_{ic}^{-1} (ns)
ZnC1	DMF	612	2.0	0.066	0.92	0.01	30	2	143
	water	611	1.8	0.030	0.88	0.09	61	2	20
FbC1	DMF	639	8.4	0.200	0.73	0.07	42	11	119
	water	637	8.2	0.140	0.76	0.10	58	11	82
ZnC2	DMF	613	2.1	0.080	0.91	0.01	26	2	207
	water	614	1.8	0.013	0.93	0.06	138	2	31
FbC2	DMF	640	10.2	0.250	0.63	0.12	41	16	85
	water	638	9.7	0.170	0.68	0.15	57	14	65
ZnC3	DMF	682	5.1	0.340	0.48	0.18	15	11	28
	water	700	*c*	*c*	*c*	*c*	*c*	*c*	*c*
FbC3	DMF	692	6.0	0.330	0.43	0.24	18	14	25
	water	710	*c*	*c*	*c*	*c*	*c*	*c*	*c*

[a]The typical errors (percent of value) of the photophysical properties are as follows: τ_S (±7%), Φ_f (±5%), Φ_{isc} (±15%), Φ_{ic} (±20%), k_f (±10%), k_{isc} (±20%), k_{ic} (±25%). The error bars for τ_S, Φ_f, and Φ_{isc} were determined from select repeat measurements, and those for the Φ_{ic}, k_f, k_{isc} and k_{ic} were obtained from propagation of errors. [b]The samples in water contained 5% DMF as a cosolvent. [c]Not examined due to low solubility.

Some important characteristic features gleaned from Table 3.2 are as follows: (1) The Φ_f values of the free base chlorins (**FbC1**, **FbC2**) are greater than the zinc chlorins (**ZnC1**, **ZnC2**), and are similar for the two chlorin–chalcones (**FbC3**, **ZnC3**). (2) The τ_s values of the zinc chlorins are much shorter than the free base chlorins. These changes can be traced

largely to greater k_{isc} values for the zinc chelates relative to the free base forms, as expected due to more facile intersystem crossing associated with the heavy-atom effect on spin-orbit coupling in the metallochlorins (Table 3.2). Metalation only increases k_{isc} modestly for chlorin–chalcone **ZnC3** metalation relative to **FbC3**. The k_{ic}^{-1} values decrease (k_{ic} increases) for chlorins **ZnC1**, **FbC1**, **ZnC2** and **FbC2** in water versus DMF. As noted above, the low solubility of the two chlorin–chalcones (**ZnC3** and **FbC3**) precludes the photophysical studies in water. In each case, the calculated radiative rate constant (k_f) in water is reduced considerably from the values in DMF. Similarly, the intensity of the Q_y band relative to Soret is either reduced or similar in water versus DMF (Table 3.1). The effects are in the same direction and in good agreement considering experimental error. The connection between these two observables is the direct proportionality of the Einstein coefficients for absorption and spontaneous emission. This connection explains the slight diminution in relative Q_y absorption intensity (Table 3.1) and the moderate decrease of Φ_f (Table 3.2) in water compared to DMF. Some small change in radiative probability for the compounds in the two media is expected due to the difference in refractive indices. However, other effects may also come into play, including the influence of the media on the relative energies of the frontier molecular orbitals of the complexes. The latter issue has not been explored in detail for tetrapyrroles.

(C) Effect of concentration on spectral properties. Absorption *versus* concentration studies were conducted to assess the aqueous solution properties of the PEGylated chlorins over a 1000-fold range of concentration (~450 μM to ~0.45 μM). The methodology for this type of study has been previously reported in detail;[62] the same

approach was utilized herein. The spectral properties of the PEGylated chlorins **ZnC2** and **FbC2** in neat deionized water are shown in Figure 3.3; data for **ZnC1** and **FbC1** are shown in Supplimentary information. **ZnC2** exhibits almost unchanged spectral properties over a concentration range of 1000-fold, indicating exceptionally high solubility of this chlorin in water. On the other hand, **FbC2** exhibits changes in the shape of the B bands at higher concentrations (45 μM) indicating some degree of aggregation. The absorption spectra of chlorin–chalcones, **ZnC3** and **FbC3** exhibit clear broadening in neat water (see Supplimentary information) at ~5 μM, which indicates limited water solubility of these compounds.

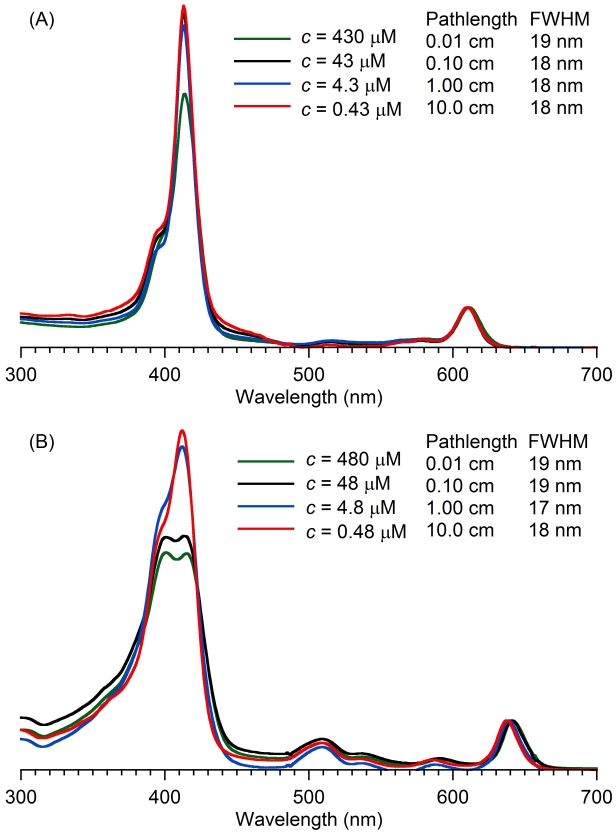

Figure 3.3. Absorption versus concentration of **ZnC2** and **FbC2** over a 1000-fold range. The spectra are normalized at the Q_y band; the path length of the sample cell and FWHM of the Q_y band are also listed in the inset. The concentrations are based on the absorbance of the ~5 μM solution measured at the B band (assuming[51] ε = 160,000 $M^{-1}cm^{-1}$).

(IV) Flow cytometry

The development of fluorophores with spectrally distinct emission bands (i.e., distinct "colors") as well as supporting technology that enables polychromatic flow cytometry is critically important for achieving increased accuracy and efficacy in clinical diagnostics.[4-6] In this regard, the 405 nm (violet) diode laser is becoming one of the most commonly used excitation sources in flow cytometers.[5] This excitation wavelength is ideal for chlorins

because these molecules typically absorb strongly near 405 nm; the resulting emission in the red region affords an effective Stokes' shift of >200 nm (Figure 3.1). To demonstrate the use of chlorins in flow cytometry, chlorin-labeled antibodies were detected using antibody-capture compensation beads, a tool frequently used for setting up multicolor flow cytometry experiments to determine proper corrections due to spectral overlap between fluorophore-labeled reagents.[63]

The chlorin **FbC2-R-NHS** was used to label mouse IgG antibody for detection using mouse IgG antibody-specific compensation beads. The antibody was labeled at room temperature for 3 h with a 35-fold molar excess of **FbC2-R-NHS**. The conjugate was dialyzed against a 20kD molecular weight cutoff membrane to remove byproducts, and the labeled antibody was further purified by affinity binding to Protein A agarose beads. The resulting chlorin–antibody conjugate **FbC2–Ab** had a fluorophore/protein ratio of 2.2 on the basis of absorption spectroscopy. This ratio is relatively low but it ensures minimal dye–dye quenching on the antibody. Flow cytometry experiments used a 405-nm laser for excitation with 600 nm longpass and 620/60 nm bandpass filters for emission. Figure 3.4 shows a histogram of the flow cytometry signals for the **FbC2–Ab**-bound compensation beads, for unbound beads (negative population), and for beads bound to a monoclonal antibody labeled with Brilliant Violet 650 (**BV650–Ab**, the positive control). The latter dye is from a recently introduced dye family based on semiconducting polymers that are among the brightest fluorophores available for flow cytometry.[64] The **FbC2–Ab** exhibits roughly the same fluorescence intensity as a four-fold dilution of the **BV650–Ab** for the same relative protein concentrations. Figure 3.5 shows the relative emission spectral overlap of both dyes with the

bandpass filter. The **BV650–Ab** is a commercial product with an undisclosed fluorophore/protein ratio, so a more precise comparison of relative dye spectral properties was not possible.

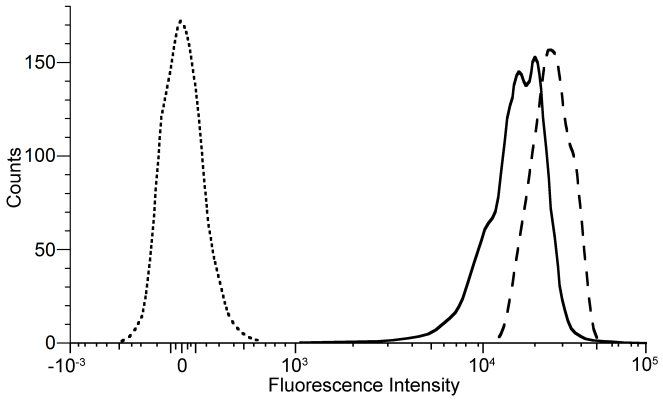

Figure 3.4. Histogram from a flow cytometry experiment using compensation beads stained with either 0.5 μg of chlorin–antibody **FbC2–Ab** (solid line) or 0.12 μg of Brilliant Violet 650–antibody **BV650–Ab** (dashed line), plus unstained beads (dotted line). The analysis used the 405 nm violet laser with 600 nm longpass and 620/60 nm bandpass filters.

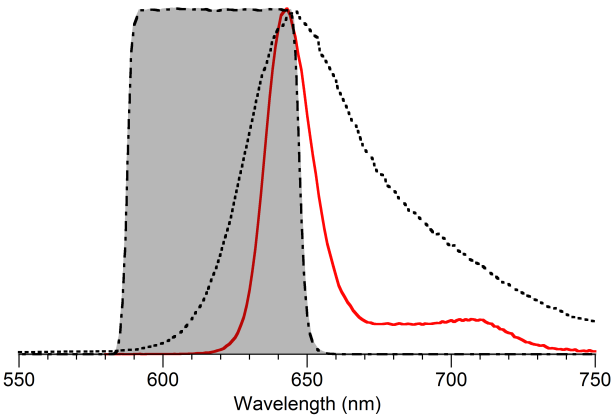

Figure 3.5. Fluorescence spectra of chlorin **FbC2-R-NHS** (red line) and Brilliant Violet 650 (dotted line) overlaid with the Chroma bandpass filter ET620/60 (shadowed gray).

The flow cytometry data suggest that chlorins should prove valuable as labels for polychromatic experiments, especially ones requiring a large number of fluorophores excited from a violet laser. Although not as bright as Brilliant Violet 650, **FbC2-R-NHS** has far narrower emission (FWHM <20 nm) than the commercial label (FWHM ~50 nm; Figure 3.5). Thus, within the red spectral range, it should be possible to discriminate more chlorin-labeled biomolecules with less spectral overlap ("spillover")[63] than with other fluorophore families currently available for flow cytometry. Figure 3.5 suggests that the overall advantage of the narrow-emitting chlorins would be further enhanced if the filter bandpass were reduced (e.g., from 60 nm to 30 nm). This would (1) fit more discrete emission channels in a given wavelength span to enhance multiplexing; (2) collect most of the emission from the chlorin but only a fraction from current dyes with broader emission; and (3) effectively collapse any apparent greater (integrated) brightness of another dye compared to a chlorin.

Conclusions

The installation of PEG groups in a facially encumbering arrangement enables aqueous solubilization of the hydrophobic, disk-like chlorin macrocycle. The resulting PEGylated chlorins are water-soluble but neutral and nonionic. A single PEG-substituted 2,4,6-trialkoxy arene (for **ZnC1**, **FbC1**, **ZnC2**, **FbC2**) suffices to impart aqueous solubility, whereas PEG groups at the terminus of chalcones (for **FbC3**, **ZnC3**) were only partially effective in this regard. Chlorins **ZnC1**, **FbC1** or **ZnC2**, **FbC2** are substituted with fewer

PEG units (12 units or 18 units in total, respectively) than **T(*p*-PEG$_{10}$)PP** (40 units in total; Chart 3.2), yet the former designs impart significant solubility of the macrocycle in water. A distinct feature of the synthetic chlorins is the relatively sharp long-wavelength absorption and companion fluorescence emission band. Such sharp bands are very attractive for use in polychromatic flow cytometry, light-harvesting, and energy-cascade processes.

Acknowledgment

Synthesis and photophysical characterization were supported by the Photosynthetic Antenna Research Center (PARC), an Energy Frontier Research Center funded by the U.S. Department of Energy, Office of Science, Office of Basic Energy Sciences, under Award No. DE-SC0001035. Flow cytometry studies were supported by a grant to NIRvana Sciences (1R41EB020470) from the National Institutes of Health Small Business Technology Transfer Program. Cytometry was performed at the UNC Flow Cytometry Core Facility, which is supported in part by P30 CA016086 Cancer Center Core Support Grant to the UNC Lineberger Comprehensive Cancer Center. Mass spectra were obtained at the Mass Spectrometry Laboratory for Biotechnology at North Carolina State University. Partial funding for the facility was obtained from the North Carolina Biotechnology Center and the National Science Foundation.

Experimental section

(I) General methods

^{1}H NMR (400 MHz) spectra and ^{13}C NMR spectra (100 MHz) were collected at room

temperature in $CDCl_3$ unless noted otherwise. Silica gel (40 μm average particle size) was used for adsorption column chromatography. Size-exclusion chromatography (SEC) was carried out at the preparative level using Bio Beads S-X3 (200–400 mesh) and elution with toluene (HPLC grade). All solvents were reagent grade and were used as received unless noted otherwise. THF was freshly distilled from sodium/benzophenone ketyl. Electrospray ionization mass spectrometry (ESI-MS) data are reported for the molecular ion or cationized molecular ion. Matrix-assisted laser-desorption mass spectrometry (MALDI-MS) was performed with the matrix 1,4-bis(5-phenyl-2-oxaxol-2-yl)benzene.[65] Sonication was carried out using a benchtop sonication bath. Compounds **2f**,[47] **3c**,[18] **4**[50] and **4-Br**[8](ref 57) were prepared as described in the literature.

(II) Synthesis

2,4,6-Tris(propargyloxy)benzaldehyde (1a). Following an alkylation procedure,[33] a solution of 2,4,6-trihydroxybenzaldehyde (5.05 g, 32.7 mmol) in anhydrous DMF (150 mL) was treated with K_2CO_3 (27.6 g, 200. mmol), and the resulting suspension was heated to 60 °C. After 30 min, propargyl bromide (80% in toluene, 11.5 mL, 105 mmol) was added, and the temperature was increased to 80 °C. After stirring for 1.5 h, the reaction mixture was allowed to cool to room temperature, and then diluted with ethyl acetate (500 mL). The organic fraction was washed [water (3 × 200 mL) and brine (2 × 200 mL)], dried (Na_2SO_4), and concentrated to obtain a brown solid (7.65 g, 87%): mp 137–139 °C; ^{1}H NMR (300 MHz) δ 2.56 (t, J = 2.4 Hz, 2H), 2.60 (t, J = 2.4 Hz, 1H), 4.76 (d, J = 2.4 Hz, 2H), 4.78 (d, J = 2.4 Hz, 4H), 6.39 (s, 2H), 10.38 (s, 1H); ^{13}C NMR δ 12.9, 56.0, 56.6, 76.5, 77.4, 93.8, 95.0,

110.3, 161.5, 163.2, 187.2; ESI-MS obsd 269.08107, calcd 269.08084 [$(M + H)^+$, M = $C_{16}H_{12}O_4$].

2,4,6-Tris(3,6,9,12-tetraoxatridecyloxy)benzaldehyde (1b). Following an alkylation procedure,[33] a solution of 2,4,6-trihydroxybenzaldehyde (0.45 g, 2.9 mmol) in anhydrous DMF (5.0 mL) was treated with K_2CO_3 (1.5 g, 12 mmol), and the resulting suspension was heated to 60 °C. After 30 min, 1-bromo-3,6,9,12-tetraoxatridecane (3.0 g, 11 mmol) was added. The mixture was heated at 80 °C and stirred for 1.5 h. The reaction mixture was allowed to cool to room temperature, and then diluted with CH_2Cl_2. The mixture was washed with brine. The organic layer was dried (Na_2SO_4) and concentrated. Chromatography (silica, CH_2Cl_2 with 5% MeOH) afforded the title compound (0.77 g, 36%) and 2,4-bis(3,6,9,12-tetraoxatridecyloxy)-6-hydroxybenzaldehyde (**1b′**, 0.30 g, 20%), each as a pale yellow liquid. Data for **1b**: ^{1}H NMR δ 3.38 (s, 9H), 3.53–3.56 (m, 6H), 3.63–3.72 (m, 30H), 3.85–3.91 (m, 6H), 4.14–4.17 (m, 6H), 6.11 (s, 2H), 10.36 (s, 1H); ^{13}C NMR δ 59.0, 69.6, 68.7, 69.3, 70.6, 70.8, 71.0, 71.9, 92.2, 109.4 163.0, 165.0, 187.4; ESI-MS obsd 725.3942, calcd 725.3954 [$(M + H)^+$, M = $C_{34}H_{60}O_{16}$]. Data for **1b′**: ^{1}H NMR δ 3.38 (s, 6H), 3.54–3.56 (m, 4H), 3.63–3.73 (m, 20H), 3.84–3.89 (m, 4H), 4.13–4.16 (m, 4H), 5.97 (dd, J = 21.7 Hz, J = 2.01 Hz, 2H), 10.12 (s, 1H), 12.48 (s, 1H); ^{13}C NMR δ 59.0, 67.8, 68.1, 69.2, 70.6, 70.8, 70.9, 71.9, 91.84, 91.90, 93.5, 93.6, 106.1, 162.6, 166.2 167.1, 192.0; ESI-MS obsd 535.2725, calcd 535.2749 [$(M + H)^+$, M = $C_{25}H_{42}O_{12}$].

5-[2,4,6-Tris(propargyloxy)phenyl]dipyrromethane (2a). Following a reported procedure,[47] a solution of aldehyde **1a** (2.68 g, 10.0 mmol) in pyrrole (69.3 mL, 1.0 mol) was

degassed with a stream of argon for 10 min. $InCl_3$ (221 mg, 1.00 mmol) was added, and the mixture was stirred for 1.5 h under argon flow. Powdered NaOH (1.2 g) was added, and the mixture was stirred for 45 min. The mixture was filtered. The filtrate was concentrated under high vacuum (to remove excess pyrrole) and then diluted with ethyl acetate (100 mL). The mixture was washed with water, dried (Na_2SO_4), concentrated and chromatographed [silica, hexanes/ethyl acetate (4:1)] to give a viscous oil (2.03 g, 52%): ^{1}H NMR (300 MHz) δ 2.50–2.57 (m, 3H), 4.52 (b, 4H), 4.66 (d, *J* = 2.7 Hz, 2H), 5.90–5.94 (m, 2H), 6.07–6.12 (m, 3H), 6.44 (s, 2H), 6.62–6.66 (m, 2H), 7.64–7.56 (b, 2H); ^{13}C NMR δ 14.0, 32.8, 56.2, 57.6, 76.1, 76.2, 78.4, 78.6, 96.2, 106.3, 108.0, 115.2, 116.5, 116.8, 132.8, 157.2, 157.8; ESI-MS obsd 383.13838, calcd 383.13902 [$(M + H)^+$, M = $C_{24}H_{20}N_2O_3$].

5-[2,4,6-Tris(3,6,9,12-tetraoxatridecyloxy)phenyl]dipyrromethane (2b). Following a standard procedure,[47] a solution of pyrrole (7.4 mL, 0.11 mol) and **1b** (0.77 g, 1.1 mmol) was degassed with a stream of argon for 10 min. $InCl_3$ (2.4 mg, 11 μmol) was added, and the mixture was stirred under argon at room temperature for 1.5 h. The mixture turned yellow during the course of the reaction. Powdered NaOH (0.13 g, 3.3 mmol) was added to quench the reaction. After stirring for 45 min, the mixture was filtered by gravity flow. The filtrate was concentrated and chromatographed (silica, CH_2Cl_2 with 2% MeOH) to afford a pale yellow liquid (0.66 g, 74%): ^{1}H NMR δ 3.36 (s, 6H), 3.37 (s, 3H), 3.50–3.57 (m, 15H), 3.62–3.70 (m, 24H), 3.80–3.82 (m, 3H), 4.00–4.07 (m, 6H), 5.86 (s, 2H), 5.85–5.87 (m, 2H), 6.10 (s, 3H), 6.60–6.61 (m, 2H), 9.20 (s, 2H); ^{13}C NMR δ 32.6, 59.0, 67.5, 69.6, 70.43, 70.55, 70.75, 70.79, 71.9, 93.2, 105.5, 107.2, 113.5, 115.9; ESI-MS obsd 841.4682, calcd 841.4698 [$(M + H)^+$, M = $C_{42}H_{68}N_2O_{15}$].

Streamlined synthesis of 2b. A solution of 2,4,6-trihydroxybenzaldehyde (0.82 g, 5.3 mmol) in anhydrous DMF (10.6 mL) was treated with K_2CO_3 (2.4 g, 18 mmol), and the resulting suspension was heated to 60 °C. After 30 min, 1-bromo-3,6,9,12-tetraoxatridecane (5.0 g, 18 mmol) was added, and the temperature was raised to 80 °C. After 16 h, the reaction mixture was concentrated under vacuum (40 mmHg) at 60 °C. The resulting liquid was diluted with CH_2Cl_2, dried (Na_2SO_4) and filtered. The filtrate was concentrated in a 100-mL flask to afford a pale yellow liquid. Pyrrole (37 mL, 0.54 mol) was added, and the mixture was degassed with a stream of argon for 10 min. $InCl_3$ (0.60 g, 3.0 mmol) was added, and the mixture was stirred under argon at room temperature. After 1 h, ^{1}H NMR analysis showed the reaction was not complete. Additional $InCl_3$ (0.60 g, 3.0 mmol) was added, and the mixture was stirred for 2.5 h. NaOH (0.60 g, 0.020 mol) was added to quench the reaction. After stirring for 45 min, the mixture was filtered by gravity flow. The filtrate was concentrated and chromatographed (silica, CH_2Cl_2 with 2% MeOH) to afford a pale yellow liquid (2.4 g, 54%). The characterization data (^{1}H NMR) were consistent with those reported above.

1-Formyl-5-[2,4,6-tris(propargyloxy)phenyl]dipyrromethane (3a). Following a standard procedure,[48] the Vilsmeier reagent was prepared by treatment of dry DMF (2 mL) with $POCl_3$ (341 μL, 3.65 mmol) at 0 °C and stirring of the resulting mixture for 10 min under argon. In a separate flask, a solution of **2a** (1.30 g, 3.38 mmol) in DMF (15 mL) was treated with the freshly prepared Vilsmeier reagent at 0 °C. The resulting mixture was stirred at 0 °C for 1.5 h. The reaction mixture was treated with saturated aqueous NaOAc (~15 mL) for 2 h. CH_2Cl_2 was added, then the organic phase was washed (water, brine), dried

(Na_2SO_4), concentrated, and chromatographed [silica, hexanes/ethyl acetate (3:2)] to afford an orange oil (713 mg, 51%): ^{1}H NMR δ 2.53 (t, *J* = 2.4 Hz, 2H), 2.56 (t, *J* = 2.4 Hz, 1H), 4.56 (d, *J* = 2.4 Hz, 4H), 4.66 (d, *J* = 2.4 Hz, 2H), 5.92–5.94 (m, 1H), 6.06 (s, 1H), 6.11–6.12 (m, 2H), 6.40 (s, 2H), 6.68–6.70 (m, 1H), 6.83–6.84 (m, 1H), 8.90 (s, 1H), 9.26 (s, 1H), 9.33 (s, 1H); ^{13}C NMR δ 32.7, 32.8, 56.8, 76.1, 76.2, 76.4, 77.9, 78.07, 95.44, 95.49, 107.7, 107.9, 109.4, 112.7, 117.6, 122.2, 129.8, 131.5, 144.1, 156.7, 158.2, 177.9; ESI-MS obsd 413.14984, calcd 413.14958 [$(M + H)^+$, M = $C_{25}H_{20}N_2O_4$].

1-{4-[2-(*tert*-Butoxy)-2-oxoethoxy]phenyl}-5-[2,4,6-tris(3,6,9,12-tetraoxatridecyloxy)phenyl]dipyrromethane (3b). Following a standard procedure[47] with slight modification of reaction time and reagent equivalents, a solution of **2b** (840. mg, 1.00 mmol) in THF (2.0 mL) was treated with EtMgBr (2.8 mL, 0.9 M, 2.5 mmol) at room temperature for 30 min. The solution was cooled to –78 °C, whereupon a solution of **6** (202 mg, 1.20 mmol) in THF (2.4 mL) was added. After 1 h, the reaction mixture was quenched by addition of saturated aqueous NH_4Cl solution (10 mL). The mixture was extracted with CH_2Cl_2 (3 × 20 mL). The organic layer was dried (Na_2SO_4), concentrated, and chromatographed (silica, CH_2Cl_2 with 2–5% MeOH) to afford a pale yellow liquid (439 mg, 41%): ^{1}H NMR δ 1.50 (s, 9H), 3.36 (s, 6H), 3.37 (s, 3H), 3.51–3.55 (m, 6H), 3.60–3.73 (m, 33H), 3.82–3.84 (m, 3H), 3.97–4.16 (m, 6H), 4.58 (s, 2H), 5.90–5.92 (m, 1H), 6.05–6.07 (m, 1H), 6.08–6.10 (m, 1H), 6.11–6.15 (m, 3H), 6.71–6.74 (m, 2H), 6.91–6.96 (m, 2H), 7.81–7.85 (m, 2H), 9.41 (s, 1H), 9.90 (s, 1H); ^{13}C NMR δ 28.0, 32.9, 59.0, 65.5, 67.5, 69.53, 70.46, 70.71, 70.77, 71.83, 82.6, 93.1, 107.0–107.3 (m), 109.0, 111.3, 114.0, 117.8, 119.7, 129.2, 130.5, 130.7, 132.2, 143.5, 157.2, 159.3, 160.5, 167.5, 182.3; ESI-MS obsd

1075.5566, calcd 1075.5585 [$(M + H)^+$, M = $C_{55}H_{82}N_2O_{19}$].

4-[2-(*tert*-Butoxy)-2-oxoethoxy]benzoic acid (5). Following a procedure for phenol alkylation,[54] a solution of 4-hydroxybenzoic acid (3.00 g, 21.7 mmol) in THF (43.4 mL) at 0 °C under argon was treated with 40% aq *n*-Bu_4POH (30.3 mL, 43.4 mmol), whereupon *tert*-butyl bromoacetate (3.20 mL, 21.7 mmol) was added. The resulting reaction mixture was allowed to warm to room temperature for 1 h. The organic solvent was removed under vacuum, and the aqueous residue was acidified with 2N aqueous HCl. No product precipitated after acidification, so ethyl acetate and brine were added. The organic phase was washed (water), dried (Na_2SO_4), and concentrated to give a colorless oil. The resulting oil was filtered through a silica pad with ethyl acetate. The filtrate was chromatographed [silica, hexanes/ethyl acetate (3:1)] to afford a white solid (4.76 g, 87%): mp 114–116 °C; ^{1}H NMR δ 1.46 (s, 9H), 4.57 (s, 2H), 6.91 (d, *J* = 9.0 Hz, 2H), 8.04 (d, *J* = 9.0 Hz, 2H), 11.23 (br s, 1H); ^{13}C NMR δ 28.0, 65.5, 82.9, 114.3, 122.6, 132.4, 162.3, 167.5, 171.8; ESI-MS obsd 275.08850, calcd 275.08899 [$(M + Na)^+$, M = $C_{13}H_{16}O_5$].

***S*-2-Pyridyl 4-[2-(*tert*-butoxy)-2-oxoethoxy]benzothioate (6).** Following a reported procedure,[55] a sample of **5** (4.76 g, 18.8 mmol) was dissolved in anhydrous CH_2Cl_2 (188 mL) under argon and several drops of DMF were added. The mixture was cooled to 0 °C and treated dropwise with oxalyl chloride (2.40 mL, 28.3 mmol). The resulting reaction mixture was allowed to warm to room temperature for 40 min, and then the solvent was removed under vacuum to afford a colorless oil. The resulting oil was dissolved in THF (37.6 mL) and treated with 2-mercaptopyridine (2.10 g, 18.8 mmol) under argon. After stirring for 30 min at room temperature, the reaction mixture was treated with diethyl ether/aqueous

$NaHCO_3$. The organic phase was washed (water), dried (Na_2SO_4), concentrated, and chromatographed [silica, hexanes/ethyl acetate (3:1)] to afford a white solid (2.8 g, 45%): mp 105–106 °C; ^{1}H NMR δ 1.49 (s, 9H), 4.60 (s, 2H), 6.96 (d, J = 9.0 Hz, 2H), 7.31–7.34 (m, 1H), 7.71–7.73 (m, 1H), 7.76–7.80 (m, 1H), 8.00 (d, J = 9.0 Hz, 2H), 8.66–8.68 (m, 1H); ^{13}C NMR δ 28.2, 65.7, 83.0, 114.7, 123.6, 129.9, 130.1, 131.1, 137.2, 150.56, 150.64, 162.5, 167.3; ESI-MS obsd 346.11081, calcd 346.11076 [$(M + H)^+$, M = $C_{18}H_{19}NO_4S$].

Streamlined synthesis of 6. A solution of 4-hydroxybenzoic acid (6.0 g, 43 mmol) in THF (86 mL) at 0 °C under argon was treated with 40% aq *n*-Bu_4POH (60. mL, 87 mmol) followed by *tert*-butyl bromoacetate (6.4 mL, 43 mmol). The resulting reaction mixture was allowed to warm to room temperature for 1 h. Ethyl acetate (300 mL) and aqueous HCl solution (300 mL, pH = 2 by pH test paper) were added to the reaction mixture. The organic phase was separated and washed with aqueous HCl solution (150 mL × 3, pH = 2 by pH test paper), dried (Na_2SO_4), and then concentrated to give a white solid. Recrystallization (hot water) afforded **6** (8.2 g, 30. mmol, 69%), which was dissolved in its entirety in anhydrous CH_2Cl_2 (380 mL) containing 1 mL of DMF under argon. The mixture was cooled to 0 °C and treated dropwise with oxalyl chloride (4.8 mL, 56 mmol). The resulting reaction mixture was allowed to warm to room temperature for 40 min, and then the solvent was removed under vacuum to afford a colorless oil. The oil was dissolved in THF (75 mL) and treated with 2-mercaptopyridine (4.7 g, 45 mmol) under argon. After stirring for 30 min at room temperature, the reaction mixture was treated with diethyl ether/aqueous $NaHCO_3$. The organic phase was washed (water), dried (Na_2SO_4), and concentrated. The resulting solid was recrystallized (hot ethanol) to afford a yellow solid (4.7 g, 32% from 4-hydroxybenzoic

acid). The characterization data (^{1}H NMR) were consistent with those reported above.

Zn(II)-10-[2,4,6-Tris(propargyloxy)phenyl]-18,18-dimethylchlorin (pro-ZnC1). Following a standard procedure,[47] a solution of **3a** (540 mg, 1.31 mmol) in anhydrous THF (13 mL) was treated with NBS (233 mg, 1.31 mmol) under argon at –78 °C. The reaction mixture was stirred for 1 h at –78 °C, after which the cooling bath was removed. Upon reaching 0 °C, hexanes and water were added. The mixture was extracted with ethyl acetate. The organic layer was dried (Na_2SO_4), concentrated, and chromatographed [silica, hexanes/ethyl acetate (2:1)] to afford 9-bromo-1-formyl-5-[2,4,6-tris(propargyloxy)phenyl]dipyrromethane (**3a-Br**[9]) as an orange oil (440 mg, 68%): ^{1}H NMR δ 2.56 (t, J = 2.4 Hz, 2H), 2.57 (t, J = 2.4 Hz, 1H), 4.62 (d, J = 2.4 Hz, 4H), 4.70 (d, J = 2.4 Hz, 2H), 5.96–5.97 (m, 1H), 6.00 (s, 1H), 6.04–6.05 (m, 2H), 6.42 (s, 2H), 6.85–6.87 (m, 1H), 8.76 (s, 1H), 9.05 (s, 1H), 9.20 (s, 1H). Bromodipyrromethane **3a-Br**[9] in $CDCl_3$ solution darkened and decomposed, and hence was used directly in the chlorin-forming process.

Following a general procedure,[49] a solution of **4** (170 mg, 0.896 mmol) and **3a-Br**[9] (440 mg, 0.896 mmol) in CH_2Cl_2 (24 mL) was treated with a solution of *p*-TsOH·H_2O (852 mg, 4.48 mmol) in methanol (6 mL) under argon. The reaction mixture immediately turned red. The mixture was stirred for 30 min under argon, then treated with 2,2,6,6-tetramethylpiperidine (1.10 mL, 6.72 mmol) and concentrated to dryness. The resulting brown solid was suspended in acetonitrile (90 mL) followed by the successive addition of 2,2,6,6-tetramethylpiperidine (3.00 mL, 17.9 mmol), $Zn(OAc)_2$ (2.46 g, 13.4 mmol), and AgOTf (691 mg, 2.69 mmol). The resulting suspension was refluxed for 22 h exposed to air.

The crude mixture was filtered through a silica pad with CH_2Cl_2. The filtrate was chromatographed [silica, hexanes/CH_2Cl_2 (1:1)] to afford a green solid (86 mg, 15%): ^{1}H NMR (THF-d_8) δ 2.06 (s, 6H), 2.65–2.67 (m, 3H), 4.38 (d, J = 2.8 Hz, 4H), 4.55 (s, 2H), 5.03 (d, J = 2.8 Hz, 2H), 6.93 (s, 2H), 8.46 (d, J = 4.4 Hz, 1H), 8.54 (d, J = 4.4 Hz, 1H), 8.60–8.66 (m, 3H), 8.74 (d, J = 4.4 Hz, 1H), 8.74 (d, J = 4.4 Hz, 1H), 9.04 (d, J = 4.4 Hz, 1H), 9.55 (s, 1H); ^{13}C NMR (THF-d_8) δ 29.6, 30.8, 45.1 50.9, 57.4, 75.9, 79.0, 93.6, 94.7, 96.0, 108.6, 114.2, 116.0, 126.4, 126.5, 127.7, 127.8, 131.8, 132.2, 145.7, 146.1, 147.2, 148.3, 153.0, 153.4, 158.1, 159.2, 159.6, 168.4; ESI-MS obsd 640.14376, calcd 640.14474 (M^+, M = $C_{37}H_{28}N_4O_3Zn$); λ_{abs} (toluene) 407, 609 nm.

Zn(II)-10-[2,4,6-Tris(2,5,8,11,14,17-hexaoxanonadecyl-1*H*-1,2,3-triazol-4-ylmethoxy)phenyl]-18,18-dimethylchlorin (ZnC1). The Cu(I) catalyst was prepared by treatment of $CuSO_4 \cdot 5H_2O$ (15.7 mg, 0.0630 mmol) and sodium ascorbate (25.0 mg, 0.126 mmol) with 600 μL deionized H_2O under argon. The reaction mixture turned brown immediately and was stirred until homogeneous. In a separate vial, a solution of **pro-ZnC1** (20.0 mg, 0.0315 mmol) and **PEG$_6$-N$_3$** (150 mg, 0.468 mmol) in DMSO (1200 μL) was treated with freshly prepared Cu(I) catalyst (300 μL) under argon. The reaction mixture was stirred at 40 °C for 16 h. H_2O was added, and the organic phase was extracted with CH_2Cl_2. The extract was washed (brine), dried (Na_2SO_4), and concentrated. The resulting mixture was purified as follows: (1) chromatography [silica, CH_2Cl_2/CH_3OH (93:7 → 19:1)], (2) preparative SEC, and (3) chromatography (silica, CH_2Cl_2 with 8% CH_3OH). The purification procedure afforded a blue oil (29 mg, 58%): ^{1}H NMR (THF-d_8) δ 1.98 (s, 6H),

2.78 (s, 6H), 2.92−2.94 (m, 4H), 3.04−3.06 (m, 4H), 3.12−3.17 (m, 6H), 3.22−3.25 (m, 4H), 3.27 (s, 3H), 3.30−3.36 (m, 12H), 3.38−3.41 (m, 4H), 3.44−3.45 (m, 2H), 3.53−3.68 (m, 28H), 3.80 (t, J = 5.2 Hz, 4H), 3.97 (t, J = 5.2 Hz, 2H), 4.52 (s, 2H), 4.62 (t, J = 5.2 Hz, 2H), 4.96 (s, 4H), 5.44 (s, 2H), 6.47 (s, 2H), 6.97 (s, 2H), 8.24 (s, 1H), 8.42 (d, J = 4.4 Hz, 1H), 8.52 (d, J = 4.0 Hz, 1H), 8.58–8.60 (m, 3H), 8.69 (d, J = 4.0 Hz, 1H), 8.76 (d, J = 4.4 Hz, 1H), 9.01 (d, J = 4.0 Hz, 1H), 9.54 (s, 1H); ^{13}C NMR (THF-d_8) δ 32.4, 47.2, 51.2, 51.9, 52.4, 60.0, 64.2, 65.0, 70.8, 71.6, 71.8, 72.12, 72.13, 72.18, 72.22, 72.31, 72.35, 72.40, 72.44, 72.5, 72.6, 72.7, 73.9, 74.0, 95.1, 96.0, 97.6, 110.5, 116.8, 117.4, 125.0, 126.4, 128.3, 129.6, 130.0, 133.7, 134.4, 145.4, 147.5, 147.8, 149.2, 150.4, 154.8, 155.4, 160.0, 161.8, 162.6,171.5; ESI-MS obsd 1625.70380, calcd 1625.69664 [$(M + Na)^+$, M = $C_{76}H_{109}N_{13}O_{21}Zn$]; λ_{abs} (toluene) 409, 609 nm.

10-[2,4,6-Tris(2,5,8,11,14,17-hexaoxanonadecyl-1*H*-1,2,3-triazol-4-ylmethoxy)-phenyl]-18,18-dimethylchlorin (FbC1). A solution of **ZnC1** (8.0 mg, 0.0050 mmol) in CH_2Cl_2 (16 mL) was treated dropwise with TFA (40 μL). After 5 min, saturated aqueous $NaHCO_3$ was added slowly. The organic layer was separated, dried ($NaSO_4$), and concentrated. The crude product was chromatographed [silica, CH_2Cl_2/CH_3OH (19:1)] to afford a green solid (7.0 mg, 89%): ^{1}H NMR (THF-d_8) δ –2.22 (s, 1H), –1.94 (s, 1H), 2.06 (s, 6H), 2.55 (s, 6H), 2.92−2.94 (m, 4H), 3.04−3.06 (m, 4H), 3.12−3.17 (m, 6H), 3.22−3.25 (m, 4H), 3.27 (s, 3H), 3.30−3.36 (m, 12H), 3.38−3.41 (m, 4H), 3.44−3.45 (m, 2H), 3.53−3.68 (m, 28H), 3.80 (t, J = 5.2 Hz, 4H), 3.97 (t, J = 5.2 Hz, 2H), 4.52 (s, 2H), 4.63 (t, J = 5.2 Hz, 2H), 5.02 (s, 4H), 5.47 (s, 2H), 6.26 (s, 2H), 7.10 (s, 2H), 8.27 (s, 1H), 8.54 (d, J = 4.4 Hz, 1H), 8.75 (d, J = 4.4 Hz, 1H), 8.82 (d, J = 4.4 Hz, 1H), 8.86 (d, J = 4.4 Hz, 1H), 8.98–9.04 (m,

3H), 9.28 (d, J = 4.4 Hz, 1H), 9.87 (s, 1H); ^{13}C NMR (THF-d_8) δ 30.5, 30.6, 46.2, 49.3, 50.1, 52.0, 58.1, 58.2, 62.4, 63.2, 68.85, 68.95, 69.6, 69.7, 69.8, 69.94, 69.95, 70.01, 70.06, 70.09, 70.23, 70.38, 70.40, 70.44, 70.51, 70.56, 70.58, 70.74, 70.76, 70.80, 72.0, 72.1, 94.0, 94.2, 96.3, 107.0, 113.1, 114.3, 122.5, 122.8, 123.0, 123.6, 124.6, 127.5, 128.3, 131.9, 132.4, 132.6, 133.8, 136.6, 139.7, 140.5, 143.5, 150.8, 154.8, 159.9, 161.2, 162.5, 174.2; ESI-MS obsd 771.90605, calcd M/2 = 771.90815 [$(M + 2H)^{2+}$, M = $C_{76}H_{111}N_{13}O_{21}$]; λ_{abs} (toluene) 408, 640 nm.

Zn(II)-18,18-Dimethyl-5-[4-(2-(*tert*-butoxy)-2-oxoethoxy)phenoxy]-10-[2,4,6-tris(3,6,9,12-tetraoxatridecyloxy)phenyl]chlorin (Pro-ZnC2). Following a standard procedure,[47] a solution of **3b** (482 mg, 449 μmol) in THF (12 mL) was treated with NBS (83.0 mg, 446 μmol) at –78 °C for 1 h. A mixture of hexanes (26 mL) and water (26 mL) was added, and the reaction mixture was allowed to warm to room temperature for 20 min. The organic phase was separated. The aqueous phase was extracted with CH_2Cl_2 (26 mL). The combined organic extract was dried (Na_2SO_4) and concentrated, whereupon THF (7.3 mL) and anhydrous methanol (1.8 mL) were added. The solution was treated with $NaBH_4$ (300. mg, 7.93 mmol) at room temperature for 45 min. The reaction mixture was quenched by the addition of saturated aqueous NH_4Cl (26 mL), and then extracted with CH_2Cl_2 (52 mL). The organic extract was dried (Na_2SO_4) and concentrated under reduced pressure without heating to ~4 mL, whereupon anhydrous CH_3CN (10 mL) was added, and again the solution was concentrated by blowing with argon to ~4 mL. The resulting solution (which contained the Eastern half) was treated with anhydrous CH_3CN (9 mL, total volume of ~13 mL of CH_3CN), Western half **4** (86.6 mg, 456 μmol) and TFA (34 μL, 447 μmol). The

reaction mixture was stirred at room temperature for 30 min and then diluted with CH_3CN (42 mL). Samples of triethylamine (1.8 mL, 14 mmol), $Zn(OAc)_2$ (1.2 g, 12 mmol), and AgOTf (0.34 mg, 1.3 mmol) were added. The resulting mixture was refluxed in the presence of air for 24 h. The reaction mixture was quenched by the addition of water, and extracted with CH_2Cl_2 (50 mL × 4). The organic extract was dried (Na_2SO_4) and concentrated. The mixture was purified by (*vide supra*): (1) flash chromatography (silica, CH_2Cl_2 with 5% MeOH), (2) preparative SEC, and (3) flash chromatography (silica, CH_2Cl_2 with 2–5% MeOH). The purification procedure afforded a blue solid (62 mg, 11%): ^{1}H NMR δ 1.60 (s, 9H), 1.77–1.80 (m, 4H), 1.89–2.18 (m, 12H), 2,02 (s, 6H), 2.23–2.41 (m, 8H), 2.46 (s, 6H), 2.99–3.02 (m, 4H), 3.40 (s, 3H), 3.57–3.60 (m, 2H), 3.68–3.80 (m, 8H), 3.84–3.87 (m, 2H), 3.89–3.92 (m, 4H), 4.01–4.04 (m, 2H), 4.35–4.37 (m, 2H), 4.49 (s, 2H), 4.77 (s, 2H), 6.54 (s, 2H), 7.19 (d, J = 8.8 Hz, 2H), 7.69 (d, J = 8.8 Hz, 2H), 8.30, 8.33 (AB, J = 4.4 Hz, 2H), 8.47 (s, 1H), 8.51 (d, J = 4.4 Hz, 1H), 8.53 (s, 1H), 8.58 (d, J = 4.4 Hz, 1H), 8.610 (d, J = 4.4 Hz, 1H), 8.614 (d, J = 4.4 Hz, 1H); ^{13}C NMR δ 28.2, 31.1, 45.0, 50.5, 58.2, 59.1, 66.0, 67.7, 68.64, 68.71, 68.89, 68.95, 69.14, 69.17, 69.5, 69.9, 70.7, 70.9, 71.9, 82.5, 93.4, 93.9, 95.8, 112.6, 115.1, 115.7, 123.2, 126.1, 126.9, 127.5, 128.6, 132.4, 132.6, 134.6, 136.4, 145.4, 146.8, 147.3, 148.6, 153.1, 153.2, 157.3, 158.7, 159.9, 160.4, 168.3, 169.7; ESI-MS obsd 1303.5576, calcd 1303.5614 [$(M + H)^+$, M = $C_{67}H_{90}N_4O_{18}Zn$].

5-[4-(Carboxymethoxy)phenyl]-18,18-dimethyl-10-[2,4,6-tris(3,6,9,12-tetraoxatridecyloxy)phenyl]chlorin (FbC2). Following a standard procedure,[62] a solution of **pro-ZnC2** (15 mg, 12 μmol) in CH_2Cl_2 (4.2 mL) was treated with TFA (1.1 mL). The reaction mixture was stirred at room temperature for 3 h. Water (~6 mL) was added. The

organic phase was separated, washed with water (6 mL × 3), dried (Na_2SO_4) and concentrated. Hexanes (HPLC-grade) was added to the residue, and the suspension was sonicated for 3 min followed by centrifugation. The supernatant was discarded to afford a brown solid (11 mg, 80%): ^{1}H NMR (the CO_2H proton peaks were not observed) δ –1.91 (br s, 2H), 2.06 (s, 6H), 2.14–2.28 (m, 6H), 2.61–2.63 (m, 4H), 2.91–2.93 (m, 6H), 3.02–3.08 (m, 2H), 3.18–3.21 (m, 4H), 3.25 (s, 6H), 3.28–3.31 (m, 4H), 3.41 (s, 3H), 3.59–3.61 (m, 2H), 3.69–4.05 (m, 18H), 4.37–4.40 (m, 2H), 4.60 (s, 2H), 4.88 (s, 2H), 6.55 (s, 2H), 7.24 (d, *J* = 8.2 Hz, 2H), 8.02 (d, *J* = 8.2 Hz, 2H), 8.35, 8.50 (AB, *J* = 4.2 Hz, 2H), 8.72–8.75 (m, 3H), 8.80 (d, *J* = 4.8 Hz, 1H), 8.83 (s, 1H), 8.90 (s, 1H); ^{13}C NMR δ 31.2, 46.3, 51.8, 58.70, 58.79, 59.0, 65.2, 65.8, 67.7, 68.5, 69.1, 69.3, 69.41, 69.53, 69.62, 69.77, 69.83, 70.53, 70.65, 70.70, 70.9, 71.5, 71.9, 92.72, 92.80, 94.6, 96.1, 112.80, 112.93, 113.2, 114.1, 121.2, 122.6, 123.2, 128.0, 128.4, 131.2, 131.7, 134.4, 134.9, 135.6, 135.92, 140.04, 140.26, 151.4, 153.5, 157.4, 159.9, 160.8, 163.2, 170.8, 174.2; ESI-MS obsd 1185.5815, calcd 1185.5853 [$(M + H)^+$, M = $C_{63}H_{84}N_4O_{18}$].

Zn(II)-5-[4-(Carboxymethoxy)phenyl]-18,18-dimethyl-10-[2,4,6-tris(3,6,9,12-tetraoxatridecyloxy)phenyl]chlorin (ZnC2). A solution of **FbC2** (11 mg, 9.3 μmol) in CH_2Cl_2 (0.5 mL) was treated with a solution of $Zn(OAc)_2 \cdot 2H_2O$ (30.0 mg, 136 μmol) in methanol (0.5 mL). The reaction mixture was stirred at room temperature for 16 h, and then treated with water (~4 mL). The organic phase was separated, washed with water (4 mL × 3), dried (Na_2SO_4) and concentrated. HPLC-grade hexanes was added to the residue, and the suspension was sonicated for 3 min followed by centrifugation. The supernatant was discarded to afford a blue solid (11 mg, 95%): ^{1}H NMR ($CDCl_3$, 300 MHz, the CO_2H proton

peaks were not observed) δ 2.02 (s, 6H), 2.08–2.69 (m, 24H), 2.71 (s, 6H), 2.93–3.05 (m, 4H), 3.40 (s, 3H), 3.57–3.60 (m, 4H), 3.68–3.94 (m, 10H), 4.01–4.04 (m, 4H), 4.35–4.38 (m, 2H), 4.48 (s, 2H), 4.77 (br s, 2H), 6.53 (s, 2H), 7.17 (d, J = 8.3 Hz, 2H), 7.94 (d, J = 8.3 Hz, 2H), 8.26, 8.34 (AB, J = 4.3 Hz, 2H), 8.47 (s, 1H), 8.50 (d, J = 4.4 Hz, 1H) 8.52 (s, 1H), 8.57–8.61 (m, 3H); ^{13}C NMR δ 31.0, 45.0, 58.2, 59.0, 68.6, 68.8, 69.0, 69.2, 69.8, 70.50, 70.62, 71.9, 114.9, 125.3, 128.2, 129.0, 137.8, 159.8, 169.8; ESI-MS obsd 1247.4956, calcd 1247.4988 [$(M + H)^+$, M = $C_{63}H_{82}N_4O_{18}Zn$].

17,18-Dihydro-18,18-dimethyl-5-[4-(succinimidooxycarbonylmethoxy)phenyl]-10-[2,4,6-tris(3,6,9,12-tetraoxatridecyloxy)phenyl]porphyrin (FbC2-NHS). Following a standard procedure,[39] a mixture of **FbC2** (4.0 mg, 3.4 μmol), *N*-hydroxysuccinimide (0.47 mg, 4.1 μmol) and EDC (0.78 mg, 4.1 μmol) in CH_2Cl_2 (5.0 mL) was stirred in the dark at room temperature. After 6 h, the reaction mixture was diluted with CH_2Cl_2 (3 mL) and washed with water. The organic layer was separated, dried (Na_2SO_4) and concentrated to a red-brown solid (4.6 mg, ~80% purity estimated by ^{1}H NMR spectroscopy and MALDI-MS): MALDI-MS obsd 1283.73, calcd 1282.60 [$(M + H)^+$, M = $C_{67}H_{87}N_5O_{20}$]; λ_{abs} (CH_2Cl_2) 414, 508, 641 nm.

17,18-Dihydro-18,18-dimethyl-5-(4-((42-(succinimidooxy)-2,42-dioxo-6,9,12,15,18,21,24,27,30,33,36,39-dodecaoxa-3-azadotetracontyl)oxy)phenyl)-10-(2,4,6-tris(3,6,9,12-tetraoxatridecyloxy)phenyl)porphyrin (FbC2-R-NHS). A mixture of **FbC2-NHS** (5.5 mg, 80% purity, 3.4 μmol), $H_2N(C_2H_4O)_{12}C_2H_4CO_2H$ (2.5 mg, 4.0 μmol) in dry CH_2Cl_2 (1.7 mL) was stirred in the dark at room temperature. After 6 h, the reaction mixture

was diluted with CH_2Cl_2 (3 mL) and washed with water. The organic layer was separated, dried (Na_2SO_4) and concentrated. The resulting material was treated with *N*-hydroxysuccinimide (0.29 mg, 2.5 μmol) and EDC (0.48 mg, 2.5 μmol) in CH_2Cl_2 (2.1 mL) in the dark at room temperature. After 20 h, the reaction mixture was diluted with CH_2Cl_2 (3 mL) and washed with aqueous HCl solution (pH = 5). The organic layer was separated, dried (Na_2SO_4) and concentrated. The resulting material was treated with hexanes/ethyl acetate (1:2), sonicated, and centrifuged. The supernatant was discarded, leaving a red-brown solid (3.8 mg, ~80% purity estimated by ^{1}H NMR and MALDI-MS): MALDI-MS obsd 1882.75, calcd 1881.95 [$(M + H)^+$, M = $C_{94}H_{140}N_6O_{33}$]; λ_{abs} (CH_2Cl_2) 414, 508, 641 nm.

3,13-Dibromo-10-[(4-methoxycarbonyl)phenyl]-18,18-dimethylchlorin (pro-FbC3-Br^{3,13}). Following a reported procedure,[18] a solution of **3c** (1.70 g, 5.52 mmol) in anhydrous THF (55 mL) was treated with NBS (1.96 g, 11.0 mmol) under argon at –78 °C. The reaction mixture was stirred for 1 h at –78 °C, after which the cooling bath was removed. Upon reaching –20 °C, hexanes and water were added. The mixture was extracted with ethyl acetate. The organic layer was dried (Na_2SO_4) and concentrated to afford 8,9-dibromo-5-[(4-methoxycarbonyl)phenyl]dipyrromethane (**3c-Br^{8,9}**) as a yellow oil, which was used in the next step without further purification.

Following a general procedure,[49] a solution of **4-Br^8** (5.5 mmol) and **3c-Br^{8,9}** (1.48 g, 5.50 mmol) in CH_2Cl_2 (140 mL) was treated with a solution of *p*-TsOH·H_2O (5.20 g, 27.5 mmol) in methanol (37 mL) under argon. The reaction mixture immediately turned red. The mixture was stirred for 30 min under argon, then treated with 2,2,6,6-tetramethylpiperidine (7.00 mL, 41.3 mmol) and concentrated to dryness. The resulting brown solid was

suspended in acetonitrile (550 mL) followed by the successive addition of 2,2,6,6-tetramethylpiperidine (23.60 mL, 137.5 mmol), $Zn(OAc)_2$ (25.00 g, 137.5 mmol), and AgOTf (4.20 g, 16.5 mmol). The resulting suspension was refluxed for 22 h exposed to air. The crude mixture was filtered through a silica pad with CH_2Cl_2. The filtrate was concentrated. The resulting crude product was dissolved in anhydrous CH_2Cl_2 (100 mL). TFA (500 μL) was added dropwise to the resulting mixture. After 10 min, saturated aqueous $NaHCO_3$ was added slowly. The organic layer was dried ($NaSO_4$), concentrated and chromatographed [silica, hexanes/CH_2Cl_2 (2:1)] to afford a green solid (332 mg, 10%): ^{1}H NMR δ –2.19 (br s, 1H), –1.79 (br s, 1H), 2.00 (s, 6H), 4.10 (s, 3H), 4.60 (s, 2H), 8.15 (d, *J* = 8.0 Hz, 2H), 8.40 (d, *J* = 8.0 Hz, 2H), 8.47 (d, *J* = 4.4 Hz, 1H), 8.73 (s, 1H), 8.75 (s, 1H), 8.91 (d, *J* = 4.4 Hz, 1H), 8.93 (s, 1H), 9.11 (s, 1H), 9.82 (s, 1H); ^{13}C NMR δ 31.3, 46.6, 52.1, 52.7, 94.9, 95.7, 106.0, 113.9, 118.8, 120.3, 124.7, 128.4, 128.8, 129.9, 132.3, 132.5, 133.4, 134.0, 134.2, 137.3, 140.2, 145.9, 151.3, 152.5, 159.6, 163.8, 167.5, 176.1; ESI-MS obsd 631.03316, calcd 631.03388 [$(M + H)^+$, M = $C_{30}H_{24}Br_2N_4O_2$]; λ_{abs} (toluene) 411, 652 nm.

3,13-Diacetyl-10-[(4-methoxycarbonyl)phenyl]-18,18-dimethylchlorin (pro-FbC3-A^{3,13}). Following a procedure for Stille coupling of chlorins,[58] a mixture of **pro-FbC3-Br^{3,13}** (100. mg, 0.158 mmol), tributyl(1-ethoxyvinyl)tin (267 μL, 0.790 mmol), and $(Ph_3P)_2PdCl_2$ (22.2 mg, 0.0316 mmol) was stirred in CH_3CN/DMF [8 □L (3:2)] under argon for 4 h at 83 °C in a Schlenk line. The reaction mixture was treated with 10% aqueous HCl (5 mL) at room temperature for 20 min. CH_2Cl_2 was added. The organic layer was separated, washed (saturated aqueous $NaHCO_3$, water, and brine), dried (Na_2SO_4), concentrated, and chromatographed [silica, CH_2Cl_2/CH_3OH (99:1)]. The resulting solid

product was washed [hexanes/ethyl ether (20:1)] five times (to remove impurities derived from the tin reagent) to afford a brown solid (80 mg, 90%): ^{1}H NMR δ –1.78 (br s, 1H), –1.58 (br s, 1H), 1.99 (s, 6H), 3.04 (s, 3H), 3.12 (s, 3H), 4.14 (s, 3H), 4.57 (s, 2H), 8.06 (d, J = 8.0 Hz, 2H), 8.38–8.40 (m, 3H), 8.77 (s, 1H), 8.84 (d, J = 4.0 Hz, 1H), 8.94 (s, 1H), 9.17 (s, 1H), 10.14 (s, 1H), 10.53 (s, 1H); ^{13}C NMR δ 29.8, 29.9, 31.1, 46.4, 52.3, 52.7, 66.1, 96.6, 99.3, 109.0, 122.1, 127.8, 128.3, 130.07, 130.12, 131.3, 132.3, 133.0, 133.2, 134.0, 134.1, 135.0, 137.4, 138.1, 145.8, 153.6, 154.7, 165.9, 167.4, 176.8, 196.7, 196.9; ESI-MS obsd 559.23347, calcd 559.23398 [$(M + H)^+$, M = $C_{34}H_{30}N_4O_4$]; λ_{abs} (toluene) 433, 686 nm.

5-(4-Carboxyphenyl)-18,18-dimethyl-3,13-bis{(*E*)-3-[2,4,6-tris(3,6,9,12-tetraoxatridecyloxy)phenyl]prop-2-en-1-only}chlorin (FbC3). A mixture of **pro-FbC3-A**[3,13] (50.0 mg, 0.0895 mmol), benzaldehyde **1b** (649 mg, 0.895 mmol), and NaOH (143 mg, 3.58 mmol) in absolute ethanol (45 mL) was refluxed in the open air upon microwave irradiation at 60 W. The microwave irradiation protocol was follow: (1) heat from room temperature to 100 °C (irradiate for 2 min), (2) hold at 100 °C (irradiate for 18 min), (3) allow to cool to room temperature. The reaction mixture was concentrated. The resulting crude product was dissolved in CH_2Cl_2 and washed with a saturated aqueous solution of NH_4Cl. The organic layer was separated, dried (Na_2SO_4), concentrated. The mixture was purified as follows: (1) flash chromatography (silica, CH_2Cl_2 with 5% MeOH), (2) preparative SEC (toluene), and (3) flash chromatography (silica, CH_2Cl_2 with 10% MeOH). The purification procedure afforded a blue solid (98 mg, 56%): ^{1}H NMR δ –1.52 (br s, 1H), –1.36 (br s, 1H), 2.07 (s, 6H), 3.24 (s, 6H), 3.31 (s, 6H), 3.36–3.37 (m, 4H), 3.39 (s, 3H), 3.40 (s, 3H), 3.44–3.50 (m, 8H), 3.51–3.52 (m, 16H), 3.55–3.58 (m, 8H), 3.61–3.63 (m, 4H),

3.65–3.76 (m, 28H), 3.79–3.82 (m, 4H), 3.86–3.90 (m, 2H), 3.90–3.95 (m, 6H), 4.04–4.09 (m, 4H), 4.15–4.20 (m, 2H), 4.20–4.22 (m, 2H), 4.25–4.29 (m, 4H), 4.30–4.34 (m, 4H), 4.67 (s, 2H), 6.26 (s, 2H), 6.27 (s, 2H), 8.29 (d, J = 8.0 Hz, 2H), 8.46 (d, J = 16.0 Hz, 1H), 8.52–8.54 (m, 3H), 8.62 (d, J = 16.0 Hz, 1H), 8.67 (d, J = 15.6 Hz, 1H), 8.72 (d, J = 15.6 Hz, 1H), 8.93 (s, 1H), 8.00 (d, J = 4.4 Hz, 1H), 9.22 (s, 1H), 9.49 (s, 1H), 10.34 (s, 1H), 10.81 (s, 1H), the $-CO_2H$ proton was not detected; ^{13}C NMR δ 31.2, 46.4, 52.4, 59.0, 59.1, 67.7, 68.2, 68.3, 69.4, 69.6, 69.7, 70.3, 70.40, 70.44, 70.52, 70.56, 70.61, 70.67, 70.70, 70.9, 71.8, 72.0, 92.6, 92.8, 96.2, 99.2, 107.4, 109.1, 121.7, 124.6, 125.5, 126.5, 128.6, 129.9, 132.4, 132.5, 132.9, 133.9, 134.2, 134.7, 135.5, 136.2, 137.1, 138.4, 138.6, 146.4, 153.3, 154.2, 161.1, 161.2, 162.38, 162.48, 165.4, 168.8, 176.5, 189.6, 190.2; ESI-MS obsd 979.49094, calcd M/2 = 979.49094 [$(M + 2H)^{2+}$, M = $C_{101}H_{144}N_4O_{34}$]; λ_{abs} (toluene) 442, 686 nm.

Zn(II)-5-(4-Carboxyphenyl)-18,18-dimethyl-3,13-bis{(*E*)-3-[2,4,6-tris(3,6,9,12-tetraoxatridecyloxy)phenyl]prop-2-en-1-only}chlorin (ZnC3). A solution of **FbC3** (15 mg, 7.7 μmol) in $CHCl_3$ (0.5 mL) was treated with a solution of $Zn(OAc)_2$ (27.0 mg, 150 μmol) in methanol (0.5 mL). The reaction mixture was stirred at room temperature for 16 h, and then treated with water (~4 mL). The organic phase was separated, washed with water (4 mL × 3), dried (Na_2SO_4) and concentrated. HPLC-grade hexanes was added to the residue, and the suspension was sonicated followed by centrifugation. The supernatant was discarded to afford a green solid (13 mg, 84%): ^1H NMR (THF-d_8) δ 2.10 (s, 6H), 3.24 (s, 6H), 3.31 (s, 6H), 3.36–3.37 (m, 4H), 3.39 (s, 3H), 3.40 (s, 3H), 3.44–3.50 (m, 8H), 3.51–3.52 (m, 16H), 3.55–3.58 (m, 8H), 3.61–3.63 (m, 4H), 3.65–3.76 (m, 28H), 3.79–3.82 (m, 4H), 3.86–3.90 (m, 2H), 3.90–3.95 (m, 6H), 4.04–4.09 (m, 4H), 4.15–4.20 (m, 2H), 4.20–4.22 (m, 2H),

4.25–4.29 (m, 4H), 4.30–4.34 (m, 4H), 4.60 (s, 2H), 6.35 (s, 2H), 6.41 (s, 2H), 8.24 (d, *J* = 8.0 Hz, 2H), 8.41–8.45 (m, 3H), 8.47–8.48 (m, 3H), 8.61 (d, *J* = 15.6 Hz, 1H), 8.70 (s, 1H), 8.80 (d, *J* = 15.6 Hz, 1H), 8.91 (d, *J* = 4.4 Hz, 1H), 9.18 (s, 1H), 9.47 (s, 1H), 10.06 (s, 1H), the $-CO_2H$ proton was not detected; ESI-MS obsd 1032.42903, calcd M/2 = 1032.42907 [$(M + 2Na)^{2+}$, M = $C_{101}H_{142}N_4O_{34}Zn$]; λ_{abs} (toluene) 447, 666 nm.

(III) Photophysical measurements

All studies were performed at room temperature for compounds in DMF, or in HPLC-grade water (Sigma Aldrich) with 5% DMF. The small amount of DMF was employed to pre-solubilize any solid compound with limited solubility in pure water, and this method was used in all cases for consistency. To simplify the presentation, the solvent consisting of water plus 5% DMF is referred to as "water". Dilute (μM) argon-purged samples were used for static emission spectral, fluorescence quantum yield (Φ_f) and singlet excited-state lifetime (τ_S) studies. Static emission spectra were acquired using 2–4 nm excitation and detection bandwidths and corrected for instrument spectral response. The Φ_f values were determined for samples having $A \leq 0.1$ at λ_{exc} (typically in the Soret region) using replicate measurements with an integrating sphere (Horiba, Quanti-Phi).

Singlet excited-state lifetimes (τ_S) are the average result of two measurements. The first method used a stroboscopic fluorescence decay apparatus with an ~1 ns Gaussian instrument response function (Laser Strobe TM-3; Photon Technology International) and samples excited in the blue to green spectral regions by a dye laser pumped by a nitrogen laser. The second method utilized transient absorption spectroscopy employing ~100 fs

excitation flashes (typically in the Q_x region) from an ultrafast laser system (Spectra Physics) and acquisition of difference spectra (360–900 nm) using a white-light pulsed laser (~1 ns rise time) in 100-ps time bins with variable pump-probe spacing up to 0.5 ms (Ultrafast Systems, EOS). The latter apparatus was also used to determine the yield of $S_1 \rightarrow T_1$ intersystem crossing (Φ_{isc}) by comparing the extent of bleaching of the ground-state B_x, Q_x or Q_y absorption bands (relative to the featureless excited-state absorption) for the T_1 state at long times compared to that due to S_1 right after the flash. The contribution of stimulated emission (to S_1 spectra) was taken into account for studies in the Q_y region.

(IV) Flow cytometry measurements

(A) Instrumentation and software. Samples were analyzed at the University of North Carolina Core Flow Cytometry Facility on a 19-parameter LSR-II SORP flow cytometer (BD Biosciences, San Joe, CA) equipped with seven lasers (355, 405, 488, 532, 561, 594, and 633 nm) using FACSDiva 8.0 acquisition software. The longpass filter in the "A" detector channel of the 355 nm laser was replaced with a 600 nm longpass filter provided with the instrument and the standard bandpass filter in this channel was replaced with a 620/60 nm bandpass filter (ET620/60, Chroma Technology Corp., Bellows Falls, VT). Data were collected using the 100 mW 405 nm laser. Post-experimental analysis was performed with FlowJo software (version 10.0.8, FlowJo, LLC, Ashland, OR).

(B) Materials. Simply Cellular™ anti-mouse for violet laser compensation standard beads (Bangs Laboratories, Fishers, IN) were used for all flow cytometry experiments. Antibodies used included BD Horizon Brilliant Violet 650-labeled CD8 clone RPA–T8

(**BV650–Ab**, positive control) and Protein A-purified mouse IgG (MU-003-C, ImmunoReagents, Raleigh, NC).

(C) Bioconjugation to form FbC2–Ab. Prior to bioconjugation, dialysis was used to exchange antibodies into 50 mM borate buffer (pH 8.5). The chlorin **FbC2-R-NHS** (0.1 mg) was dissolved in 20 μL of the borate buffer and added to 0.25 mg of mouse IgG solution to achieve a 35-fold ratio of fluorophore to protein in a final reaction volume of 86 μL. This reaction solution was gently rotated in a microcentrifuge tube protected from light for 3 h at ambient temperature and then dialyzed against phosphate buffered saline (PBS) with a 20 kD MWCO dialysis membrane for at least 4 h at ambient temperature to remove unreacted materials. The chlorin–antibody bioconjugate was further purified by affinity purification using Pierce Protein A Agarose beads (Thermo Scientific, Rockford, IL) and the manufacturer's protocol for immunoprecipitation. The resulting chlorin–antibody bioconjugate, **FbC2–Ab**, exhibited a fluorophore/protein ratio of 2.2 as determined by absorption spectroscopy using a molar absorption coefficient for the chlorin ($\varepsilon_{414\ nm}$ = 160,000 $M^{-1}cm^{-1}$; $\varepsilon_{280\ nm}$ = 22,000 $M^{-1}cm^{-1}$) and for the antibody[66] ($\varepsilon_{280\ nm}$ = 210,000 $M^{-1}cm^{-1}$). The value for the chlorin was drawn from that the chlorin analogue lacking any meso-substituents.[51]

(D) Staining of compensation beads. All preparations used PBS with 0.5% bovine serum albumin (BSA) as the buffer for all steps. For blanks (negative controls), 1 drop of the anti-mouse compensation bead solution was added to buffer and adjusted to a final volume of 250 μL. Blanks were treated by the following sequence of washes and centrifugation but

without antibody addition, then resuspended in 1.0 mL buffer. For labeled antibodies, 1.0 mL aliquots of bead solution were prepared from 4 drops of beads, then 50 μL was aliquoted per sample. For the experiment shown in Figure 3.4, 0.5 μg of **FbC2–Ab**, and 0.12 μg of the positive control Brilliant Violet 650-labeled antibody (**BV650–Ab**) were added to each aliquot, and each sample was mixed gently for 30 min at ambient temperature in the dark. Solutions were washed twice by addition of buffer (1mL) to each tube, centrifugation at 3000 × g for 3 min, and removal of supernatant. Samples were resuspended in 1.0 mL of buffer for analysis.

(E) Experiment and data analysis. The **FbC2–Ab** and the positive control **BV650–Ab** were excited with the 405 nm laser and read in channel A with a 600 nm longpass filter and a 620/60 nm bandpass filter in place. Compensation beads were identified on the basis of forward and side light scatter. Gating was applied to exclude events with both lower and higher scatter than single beads and all further data were analyzed using this gating. For all experiments, 5000 gated events were collected.

Supplimentary information

(I) Click reaction conditions

Table 3.3. Conditions for click reaction of **pro-ZnC1** with **PEG_6-N_3** to form **ZnC1**.

Entry	Cu (I) amount	Solvent	Temp., Time	Result[a]
1	0.03 equiv	Butanol/H_2O (2:1)	RT, 16 h	**Pro-ZnC1**
2	0.03 equiv	CH_3CN/H_2O (2:1)	RT, 16 h	**Pro-ZnC1**

Table 3.3. Continued.

3	0.1 equiv	CH_3CN/H_2O (1:1)	40 °C, 36 h	mono-, di-, tri-derivatized chlorins, minor **Pro-ZnC1**
4	0.2 equiv	CH_3CN/H_2O (2:1)	40 °C, 16 h	Same as entry 3
5	1 equiv	DMSO/H_2O (4:1)	40 °C, 16 h	**ZnC1**

[a]Results are based on TLC analysis and MALDI-MS.

(II) Exploratory molecular designs

Several targets that were pursued are shown in Chart 3.6. The limitations of each design with regard to syntheses, and the synthetic procedures and characterization, are provided herein. Much promising chemistry was accomplished, which potentially can be exploited in other synthetic routes.

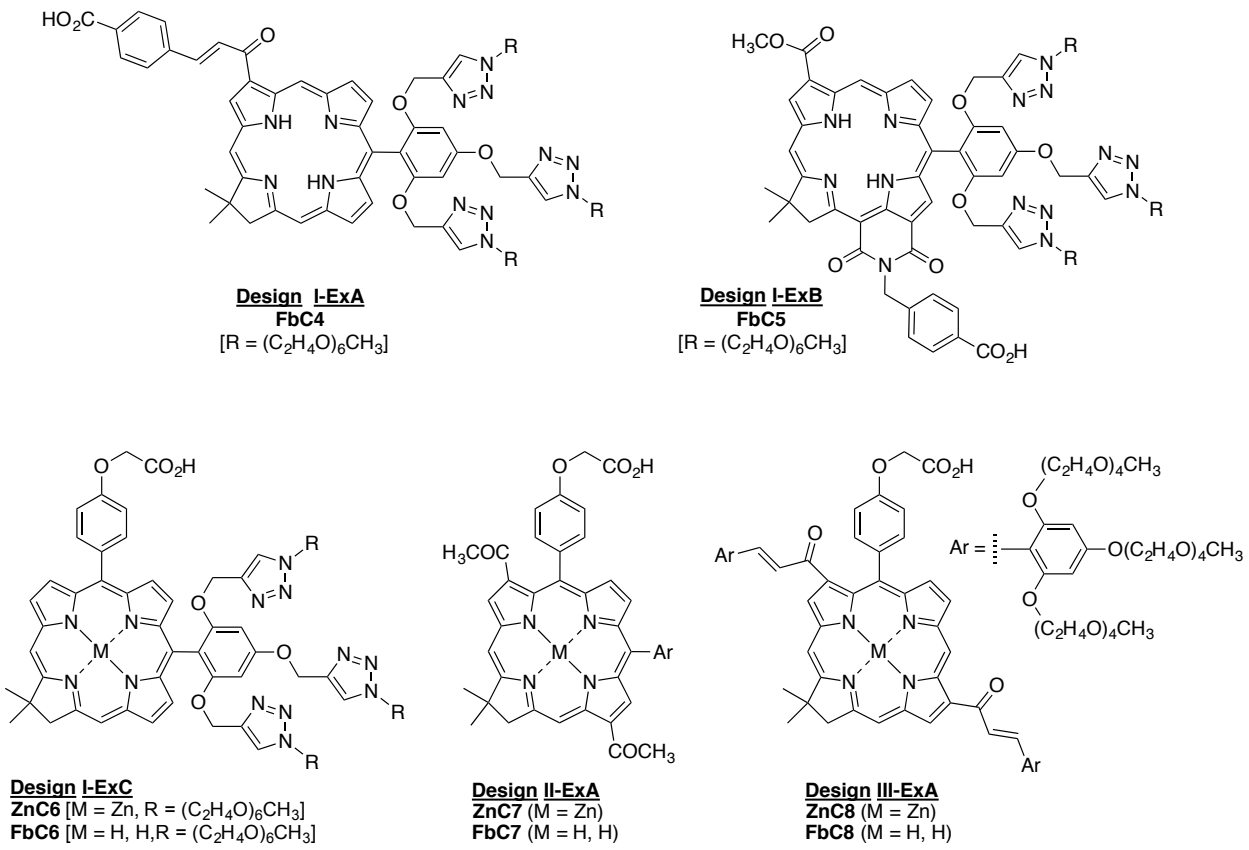

Chart 3.6. Attempted target chlorins.

(A) Design I-ExA. In this attempted design (Scheme 3.7), the chalcone moieties would be incorporated at the 3-position to achieve wavelength-tunable and bioconjugatable chlorins. Here, chalcone formation entails an aldol condensation of the 3-acetylchlorin and 4-formylbenzoic acid under basic conditions. The synthesis started by protection of **1a** with TMSCl in the presence of DBU and a catalytic amount of AgCl, thereby affording the TMS-protected tris(propargyloxy)benzaldehyde **1d** in 63% yield.[68,69] The condensation of **1d** and pyrrole with $InCl_3$ unexpectedly gave TMS-cleaved dipyrromethane **2a** (not shown) instead of the corresponding dipyrromethane **2d**. TMS cleavage may happen when NaOH powder

was added to quench the reaction; the use of NaOH addition is essential for dipyrromethane formation with $InCl_3$.[47] TFA was then used as catalyst,[70] and 0.1 N aqueous NaOH was added to quench the reaction, which gave **2d** in 47% yield.

Vilsmeier formylation of TMS-protected dipyrromethane **2d** with $POCl_3$/DMF afforded 1-formyldipyrromethane **3d** in 33% yield. Bromination of **3d** with 1 equiv of NBS at –78 °C afforded **3d-Br**[9], which was used in next step without further purification. The chlorin-forming reaction was carried out under standard conditions.[49] However, the reaction provided a mixture of zinc chlorins wherein 1–3 TMS protecting groups were cleaved, and no desired chlorin **pro-ZnC4-Br**[3] was observed. The presence of the base TMPi might cause TMS deprotection during the oxidative cyclization. If successful, a Stille coupling reaction would replace the 3-bromo group with an acetyl moiety, but the synthesis was ceased here to avoid competing Sonogashira side reactions of the unprotected alkyne groups.

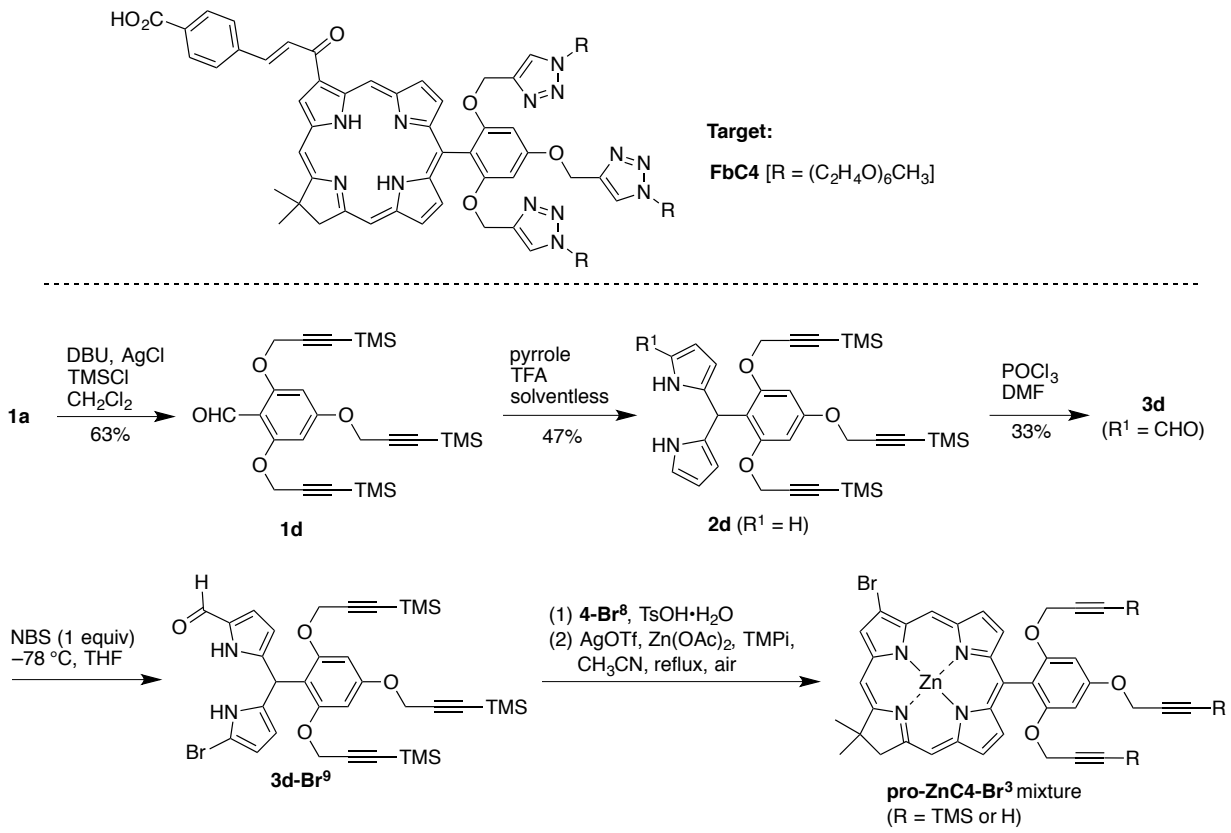

Scheme 3.7. Attempted synthesis of TMS-protected trispropargyl chlorin.

(B) Design I-ExB. To avoid competing Sonogashira reaction with unprotected alkyne groups, an alternative strategy is to carry out the click reaction before Pd-catalyzed reactions. This strategy was employed to synthesize a target chlorin-imide (Scheme 3.8). The target chlorin-imide was expected to exhibit Q_y absorption ~705 nm, which could fill the spectral window between that of synthetic chlorins (603–687 nm) and bacteriochlorins (707–792 nm).[71] In this design, a bioconjugatable tether would be introduced at the imide ring at the stage of ring closure, and water-solubility achieved by click reaction between the alkynes and **PEG$_6$-N$_3$**. Bromination[72] of **3a** with 2 equiv of NBS at –78 °C afforded **3a-Br^{8,9}** in 54%

yield. Note: **3a-Br**[8,9] was unstable and decomposed quickly at room temperature; hence, the bromination was conducted immediately prior to the synthesis of the chlorin.

The chlorin-forming reaction was carried out under standard conditions,[49] which afforded zinc chlorin **pro-ZnC5-Br**[3,13] in 6% yield. Treatment of **pro-ZnC5-Br**[3,13] and **PEG$_6$-N$_3$** with a stoichiometric amount of Cu(I) in DMSO/H_2O (4:1) at 40 °C gave the zinc triazole-PEG-chlorin **ZnC5-Br**[3,13] in 43% yield. The dibromochlorin **ZnC5-Br**[3,13] was subjected to carbonylation with CO in DMF/toluene (1:1) in the present of a stoichiometric amount of $Pd(PPh_3)_4$. Subsequent treatment of the resulting acylpalladium intermediate with NaOMe in methanol afforded chlorin-diester **ZnC5-Es**[3,13] in 34% yield.

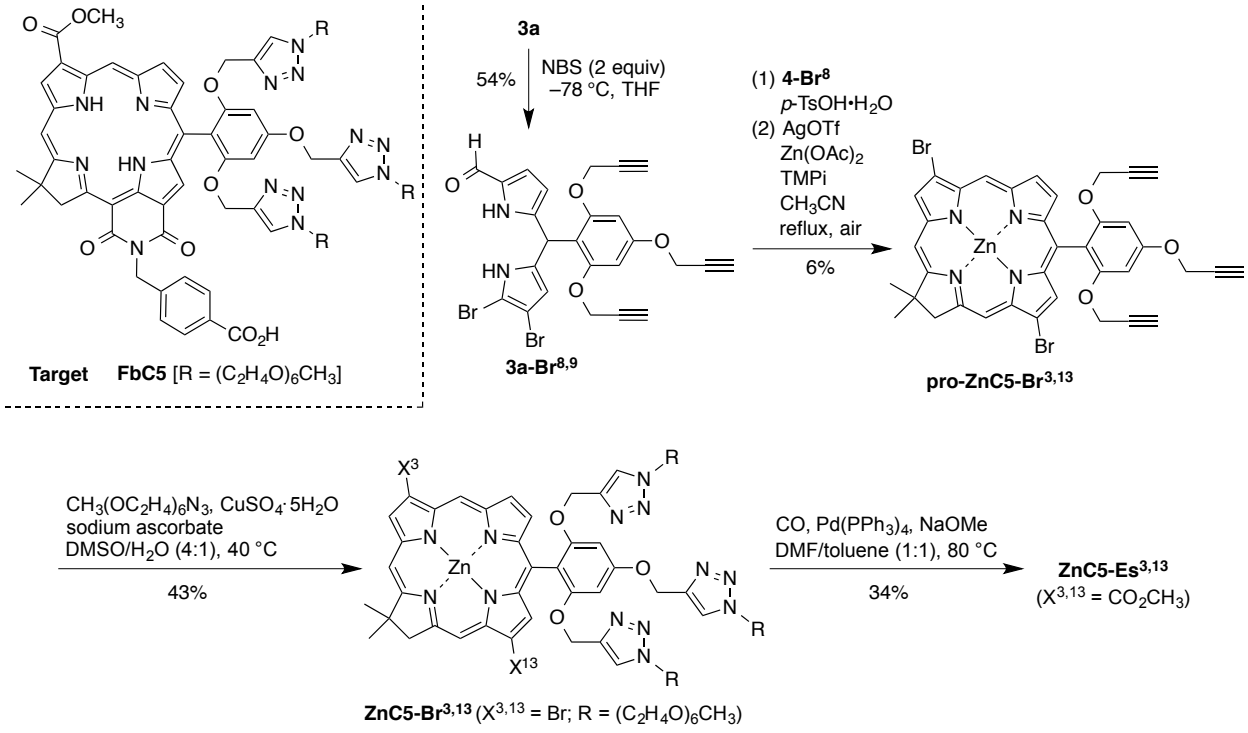

Scheme 3.8. Synthesis approach toward a chlorin-imide.

The successful formation of **ZnC5-Es**[3,13] provided an attractive methodology to synthesize water-soluble chlorins wherein only moderate derivatization is required after chlorin formation. For example, the target chlorin-chalcone **FbC4** (Scheme 3.7, upper panel) would be synthesized in a similar way: after preparation of the alkyne-unprotected chlorin **pro-ZnC4-Br**[3], a click reaction could be carried out first, followed by Stille coupling reaction to introduce the acetyl group. The last step would entail aldol condensation between the acetylchlorin and 4-formylbenzoic acid to incorporate a bioconjugatable tether. However, for the synthesis of the chlorin-imide, the limitation of this strategy came from the lengthy elaboration of the chlorin. Two more steps (regioselective 15-bromination, Pd-mediated carbonylation followed by ring closure to form the imide) remain to form the target chlorin-imide from **ZnC5-Es**[3,13], but a total yield of **ZnC5-Es**[3,13] from Eastern half **3a** was less than 1%. At the same time, PEG groups were carried through all of the steps for chlorin derivatization, which complicated purification.

(C) Design I-ExC. Target chlorins **ZnC6** and **FbC6** were pursued on the basis of the success of **ZnC1** and **FbC1**. The same PEGylation strategy was adopted with the only difference the requirement to introduce a bioconjugable tether at the 5-position. Acylation of dipyrromethane **2a** with thioester **6** afforded monoacyldipyrromethane **3e** in 28% yield along with recovery of unreacted dipyrromethane **2a** in 27% yield (Scheme 3.9). Acyldipyrromethane **3e** was brominated selectively at the remaining free α-position by treatment[56] with NBS in THF at –78 °C, affording **3e-Br**[9] in 76% yield. The reduction of bromoacyldipyrromethane **3e-Br**[9] under the standard conditions[49,53] with excess $NaBH_4$ in THF/MeOH (4:1) was inefficient, as only the starting material **3e-Br**[9] was observed by TLC

analysis, and none of the desired dipyrromethanecarbinol was detected. Unlike the analogous **3a-Br**[9], which was unstable, compound **3e-Br**[9] was sufficiently stable for routine handling. The low conversion yield upon acylation of **2a** to **3e** and the failure of subsequent reduction might be attributed to the reactive terminal alkynyl groups. One workaround would entail the protection of terminal alkynyl groups and removal thereof prior to the click reaction, but this was not investigated.

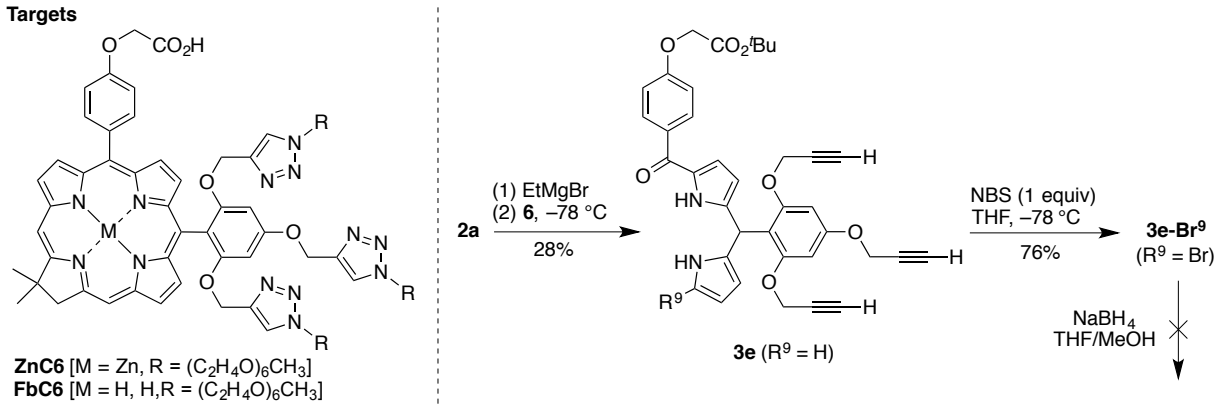

Scheme 3.9. Synthesis of 5-substituted chlorin precursors.

(D) Design II-ExA. Another attempted design (for **ZnC7** and **FbC7**) entailed introduction of auxochromes at the 3- and 13-positions of PEGylated chlorins, which would be synthesized via pre-installation of the PEG moieties. Bromination of **3b** with 2 equiv of NBS at –78 °C afforded the desired compound **3b-Br**[8,9], but a tribrominated impurity (not shown) could not be removed (Scheme 3.10). The inability to purify dipyrromethane **3b-Br**[8,9] caused this approach to be discontinued.

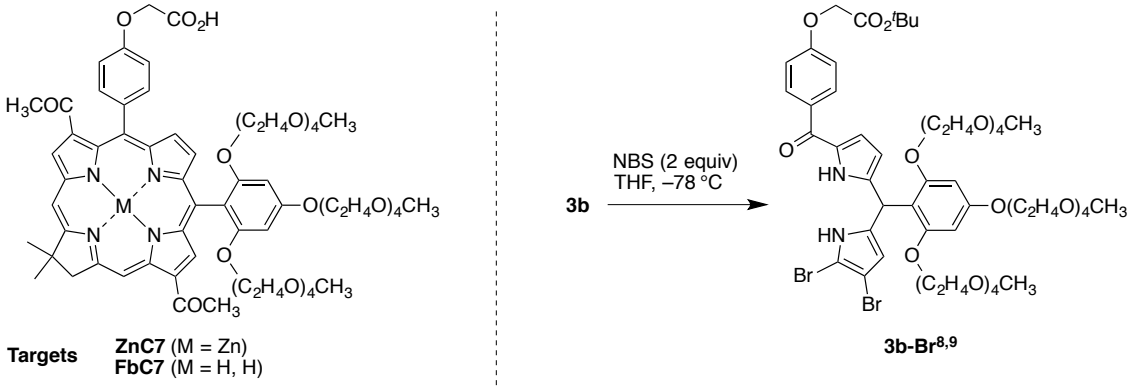

Scheme 3.10. Synthesis of 5-substituted chlorin precursors.

(E) Design III-ExA. A chalcone design was employed here by derivatization of the 3,12-positions of the chlorin to achieve wavelength tunability and water solubility. The 5-position was assigned to the bioconjugatable tether. Thus, dipyrromethane **2f** was acylated[47] with thioester **6** to form monoacyldipyrromethane **3f** in 62% yield (Scheme 3.11). Acyldipyrromethane **4c** was brominated selectively at the 7,9-positions by treatment with 2 equiv of NBS in THF at –78 °C,[72] affording **3f-Br**^{7,9} in 84% yield. Attempts to reduce bromoacyldipyrromethane **3f-Br**^{7,9} under the standard conditions[49] with excess $NaBH_4$ in THF/MeOH (4:1) were unsuccessful: starting material **3f-Br**^{7,9} was observed by TLC analysis after reduction, and the yield of the chlorin-forming reaction to produce **pro-FbC8-Br**^{3,12} was a meager 0.7%.

Stille coupling[55] of 3,12-dibromochlorin **pro-FbC8-Br**^{3,12} with tributyl(1-ethoxyvinyl)tin and a catalytic amount of $(Ph_3P)_2PdCl_2$ in CH_3CN/DMF (3:2) followed by acidic hydrolysis gave 3,12-diacetylchlorin **pro-FbC8-A**^{3,12} in 42% yield. The expected Q_y band of **pro-FbC8-A**^{3,12} is ~690 nm in toluene, on the basis of estimated derived from

estimated value the known 5-unsubstituted chlorins that contain 3,12- or 3,13-diacetyl groups.[56,73] However, the Q_y band of **pro-FbC8-A**^{3,12} appeared at 671 nm in toluene. The failure to achieve the desired wavelength along with absymally low yield of chlorin formation prompted us to abandon this strategy and avoid a chlorin design with a 5-substituent.

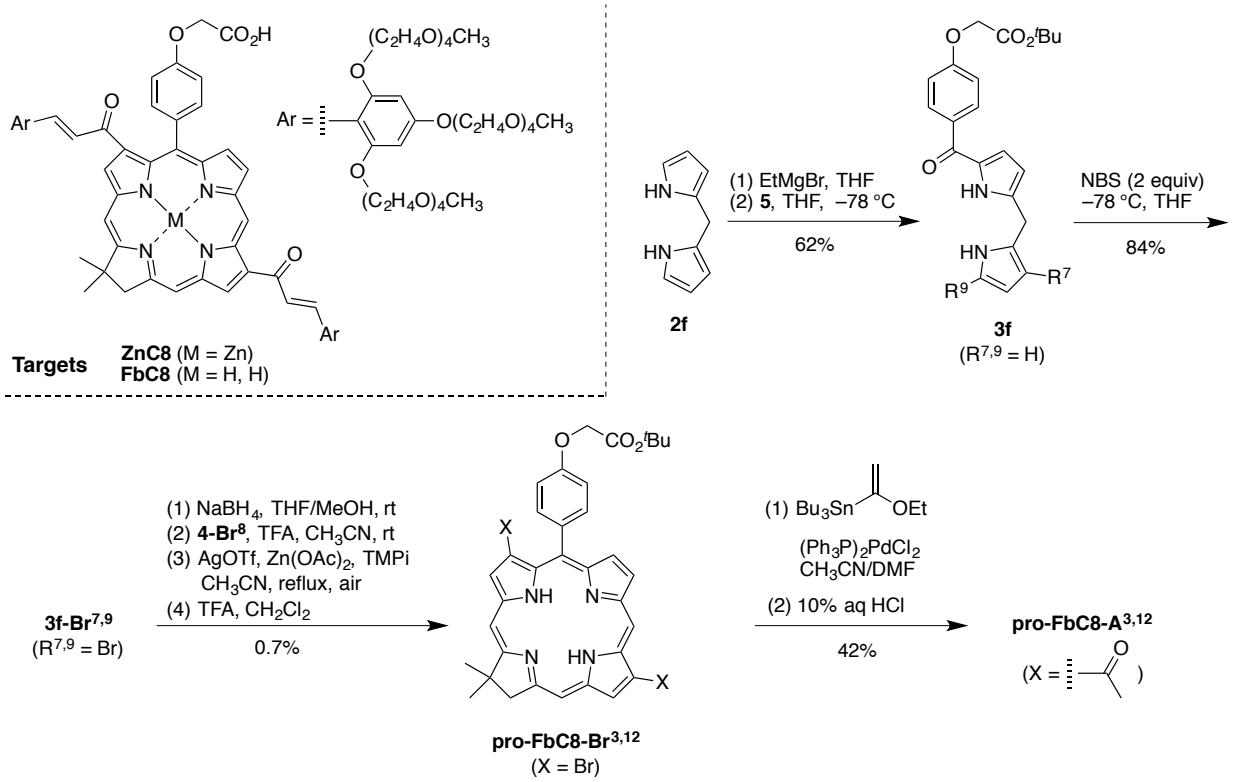

Scheme 3.11. Synthesis of a diacetylchlorin with a bioconjugatable tether at the 5-position.

(F) Experimental procedures and characterization

2,4,6-Tris(3-trimethylsilylpropargyloxy)benzaldehyde (1d). Following a trimethylsilyl protection procedure,[68,69] DBU (23.80 g, 156.5 mmol) was added to a mixture

of benzaldehyde **1a** (7.00 g, 26.1 mmol) and AgCl (2.20 g, 15.7 mmol) in anhydrous CH_2Cl_2 (50 mL). The reaction mixture was then heated under reflux, whereupon chlorotrimethylsilane (25.50 g, 234.9 mmol) was added dropwise. After refluxing with stirring for 36 h, the mixture was allowed to cool to room temperature. The mixture was diluted with hexanes, and then washed with aqueous $NaHCO_3$, 2 M HCl, and water. The resulting organic phase was dried (Na_2SO_4), concentrated, and chromatographed [silica, hexanes/ethyl acetate (9:1)] to afford a light yellow oil (8.0 g, 63%): ^{1}H NMR δ 0.13 (s, 18H), 0.15 (s, 9H), 4.68 (s, 2H), 4.70 (s, 4H), 6.35 (s, 2H), 10.31 (s, 1H); ^{13}C NMR δ –0.40, 56.9, 57.7, 93.6, 93.7, 94.1, 98.8, 99.15, 110.3; ESI-MS obsd 485.20011, calcd 485.19942 [$(M + H)^+$, M = $C_{25}H_{36}O_4Si_3$].

5-[2,4,6-Tris(3-trimethylsilylpropargyloxy)phenyl]dipyrromethane (2d). Following a reported procedure,[47,74] a solution of benzaldehyde **1d** (6.00 g, 12.4 mmol) and pyrrole (33.2 g, 49.5 mmol) was degassed with a stream of argon for 10 min, and then TFA (95.0 μL, 1.24 mmol) was added. The solution was stirred for 20 min, and then diluted with CH_2Cl_2. The organic phase was washed (0.1 N aqueous NaOH, H_2O), dried (Na_2SO_4), concentrated and chromatographed [silica, hexanes/ethyl acetate (20:1)] to afford a light yellow oil (3.5 g, 47%): ^{1}H NMR δ 0.19 (s, 9H), 0.20 (s, 18H), 4.50 (s, 2H), 4.63 (s, 4H), 5.93 (s, 1H), 6.09–6.10 (m, 4H), 6.40 (s, 2H), 6.63–6.64 (m, 2H), 8.57 (s, 2H); ^{13}C NMR δ –0.12, –0.03, 32.8, 57.2, 58.6, 92.8, 93.3, 94.8, 96.3, 99.9, 100.2, 106.3, 108.0, 115.1, 116.4, 116.7,133.0, 158.2; ESI-MS obsd 601.27373, calcd 601.27325 [$(M + H)^+$, M = $C_{33}H_{44}N_2O_3Si_3$].

1-Formyl-5-[2,4,6-tris(3-trimethylsilylpropargyloxy)phenyl]dipyrromethane (3d). The Vilsmeier reagent was prepared by treatment of dry DMF (2.5 mL) with $POCl_3$ (542 μL, 5.80 mmol) at 0 °C and stirring of the resulting mixture for 10 min under argon. In a separate flask, a solution of **2d** (3.50 g, 5.80 mmol) in DMF (30 mL) was treated with the freshly prepared Vilsmeier reagent at 0 °C. The resulting mixture was stirred at 0 °C for 1.5 h. The reaction mixture was treated with saturated aqueous NaOAc (~25 mL) for 2 h. CH_2Cl_2 was added to reaction mixture, then the organic phase was washed (water, brine), dried (Na_2SO_4), concentrated, and chromatographed [silica, hexanes/ethyl acetate (9:1)] to afford an orange oil (1.2 g, 33%): ^{1}H NMR δ 0.19 (s, 18H), 0.20 (s, 9H), 4.52 (s, 2H), 4.54 (s, 2H), 4.65 (s, 2H), 5.90–5.92 (m, 1H), 6.07 (s, 1H), 6.12–6.16 (m, 2H), 6.40 (s, 2H), 6.70–6.72 (m, 1H), 6.83–6.85 (m, 1H), 8.98 (s, 1H), 9.06 (s, 1H), 9.33 (s, 1H); ^{13}C NMR δ –0.08, 33.1, 57.2, 58.2, 93.4, 93.7, 95.6, 99.58, 99.69, 108.0, 109.6, 112.6, 117.7, 122.3, 130.1, 131.6, 144.6, 157.1, 158.7, 178.1; ESI-MS obsd 629.26867, calcd 629.26816 [$(M + H)^+$, M = $C_{34}H_{44}N_2O_4Si_3$].

Zn(II)-3-Bromo-10-[2,4,6-tris(3-trimethylsilylpropargyloxy)phenyl]-18,18-dimethyl-chlorin (pro-ZnC4-Br^3). Following a standard procedure,[75] a solution of **3d** (1.2 g, 1.9 mmol) in anhydrous THF (19 mL) was treated with NBS (340 mg, 1.9 mmol) under argon at –78 °C. The reaction mixture was stirred for 1 h at –78 °C, after which the ice bath was removed and the reaction mixture was allowed to warm to room temperature. Upon reaching 0 °C, hexanes and water were added. The mixture was extracted with ethyl acetate. The organic layer was dried (Na_2SO_4) and concentrated to afford 9-bromo-1-formyl-5-[2,4,6-tris(3-trimethylsilyl- propargyloxy)phenyl]dipyrromethane (**3d-Br^9**) as a yellow oil, which

was used in the next step without further purification: ^{1}H NMR δ 0.19 (s, 18H), 0.20 (s, 9H), 4.47–4.61 (m, 4H), 4.65 (s, 2H), 5.91–5.93 (m, 1H), 5.98 (s, 1H), 6.03–6.08 (m, 2H), 6.40 (s, 2H), 6.84–6.86 (m, 1H), 8.91 (s, 1H), 9.00 (s, 1H), 9.35 (s, 1H).

Following a general procedure,[49] a solution of **4-Br**[8] (511 mg, 1.90 mmol) and **3d-Br**[9] (1.90 mmol) in CH_2Cl_2 (50 mL) was treated with a solution of *p*-TsOH·H_2O (1.80 g, 9.50 mmol) in methanol (12.6 mL) under argon. The reaction mixture immediately turned red. The mixture was stirred for 30 min under argon, then treated with 2,2,6,6-tetramethylpiperidine (2.40 mL, 14.0 mmol) and concentrated to dryness. The resulting brown solid was suspended in acetonitrile (190 mL) followed by the successive addition of 2,2,6,6-tetramethylpiperidine (8.10 mL, 47.5 mmol), $Zn(OAc)_2$ (5.20 g, 28.5 mmol), and AgOTf (1.40 g, 5.70 mmol). The resulting suspension was refluxed for 22 h exposed to air. The crude mixture was filtered through a silica pad with CH_2Cl_2. The crude product was a mixture of chlorins with TMS cleaved and partially cleaved.

Zn(II)-3,13-Dibromo-10-[2,4,6-tris(propargyloxy)phenyl]-18,18-dimethylchlorin (pro-ZnC5-Br[3,13]**).** Following a standard procedure,[75] a solution of **3a** (948 mg, 2.30 mmol) in anhydrous THF (23 mL) was treated with NBS (818 mg, 4.60 mmol) under argon at –78 °C. The reaction mixture was stirred for 1 h at –78 °C, after which the ice bath was removed. Upon reaching –20 °C, hexanes (20 mL) and water (20 mL) was added. The mixture was extracted with ethyl acetate. The organic layer was dried (Na_2SO_4), concentrated and chromatographed [silica, hexanes/ethyl acetate (4:1)] to afford 8,9-dibromo-1-formyl-5-[2,4,6-tris(propargyloxy)- phenyl]dipyrromethane (**3a-Br**[8,9]) as a yellow oil (710 mg, 54%): ^{1}H NMR δ 2.57 (t, J = 2.4 Hz, 2H), 2.58 (t, J = 2.4 Hz, 1H), 4.63 (d, J = 2.4 Hz, 4H), 4.70 (d,

J = 2.4 Hz, 2H), 5.89–5.91 (m, 1H), 6.10 (d, *J* = 3.0 Hz, 1H), 6.21 (s, 1H), 6.43 (s, 2H), 6.85–6.87 (m, 1H), 9.21 (s, 1H), 9.24 (s, 1H), 9.43 (s, 1H). Dibromodipyrromethane **1e** in $CDCl_3$ solution darkened and decomposed, and hence was used directly in the chlorin-forming process.

Following a general procedure,[49] a solution of **4-Br**[8] (161 mg, 0.600 mmol) and **3a-Br**[8,9] (342 mg, 0.600 mmol) in CH_2Cl_2 (16 mL) was treated with a solution of *p*-TsOH·H_2O (570. mg, 3.00 mmol) in methanol (4 mL) under argon. The reaction mixture immediately turned red. The mixture was stirred for 30 min under argon, then treated with 2,2,6,6-tetramethylpiperidine (0.76 mL, 4.5 mmol) and concentrated to dryness. The resulting brown solid was suspended in acetonitrile (60 mL) followed by the successive addition of 2,2,6,6-tetramethylpiperidine (2.6 mL, 15.0 mmol), $Zn(OAc)_2$ (1.65 g, 9.00 mmol), and AgOTf (463 mg, 1.80 mmol). The resulting suspension was refluxed for 22 h exposed to air. The crude mixture was filtered through a silica pad with CH_2Cl_2. The crude product was chromatographed [silica, hexanes/CH_2Cl_2 (1:2)] to afford a green solid (28 mg, 6%): ESI-MS obsd 795.96584, calcd 795.96576 [M^+, M = $C_{37}H_{26}Br_2N_4O_3Zn$].

Zn(II)-3,13-Dibromo-10-[2,4,6-tris(2,5,8,11,14,17-hexaoxanonadecyl-1*H*-1,2,3-triazol-4-ylmethoxy)phenyl]-18,18-dimethylchlorin (ZnC5-Br[3,13]**).** The Cu(I) catalyst was prepared by treatment of $CuSO_4·H_2O$ (15 mg, 0.060 mmol) and sodium ascorbate (24.0 mg, 0.120 mmol) with 600 μL of DI H_2O under argon. The reaction mixture turned brown immediately and was stirred until homogeneous. In a separate vial, **pro-ZnC5-Br**[3,13] (24 mg, 0.030 mmol) and **PEG$_6$-N$_3$** (87 mg, 0.27 mmol) in DMSO (1.2 mL) were treated with freshly prepared Cu (I) catalyst (300 μL) under argon. The reaction mixture was stirred at 40 °C for

16 h. Upon cooling to room temperature, H_2O was added and organic phase was extracted with CH_2Cl_2. The extract was washed (brine), dried (Na_2SO_4), concentrated, and chromatographed [silica, CH_2Cl_2 /CH_3OH (93:7)] to afford a green solid (23 mg, 43%): ESI-MS obsd 1760.54352, calcd 1760.54355 [$(M + H)^+$, M = $C_{76}H_{107}Br_2N_{13}O_{21}Zn$].

Zn(II)-3,13-Bis(methoxycarbonyl)-10-[2,4,6-tris(2,5,8,11,14,17-hexaoxanonadecyl-1*H*-1,2,3-triazol-4-ylmethoxy)phenyl]-18,18-dimethylchlorin (ZnC5-Es[3,13]). Samples of **ZnC5-Br[3,13]** (10 mg, 0.0057 mmol) and $Pd(PPh_3)_4$ (13.2 mg, 0.0114 mmol) were dried in a Schlenk flask under high vacuum for 1 h. The solvent DMF/toluene (1:1) was purged with argon (30 min) and subsequently with CO (30 min). The reaction flask was filled with CO gas and DMF/toluene [0.6 mL, (1:1)]. CO gas was bubbled through the stirred reaction mixture for 2 h. Then excess NaOMe (6.2 mg, 0.11 mmol) in MeOH (285 μL) was added to the reaction mixture. The latter was stirred at 80 °C for 5 min before being cooled to room temperature. A saturated aqueous solution of NH_4Cl was added, and the mixture was extracted with CH_2Cl_2. The organic layer was separated, filtered through Celite (CH_2Cl_2), and concentrated. Column chromatography [silica, CH_2Cl_2/CH_3OH (7:93)] afforded a green oil (3.0 mg, 34%): MALDI-MS obsd 1742.0881, calcd 1742.7158 [$(M + Na)^+$, M = $C_{80}H_{113}N_{13}O_{25}Zn$].

1-{4-[2-(*tert*-Butoxy)-2-oxoethoxy]phenoxy}-5-[2,4,6-tris(propargyloxy)phenyl]dipyrromethane (3e). Following a general procedure,[76] EtMgBr (0.9 M solution in THF, 2.66 mL, 2.39 mmol) was added dropwise to a solution of **2a** (459 mg, 1.19 mmol) in THF (1.2 mL) over a 5 min period. The solution was stirred at room temperature for 10 min before cooling to –78 °C. A solution of **6** (412 mg, 1.19 mmol) in

THF (1.2 mL) was added, and the mixture was stirred at –78 °C for 30 min. The cooling bath was removed and the reaction mixture was allowed to warm to room temperature for 1 h before saturated aqueous NH_4Cl was added. The aqueous layer was removed and washed with CH_2Cl_2. The combined organic extract was washed with brine, concentrated, and chromatographed [silica, hexanes/ethyl acetate (3:1)] to recover starting material **2a** (126 mg) as the first fraction followed by the title compound as a yellow oil (203 mg, 28%): ^{1}H NMR δ 1.44 (s, 9H), 2.53–2.57 (m, 3H), 4.57 (s, 2H), 4.59 (d, *J* = 2.4 Hz, 4H), 4.68 (d, *J* = 2.4 Hz, 2H), 5.92–5.95 (m, 1H), 6.10 (s, 1H), 6.12–6.13 (m, 2H), 6.43 (s, 2H), 6.70–6.72 (m, 1H), 6.73–6.76 (m, 1H), 6.93 (d, *J* = 9 Hz, 2H), 7.84 (d, *J* = 9 Hz, 2H), 8.83 (s, 1H), 9.27 (s, 1H); ^{13}C NMR δ 28.15, 33.0, 56.2, 57.2, 65.7, 76.2, 76.4, 78.1, 82.8, 95.7, 107.6, 108.0, 109.3, 114.2, 117.5, 119.9, 129.8, 130.4, 131.0, 132.3, 142.5, 156.8, 158.2, 160.7, 167.7, 182.8; ESI-MS obsd 619.24297, calcd 619.24388 [$(M + H)^+$, M = $C_{37}H_{34}N_2O_7$].

9-Bromo-1-{4-[2-(*tert*-butoxy)-2-oxoethoxy]phenyl}-5-[2,4,6-tris(propargyloxy)phenyl]dipyrromethane (3e-Br^9). Following a general procedure,[56] a solution of **3e** (77.0 mg, 0.124 mmol) in anhydrous THF (2.5 mL) was treated with NBS (22.1 mg, 0.124 mmol) under argon at –78 °C. The reaction mixture was stirred for 1 h at –78 °C, after which the ice bath was removed and the reaction mixture was allowed to warm to room temperature. Upon reaching 0 °C, hexanes and water were added. The mixture was extracted with ethyl acetate. The organic layer was dried (Na_2SO_4), concentrated, and chromatographed [silica, hexanes/ethyl acetate (3:1)] to afford an orange oil (67 mg, 76%): ^{1}H NMR δ 1.48 (s, 9H), 2.56–2.57 (m, 3H), 4.56 (s, 2H), 4.62 (d, *J* = 2.4 Hz, 4H), 4.68 (d, *J* = 2.4 Hz, 2H), 5.95–5.96 (m, 1H), 6.02 (s, 1H), 6.03–6.04 (m, 2H), 6.42 (s, 2H), 6.73–6.75

(m, 1H), 6.93 (d, J = 9 Hz, 2H), 7.84 (d, J = 9 Hz, 2H), 8.80 (s, 1H), 9.38 (s, 1H); ^{13}C NMR δ 28.11, 33.2, 56.1, 57.1, 65.6, 76.3, 76.6, 77.8, 78.2, 82.8, 95.5, 96.8, 109.4, 110.0, 112.3, 114.2, 119.7, 130.0, 131.0, 132.0, 132.1, 141.4, 156.6, 158.4, 160.7, 167.6, 182.9; ESI-MS obsd 697.15421, calcd 697.15439 [$(M + H)^+$, M = $C_{37}H_{33}BrN_2O_7$].

8,9-Dibromo-1-{4-[2-(*tert*-butoxy)-2-oxoethoxy]phenyl}-5-[2,4,6-tris(3,6,9,12-tetraoxatridecyloxy)phenyl]dipyrromethane (3b-Br^{8,9}). A solution of **3b** (1.14 g, 1.06 mmol) in anhydrous THF (10 mL) was treated with NBS (377.3 mg, 2.12 mmol) under argon at –78 °C. The reaction mixture was stirred for 1 h at –78 °C, after which the ice bath was removed and the reaction mixture was allowed to warm. Upon reaching –20 °C, hexanes (20 mL) and water (20 mL) were added. The mixture was extracted with ethyl acetate. The organic layer was dried (Na_2SO_4), concentrated, and chromatographed [silica, CH_2Cl_2/CH_3OH/ (97:3)] to afford the title compound mixed with tribromodipyrromethane in a ratio of 5:1 on the basis of ^{1}H NMR analysis (1000 mg, impure).

1-{4-[2-(*tert*-Butoxy)-2-oxoethoxy]phenyl}dipyrromethane (3f). Following a general procedure,[76] EtMgBr (1 M solution in THF, 6.2 mL, 6.2 mmol) was added dropwise to a solution of **2f** (0.45 g, 3.1 mmol) in THF (3.4 mL) over a 5 min period. The solution was stirred at room temperature for 10 min before cooling to –78 °C. A solution of **6** (1.07 mg, 3.10 mmol) in THF (3.4 mL) was added, and the mixture was stirred at –78 °C for 30 min. The cooling bath was removed, and the reaction mixture was allowed to warm to room temperature for 1 h before saturated aqueous NH_4Cl was added. The aqueous layer was removed and washed with CH_2Cl_2. The combined organic layer was washed with brine, concentrated, and chromatographed [silica, hexanes/ethyl acetate (4:1)] to recover starting

material **2f** as the first fraction followed by the title compound, which upon concentration gave a white solid (734 mg, 62%): mp 120–122 °C; ^{1}H NMR δ 1.52 (s, 9H), 4.09 (s, 2H), 4.59 (s, 2H), 6.066–6.069 (m, 1H), 6.12–6.15 (m, 2H), 6.62–6.64 (m, 1H), 6.80–6.82 (m, 1H), 6.95 (d, *J* = 8.4 Hz, 2H), 7.86 (d, *J* = 8.4 Hz, 2H), 8.63 (s, 1H), 10.17 (s, 1H); ^{13}C NMR δ 27.9, 49.1, 83.0, 106.3, 106.4, 108.1, 108.2, 109.6, 109.7, 114.2, 117.6, 121.5, 127.9, 130.1, 131.1, 131.9, 139.6, 160.8, 167.8, 183.8; ESI-MS obsd 381.18073, calcd 381.18008 [(M + H)$^+$, M = $C_{22}H_{24}N_2O_4$].

3,12-Dibromo-5-[4-(carboxymethoxy)phenyl]-18,18-dimethylchlorin (pro-FbC8-Br^{3,12}). Following a standard procedure,[72] a solution of **3f** (734 mg, 1.93 mmol) in anhydrous THF (38 mL) was treated with NBS (686 mg, 3.86 mmol) under argon at –78 °C. The reaction mixture was stirred for 1 h at –78 °C, after which the cooling bath was removed and the reaction mixture was allowed to warm. Upon reaching –20 °C, hexanes (38 mL) and water (38 mL) were added. The mixture was extracted with ethyl acetate. The organic layer was dried (Na_2SO_4), concentrated, and chromatographed [silica, hexanes/ethyl acetate (4:1)] to afford 7,9-dibromo-1-[4-(2-(*tert*-butoxy)-2-oxoethoxy)phenyl]dipyrromethane (**3f-Br^{7,9}**) as a light yellow solid (878 mg, 84%): ^{1}H NMR δ 1.49 (s, 9H), 4.05 (s, 2H), 4.59 (s, 2H), 6.00 (d, *J* = 3 Hz, 1H), 6.27–6.29 (m, 1H), 6.87–6.89 (m, 1H), 6.98 (d, *J* = 9 Hz, 2H), 7.87 (d, *J* = 9 Hz, 2H), 10.45 (s, 1H), 11.52 (s, 1H).

Following a general procedure,[77] a solution of **3f-Br^{7,9}** (878 mg, 1.63 mmol) in anhydrous THF (26 mL) and anhydrous methanol (6.6 mL) was treated with $NaBH_4$ (616 mg, 16.3 mmol) at room temperature for 30 min. The reaction mixture was quenched by the addition of saturated aqueous NH_4Cl, and then extracted with ethyl acetate. The combined

organic phase was washed with brine, dried (Na_2SO_4), and concentrated. The resulting oil was dissolved in CH_3CN (16 mL) containing **4-Br**[8] (439 mg, 1.63 mmol) and TFA (125 μL, 1.63 mmol). The resulting mixture was stirred at room temperature for 30 min and then diluted with CH_3CN. Sample of 2,2,6,6-tetramethylpiperidine (4.16 mL, 24.5 mmol), $Zn(OAc)_2$ (4.49 g, 24.5 mmol) and AgOTf (1.26 g, 4.89 mmol) were added successively. The resulting suspension was refluxed for 22 h exposed to air. The crude mixture was filtered through a silica pad with ethyl acetate. The filtrate was concentrated, dissolved in anhydrous CH_2Cl_2 (100 mL), and treated dropwise with TFA (150 μL). After 10 min, saturated aqueous $NaHCO_3$ was added slowly. The organic layer was dried ($NaSO_4$), concentrated and chromatographed [silica, hexanes/CH_2Cl_2 (1:1)] to afford a green solid (8.0 mg, 0.7%): ^{1}H NMR δ –2.12 (br s, 1H), –1.52 (br s, 1H), 1.61 (s, 6H), 2.00 (s, 6H), 4.51 (s, 2H), 4.79 (s, 2H), 7.22 (d, *J* = 8.8 Hz, 2H), 7.84 (d, *J* = 8.8 Hz, 2H), 8.50 (d, *J* = 4.4 Hz, 1H), 8.75 (s, 1H), 8.77 (s, 1H), 8.85 (s, 1H), 8.90 (d, *J* = 4.4 Hz, 1H), 8.96 (s, 1H), 9.82 (s, 1H); ^{13}C NMR δ 28.3, 29.8, 31.3, 40.3, 46.7, 51.5, 66.2, 82.7, 94.7, 96.2, 105.6, 113.1, 116.6, 118.8, 121.8, 124.2, 128.7, 130.1, 132.1, 132.7, 133.2, 134.6, 138.6, 139.3, 151.4, 154.4, 158.4, 164.8, 168.3, 174.8; ESI-MS obsd 703.09084, calcd 703.09139 [$(M + H)^+$, M = $C_{34}H_{32}Br_2N_4O_3$]; λ_{abs} (toluene) 401, 647 nm.

3,12-Diacetyl-5-[4-(carboxymethoxy)phenyl]-18,18-dimethylchlorin (pro-FbC8-A[3,12]). Following a procedure for Stille coupling of chlorins,[56] a mixture of **pro-FbC8-Br**[3,12] (8.0 mg, 0.011 mmol), tributyl(1-ethoxyvinyl)tin (20. μL, 0.055 mmol), and $(Ph_3P)_2PdCl_2$ (1.6 mg, 0.0022 mmol) was stirred in CH_3CN/DMF [600 μL (3:2)] under argon for 4 h at 83 °C in a Schlenk line. The reaction mixture was treated with 10% aqueous HCl (2 mL) at

room temperature for 20 min. CH_2Cl_2 was added. The organic layer was separated, washed (saturated aqueous $NaHCO_3$, water, and brine), dried (Na_2SO_4), concentrated, and chromatographed [silica, CH_2Cl_2/ethyl acetate (49:1)] to afford a brown oil (3.2 mg, 42%): ^{1}H NMR δ –1.97 (br s, 1H), –1.56 (br s, 1H), 1.61 (s, 6H), 2.04 (s, 6H), 2.17 (s, 3H), 3.27 (s, 3H), 4.57 (s, 2H), 4.79 (s, 2H), 7.24 (d, *J* = 8.4 Hz, 2H), 8.02 (d, *J* = 8.4 Hz, 2H), 8.61 (d, *J* = 4.4 Hz, 1H), 8.89 (s, 1H), 8.95 (s, 1H), 8.98 (s, 1H), 9.03 (d, *J* = 4.4 Hz, 1H), 9.27 (s, 1H), 10.81 (s, 1H); ^{13}C NMR δ 28.4, 29.9, 30.1, 31.3, 31.9, 47.0, 51.4, 66.1, 82.9, 96.6, 98.4, 109.3, 113.8, 121.2, 125.5, 126.5, 132.1, 133.1, 133.6, 135.1, 136.6, 137.0, 137.7, 143.3, 153.4, 155.5, 158.8, 163.6, 168.1, 175.4, 197.2, 201.3; ESI-MS obsd 631.29117, calcd 631.29150 [$(M + H)^+$, M = $C_{38}H_{38}N_4O_5$]; λ_{abs} (toluene) 430, 671 nm.

(III) Absorption spectra

The spectral properties of the PEGylated chlorins **ZnC1** and **FbC1** are shown in Figure 3.6. **ZnC1** exhibited almost unchanged spectroscopic properties over a concentration range of 1000-fold, indicating high solubility of the chlorin in water. On the other hand, at higher concentrations, **FbC1** exhibited no significant broadening in the Q_y band, but the shape of the B bands changed at concentrations ~800 μM showing some degree of aggregation.

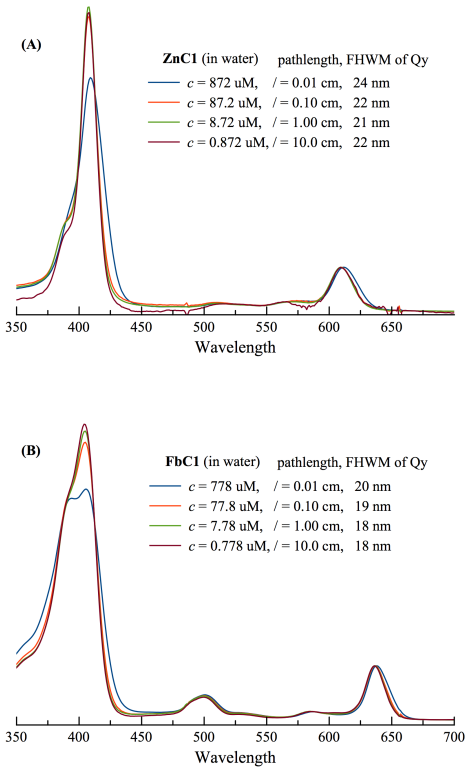

Figure 3.6. Absorption versus concentration of **ZnC1** and **FbC1** over a range of 1000-fold. The spectra are normalized at the Q_y band; the FWHM of the Q_y band is shown in the inset.

Absorption spectra of **ZnC3** and **FbC3** in neat water at ~5 μM are shown in Figure 3.7. Obvious broadening of the spectra is evident.

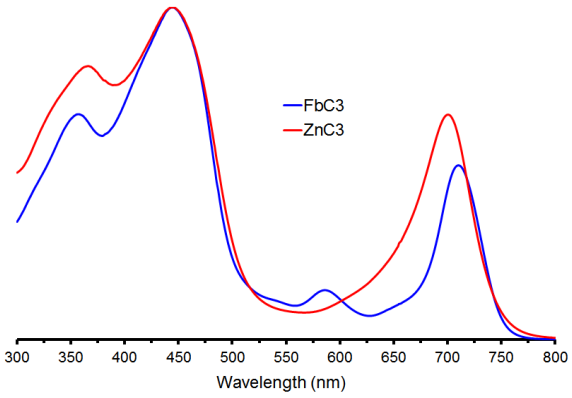

Figure 3.7. Absorption spectra of PEGylated chlorins in H_2O.

(IV) Purification of PEGylated compounds

One essential issue arising from the pre-installation route concerns the purification process. During flash chromatography, PEGylated compounds possessing high polarity tended to bind tightly to silica gel. When the crude mixture containing the desired product was mixed with PEG-containing impurities, the resolution of the flash chromatography process was compromised. A typical flash chromatography (3 cm dia. × 15 cm) procedure entails: (1) pack the column and load the crude mixture with CH_2Cl_2 (or ethyl acetate); (2) elute with one column volume of CH_2Cl_2 (or ethyl acetate) to remove impurities while the PEGylated precursors remained bound or near the top of the column; and (3) elute with CH_2Cl_2 with a gradual increase of 0.5–5% MeOH (or EtOH with ethyl acetate[78]) to remove PEG-containing impurities and isolate the desired product. The PEGylated precursors **1b**, **1b**′, and **2b** generally were obtained with good purity following the above procedure. For acylation of **2b**, the crude mixture often contained ~20% of unreacted starting material **2b**. Isolation of **3b** with good purity required prolonged elution (2–3 h) in step 3.

The purification of the PEGylated chlorins proceeded in the same manner as employed for separation of multiporphyrin arrays.[60] A general purification procedure for the crude PEGylated chlorin is as follows, which afforded the PEGylated chlorins **ZnC1**, **pro-ZnC2**, and **FbC3** in good purity:

(1) Silica chromatography (2 cm dia. × 10 cm) was eluted with CH_2Cl_2 (0.5–5% MeOH).

(2) Size-exclusion chromatography (4 cm dia. × 40 cm; Bio Beads S-X3, 200–400 mesh; flow rate: ~1.5 ml/min) was eluted with toluene (HPLC grade).

(3) Flash silica chromatography (2 cm dia. × 4 cm) was eluted with CH_2Cl_2 (0.5–10% MeOH, HPLC grade).

(V) 3-Dimensional conformation

The conformation of the 2,4,6-trisubstituted aryl motif was examined by ^{1}H NMR spectroscopy. Protons on the PEG chain typically resonate at 3.4–4.6 ppm, depending on the terminal substitution groups. Indeed, the PEGylated precursors **1b**, **1b′**, **2b**, and **3b** exhibited a complicated resonance pattern in this region in the ^{1}H NMR spectra. No significant difference was found between the resonances of protons from the *ortho*- and *para*-PEG chains in the non-macrocyclic precursors. However, for the PEGylated chlorins a significant difference was observed. The protons of the *para*-PEG chain resonated similarly to that of a typical PEG-chain, while the protons of the *ortho*-PEG chains resonated at a higher frequency, ranging from 1.7–3.2 ppm. A ^{1}H NMR spectrum of PEGylated chlorins is demonstrated by **pro-FbC2** and shown in Figure 3.8. The *ortho*-PEG chains are conformationally restricted to above and below the macrocycle plane and thus are magnetically more shielded due to the aromatic ring-current effect. Although detailed

analyses and assignments of PEG-protons do not relate to our main interests, the different resonance regions clearly show that the desired geometric design was achieved.

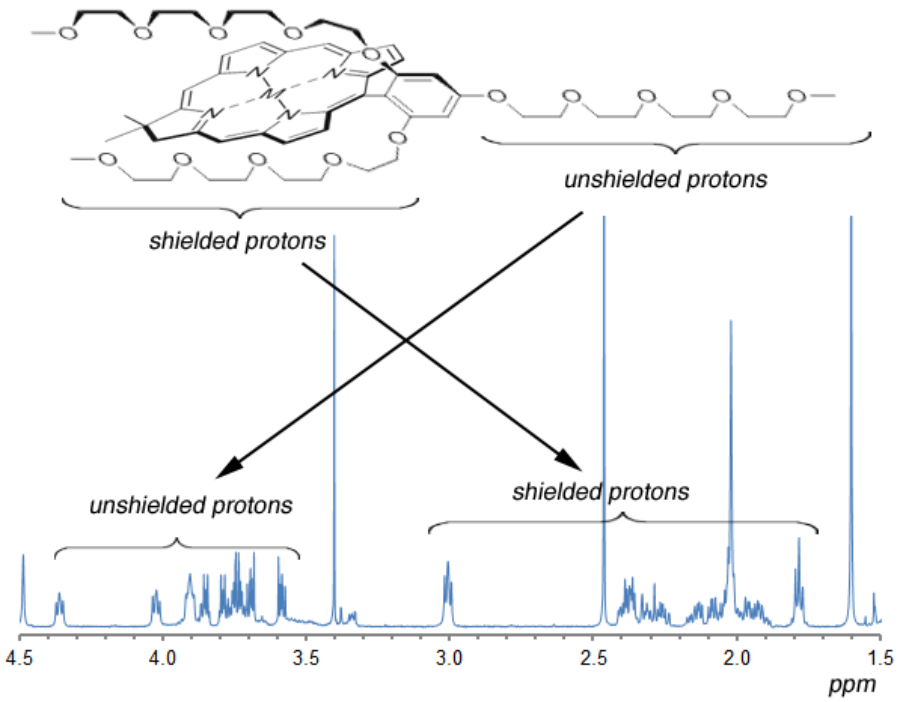

Figure 3.8. ^{1}H NMR spectrum (in $CDCl_3$ at room temperature) of **pro-ZnC2** and illustrative representation of shielded and unshielded protons. Note: the scheme only represents the relative orientation of the chlorin and the PEG moiety and does not reflect the actual size and conformation.

References

1 N. Y. Kiang, J. Siefert, Govindjee and R. E. Blankenship, *Astrobiol.*, 2007, **7**, 222–251.

2 K. Licha, *Top. Curr. Chem.,* 2002, **222**, 1–29.

3 J. B. Dawson, D. J. Barker, D. J. Ellis, E. Grassam, J. A. Cotterill, G. W. Fisher and J.

W. Feather, *Phys. Med. Biol.*, 1980, **25**, 695–709.

4 P. K. Chattopadhyay, C.-M. Hogerkorp and M. Roederer, *Immunology*, 2008, **125**, 441–449.

5 P. K. Chattopadhyay and M. Roederer, *Methods*, 2012, **57**, 251–258.

6 S. C. Bendall, G. P. Nolan, M. Roederer and P. K. Chattopadhyay, *Trends Immunol.*, 2012, **33**, 323–332.

7 J. Fabian, H. Nakazumi and M. Matsuoka, *Chem. Rev.*, **1992**, 92, 1197–1226.

8 S. Stoyanov, in *Near-Infrared Applications in Biotechnology*, ed. R. Raghavachari, Marcel Dekker Inc., New York, 2001, pp. 35–93.

9 H. Scheer, in *Chlorophylls and Bacteriochlorophylls. Biochemistry, Biophysics, Functions and Applications*, ed. B. Grimm, R. J. Porra, W. Rüdiger and H. Scheer, Springer: Dordrecht, The Netherlands, 2006, Advances in Photosynthesis and Respiration, vol. 25, pp. 1−26.

10 V. Y. Pavlov and G. V. Ponomarev, *Chem. Heterocycl. Compd.*, 2004, **40**, 393−425.

11 T. S. Balaban, H. Tamiaki and A. R. Holzwarth, *Top. Curr. Chem.*, 2005, **258**, 1−38.

12 H. Tamiaki and M. Kunieda, in *Handbook of Porphyrin Science*, ed. K. M. Kadish, K. M. Smith and R. Guilard, World Scientific Co.: Singapore, 2011, vol. 11, pp. 223−290.

13 I. Yoon, D. Demberelnyamba, J. Z. Li and Y. K. Shim, in *Handbook of Porphyrin Science*, ed. K. M. Kadish, K. M. Smith and R. Guilard, World Scientific Co.: Singapore, 2014, vol. 33, pp. 167−224.

14 A. A. Ryan and M. O. Senge, *Photochem. Photobiol. Sci.*, 2015, **14**, 638−660.

15 J. S. Lindsey, *Chem. Rev.*, 2015, **115**, 6534–6620.

16 J. A. S. Cavaleiro, M. G. P. M. S. Neves and A. C. Tomé, *Arkivoc*, 2003, **14**, 107–130.

17 A. M. G. Silva and J. A. S. Cavaleiro, in *Prog. Heterocycl. Chem.*, ed. G. W. Gribble and J. A. Joule, Elsevier: Amsterdam, 2008, vol. 19, pp. 44–69.

18 Z. Yu and M. Ptaszek, *J. Org. Chem.*, 2013, **78**, 10678–10691.

19 Z. Yu, C. Pancholi, G. V. Bhagavathy, H. S. Kang, J. K. Nguyen and M. Ptaszek, *J. Org. Chem.*, 2014, **79**, 7910–7925.

20 A. Meares, A. Satraitis, N. Santhanam, Z. Yu and M. Ptaszek, *J. Org. Chem.*, 2015, **80**, 3858–3869.

21 C. Brückner, *Acc. Chem. Res.*, DOI: 10.1021/acs.accounts.6b00043.

22 J. Jiang, M. Taniguchi and J. S. Lindsey, *New J. Chem.,* 2015, **39**, 4534–4550.

23 P. Hambright, in *The Porphyrin Handbook*, ed. K. M. Kadish, K. M. Smith and R. Guilard, Academic Press: San Diego, CA, 2000, vol. 3, pp. 129–210.

24 S. Pisarek, K. Maximova and D. Gryko, *Tetrahedron*, 2014, **70**, 6685–6715.

25 N. Larson and H. Ghandehari, *Chem. Mater.*, 2012, **24**, 840–853.

26 A. Kolate, D. Baradia, S. Patil, I. Vhora, G. Kore and A. Misra, *J. Control. Release*, 2014, **192**, 67–81.

27 J. Herzberger, K. Niederer, H. Pohlit, J. Seiwert, M. Worm, F. R. Wurm and H. Frey, *Chem. Rev.*, 2016, **116**, 2170–2243.

28 T. Aida, A. Takemura, M. Fuse and S. Inoue, *J. Chem. Soc., Chem. Commun.*, 1988, 391–393.

29 K. E. Borbas, V. Chandrashaker, C. Muthiah, H. L. Kee, D. Holten and J. S. Lindsey, *J. Org. Chem*., 2008, **73**, 3145–3158.

30 K. E. Borbas, P. Mroz, M. R. Hamblin and J. S. Lindsey, *Bioconjugate Chem*., 2006, **17**, 638–653.

31 Z. Yao, K. E. Borbas and J. S. Lindsey, *New J. Chem.*, 2008, **32**, 436–451.

32 K. E. Borbas, H. L. Kee, D. Holten and J. S. Lindsey, *Org. Biomol. Chem.*, 2008, **6**, 187–194.

33 A. Z. Muresan and J. S. Lindsey, *Tetrahedron*, 2008, **64**, 11440–11448.

34 J. Jiang, C.-Y. Chen, N. Zhang, P. Vairaprakash and J. S. Lindsey, *New J. Chem.*, 2015, **39**, 403–419.

35 J. Jiang, E. Yang, K. R. Reddy, D. M. Niedzwiedzki, C. Kirmaier, D. F. Bocian, D. Holten and J. S. Lindsey, *New J. Chem.*, 2015, **39**, 5694–5714.

36 J. M. Harris, in *Poly(ethylene glycol) Chemistry – Biotechnical and Biomedical Applications*, ed. J. M. Harris, Plenum Press: New York, 1992, pp. 1–14.

37 S. Zalipsky and J. M. Harris, in *Poly(ethylene glycol) Chemistry and Biological Applications*, ed. J. M. Harris and S. Zalipsky, American Chemical Society: Washington, DC, 1997, pp. 1–13.

38 M. S. Thompson, T. P. Vadala, M. L. Vadala, Y. Lin and J. S. Riffle, *Polymer*, 2008, **49**, 345–373.

39 N. Zhang, J. Jiang, M. Liu, M. Taniguchi, A. K. Mandal, R. B. Evans-Storm, J. B. Pitner, C. Kirmaier, D. F. Bocian, D. Holten and J. S. Lindsey, *companion submitted paper*.

40 J. Jiang, K. R. Reddy, M. P. Pavan, E. Lubian, M. A. Harris, J. Jiao, D. M. Niedzwiedzki, C. Kirmaier, P. S. Parkes-Loach, P. A. Loach, D. F. Bocian, D. Holten and J. S. Lindsey, *Photosynth. Res.,* 2014, **122**, 187–202.

41 F. Giuntini, C. M. A. Alonso and R. W. Boyle, *Photochem. Photobiol. Sci.*, 2011, **10**, 759–791.

42 M. F. Grahn, A. McGuinness, M. L. de Jode, A. Giger, A. S. Dhiman, C.-M. Cheung, S. Pavitt, R. Benzie and N. S. Williams, *Proc. SPIE*, 1997, **3191**, 180–186.

43 D. Li, P. Li, H. Lin, Z. Jiang, L. Guo and B. Li, *J. Photochem. Photobiol. B: Biol.*, 2013, **127**, 28–37.

44 J. L. Worlinsky, S. Halepas and C. Brückner, *Org. Biomol. Chem.*, 2014, **12**, 3991–4001.

45 D. Ra, K. A. Gauger, K. Muthukumaran, T. Balasubramanian, V. Chandrashaker, M. Taniguchi, Z. Yu, D. C. Talley, M. Ehudin, M. Ptaszek and J. S. Lindsey, *J. Porphyrins Phthalocyanines*, 2015, **19***,* 547–572.

46 F. Dumoulin and V. Ahsen, *J. Porphyrins Phthalocyanines*, 2011, **15**, 481–504.

47 J. K. Laha, S. Dhanalekshmi, M. Taniguchi, A. Ambroise and J. S. Lindsey, *Org. Process Res. Dev.*, 2003, **7**, 799–812.

48 M. Ptaszek, B. E. McDowell and J. S. Lindsey, *J. Org. Chem.*, 2006, **71**, 4328–4331.

49 M. Taniguchi, D. Ra, G. Mo, T. Balasubramanian and J. S. Lindsey, *J. Org. Chem.*, 2001, **66**, 7342–7354.

50 M. Ptaszek, J. Bhaumik, H.-J. Kim, M. Taniguchi and J. S. Lindsey, *Org. Process Res. Dev.*, 2005, **9**, 651–659.

51 M. Taniguchi, M. Ptaszek, B. E. McDowell, P. D. Boyle and J. S. Lindsey, *Tetrahedron*, 2007, **63**, 3850–3863.

52 A. R. Battersby, C. J. R. Fookes and R. J. Snow, *J. Chem. Soc. Perkin Trans. 1*, 1984, 2725−2732.

53 J.-P. Strachan, D. F. O'Shea, T. Balasubramanian and J. S. Lindsey, *J. Org. Chem.*, 2000, **65**, 3160–3172. Additions and Corrections: J.-P. Strachan, D. F. O'Shea, T. Balasubramanian and J. S. Lindsey, *J. Org. Chem.*, 2001, **66**, 642.

54 P. Liu, L. Huang and M. M. Faul, *Tetrahedron Lett.*, 2007, **48***,* 7380–7382.

55 K. P. Cusack, E. C. Breinlinger, S. R. Fix-Stenzel, R. H. Stoffel, K. R. Woller, A. D. Hobson and P. Grongsaard, US Pat. Appl., 0 207 704, 2011.

56 J. K. Laha, C. Muthiah, M. Taniguchi, B. E. McDowell, M. Ptaszek and J. S. Lindsey, *J. Org. Chem.*, 2006, **71**, 4092–4102. Additions and Corrections: J. K. Laha, C. Muthiah, M. Taniguchi, B. E. McDowell, M. Ptaszek and J. S. Lindsey, *J. Org. Chem.*, 2009, **74**, 5122.

57 M. Krayer, T. Balasubramanian, C. Ruzié, M. Ptaszek, D. L. Cramer, M. Taniguchi and J. S. Lindsey, *J. Porphyrins Phthalocyanines*, 2009, **13**, 1098–1110.

58 J. K. Laha, C. Muthiah, M. Taniguchi and J. S. Lindsey, *J. Org. Chem.*, 2006, **71**, 7049–7052.

59 C. Ruzié, M. Krayer and J. S. Lindsey, *Org. Lett*., 2009, **11**, 1761–1764.

60 R. S. Loewe, K.-Y. Tomizaki, W. J. Youngblood, Z. Bo and J. S. Lindsey, *J. Mater. Chem.*, 2002, **12**, 3438–3451.

61 J. M. Yuen, M. A. Harris, M. Liu, J. R. Diers, C. Kirmaier, D. F. Bocian, J. S. Lindsey

and D. Holten, *Photochem. Photobiol.*, 2015, **91**, 331–342.

62 J. Jiang, P. Vairaprakash, K. R. Reddy, T. Sahin, M. P. Pavan, E. Lubian and J. S. Lindsey, *Org. Biol. Chem.*, 2014, **12**, 86–103.

63 R. Nguyen, S. Perfetto, Y. D. Mahnke, P. Chattopadhyay and M. Roederer, *Cytometry Part A*, 2013, **83A**, 306–315.

64 P. K. Chattopadhyay, B. Gaylord, A. Palmer, N. Jiang, M. A. Raven, G. Lewis, M. A. Reuter, A. K. M. N. Rahman, D. A. Price, M. R. Betts and M. Roederer, *Cytometry Part A*, 2012, **81A**, 456–466.

65 N. Srinivasan, C. A. Haney, J. S. Lindsey, W. Zhang and B. T. Chait, *J. Porphyrins Phthalocyanines,* 1999, **3**, 283–291.

66 Tech Tip #6, Thermo Fisher Scientific, Inc., 2008.

67 M. Liu, C.-Y. Chen, A. K. Mandal, V. Chandrashaker, R. B. Evans-Storms, J. B. Pitner, D. F. Bocian, D. Holten and J. S. Lindsey, *Chem. Sci.*, 2016.

68 J. T. Wiltshire and G. G. Qiao, *J. Polym. Sci.: Part A: Polym. Chem.*, 2009, **47**, 1485–1498.

69 E. H. H. Wong, M. H. Stenzel, T. Junkers and C. Barner-Kowollik, *Macromolecules*, 2010, **43**, 3785–3793.

70 C.-H. Lee and J. S. Lindsey, *Tetrahedron*, 1994, **50**, 11427–11440.

71 M. Ptaszek, D. Lahaye, M. Krayer, C. Muthiah and J. S. Lindsey, *J. Org. Chem.*, 2010, **75**, 1659–1673.

72 O. Mass, M. Ptaszek, M. Taniguchi, J. R. Diers, H. L. Kee, D. F. Bocian, D. Holten and J. S. Lindsey, *J. Org. Chem.*, 2009, **74**, 5276–5289.

73 O. Mass, D. R. Pandithavidana, M. Ptaszek, K. Santiago, J. W. Springer, J. Jiao, Q. Tang, C. Kirmaier, D. F. Bocian, D. Holten and J. S. Lindsey, *New J. Chem.*, 2011, **35**, 2671–2690.

74 B. J. Littler, M. A. Miller, C.-H. Hung, R. W. Wagner, D. F. O'Shea, P. D. Boyle and J. S. Lindsey, *J. Org. Chem.*, 1999, **64**, 1391–1396.

75 M. Ptaszek, B. E. McDowell, M. Taniguchi, H.-J. Kim and J. S. Lindsey, *Tetrahedron*, 2007, **63**, 3826–3839.

76 S. H. H. Zaidi, K. Muthukumaran, S.-I. Tamaru and J. S. Lindsey, *J. Org. Chem.*, 2004, **69**, 8356–8365.

77 H. L. Kee, C. Kirmaier, Q. Tang, J. R. Diers, C. Muthiah, M. Taniguchi, J. K. Laha, M. Ptaszek, J. S. Lindsey, D. F. Bocian and D. Holten, *Photochem. Photobiol*., 2007, **83**, 1110–1124.

78 J. P. Taygerly, L. M. Miller, A. Yee and E. A. Peterson, *Green Chem.*, 2012, **14**, 3020–3025.

CHAPTER 4

Bioconjugatable, PEGylated Hydroporphyrins for Photochemistry and Photomedicine. Narrow-Band, Near-Infrared-Emitting Bacteriochlorins

Preamble. This contents in this chapter have been submitted[52] with contributions from the following individuals. Nuonuo Zhang: synthesis of **B3**, **B4, B5** and corresponding precursors. Jianbin Jiang: synthesis of **B2** and corresponding presursors. Amit Kumar Mandal (Holten group, Washington University, St. Louis): photophysical property studies on PEGylated bacteriochlorins. Rosemary B. Evans-Storms and J. Bruce Pitner (NIRvana Sciences, Research Triangle Park): flow cytometry study.

Introduction

Photochemistry in the NIR spectral region (700–1400 nm) has been far less explored than the visible or ultraviolet regions owing chiefly to availability of suitable chromophores. Yet, the NIR presents a number of distinct opportunities. The broadest spectral distribution of sunlight harvested for photosynthesis is achieved by anoxygenic bacteria, which deploy bacteriochlorophylls in light-harvesting assemblies that capture light with wavelengths in the 700–900 nm region, and in some cases to ~1000 nm.[1] An optical window for penetration of soft tissue by light occurs with midpoint near ~800 nm.[2] More generally, NIR light gives rise to excited states of relatively low energy (~30–40 kcal/mol), far less than that of typical chemical bonds, versus ultraviolet light which affords excited-state energies (up to ~140

kcal/mol) that exceed those of many chemical bonds.

Our work over the past decade has focused on developing synthetic bacteriochlorins as a class of compounds for use in diverse photochemical studies.[3] A number of routes are available for gaining access to bacteriochlorins.[4-13] The synthetic bacteriochlorins contain the core chromophore of natural bacteriochlorophylls[14] yet also afford amenability toward molecular tailoring to meet diverse objectives (Chart 4.1). The presence of a geminal dimethyl group in each pyrroline ring stabilizes the macrocycle toward adventitious dehydrogenation. One objective has been to gain access to a palette of water-soluble, bioconjugatable, wavelength-tunable bacteriochlorins.[15] In energy sciences, such bacteriochlorins can be employed in light-harvesting architectures and as constituents of energy-transfer cascades.[16,17] In photomedicine, the bacteriochlorins are effective in photodynamic therapy[18,19] and in optical imaging.[20-25] In clinical diagnostics, the bacteriochlorins are candidates for fluorescent markers in flow cytometry.[26] For polychromatic flow cytometry,[27-29] a palette of bacteriochlorins spanning the NIR spectral region would complement that of a corresponding set of chlorins in the red spectral region as described in the companion paper.[30]

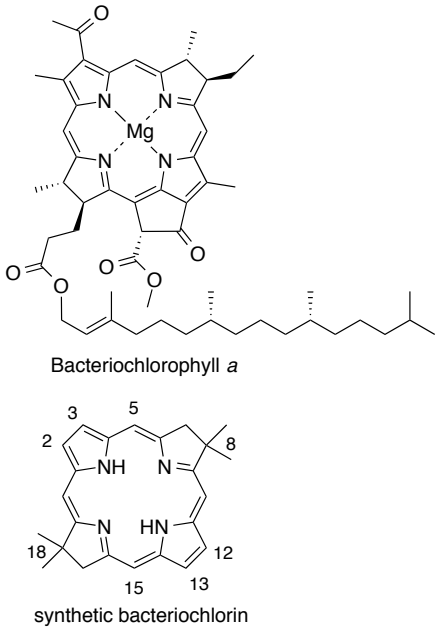

Chart 4.1. Natural and synthetic bacteriochlorins

The construction of bacteriochlorins with the combination of features for water solubility, bioconjugation, and wavelength tunability has proven to be very challenging. The general structure of the synthetic bacteriochlorins is shown in Chart 4.1. Installing a single bioconjugatable tether has been achieved in a straightforward manner by regioselective 15-bromination of a 5-methoxybacteriochlorin followed by Pd-mediated coupling.[11] Tuning the position of the long-wavelength (Q_y) absorption band from ~700–900 nm has chiefly been achieved by appropriate choice of auxochromes located at the β-pyrrolic (2, 3, 12, 13) positions about the perimeter of the macrocycle.[3] Indeed, a palette of lipophilic bacteriochlorins bearing diverse tethers was recently prepared for bio-orthogonal labeling.[31] On the other hand, achieving water solubility has proved quite challenging alone and has been even more daunting to accomplish while maintaining the other desired features of

bioconjugation and wavelength tunability.[15]

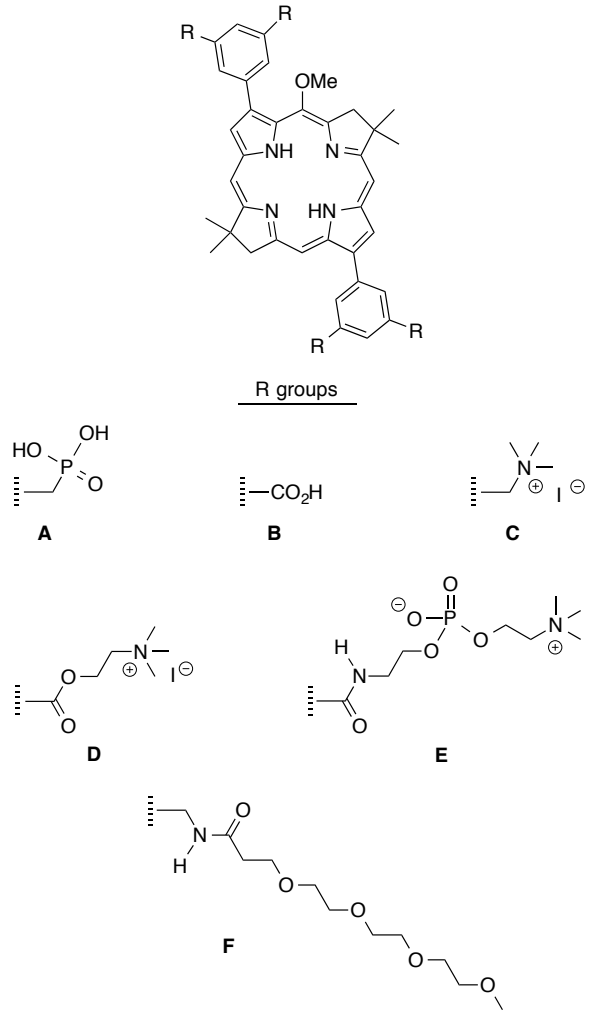

Chart 4.2. Water-solubilization motifs with bacteriochlorins.

In the companion paper, a general strategy for water-solubilization of chlorins entailed use of PEG groups located at the 2,6-positions of a meso-aryl substituent, which caused the polar groups to project above and below the plane of the macrocycle.[30] The

present synthetic route to bacteriochlorins is not amenable to incorporation of such sterically hindered 2,6-substituted aryl groups at any macrocycle position. Accordingly, we recently incorporated 3,5-disubstituted aryl groups located at the β-pyrrole positions wherein the 3,5-substituents are quite polar.[15] The substituents **A–F** are shown in Chart 4.2. The polar substituents are not thrust over the plane of the macrocycle as in the case for the 2,6-substitution pattern with chlorins, but still imparted a significant degree of aqueous solubility. The substituents include phosphonate (**A**), carboxylate (**B**), ammonium (**C**), choline-ester (**D**), phosphatidylcholine-ester (**E**), and oligoethyleneoxy (PEG, **F**) units. The common scaffold resulted in each bacteriochlorin exhibiting essentially the same spectral properties.[15] Among these various motifs, the PEG group was most attractive for aqueous solubilization and bioconjugation. The nonionic nature of the PEG facilitates handling – the PEG derivatives are soluble in both water and organic solvents,[32,33] but readily partition from water into dichloromethane thereby enabling partitioning of crude reaction mixtures. Moreover, the PEG group is compatible with bioconjugation strategies without cross-reactions as can occur with carboxylates, phosphonates, and amines.

In this paper, we report the design and synthesis of five bioconjugatable bacteriochlorins (**B1–B5**) that bear PEG groups at the 3,5-positions of appended aryl moieties (Chart 4.3). The five bacteriochlorins were prepared by elaboration of the bacteriochlorin building blocks **BC-Br^{3,13}** and **BC-Br^{2,12}Es^{3,13}**, which in turn were obtained by *de novo* synthesis.[10-13] The bacteriochlorins afford distinct Q_y band positions owing to the presence of auxochromes at the macrocycle β-positions (2,12-, 3,13-, 7-sites) and meso-positions (15-site), and hence are of interest for use in light-harvesting and in flow cytometry.

Two benchmark bacteriochlorins (**I**, **II**) lacking bioconjugatable groups also were prepared. The bacteriochlorins have been characterized for solubility in dilute aqueous solution. The spectroscopic properties of bacteriochlorin **I** were reported previously;[15] the synthesis is provided herein. The photophysical properties, including rate constants and yields for fluorescence emission, have been measured. One bacteriochlorin was attached to an antibody and examined via flow cytometry. Taken together, the advances reported herein broaden the scope of synthetically accessible chromophores for use in the NIR spectral region, particularly where sharp absorption and emission bands are advantageous.

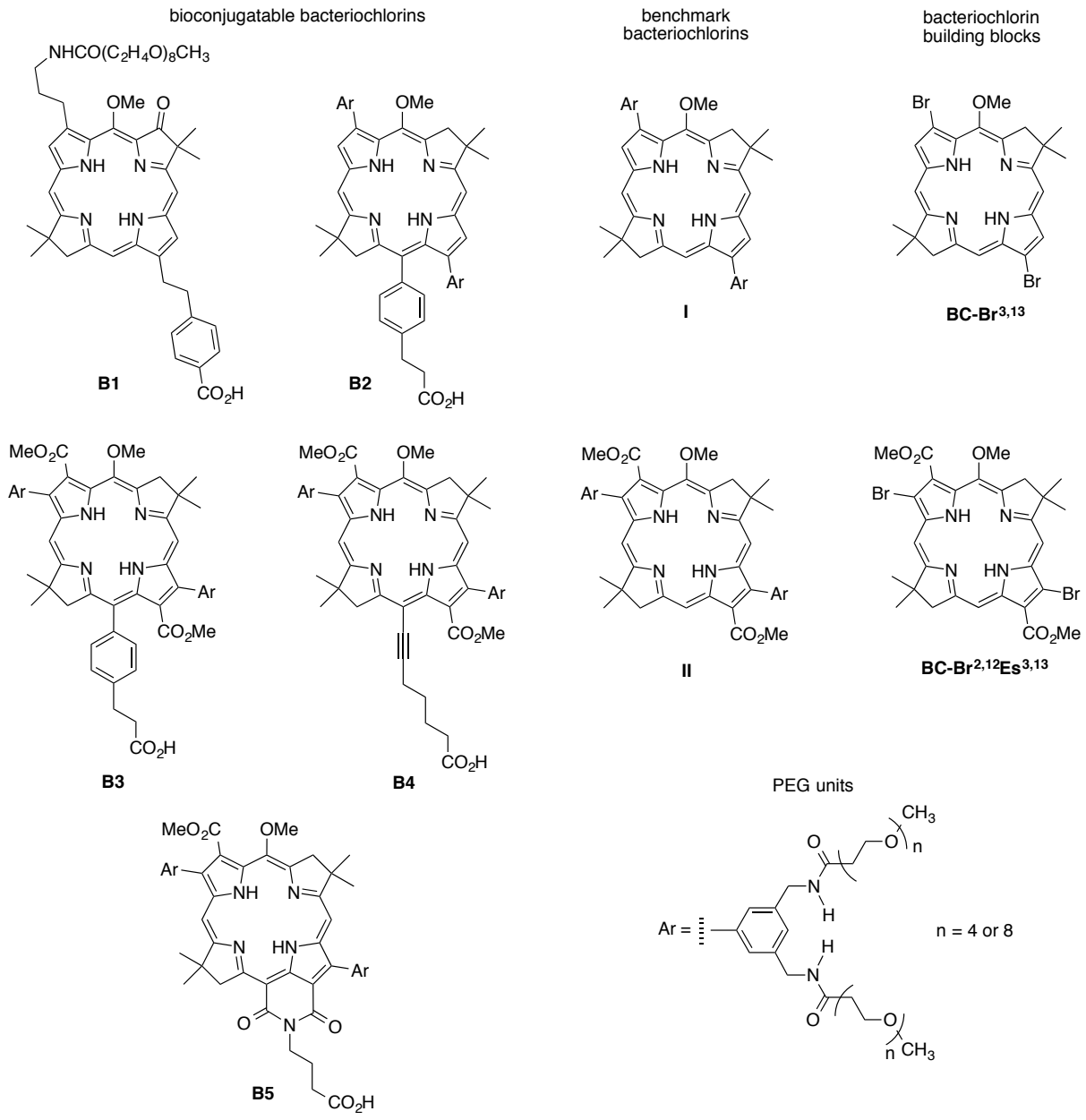

Chart 4.3. Target PEGylated bacteriochlorins and precursor building blocks.

Results and discussion

(I) Synthesis

(A) Bacteriochlorin B1. An oxobacteriochlorin was synthesized to shift the Q_y band hypsochromically into the red spectral region. Treatment of **BC-Br**[3,13] with MnO_2 in CH_2Cl_2 afforded oxobacteriochlorin **B6** in 54% yield.[34] The steric hindrance caused by the methoxy group at the 5-position causes Pd-mediated coupling with the 3,13-dibromobacteriochlorin to proceed regioselectively at the 13-position.[24,35,36] therefore, the Sonogashira coupling reaction of **B6** with methyl 4-ethynylbenzoate **1** regioselectively proceeded at the 13-position of the macrocycle to give ethynylbacteriochlorin **B7** in 42% yield (Scheme 4.1). Further reaction of **B7** with $Pd(PPh_3)_2Cl_2$ and Et_3N in DMF at 80 °C gave unsymmetrically substituted derivative **B8**.[35] The alkynes in **B8** were reduced[37] to the fully saturated alkyl moieties by catalytic hydrogenation to obtain dialkylbacteriochlorin **B9** in 85% yield. Absorption spectroscopy was used to monitor the reduction, given that prolonged reaction afforded side products. The Boc groups were deprotected by treatment with 17% TFA in CH_2Cl_2 to release free amine. The methyl group was removed under 4 M aqueous NaOH solution to afford the carboxylic acid. Without purification, PEGylation of deprotected bacteriochlorin with **PEG$_8$-NHS** was carried out directly in the presence of Cs_2CO_3 to give target oxobacteriochlorin **B1** in 63% yield.

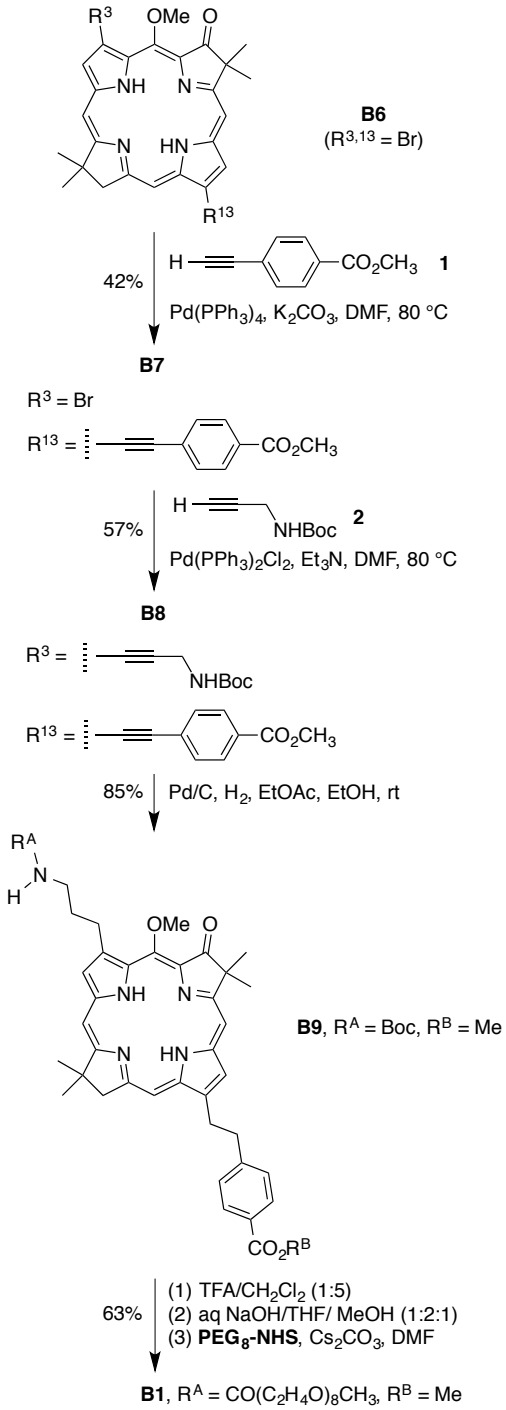

Scheme 4.1. Synthesis of a PEGylated oxobacteriochlorin.

(B) Bacteriochlorins B2 and I. Suzuki coupling reaction of **BC-Br**[3,13] with the coupling partner **3** previously gave the corresponding 3,13-diarylbacteriochlorin **B10** in 85% yield (Scheme 4.2).[15] This procedure was carried out here at 6-fold larger scale in 90% yield. The four Boc groups were smoothly removed upon treatment with 40% TFA in CH_2Cl_2 to give bacteriochlorin **B11** in 78% yield.[15] The tetraaminobacteriochlorin **B11** was subjected to PEGylation with **PEG_4-NHS** to give the water-soluble benchmark bacteriochlorin **I** in 80% yield.

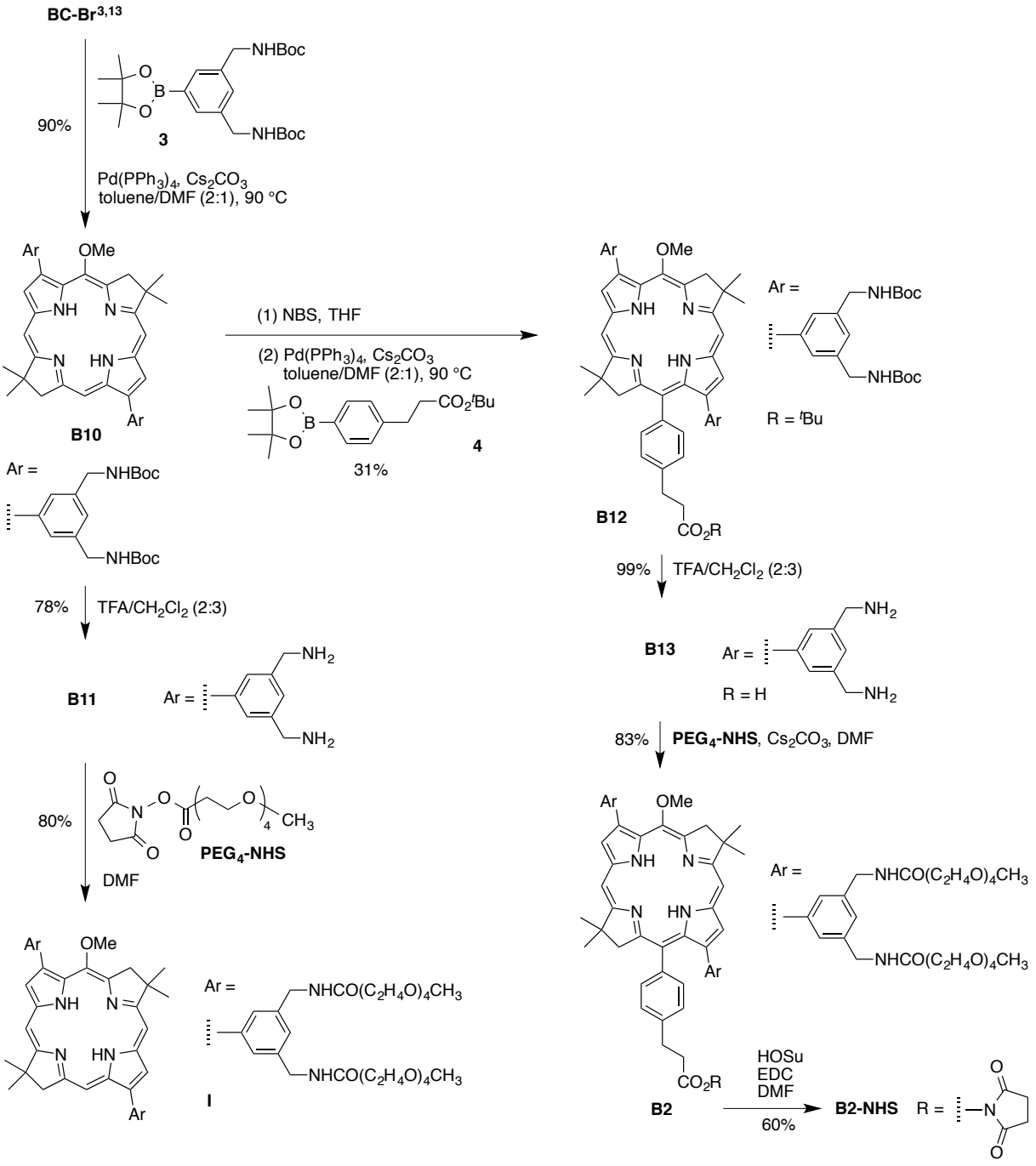

Scheme 4.2. Synthesis of PEGylated bacteriochlorins.

Bromination of bacteriochlorin **B10** with NBS afforded the 15-brominated bacteriochlorin[11] along with an almost equal amount of unreacted bacteriochlorin (on the assumption of equal desorption and ionization efficiencies upon MALDI mass spectrometry) (Scheme 4.2). The crude reaction mixture was not separable by column chromatography, and was used directly in the next step. The Suzuki coupling reaction with partner **4**[38] gave the corresponding 3,5-diaryl-15-(carboxyaryl)bacteriochlorin **B12** in 31% yield from two steps. Upon treatment of 40% TFA in CH_2Cl_2, four Boc groups were removed smoothly, as well as the *tert*-butyl protecting group. The amine-containing bacteriochlorin **B13** was subjected to PEGylation in the presence of Cs_2CO_3 to afford the water-soluble PEGylated bacteriochlorin **B2** in 83% yield. The aforementioned synthesis of **B2** was based on a small-scale synthesis (~10 mg); a larger scale synthesis afforded ~40 mg of **B2** starting from **B10** (Supplimentary information).

(C) Bacteriochlorins B3, **B4** and **II.** The Suzuki coupling reaction of the dibromobacteriochlorin bearing two ester groups **BC-Br^{2,12}Es^{3,13}** with **3** gave Boc-protected bacteriochlorin **B14** in 80% yield (Scheme 4.3). Bacteriochlorin **B14** was treated with 20% TFA in CH_2Cl_2 to unveil the four primary amines, which were used as handles for attaching four PEG_8 units to give benchmark bacteriochlorin **II** in 54% yield. Bromination of bacteriochlorin **B14** with NBS gave the 15-brominated bacteriochlorin **B15** in 50% yield. Sonogashira coupling of **B15** initially with *tert*-butyl 6-heptynoate did not afford the desired product, while the unprotected 6-heptynoic acid (**5**) gave bacteriochlorin **B16** in 15% yield. Deprotection of the four amines followed by PEGylation with **PEG_4-NHS** afforded the water-soluble bioconjugatable bacteriochlorin **B4** in 55% yield from two steps.

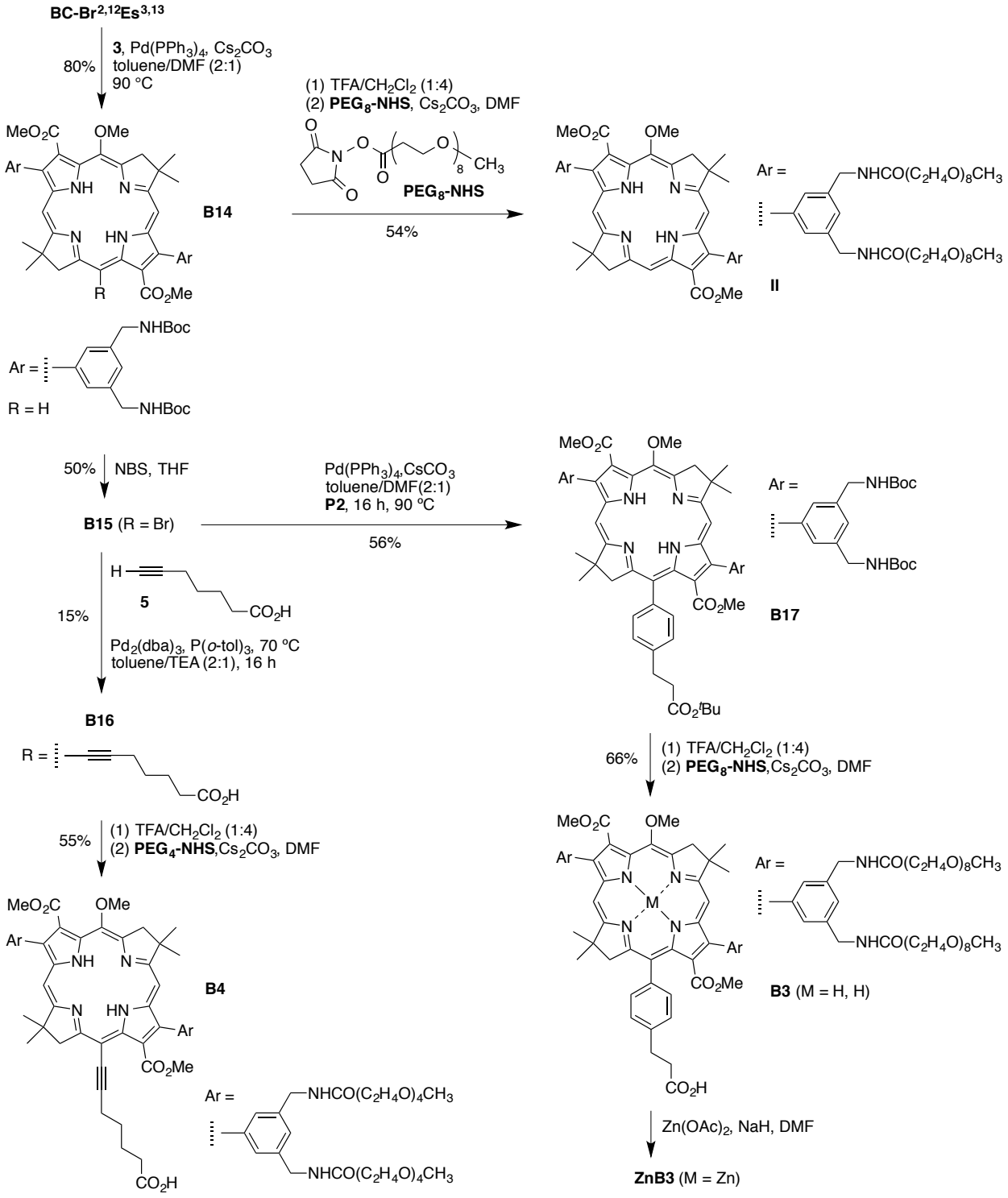

Scheme 4.3. Synthesis of PEGylated bacteriochlorin–diesters.

Target bacteriochlorin **ZnB3** with a predicted Q_y absorption band at ~760 nm was designed using the same strategy as for bacteriochlorin **B2** (Scheme 4.3). Suzuki coupling reaction of **B15** with compound **4** smoothly afforded bacteriochlorin **B17** in 56% yield. Cleavage of Boc and *tert*-butyl protecting groups using 20% TFA in CH_2Cl_2 followed by PEGylation of the four amino groups with **PEG$_8$-NHS** yielded **B3** in 66% yield. Bacteriochlorin **B3** was metalated with zinc (in DMF containing NaH)[39] to tune the wavelength from 742 nm to 754 nm. However, the resulting zinc-metalated bacteriochlorin **ZnB3** demetalated to give the free-base bacteriochlorin **B3** on standing for 2 h in solution at ambient temperature or as a solid overnight at –20 °C.

(D) Bacteriochlorin B5. A further design entails the synthesis of a bacteriochlorin–imide. Carbamoylation[3] of **B15** with CO (ambient pressure) and *tert*-butyl 4-aminobutanoate hydrochloride **6** gave the corresponding bacteriochlorin–imide **B18** in 25% yield (Scheme 4.4). Satisfactory separation of **B18** from various byproducts by column chromatography required a very slow rate of elution. Each fraction was collected and preliminarily identified by absorption spectroscopy, and the desired product was further characterized by MALDI-MS, ESI-MS and ^{1}H NMR spectroscopy. The four Boc and one *tert*-butyl groups were easily removed upon treatment with 20% TFA in CH_2Cl_2. The amine-containing bacteriochlorin was subjected to PEGylation with **PEG$_8$-NHS** in the presence of Cs_2CO_3 to afford the water-soluble PEGylated bacteriochlorin **B5** in 68% yield. A preceding model reaction of **B18** (not in pure form, containing <10 mol% of **B14**) was conducted for deprotection and PEGylation with **PEG$_4$-NHS**, and the PEGylated bacteriochlorin was found to afford broad absorption band and low fluorescence quantum yield (Φ_f) in water (0.0055). We assumed the poor

water-solubility and low Φ_f was derived from the short PEG_4 chain, and switched to the longer PEG reagent **PEG_8-NHS** for the synthesis of **B5**.

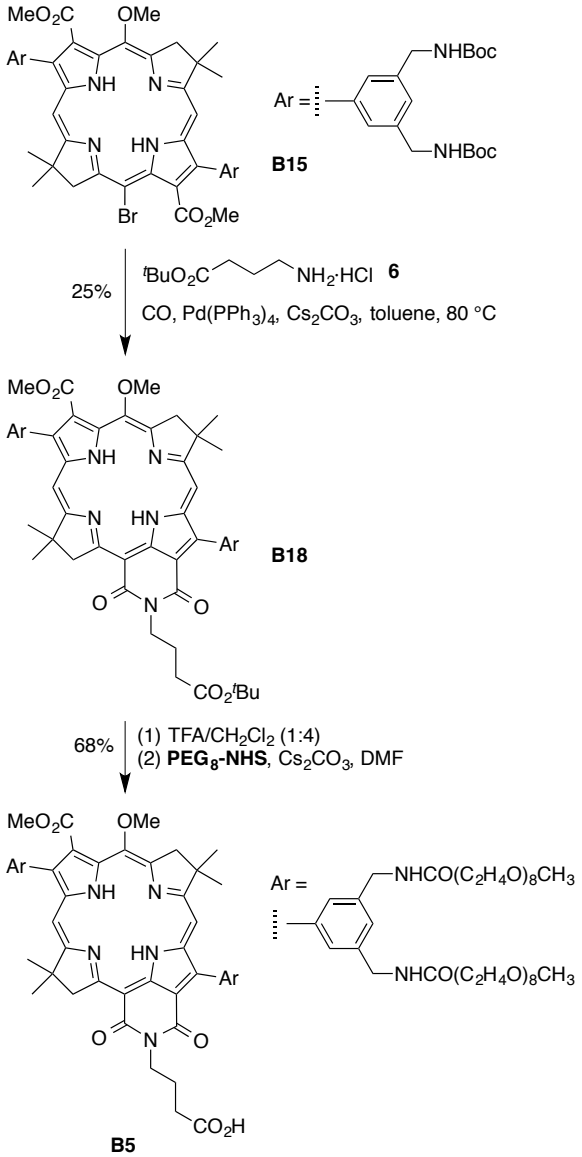

Scheme 4.4. Synthesis of a PEGylated bacteriochlorin–imide.

The PEGylated, bioconjugatable bacteriochlorins **B1–B5**, the benchmarks **I** and **II**, and the corresponding precursors typically were characterized by absorption and fluorescence spectroscopy (not for precursors), ^{1}H NMR spectroscopy, ^{13}C NMR spectroscopy (where quantity and solubility allowed), MALDI-MS and ESI-MS. Several other target molecules were also designed with expectation to tune the wavelength and were the subject of exploratory syntheses (see the Supplimentary information).

The routes for preparation of **B2**–**B5** are amenable to scale-up given the following attributes: (i) Each step for bacteriochlorin derivatization has a moderate to good yield (except 15% and 25% yields for the preparation of bacteriochlorin **B16** and **B18**, respectively). (ii) Each target compound or the corresponding intermediate is stable enough for purification and storage. (iii) The relatively expensive PEG reagents were used in the final step to make the purification facile (no column chromatography) and the synthesis more economical. The bacteriochlorin building block **BC-Br^{3,13}** or **BC-Br^{2,12}Es^{3,13}** could be prepared within three weeks in a scale of hundreds of mgs for each, and the diversification of these two precursors to the three target compounds could be achieved within three additional weeks in a 50–100 mg scale. The procedures for the four-step conversion of **BC-Br^{3,13}** to **B2** and of **BC-Br^{2,12}Es^{3,13}** to **B4** are described in the Supplimentary information.

(II) Photophysical properties

(A) Absorption and fluorescence properties. The absorption and emission spectra of **B1**, **B2**, **B3**, and **B4** were collected in water at room temperature; the spectra of **B5** were collected in DMSO (Figure 4.1). The absorption and fluorescence spectra of the same five

bacteriochlorins collected in DMF and water are shown in Figure 4.2, along with those for PEGylated benchmarks **I** and **II**, which lack a bioconjugatable tether. The absorption and fluorescence spectra for **B9**, the non-PEGylated precursor of **B1** were also obtained; these spectra were measured only in DMF (see Supplimentary information) because **B9** is insoluble in water. Each absorption spectrum shown in Figure 4.2 is normalized to the total intensity (300–1000 nm) obtained by integration when plotted in wavenumbers (cm^{-1}), which is convenient for comparing effects of substituents on relative band intensities.[40]

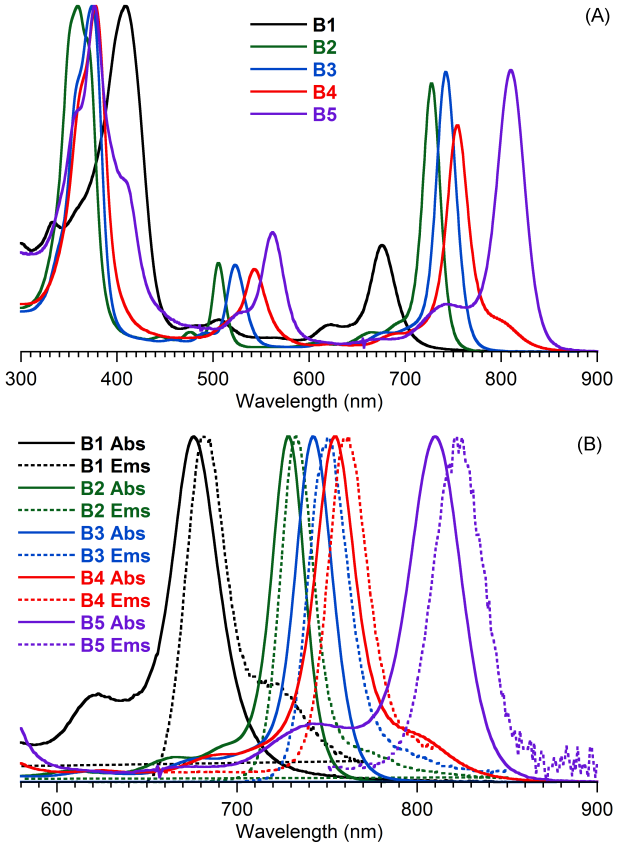

Figure 4.1. (A) Absorption spectra of PEGylated bacteriochlorins normalized at the Soret

maximum. (B). Normalized Q_y-region absorption (solid lines) and fluorescent (dotted lines) spectra of bacteriochlorins. **B1**, **B2**, **B3**, and **B4** are in water, whereas **B5** is in DMSO.

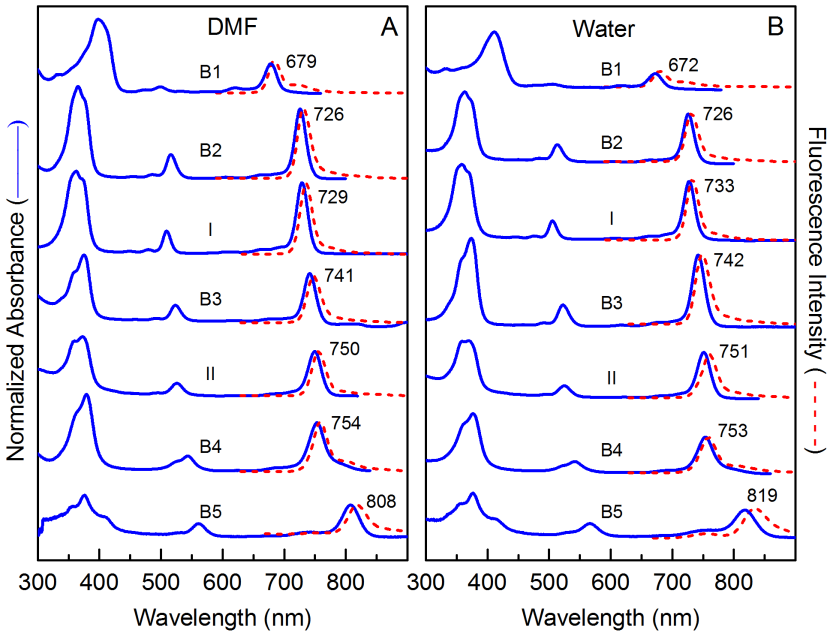

Figure 4.2. Absorption (blue solid) and fluorescence (red dashed) spectra of bacteriochlorins in (A) DMF or (B) water with 5% DMF as a co-solvent. Emission spectra were collected using excitation at the Soret maximum and are normalized to the Q_y absorption intensity for ease of presentation.

The absorption spectra of the bacteriochlorins exhibit general features expected for this genre of macrocycle in three spectral domains. These regions are an intense NIR Q_y band (670–820 nm), weaker visible Q_x band (500–580 nm), and the strong near-UV (NUV) B_x and B_y features (360–400 nm), also known as the Soret bands. Typically a weaker (1,0) satellite feature can be resolved to higher energy than each (0,0), or origin, band. There is considerable overlap of the B_y and B_x origin and vibronic components in the NUV. The peak positions for the various absorption features are listed in Table 4.1.

Table 4.1. Spectral properties of bacteriochlorins.[a]

Compound	Solvent	B_{max} abs (nm)	Q_y abs (nm)	Q_y abs fwhm	I_{Qy}/I_B	$\sum Q_y/\sum B$	Q_y em (nm)	Q_y em fwhm
B9 = B170	DMF	397	679	23	0.41	0.23	686	26
B1 = B171	DMF	398	679	22	0.40	0.23	684	26
	Water	411	672	25	0.29	0.20	679	32
B2 = B152	DMF	366	726	21	0.75	0.48	731	25
	Water	362	726	21	0.69	0.40	731	25
I = B154[b]	DMF	363	729	22	0.86	0.53	735	24
	PBS[c]	358	727	22	0.77	0.49	733	23
B3 = B172	DMF	375	741	23	0.74	0.52	748	27
	Water	374	742	24	0.81	0.57	750	28
II = B164	DMF	373	750	24	0.79	0.42	756	27
	Water	369	751	26	0.75	0.40	760	31
B4 = B156	DMF	377	754	30	0.63	0.55	760	31
	Water	368	753	32	0.62	0.52	759	33
B5 = B155	DMF	375	808	32	0.78	0.50	819	35
	Water	376	819	36	0.50	0.38	834	44

[a]All data acquired at room temperature in DMF or water with 5% DMF as a cosolvent. [b]From reference 15. [c]PBS is standard aqueous phosphate buffered saline solution.

Bacteriochlorins **B3**, **B4** and **II** and possess ester groups at the 3,13-positions, which result in a bathochromic shift in the Q_y band of ~16 nm, ~28 nm and ~25 nm, respectively relative to that for **B2** (in DMF or water). **B3** and **B4** differ from **II** by the presence of a bioconjugatable tether via phenylation or ethynylation, respectively. **B5** differs from the other bacteriochlorins by the six-membered imide ring spanning the 13–15 positions, giving rise to a ~50 nm bathochromic shift of the Q_y absorption band (808 nm in DMF and 819 nm in water) compared to **B4** and **II** (750–754 nm).

The Q_y absorption bands of the bacteriochlorins have a full-width-at-half-maximum

(FWHM) in the range 21–32 nm (25 nm average) in DMF and 21–36 nm (27 nm average) in water. The greater FWHM in water versus DMF is generally paralleled by a decrease in Q_y peak intensity (relative to the Soret maximum). The absorption profile for **B5** in water (Figure 4.2B) shows an apparent increase in baseline starting at ~600 nm and increasing into the NUV region as may be expected for light scattering, perhaps due to formation of small aggregates. The extent of scattering is comparatively less for the same compound in DMF (Figure 4.2A).

Each bacteriochlorin fluorescence spectrum in both DMF and water (Figure 4.2) is dominated by the Q_y origin band, with evidence in some cases of the weaker (0,1) band to longer wavelength. The Q_y fluorescence maximum is (Stokes') shifted to longer wavelength than Q_y absorption peak by relatively small amount (5–7 nm) for all the cases, except **B3** and **II** in water (8–9 nm) and **B5** in DMF (11 nm) or water (15 nm).

(B) Excited-state properties. The measured excited-state properties of the bacteriochlorins are the lifetime (τ_S) of the lowest singlet excited state (S_1/Q_y), the $S_1 \rightarrow S_0$ fluorescence quantum yield (Φ_f) and the $S_1 \rightarrow T_1$ intersystem crossing yield (Φ_{isc}). The $S_1 \rightarrow S_0$ internal conversion yield is obtained by subtraction: $\Phi_{ic} = 1 - \Phi_f - \Phi_{isc}$. The fluorescence ($k_f$), intersystem crossing (k_{isc}), and internal conversion (k_{ic}) rate constants are obtained from these data via the expression $k_x = \Phi_x/\tau_S$, where x = f, isc or ic. The latter three values are given as corresponding time constants ($1/k_x$) in units of nanoseconds in Table 4.2, which summarizes the excited-state photophysical properties of the bacteriochlorins in DMF and water.

Table 4.2. Photophysical properties of bacteriochlorins.[a]

Compound	Solvent	Q_y em (nm)	τ_S (ns)	Φ_f	Φ_{isc}	Φ_{ic}	k_f^{-1} (ns)	k_{isc}^{-1} (ns)	k_{ic}^{-1} (ns)
B9 = B170	DMF	686	3.28	0.20	048	0.32	16	7	10
B1 = B171	DMF	684	3.03	0.19	0.50	0.31	16	6	10
	water	679	2.76	0.075	0.47	0.45	37	6	6
B2 = B152	DMF	731	3.74	0.16	0.43	0.41	23	9	9
	water	731	3.29	0.098	0.35	0.55	34	9	6
I = B154[b]	DMF	735	3.20	0.20	0.42	0.38	16	8	9
	PBS[c]	733	2.70	0.16	0.40	0.44	17	7	6
B3 = B172	DMF	748	3.27	0.21	0.47	0.32	15	7	10
	water	750	3.39	0.13	0.45	0.42	27	8	8
II = B164	DMF	756	3.02	0.11	0.32	0.57	27	9	5
	water	760	2.96	0.078	0.31	0.61	38	10	5
B4 = B156	DMF	760	3.46	0.12	0.33	0.55	28	10	6
	water	759	3.21	0.035	0.31	0.65	92	10	5
B5 = B155	DMF	819	1.70	0.13	0.29	0.58	13	6	3
	water	834	1.40	0.017	0.08	0.90	84	18	2

[a]All data were acquired at room temperature in DMF or in water with 5% DMF as cosolvent (unless indicated otherwise). The typical errors (percent of value) of the photophysical properties are as follows: τ_S (±7%), Φ_f (±5%), Φ_{isc} (±15%), Φ_{ic} (±20%), k_f (±10%), k_{isc} (±20%), k_{ic} (±25%). The error bars for τ_S, Φ_f, and Φ_{isc} were determined from select repeat measurements, and those for the Φ_{ic}, k_f, k_{isc} and k_{ic} were obtained from propagation of errors. [b]From reference 15. [c]PBS is standard aqueous phosphate buffered saline solution.

The τ_S values of all the bacteriochlorins except **B3** (and **II**) in water are 7–18% lower in water (1.4–3.4 ns) than in DMF (1.7–3.7 ns). The lifetime for bacteriochlorin–imide **B5** in DMF or water (1.7 or 1.4 ns, respectively) is shorter than that of **B2**, **B4**, **II** and **B1** in DMF (3.0–3.7 ns) and water (2.7–3.4 ns). For all the bacteriochlorins, the Φ_f values are more substantially reduced (29–87%) in water (0.017–0.16) versus DMF (0.11–0.21). The

reduction of Φ_f in water vs DMF follows the trend: **B5** (0.017 vs 0.13; 87%) > **B4** (0.035 vs 0.12; 71%) > **B1** (0.075 vs 0.19; 61%) > **B2** (0.098 vs 0.16; 39%) ~ **B3** (0.13 vs 0.21; 38% > **II** (0.078 vs 0.11; 29%) > **I** (0.16 vs 0.20; 20%).

Collectively, the above comparisons make the following key points: (1) PEGylation of **B9** to **B1** causes only a 10% drop in τ_S (3.3 to 3.0 ns) and Φ_f (0.20 to 0.19) in DMF. (Comparisons in water cannot be made because **B9** is essentially insoluble in that medium.) (2) In DMF, **B2** gives comparable τ_s and Φ_f values to non-PEGylated bacteriochlorin analogues with similar Q_y wavelength (~731 nm).[41] (3) The reduction in τ_s and Φ_f for PEGylated bacteriochlorin–imide **B5** is consistent with prior studies on non-PEGylated bacteriochlorin–imides, and primarily reflects the effect of the fused ring to give a lower S_1 energy (and longer Q_y wavelength), enhancing nonradiative decay.[41] (4) The reduction in τ_s for **B5** relative to the other bacteriochlorins may reflect in part formation of small aggregates (even dimers) in the ground or excited state or both. Such a possibility is consistent with the above-noted light scattering in the absorption spectrum for the compound in water and to some degree in DMF (Figure 4.2).

The average five-fold larger reduction of Φ_f (40%) than τ_S (15%) for the seven bacteriochlorins in water versus DMF reflects the fact that k_f is small compared to $k_{isc}+k_{ic}$; thus, the lifetime is only modestly dependent on k_f, via the expression $\tau_s = (k_f + k_{isc} + k_{ic})^{-1}$, whereas the fluorescence yield is directly proportional to k_f (and also modestly dependent through τ_s) via the expression $\Phi_f = k_f/\tau_s$. Thus, the (disparate) reductions in τ_s and Φ_f reflect in part a decrease in k_f in water versus DMF (in addition to an increase in k_{ic} as discussed

below). Examination of Table 4.2 indicates that the values for k_f for all the bacteriochlorins (except **B5**) are reduced (k_f^{-1} is larger) by a factor of 1.1–3.3 (average 1.9) in DMF versus water. The larger, 6.5-fold difference in k_f between the two media for **B5** may stem from an effect of aggregation on the excited-state decay (*vide supra*), giving a τ_s that is smaller and thus, a k_f that is smaller than the value expected for the monomer. To further explore medium effects on the Φ_f value of **B5**, fluorescence studies were carried out in a variety of solvents in addition to DMF and water (Supplimentary information).

The differences in k_f for $S_1 \rightarrow S_0$ fluorescence (Table 4.2) and the radiative probability for $S_0 \rightarrow S_1$ absorption (as reflected in $\sum Q_y/\sum B$ in Table 4.1) likely derive from multiple factors. A small difference in k_f values can be accounted for by the differences in refractive index (1.43 vs 1.33). Other potential contributions include a difference in solvent interactions with the macrocycle and peripheral substituents (e.g., H-bonding with oxo-moieties in ester or acid groups) that alter the relative energies of the bacteriochlorin frontier molecular orbitals.

Examination of Table 4.2 shows that the seven bacteriochlorins in DMF or water generally have an intersystem-crossing yield (Φ_{isc}) in the range 0.29–0.50 and a rate constant (k_{isc}) of $(6–10\ ns)^{-1}$. The exception is **B5** in water which has $\Phi_{isc} = 0.08$ and $k_{isc} = (18\ ns)^{-1}$, values likely compromised by aggregation effects. Except for **B5** in water, the values of the other cases are comparable but perhaps slightly smaller than those found for diverse bacteriochlorins having Q_y wavelength (and S_1 energies) in the same range.[3,41]

The yield of $S_1 \rightarrow S_0$ internal conversion (Φ_{ic}) for the bacteriochlorins listed in Table

4.2 generally is in the range 0.31 to 0.58 for the compounds in DMF and 0.42 to 0.65 in water (**B5** in water is the exception with a value of 0.90). The average increase in Φ_{ic} in water versus DMF is 25%. Examination of Table 4.2 reveals that this effect arises from generally larger rate constant (k_{ic}) for internal conversion for the bacteriochlorins in water versus DMF. This difference and a general trend of increasing k_{ic} with increasing Q_y wavelength (decreasing S_1 energy) can be seen by collecting the bacteriochlorins in three groups considering uncertainties k_{ic} values): (1) Bacteriochlorins **B1–B3** and **I** have Q_y at (684–748 nm) and $k_{ic} = (9–11\ ns)^{-1}$ in DMF and (679–750 nm) and $k_{ic} = (6–8\ ns)^{-1}$ in water. (2) Bacteriochlorins **B4** and **II** have Q_y at (756–760 nm) and $k_{ic} = (5–6\ ns)^{-1}$ in DMF and (759–760 nm) and $k_{ic} = (5\ ns)^{-1}$ in water. (3) Bacteriochlorin–imide **B5** has Q_y at (819 nm) and $k_{ic} = (3\ ns)^{-1}$ in DMF and (834 nm) and $k_{ic} = (2\ ns)^{-1}$ in water. Such a trend of increasing k_{ic} with decreasing S_1 (Q_y) energy is consistent with results for a large number of bacteriochlorins[3,41] and the energy-gap law for nonradiative decay.[42]

(C) Effect of concentration on spectral properties. Absorption versus concentration studies in neat dionized water were conducted to assess the aqueous solution properties of the bacteriochlorins over a concentration range of 1000-fold (~200–700 μM to ~0.20–0.70 μM). This type of study has been previously explained in detail,[33] and the same approach was adopted herein. The spectra for each bacteriochlorin are shown in Figure 4.3. While **B5** exhibits obvious band broadening indicating some degree of aggregation, the other PEGylated bacteriochlorins exhibit almost unchanged spectroscopic properties in the NIR and visible regions and minimal changes in the NUV region over the 1000-fold concentration

range. This observation indicates little or no aggregation of these molecules.

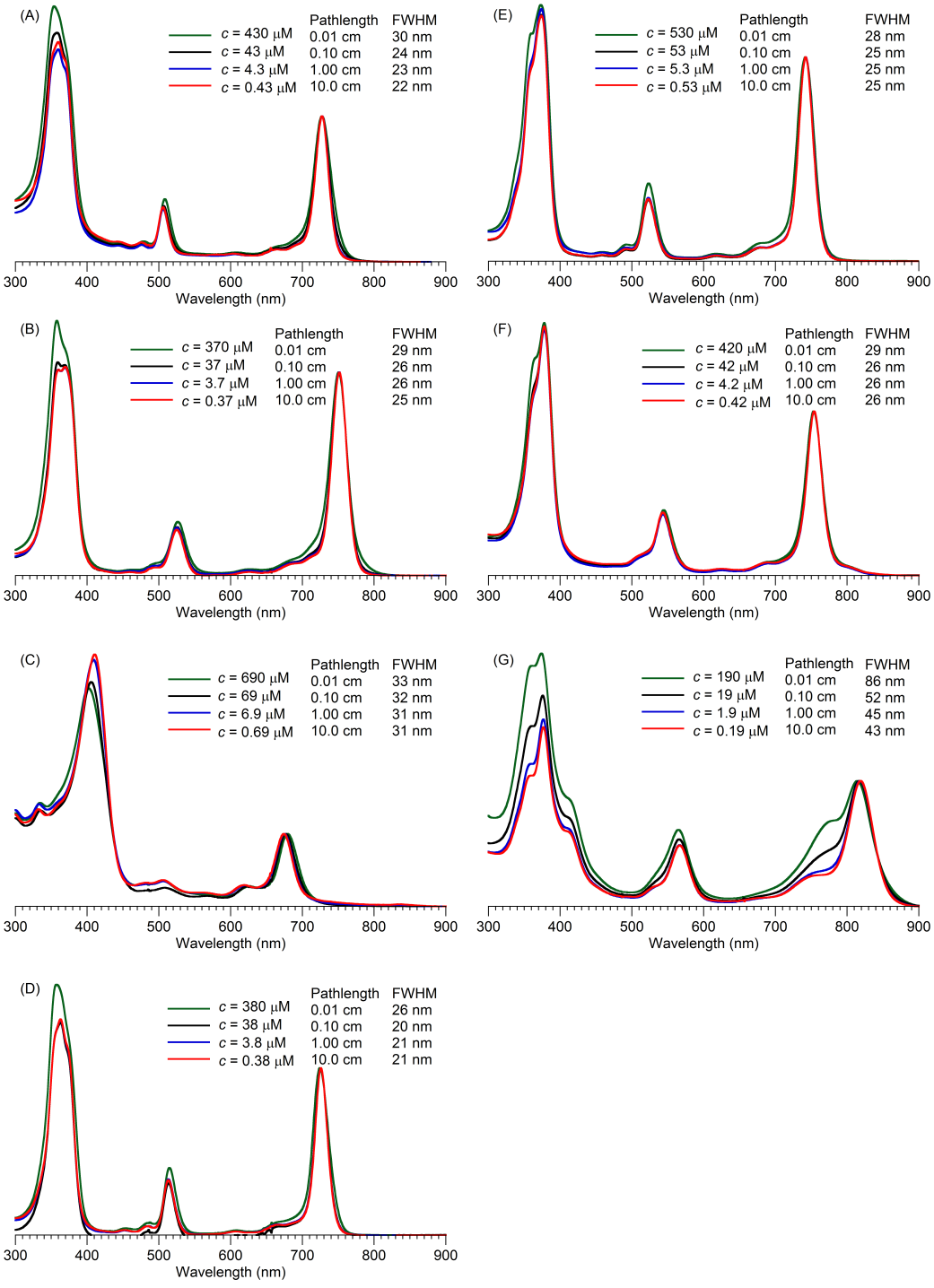

Figure 4.3. Absorption versus concentration of **I**, **B2**, **II**, **B4**, **B5** and **B1**, each over a range of 1000-fold. All spectra were recorded in water and normalized at the Q_y band. The concentration of five bacteriochlorins was calculated based on absorption in the 1-cm cuvette, assuming absorptivity at $\varepsilon(Q_y) = 120{,}000\ M^{-1}cm^{-1}$.[10]

(III) Flow cytometry

New fluorophores with spectrally distinct emission bands (i.e., distinct "colors") and instrumentation that together enable polychromatic flow cytometry are essential for advancing the field of clinical diagnostics.[27-29] Although ultraviolet lasers (UV, 355 nm) are less frequently found in flow cytometers used in the diagnostic sector than lasers that emit at longer wavelengths, UV lasers are common in research instruments where they afford important analytic attributes. The attributes include the ability to perform cell cycle analyses with DNA intercalating dyes such as 4',6-diamidino-2-phenylindole (DAPI) and Hoechst 33258, and calcium tracking with Indo-1.[44] The 355-nm excitation wavelength is nearly ideal for bacteriochlorins, which typically exhibit strong absorption in this region, with resulting emission in the NIR region, providing an effective Stokes' shift of >350 nm (Figures 4.1 and 4.2).

To examine the efficacy of bacteriochlorins in flow cytometry, bacteriochlorin-labeled antibodies were detected using antibody-capture compensation beads. Such beads are frequently used for building multicolor flow cytometry experiments to determine proper corrections due to spectral overlap between fluorophore-labeled reagents.[45] The bacteriochlorin **B2** was used to label mouse IgG antibody for detection using mouse IgG antibody-specific compensation beads. The resulting bacteriochlorin–antibody conjugate

B2–Ab had a fluorophore/protein ratio of 2.5. Flow cytometry experiments used a 355-nm laser for excitation with 685 nm longpass and 730/45 nm bandpass filters for emission. Figure 4.4 shows a histogram of the flow cytometry signals for the **B2–Ab**-bound compensation beads and for unbound beads (negative control).

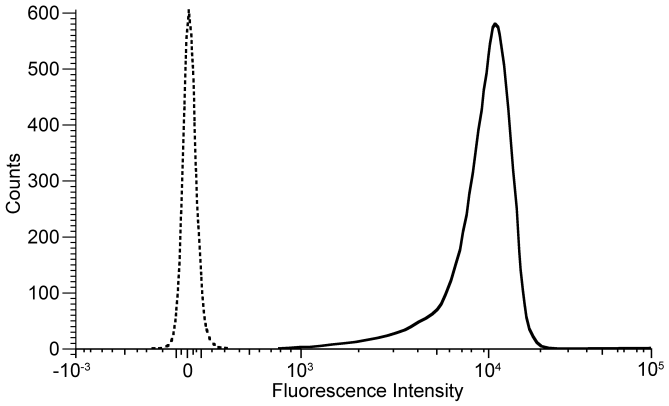

Figure 4.4. Histogram from a flow cytometry experiment using compensation beads stained with 0.8 μg of bacteriochlorin–antibody **B2–Ab** (solid line) plus unstained beads (dotted line). The analysis used the 355-nm UV laser with 685 nm longpass and 730/45 nm bandpass filters.

A wide variety of fluorophores are available, albeit with spectra chiefly in the visible region.[46] Currently, the only two commercially available dye families that contain members that can be excited at 355 nm and emit in the NIR are conductive organic polymer-based Brilliant Ultraviolet (BUV) reagents and semiconductor based Quantum dots (QDs).[47-49] Although these two fluorophore families offer large effective Stokes' shifts for multiplexing, their broad emission spectra result in considerable spectral overlap as can be seen in Figure 4.5. Thus, either two BUV fluorophores (BUV 737 and BUV 805) or two QDs (Qdot 705

and Qdot 800) could be used; however, in both cases the significant overlap between the members would require sensitivity-robbing compensation. In contrast, three or more bacteriochlorins could be used in the same window with much less spectral overlap and consequently less compensation.

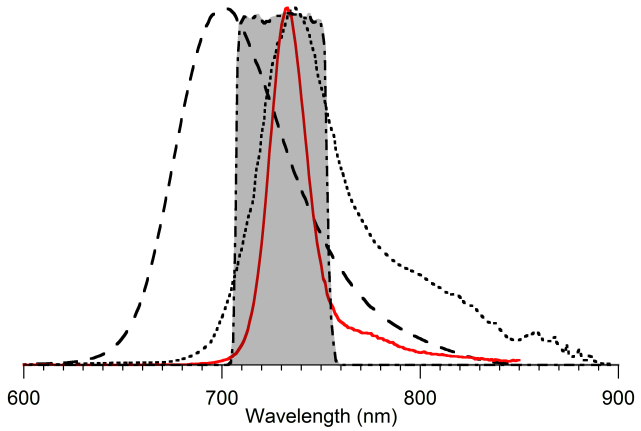

Figure 4.5. Fluorescence spectra of bacteriochlorin **B2** (red line), Qdot 705 (dashed line) and BUV-737 (dotted line) overlaid with a 730/45 nm bandpass filter (shadowed gray).

The flow cytometry data presented herein indicate that bacteriochlorins afford valuable attributes as labels for polychromatic experiments, especially those requiring a large number of fluorophores excited with a UV laser. **B2** has far narrower emission (FWHM <20 nm) than any commercially available label (FWHM > 60 nm; Figure 4.5) in this range. Accordingly, within the NIR spectral range, it should be possible to discriminate more biomolecules labeled with a palette of bacteriochlorins with less spectral overlap ("spillover")[45] than with other fluorophore families that are currently available. Figure 4.5

suggests that the overall advantage of the narrow-emitting bacteriochlorins would be further enhanced upon reduction of the filter bandpass (e.g., from 45 nm to 30 nm). Doing so would (1) fit more discrete emission channels in a given wavelength span, thereby enhancing multiplexing; (2) collect most of the emission from the bacteriochlorin but only a fraction from current fluorophores with broader emission; and (3) effectively collapse any apparent greater (integrated) brightness of another fluorophore compared to that of a bacteriochlorin.

Conclusions

Bacteriochlorins are superb chromophores for use in the NIR spectral region, yet require extensive tailoring to fulfill many photochemical applications. Strategies for the installation of PEG groups at the 3,5-positions of aryl groups attached to the bacteriochlorin macrocycle have been developed. The resulting PEGylated bacteriochlorins are water-soluble but neutral and nonionic. The PEG moieties were incorporated in the final step to facilitate purification. A single carboxylic acid group was incorporated for bioconjugation purposes. All bacteriochlorins showed excellent solubility in water, except for a bacteriochlorin–imide that gave slight aggregation at higher concentrations. One bacteriochlorin–antibody conjugate displayed a sharp signal upon ultraviolet excitation (355 nm) with NIR emission (centered at 730 nm). The synthetic bacteriochlorins are distinguished from many other NIR chromophores by the relatively sharp long-wavelength absorption band and companion fluorescence emission band. Such sharp bands are particularly attractive for use in polychromatic flow cytometry, light-harvesting, and energy-cascade processes.

Acknowledgments

Synthesis and photophysical characterization were supported by the Photosynthetic Antenna Research Center (PARC), an Energy Frontier Research Center funded by the U.S. Department of Energy, Office of Science, Office of Basic Energy Sciences, under Award No. DE-SC0001035. Flow cytometry studies were supported by a grant to NIRvana Sciences (1R41AI112302) from the National Institutes of Health Small Business Technology Transfer Program. Cytometry was performed at the UNC Flow Cytometry Core Facility, which is supported in part by P30 CA016086 Cancer Center Core Support Grant to the UNC Lineberger Comprehensive Cancer Center. Mass spectra were obtained at the Mass Spectrometry Laboratory for Biotechnology at North Carolina State University. Partial funding for the facility was obtained from the North Carolina Biotechnology Center and the National Science Foundation. Mr. Nuonuo Zhang was supported by the China Scholarship Council (CSC, 201306250076) as a visiting Ph.D. student from Tianjin University for joint research at North Carolina State University.

Experimental section.

(I) General methods.

^{1}H NMR (300 MHz) and ^{13}C NMR (100 MHz) were collected at room temperature in $CDCl_3$ unless noted otherwise. Matrix-assisted laser-desorption mass spectrometry (MALDI-MS) was performed with the matrix 1,4-bis(5-phenyl-2-oxaxol-2-yl)benzene.[50]

Electrospray ionization mass spectrometry (ESI-MS) data are reported for the molecular ion. Silica gel (40 μm average particle size) was used for column chromatography. All solvents were reagent grade and were used as received unless noted otherwise. THF was freshly distilled from sodium/benzophenone ketyl. Sonication was carried out with a benchtop open-bath sonicator. Compounds **3**,[15] **4**,[38] **BC-Br**^{3,13},[12] **BC-Br**^{2,12}**Es**^{3,13},[43] **B6**[34] and **B11**[15] were prepared following reported procedures.

(II) Photophysical measurements

Photophysical measurements were carried out as described in the companion paper.[30]

(III) Synthesis

3,13-Bis[3,5-bis(11-methoxy-3,6,9-trioxaundecylamidomethyl)phenyl]-5-methoxy-8,8,18,18-tetramethylbacteriochlorin (I). A mixture of **B11** (5.00 mg, 7.47 μmol) and **PEG$_4$-NHS** (100. mg, 299 μmol) in DMF (100 μL) was stirred under argon for 20 h. The reaction mixture was diluted with CH_2Cl_2 and washed with saturated aqueous $NaHCO_3$. The combined organic extract was dried (Na_2SO_4) and concentrated. A mixture of hexanes/CH_2Cl_2 (19:1) was added to the residue, and the suspension was sonicated (3 min) and centrifuged. The supernatant was discarded, leaving a green solid. This procedure (solvent addition–sonication–centrifuge) was conducted three more times to afford a green solid (9.2 mg, 80%): ^{1}H NMR δ –1.94 (s, 1H), –1.69 (s, 1H), 1.95 (s, 6H), 1.97 (s, 6H), 2.52–2.61 (m, 16H), 3.24 (s, 6H), 3.25 (s, 6H), 3.33–3.87 (m, 51H), 4.35 (s, 2H), 4.39 (s, 2H), 4.67 (d, J = 6.0 Hz, 4H), 4.72 (d, J = 6.0 Hz, 4H), 7.13–7.15 (m, 4H), 7.38 (s, 1H), 7.45 (s, 1H),

7.94 (s, 2H), 7.97 (s, 2H), 8.58–8.63 (m, 3H), 8.74–8.75 (m, 2H); MALDI-MS obsd 1541.8276; ESI-MS obsd 1563.8470, calcd 1563.8460 [$(M + Na)^+$, M = $C_{81}H_{120}N_8O_{21}$]; λ_{abs} (water) 359, 506, 728 nm.

3,13-Dimethoxycarbonyl-2,12-bis[3,5-bis(3,6,9,12,15,18,21,24-octaoxahexacosanyl-26-amidomethyl)phenyl]-5-methoxy-8,8,18,18-tetramethylbacteriochlorin (II). A solution of **B14** (4.6 mg, 4.2 μmol) in CH_2Cl_2 (0.80 mL) was stirred under argon for 2 min followed by addition of TFA (0.20 mL). After 1 h, the reaction mixture was dried under an argon flow. Tributylamine (50 μL) was added to the solid residue, and the resulting mixture was sonicated for 3 min. A mixture of THF/hexanes (1:1) was then added, and the resulting suspension was sonicated (5 min) and centrifuged. The supernatant was discarded to afford a dark red solid (3.3 mg), which was partially characterized as below: MALDI-MS obsd 784.05, calcd 785.41 [$(M + H)^+$, M = $C_{45}H_{52}N_8O_5$]; λ_{abs} (CH_3OH) 368, 525, 745 nm. A mixture of the resulting bacteriochlorin (3.3 mg, 4.2 μmol), Cs_2CO_3 (23 mg, 85 μmol) and **PEG_8-NHS** (50 mg, 98 μmol) in DMF (85 μL) was stirred under argon for 2.5 h. The reaction mixture was diluted with saturated aqueous $NaHCO_3$ (1.0 mL) and stirred for 2 h. The reaction mixture was extracted with CH_2Cl_2. The combined organic extract was dried (Na_2SO_4) and concentrated. A solution of hexanes/CH_2Cl_2 (2:1) was added to the residue, and the resulting suspension was sonicated (3 min) and centrifuged. The supernatant was discarded to afford a dark red solid. This procedure (solvent addition-sonication-centrifuge) was conducted three more times to afford a dark red semi-solid (5.0 mg, 54%): ^{1}H NMR (the four amide protons were not observed) δ –1.57 (s, 1H), –1.30 (s, 1H), 1.82 (s, 6H), 1.86 (s,

6H), 2.65 (m, 10H), 3.34–3.65 (m, 122H), 3.77–3.82 (m, 8H), 4.04 (s, 3H), 4.14 (s, 3H), 4.23 (s, 3H), 4.34 (s, 2H), 4.39 (s, 2H), 4.70 (s, 4H), 4.72 (s, 4H), 7.59 (s, 2H), 7.72 (s, 2H), 7.86 (s, 2H), 8.44 (s, 1H), 8.56 (s, 1H), 9.51 (s, 1H); MALDI-MS obsd 2363.15, calcd 2362.2950 [$(M + H)^+$, M = $C_{117}H_{188}N_8O_{41}$]; ESI-MS obsd 1203.6304, calcd M/2 = 1203.6336 [$(M + 2Na)^{2+}$, M = $C_{117}H_{188}N_8O_{41}$]; λ_{abs} (H_2O) 369, 525, 751 nm.

13-[(4-Carboxyphenyl)ethyl]-5-methoxy-8,8,18,18-tetramethyl-3-(26-oxo-2,5,8,11,14,17,20,23-octaoxa-27-azatriacontan-30-yl)-7-oxobacteriochlorin (B1). A solution of **B9** (6.0 mg, 8.2 μmol) in CH_2Cl_2 (1.1 mL) was stirred under argon for 2 min followed by addition of TFA (219 μL). After 1 h, the mixture was dried under an argon flow. The residue was dissolved in THF (4 mL) and methanol (2 mL). Aqueous NaOH (4 M, 2 mL) was added, and the mixture was stirred at room temperature for 16 h. Aqueous HCl solution (3 M, 8 mL) was added to stop the reaction. The mixture was extracted with CH_2Cl_2. The organic phase was washed with brine and dried over Na_2SO_4. Solvent was removed in vacuum. A mixture of the resulting crude, Cs_2CO_3 (53.4 mg, 0.164 mmol), and **PEG_8-NHS** (167 mg, 0.328 mmol) in DMF (200 μL) was stirred under argon for 2.5 h. Saturated aqueous $NaHCO_3$ (1 mL) was added. After 2 h, the organic phase was extracted by CH_2Cl_2, dried (Na_2SO_4) and concentrated. A mixture of hexanes/CH_2Cl_2 (10:1) was added to the residue, the suspension was sonicated and centrifuged. This procedure (solvent addition-sonication-centrifuge) was conducted three more times to afford a green solid (5.0 mg, 63%): ^{1}H NMR δ –1.21 (s, 1H), –1.16 (s, 1H), 1.87 (s, 6H), 1.90 (s, 6H), 2.40–2.48 (m, 2H), 2.52–2.60 (m, 2H), 3.34 (s, 3H), 3.41–3.45 (m, 4H), 3.45–3.50 (m, 8H), 3.50–3.54 (m, 6H), 3.55–

3.59 (m, 8H), 3.60–3.64 (m, 8H), 3.76–3.80 (m, 2H), 3.90–4.00 (m, 3H), 4.28 (s, 2H), 4.45 (s, 3H), 4.68 (s, 1H), 7.38 (d, J = 8.0 Hz, 2H), 7.99 (d, J = 8.0 Hz, 2H), 8.27 (s, 1H), 8.40 (m, 2H), 8.45 (s, 1H), 8.47 (s, 1H); ESI-MS obsd 1014.5407, calcd 1014.5434 [$(M+H)^+$, M = $C_{55}H_{75}N_5O_{13}$]; λ_{abs} (H_2O) 409, 676 nm.

15-[4-(3-Carboxyethyl)phenyl]-3,13-bis[3,5-bis(11-methoxy-3,6,9-trioxaundecylamidomethyl)phenyl]-5-methoxy-8,8,18,18-tetramethylbacteriochlorin (B2). A mixture of **B13** (10.0 mg, 12.2 μmol), Cs_2CO_3 (80. mg, 250 μmol) and **PEG_4-NHS** (164 mg, 490 μmol) in DMF (150 μL) was stirred under argon for 2.5 h. The reaction mixture was diluted with saturated aqueous $NaHCO_3$ (2.5 mL) and stirred for 4 h. The reaction mixture was acidified with 2N HCl solution and extracted with CH_2Cl_2. The combined organic extract was dried (Na_2SO_4) and concentrated. A mixture of hexanes/CH_2Cl_2 (19:1) was added to the residue, and the resulting suspension was sonicated (3 min) and centrifuged. The supernatant was discarded to afford a green solid. This procedure (solvent addition–sonication–centrifuge) was conducted three more times to afford a green solid (17.2 mg, 83%): ^{1}H NMR (the carboxylic acid proton was not observed) δ –1.62 (s, 1H), –1.23 (s, 1H), 1.83 (s, 6H), 1.97 (s, 6H), 2.59–2.68 (m, 16H), 2.76 (t, J = 7.8 Hz, 2H), 3.01 (t, J = 7.8 Hz, 2H), 3.25 (s, 6H), 3.26 (s, 6H), 3.34–3.89 (m, 57H), 4.35 (s, 2H), 4.44 (br, 4H), 4.68 (s, 4H), 6.98 (s, 1H), 7.10–7.14 (m, 4H), 7.39–7.46 (m, 3H), 7.97 (s, 2H), 8.54 (s, 1H), 8.61 (s, 3H); MALDI-MS obsd 1691.1589; ESI-MS obsd 845.4628, calcd M/2 = 845.4619 [$(M + 2H)^{2+}$, M = $C_{90}H_{128}N_8O_{23}$]; λ_{abs} (water) 363, 513, 726 nm. A larger-scale synthesis afforded 40.0 mg of the title compound (77% yield, see the Supplimentary

information).

3,13-Bis[3,5-bis(4,7,10,13-tetraoxaamido)phenyl]-5-methoxy-15-[(3-(4-succinimidooxycarboxyethyl)phenyl)]-8,8,18,18-tetramethylbacteriochlorin (B2–NHS). A mixture of **B2** (8.0 mg, 4.6 μmol), EDC (5.9 mg, 31 μmol), and HOSu (7.0 mg, 61 μmol) in DMF (0.10 mL) was stirred overnight under argon at room temperature. The reaction mixture was diluted with CH_2Cl_2 and washed with acidic saturated aqueous brine (0.05 N HCl). The combined organic extract was dried (Na_2SO_4) and concentrated. A mixed solvent of hexanes/CH_2Cl_2 (19:1) was added to the residue, and the suspension was sonicated for 3 min on a benchtop sonication bath and centrifuged. The supernatant was discarded, leaving a green solid (6.6 mg, 60%): ^{1}H NMR δ –1.64 (s, 1H), –1.27 (s, 1H), 1.84 (s, 6H), 1.97 (s, 6H), 2.52 (t, *J* = 5.7 Hz, 2H), 2.61 (t, *J* = 5.7 Hz, 2H), 2.81–2.94 (m, 20H), 3.31–3.84 (m, 63H), 3.92 (s, 2H), 4.35 (s, 2H), 4.39 (d, *J* = 5.7 Hz, 4H), 4.68 (d, *J* = 5.7 Hz, 4H), 6.16–6.18 (m, 4H), 6.98 (s, 1H), 7.09–7.14 (m, 4H), 7.39–7.44 (m, 3H), 7.97 (s, 2H), 8.55 (d, *J* = 1.8 Hz, 1H), 8.62 (s, 3H); MALDI-MS obsd 1787.0947; ESI-MS obsd 1808.9091, calcd 1808.9148 [$(M + Na)^+$, M = $C_{94}H_{131}N_9O_{25}$]; λ_{abs} (CH_2Cl_2) 366, 517, 729 nm ; λ_{abs} (water) 363, 513, 726 nm.

15-[4-(3-Carboxyethyl)phenyl]-3,13-dimethoxycarbonyl-2,12-bis[3,5-bis(3,6,9,12,15,18,21,24-octaoxahexacosanyl-26-amidomethyl)phenyl]-5-methoxy-8,8,18,18-tetramethylbacteriochlorin (B3). A solution of **B17** (10. mg, 7.2 μmol) in CH_2Cl_2 (0.63 mL) was stirred under argon for 2 min followed by addition of TFA (0.16 mL). After 1 h, the reaction mixture was dried under an argon flow. Tributylamine (50 μL) was

added to the solid residue, and the resulting mixture was sonicated for 3 min. A mixture of THF/hexanes (1:1) was then added, and the resulting suspension was sonicated (5 min) and centrifuged. The supernatant was discarded to afford a greenish solid (6.7 mg), which was partially characterized as below: MALDI-MS obsd 933.50, calcd 933.47 [$(M + H)^+$, M = $C_{54}H_{60}N_8O_7$]; λ_{abs} (CH_3OH) 370, 521, 736 nm. The resulting crude solid was used for the next reaction. A mixture of this solid (6.7 mg, 7.2 μmol), Cs_2CO_3 (67 mg, 0.21 mmol) and **PEG_8-NHS** (0.13 g, 0.27 mmol) in DMF (0.27 mL) was stirred under argon for 2.5 h. The reaction mixture was diluted with saturated aqueous $NaHCO_3$ (1 mL) for 2 h. The reaction mixture was extracted with CH_2Cl_2. The combined organic extract was dried (Na_2SO_4) and concentrated. A mixture of hexanes/CH_2Cl_2 (5:1) was added to the residue, and the resulting suspension was sonicated (3 min) and centrifuged. The supernatant was discarded to afford a dark red solid. This procedure (solvent addition-sonication-centrifuge) was conducted three more times to afford a dark red semi-solid (12 mg, 66%): ^{1}H NMR (the carboxylic acid proton was not observed) δ –1.53 (s, 1H), –1.23 (s, 1H), 1.75 (s, 6H), 1.85 (s, 6H), 2.58 (q, *J* = 5.7 Hz, 8H), 2.86 (t, *J* = 6.9 Hz, 2H), 3.19 (t, *J* = 6.9 Hz, 2H), 3.32–3.65 (m, 123H), 3.78 (q, *J* = 5.7 Hz, 12H), 3.86 (s, 2H), 4.14 (s, 3H), 4.28 (s, 3H), 4.36 (s, 2H), 4.65 (d, *J* = 5.7 Hz, 4H), 4.70 (d, *J* = 5.7 Hz, 4H), 7.15–7.21 (m, 4H), 7.43–7.49 (m, 4H), 7.67 (s, 1H), 7.70 (s, 1H), 7.74 (s, 2H), 7.89 (s, 2H), 8.56 (s, 1H), 8.59 (s, 1H); MALDI-MS obsd 2508.94; ESI-MS obsd 1255.6828, calcd M/2 = 1255.6771 [$(M + 2H)^{2+}$, M = $C_{126}H_{196}N_8O_{43}$]; λ_{abs} (water) 374, 522, 742 nm.

Zn(II)-15-[4-(3-Carboxyethyl)phenyl]-3,13-dimethoxycarbonyl-2,12-bis[3,5-bis(3,6,9,12,15,18,21,24-octaoxahexacosanyl-26-amidomethyl)phenyl]-5-methoxy-

8,8,18,18-tetramethylbacteriochlorin (ZnB3). Following a standard procedure,[39] a mixture of **B3** (1.0 mg, 0.4 μmol) and NaH (5.6 mg, 0.24 mmol, 600 equiv) in DMF (0.1 mL) was stirred under argon for 1 min, followed by addition of $Zn(OAc)_2$ (22 mg, 0.12 mmol, 300 equiv) at 80 °C for 16 h. The reaction mixture washed with water three times and extracted with CH_2Cl_2. The organic extract was dried (Na_2SO_4) and concentrated to give a dark red semisolid: MALDI-MS obsd 2572.9736, calcd 2572.2609 [$(M + H)^+$, M = $C1_{26}H_{194}N_8O_{43}Zn$]; λ_{abs} (H_2O) 358, 384, 563, 754 nm. The title compound was not stable in solution (toluene, DMF, or H_2O) or as solid at –20 °C, and was not characterized further.

2,12-Bis[3,5-bis(11-methoxy-3,6,9-trioxaundecylamidomethyl)phenyl]-15-(7-carboxy-1-heptyl)-3,13-dimethoxycarbonyl-5-methoxy-8,8,18,18-tetramethylbacteriochlorin (B4). A solution of **B16** (8.0 mg, 6.1 μmol) in CH_2Cl_2 (1.6 mL) was stirred under argon for 2 min followed by addition of TFA (0.40 mL). After 1 h, the reaction mixture was dried by a stream of argon to thoroughly remove the volatile components (CH_2Cl_2 and TFA). The residue was dried under high vacuum. Tributylamine (10 μL) was added to the solid residue, and the resulting mixture was sonicated for 3 min. (The thorough removal of TFA is critical to avoid decomposition of the bacteriochlorin.) A mixture of THF/hexanes (1:2) was then added, and the resulting suspension was sonicated (5 min) and centrifuged. The supernatant was discarded to afford a greenish solid (5.5 mg), which was partially characterized as follows: MALDI-MS obsd 908.3242, calcd 909.4663 [$(M + H)^+$, M = $C_{52}H_{60}N_8O_7$]; λ_{abs} (CH_3OH) 375, 543, 750 nm. A mixture of the resulting bacteriochlorin (5.5 mg, 6.1 μmol), Cs_2CO_3 (34 mg, 0.11 mmol, 17 equiv) and **PEG_4-NHS**

(72 mg, 0.22 mmol, 34 equiv) in DMF (2.0 mL) was stirred under argon for 2 h. The reaction mixture was diluted with 0.6 M aqueous $NaHCO_3$ (3.0 mL) for 2 h. The reaction mixture was extracted with CH_2Cl_2. The combined organic extract was dried (Na_2SO_4) and concentrated. A mixture of hexanes/CH_2Cl_2 (10:1) was added to the residue, and the resulting suspension was sonicated (3 min) and centrifuged. The supernatant was discarded to afford a dark red solid. This procedure (solvent addition-sonication-centrifuge) was conducted three times to afford a red solid (6.0 mg, 55%): ^{1}H NMR (the carboxylic acid proton was not observed) δ –1.38 (s, 1H), –1.16 (s, 1H), 1.82 (s, 12H), 2.00 (br, 4H), 2.51 (br, 2H), 2.59 (s, 12H), 2.83 (br, 2H), 3.23–3.65 (m, 64H), 3.77 (s, 8H), 4.05 (s, 3H), 4.11 (s, 3H), 4.23 (s, 3H), 4.29 (s, 2H), 4.40 (s, 2H), 4.68 (br, 4H), 7.45 (s, 2H), 7.84 (s, 4H), 8.49 (s, 1H), 8.52 (s, 1H); MALDI-MS obsd 1780.9208, calcd 1781.9280 [$(M + H)^+$, M = $C_{92}H_{132}N_8O_{27}$]; ESI-MS obsd 913.4495, calcd M/2 = 913.4493 [$(M + 2Na)^{2+}$, M = $C_{92}H_{132}N_8O_{27}$]; λ_{abs} (H_2O) 378, 543, 754 nm. A larger-scale synthesis afforded 20.0 mg of the title compound (86% yield, see the Supplimentary information).

2,12-Bis[3,5-bis(3,6,9,12,15,18,21,24-octaoxahexacosanyl-26-amidomethyl)phenyl]-15^2-*N*-(3-carboxypropyl)-3-methoxycarbonyl-5-methoxy-8,8,18,18-tetramethylbacteriochlorin-13, 15-dicarboimide (B5). A solution of **B18** (4.00 mg, 2.99 μmol) in CH_2Cl_2 (400 μL) was stirred under argon for 2 min followed by addition of TFA (120 μL). After 1 h, the reaction mixture was dried under an argon flow. Tributylamine (48.0 μL) was added to the solid residue, and the resulting mixture was sonicated for 3 min. A mixture of THF/hexanes (1:1) was then added, and the resulting

suspension was sonicated (5 min) and centrifuged. The supernatant was discarded to afford a dark red solid (3.00 mg, 3.40 μmol), which was used for the next reaction. A mixture of this solid (3.00 mg, 3.40 μmol), Cs_2CO_3 (22.8 mg, 70.0 μmol) and **PEG$_8$-NHS** (69.8 mg, 137 μmol) in DMF (80.0 μL) was stirred under argon for 2.5 h. The reaction mixture was diluted with saturated aqueous $NaHCO_3$ (1.00 mL) for 2 h. The reaction mixture was extracted with CH_2Cl_2. The combined organic extract was dried (Na_2SO_4) and concentrated. A mixture of hexanes/CH_2Cl_2 (2:1) was added to the residue, and the resulting suspension was sonicated (3 min) and centrifuged. The supernatant was discarded, leaving a dark red solid. This procedure (solvent addition-sonication-centrifuge) was conducted three more times to afford a dark red semi-solid (5.0 mg, 68%): ^{1}H NMR (the carboxylic acid proton and one of pyrrolic protons was overlaid with the solvent peak) δ –0.52 (s, 1H), 1.81 (s, 12H), 2.31 (br, 2H), 2.60 (m, 10H), 3.35–3.62 (m, 132H), 3.75–3.81 (m, 10H), 4.12 (s, 3H), 4.24 (s, 3H), 4.49 (br, 4H), 4.68 (s, 2H), 4.70 (s, 2H), 7.51 (s, 2H), 7.81 (s, 2H), 7.91 (s, 2H), 8.41 (s, 1H), 8.56 (s, 1H); MALDI-MS obsd 2457.98, calcd 2459.3114 [$(M + H)^+$, M = $C_{121}H_{191}N_9O_{43}$]; ESI-MS obsd 1252.1376, calcd M/2 = 1252.1416 [$(M + 2Na)^{2+}$, M = $C_{121}H_{191}N_9O_{43}$]; λ_{abs} (water) 376, 566, 818 nm, λ_{abs} (CH_2Cl_2) 376, 563, 810 nm.

3-Bromo-5-methoxy-8,8,18,18-tetramethyl-13-[(4-methoxycarbonylphenyl)ethynyl]-7-oxobacteriochlorin (B7). Following a reported procedure,[35] a mixture of **B6** (33 mg, 58 μmol), methyl 4-ethynylbenzoate (**1**, 10 mg, 64 μmol), K_2CO_3 (80 mg, 0.58 mmol), and $Pd(PPh_3)_4$ (6.7 mg, 5.8 μmol) in DMF (5.8 mL) was deaerated by three freeze-pump-thaw cycles, and then was stirred at 80 °C under argon.

After 16 h, the mixture was diluted with ethyl acetate, washed with brine and dried over Na_2SO_4. The residue was chromatographed [silica, hexanes/ CH_2Cl_2 (1:5)] to afford a brown solid (16 mg, 42%): ^{1}H NMR (400 MHz) δ –1.09 (s, 2H), 1.90 (s, 6H), 1.93 (s, 6H), 3.99 (s, 3H), 4.40 (s, 2H), 4.49 (s, 3H), 7.91 (d, *J* = 8.4 Hz, 2H), 8.17 (d, *J* = 8.4 Hz, 2H), 8.45 (s, 1H), 8.61 (s, 1H), 8.64 (d, *J* = 2.8 Hz, 1H), 8.82 (s, 1H), 8.92 (d, *J* = 1.6 Hz, 1H); ESI-MS obsd 651.1599, calcd 651.1601 [$(M + H)^+$, M = $C_{35}H_{31}BrN_4O_4$]; λ_{abs} (toluene) 411, 512, 539, 649, 712 nm.

5-Methoxy-8,8,18,18-tetramethyl-13-[(4-methoxycarbonylphenyl)ethynyl]-3-[3-(*tert*-butoxycarbonylamino)propynyl]-7-oxobacteriochlorin (B8). Following a reported procedure,[35] a mixture of **B7** (16 mg, 24 μmol), **2** (7.6 mg, 49 μmol), and $Pd(PPh_3)_2Cl_2$ (1.7 mg, 2.5 μmol) in DMF (5 mL) and Et_3N (2.5 mL) was deaerated by three freeze-pump-thaw cycles, and then was stirred at 80 °C under argon. After 3 h, the mixture was diluted with ethyl acetate, washed with brine, and dried over Na_2SO_4. The residue was chromatographed [silica, CH_2Cl_2/ethyl acetate (5:1)] to afford a yellow brown solid (10 mg, 57%): ^{1}H NMR δ –1.07 (s, 1H), –1.04 (s, 1H), 1.55 (s, 9H), 1.90 (s, 6H), 1.93 (s, 6H), 4.00 (s, 3H), 4.39 (s, 2H), 4.55 (s, 5H), 5.16 (br s, 1H), 7.91 (d, *J* = 8.1 Hz, 2H), 8.17 (d, *J* = 8.1 Hz, 2H), 8.45 (s, 1H), 8.59 (s, 1H), 8.61 (d, *J* = 2.1 Hz, 1H), 8.79 (s, 1H), 8.90 (d, *J* = 1.5 Hz, 1H); ESI-MS obsd 725.3202, calcd 725.3208 [$(M + H)^+$, M = $C_{43}H_{43}N_5O_6$]; λ_{abs} (toluene) 416, 515, 543, 655, 720 nm.

5-Methoxy-8,8,18,18-tetramethyl-13-[(4-methoxycarbonylphenyl)ethyl]-3-[3-(*tert*-butoxycarbonylamino)propyl]-7-oxobacteriochlorin (B9). Following a reported

procedure,[37] a mixture of **B8** (10.0 mg, 0.0138 mmol) and Pd/C (4.4 mg, 0.0041 mmol, 10% Pd on carbon) under an inert atmosphere was treated with ethyl acetate (1 mL) and ethanol (1 mL). The mixture was stirred at room temperature under a H_2 balloon for 4 h. The mixture was filtered through a pad of Celite and rinsed with ethyl acetate and ethanol. The filtrate was concentrated and chromatographed [silica, CH_2Cl_2/ethyl acetate (9:1)] to obtain a green solid (8.6 mg, 85%): ^{1}H NMR (400 MHz) δ –1.18 (s, 1H), –1.16 (s, 1H), 1.49 (s, 9H), 1.87 (s, 6H), 1.90 (s, 6H), 2.38–2.43 (m, 2H), 3.45–3.49 (m, 2H), 3.59 (t, *J* = 7.6 Hz, 2H), 3.90 (s, 3H), 3.95 (t, *J* = 7.6 Hz, 2H), 4.06 (t, *J* = 7.6 Hz, 2H), 4.28 (s, 2H), 4.45 (s, 3H), 4.86 (br s, 1H), 7.41 (d, *J* = 8.0 Hz, 2H), 7.99 (d, *J* = 8.0 Hz, 2H), 8.33 (s, 1H), 8.37 (s, 1H), 8.44 (s, 1H), 8.46 (s, 1H), 8.47 (s, 1H); ESI-MS obsd 733.3825, calcd 733.3834 [$(M + H)^+$, M = $C_{43}H_{51}N_5O_6$]; λ_{abs} (CH_2Cl_2) 398, 681 nm.

3,13-Bis[3,5-bis(*tert*-butoxycarbonamidomethyl)phenyl]-5-methoxy-8,8,18,18-tetramethylbacteriochlorin (B10). Following a general procedure,[11] a mixture of **BC-Br**^{3,13} (270 mg, 484 μmol), **3** (492 mg, 1.06 mmol), $Pd(PPh_3)_4$ (336 mg, 290 μmol), Cs_2CO_3 (944 mg, 2.90 mmol) and toluene/DMF [48.4 mL (2:1), deaerated by bubbling with argon for 45 min] was added to a Schlenk flask and deaerated by three freeze-pump-thaw cycles. The remaining synthesis protocol, purification procedure and characterization data (ESI-MS data were not obtained) were essentially identical with those reported previously,[15] whereupon the title bacteriochlorin was obtained in 90% yield (465 mg) versus 85% (73 mg) previously.

15-[4-(3-*tert*-Butoxycarbonylethyl)phenyl]-3,13-bis[3,5-bis(*tert*-butoxycarbonamidomethyl)phenyl]-5-methoxy-8,8,18,18-tetramethylbacteriochlorin (B12). Following a general procedure,[11] a solution of **B10** (88.0 mg, 82.3 μmol) in THF (165

mL) was treated with NBS (17.6 mg, 98.8 μmol) in THF (988 μL) at room temperature for 1.5 h. The reaction mixture was diluted with CH_2Cl_2 and washed with saturated aqueous $NaHCO_3$. The organic layer was dried (Na_2SO_4), concentrated and chromatographed [silica, CH_2Cl_2/hexanes (4:1)] to afford a red solid, which was transferred to a Schlenk flask. The resulting bacteriochlorin, **4** (67.8 mg, 0.204 mmol), $Pd(PPh_3)_4$ (19.2 mg, 16.6 μmol), and Cs_2CO_3 (82.2 mg, 0.252 mmol) were placed in the Schlenk flask and dried under high vacuum for 30 min. Toluene/DMF [4.2 mL (2:1), deaerated by bubbling with argon for 30 min] was added to the Schlenk flask under argon, and the mixture was deaerated by three freeze-pump-thaw cycles. The reaction mixture was stirred at 90 °C for 19 h. The reaction mixture was allowed to cool to room temperature and then concentrated to dryness. The residue was dissolved in ethyl acetate and washed with saturated aqueous $NaHCO_3$. The organic layer was separated, dried (Na_2SO_4), concentrated and chromatographed [silica, hexanes/ethyl acetate (8:2 to 7:3)] to provide a greenish solid (33.0 mg, 31%): ^{1}H NMR (400 MHz) δ –1.61 (s, 1H), –1.24 (s, 1H), 1.48 (s, 18H), 1.50 (s, 18H), 1.52 (s, 9H), 1.83 (s, 6H), 1.97 (s, 6H), 2.59 (t, *J* = 7.6 Hz, 2H), 2.93 (t, *J* = 7.6 Hz, 2H), 3.66 (s, 3H), 3.89 (s, 2H), 4.27 (d, *J* = 5.6 Hz, 4H), 4.37 (s, 2H), 4.56 (d, *J* = 5.6 Hz, 4H), 4.90 (br, 2H), 5.07 (br, 2H), 6.98 (s, 1H), 7.04 (d, *J* = 7.6 Hz, 2H), 7.11 (s, 2H), 7.39–7.42 (m, 3H), 7.97 (s, 2H), 8.57 (d, *J* = 2.4 Hz, 1H), 8.62–8.64 (m, 3H); ^{13}C NMR δ 28.4, 28.7, 30.0, 30.9, 31.3, 36.9, 44.7, 45.1, 45.2, 45.9, 47.8, 52.3, 63.5, 79.7, 80.8, 97.0, 97.5, 113.8, 123.1, 124.0, 125.2, 126.5, 127.2, 128.2, 129.2, 129.5, 133.6, 133.8, 134.0, 134.2, 136.2, 136.9, 137.7, 138.8, 138.9, 139.2, 139.3, 154.9, 156.1, 156.2, 160.9, 168.9, 172.7; MALDI-MS obsd 1274.9357; ESI-MS obsd

648.3581, calcd M/2 = 648.3582 [$(M + H + Na)^{2+}$, M = $C_{74}H_{96}N_8O_{11}$]; λ_{abs} (CH_2Cl_2) 367, 517, 729 nm. A larger-scale synthesis afforded 60.0 mg of the title compound (25% yield, see the Supplimentary information).

15-[4-(3-Carboxyethyl)phenyl]-3,13-bis[3,5-bis(aminomethyl)phenyl]-5-methoxy-8,8,18,18-tetramethylbacteriochlorin (B13). A solution of **B12** (15.5 mg, 12.2 μmol) in CH_2Cl_2 (730 μL) was stirred under argon for 2 min, followed by addition of TFA (470 μL). After 1 h, the reaction mixture was diluted with $CHCl_3$ and dried under an argon flow. Tributylamine (200 μL, 840 μmol) was added to the solid residue, and the mixture was sonicated for 3 min. A mixture of THF/hexanes (1:1) was then added, and the resulting suspension was sonicated (5 min) and centrifuged. The supernatant was discarded, leaving a green solid (9.90 mg, 99%): ^{1}H NMR (CD_3OD, the eight amine protons, two pyrrolic protons and one carboxylic acid proton were not observed) δ 1.82 (s, 6H), 1.98 (s, 6H), 2.57 (br, 2H), 2.89 (br, 2H), 3.69 (s, 3H), 3.88 (s, 2H), 4.06 (s, 4H), 4.28 (s, 4H), 4.37 (s, 2H), 7.12 (d, *J* = 8.1 Hz, 2H), 7.28 (s, 1H), 7.37 (s, 2H), 7.44 (d, *J* = 8.1 Hz, 2H), 7.64 (s, 1H), 8.20 (s, 2H), 8.67 (s, 1H), 8.74 (s, 2H), 8.77 (s, 1H); MALDI-MS obsd 816.0103; ESI-MS obsd 409.2308, calcd M/2 = 409.2311 [$(M + 2H)^{2+}$, M = $C_{50}H_{56}N_8O_3$]; λ_{abs} (CH_3OH) 363, 515, 726 nm. A larger-scale synthesis afforded 31.0 mg of the title compound (97% yield, see the Supplimentary information).

3,13-Dimethoxycarbonyl-2,12-bis[3,5-bis(*tert*-butoxycarbonamidomethyl)phenyl-5-methoxy-8,8,18,18-tetramethylbacteriochlorin (B14). Samples of **BC-Br^{2,12}Es^{3,13}** (46.0 mg, 68.2 μmol), **3** (69.4 mg, 150 μmol), $Pd(PPh_3)_4$ (47.3 mg, 41.0 μmol), and Cs_2CO_3 (66.7

mg, 205 μmol) were placed in a Schlenk flask and dried under high vacuum for 30 min. Toluene/DMF [6.80 mL (2:1), deaerated by bubbling with argon for 30 min] was added to the Schlenk flask under argon and the resulting mixture was deaerated by three freeze-pump-thaw cycles. The reaction mixture was stirred at 90 °C for 22 h. The reaction mixture was allowed to cool to room temperature, concentrated to dryness, diluted with ethyl acetate and washed with saturated aqueous $NaHCO_3$. The organic layer was separated, dried (Na_2SO_4), concentrated and chromatographed [silica, CH_2Cl_2/ethyl acetate (8:2 to 7:3)]. A mixture of ethyl hexanes/acetate (19:1) was added to the product, and the resulting suspension was sonicated and centrifuged. The supernatant was discarded, leaving a red solid (65.0 mg, 80%): ^{1}H NMR (THF-d_8) δ –1.45 (s, 1H), –1.15 (s, 1H), 1.57 (s, 18H), 1.58 (s, 18H), 1.98 (s, 6H), 2.03 (s, 6H), 4.09 (s, 3H), 4.23 (s, 3H), 4.35 (s, 3H), 4.51 (s, 2H), 4.56 (s, 2H), 4.63 (br, 8H), 6.91 (br, 4H), 7.62 (s, 2H), 7.90 (s, 2H), 8.06 (s, 2H), 8.72 (s, 1H), 8.83 (s, 1H), 9.73 (s, 1H); MALDI-MS obsd 1184.7352; ESI-MS obsd 1185.6251, calcd 1185.6231 [$(M + H)^+$, M = $C_{65}H_{84}N_8O_{13}$]; λ_{abs} (THF) 372, 526, 748 nm. A larger-scale synthesis afforded 326 mg of the title compound (62% yield, see the Supplimentary information).

15-Bromo-3,13-dimethoxycarbonyl-2,12-bis[3,5-bis(*tert*-butoxycarbonamidomethyl)phenyl-5-methoxy-8,8,18,18-tetramethylbacteriochlorin (B15). Following a general procedure,[11,43] a solution of **B14** (28 mg, 24 μmol, 2.0 mM) in dry THF (12 mL) was treated dropwise (10 min) with a solution of NBS (4.2 mg, 24 μmol) in dry THF (0.24 mL) and stirred at room temperature under argon for 1 h. The reaction mixture was diluted with CH_2Cl_2 and washed with saturated aqueous $NaHCO_3$. The organic

layer was separated, dried (Na_2SO_4) and concentrated. Column chromatography [silica, CH_2Cl_2/ethyl acetate/CH_3OH (100:2:1)] afforded a dark red solid (15 mg, 50%): ^{1}H NMR δ –1.61 (s, 1H), –1.36 (s, 1H), 1.48 (m, 36H), 1.83 (s, 6H), 1.85 (s, 6H), 4.11 (s, 3H), 4.15 (s, 3H), 4.26 (s, 3H), 4.35 (s, 2H), 4.20 (s, 2H), 4.58 (s, 8H), 5.05 (s, 4H), 7.47 (s, 2H), 7.84 (s, 2H), 7.88 (s, 2H), 8.53 (s, 2H); MALDI-MS obsd 1263.39; ESI-MS obsd 1263.5347, calcd 1263.5341 [$(M + H)^+$, M = $C_{65}H_{83}BrN_8O_{13}$]; λ_{abs} (CH_2Cl_2) 375, 530, 739 nm. A larger-scale synthesis afforded 250 mg of the title compound (72% yield, see the Supplimentary information).

15-(6-Carboxyhex-1-ynyl)-3,13-dimethoxycarbonyl-2,12-bis[3,5-bis(*tert*-butoxycarbonamidomethyl)phenyl]-5-methoxy-8,8,18,18-tetramethylbacteriochlorin (B16). Following a reported procedure,[38] a mixture of **B15** (50. mg, 40. μmol), $Pd_2(dba)_3$ (15 mg, 18 μmol, 0.45 equiv), and P(*o*-tol)$_3$ (30. mg, 95 μmol, 2.4 equiv) was dried under high vacuum in a Schlenk flask for 1 h. Toluene (2.6 mL) and TEA (1.3 mL) (both were bubbled with argon for 1 h) were added and the resulting mixture was degassed by three freeze-pump-thaw cycles. 6-Heptynoic acid (**5**, 50 μL, 0.40 mmol, 10 equiv) was added. The reaction mixture was stirred at 70 °C for 16 h. The reaction mixture was allowed to cool to room temperature and washed with brine and 0.20 N HCl. The organic layer was separated, dried (Na_2SO_4), concentrated to dryness and chromatographed [silica, CH_2Cl_2/ethyl acetate (2:1) to CH_2Cl_2/CH_3OH (50:1)] to afford a red solid, which was washed with hexanes to afford a red solid (8.0 mg, 15%): ^{1}H NMR (the carboxylic acid proton was not observed) δ –1.29 (s, 1H), –1.06 (s, 1H), 1.47 (s, 36H), 1.82 (s, 6H), 1.83 (s, 6H), 1.95 (br, 4H), 2.53 (br, 2H), 2.84 (t, *J*

= 7.5 Hz, 2H), 4.07 (br, 3H), 4.14 (s, 3H), 4.25 (s, 3H), 4.30 (s, 2H), 4.02 (s, 2H), 5.56 (s, 4H), 5.58 (s, 4H), 5.07 (br, 4H), 7.45 (s, 2H), 7.87 (s, 4H), 8.48 (s, 1H), 8.51 (s, 1H); MALDI-MS obsd 1308.6234; ESI-MS obsd 1309.6734, calcd 1309.6760 [$(M + H)^+$, M = $C_{72}H_{92}N_8O_{15}$]; λ_{abs} (CH_2Cl_2) 381, 546, 755 nm. A larger-scale synthesis afforded 45.0 mg of the title compound (17% yield, see the Supplimentary information).

15-[4-(3-*tert*-Butoxycarbonylethyl)phenyl]-3,13-dimethoxycarbonyl-2,12-bis[3,5-bis(*tert*-butoxycarbonamidomethyl)phenyl]-5-methoxy-8,8,18,18-tetramethylbacteriochlorin (B17). Samples of **B15** (7.0 mg, 5.5 μmol), $Pd(PPh_3)_4$ (3.8 mg, 3.3 μmol), **4** (7.2 mg, 22 μmol) and Cs_2CO_3 (8.0 mg, 23 μmol) were placed in a Schlenk flask and dried under high vacuum for 1 h. Toluene/DMF [1.5 mL (2:1), deaerated by bubbling with argon for 1 h] was added to the Schlenk flask under argon, and the resulting mixture was deaerated by three freeze-pump-thaw cycles. The reaction mixture was stirred at 90 °C for 16 h. The reaction mixture was allowed to cool to room temperature, concentrated to dryness, diluted with ethyl acetate and washed with saturated aqueous $NaHCO_3$. The organic layer was separated, dried (Na_2SO_4), concentrated and chromatographed [silica, CH_2Cl_2/ethyl acetate (2:1)] to provide a greenish solid (4.3 mg, 56%): ^{1}H NMR δ –1.50 (s, 1H), –1.19 (s, 1H), 1.46 (s, 18H), 1.47 (s, 18H), 1.52 (s, 9H), 1.74 (s, 6H), 1.84 (s, 6H), 2.75 (t, *J* = 7.7 Hz, 2H), 3.14 (t, *J* = 7.7 Hz, 2H), 3.33 (s, 3H), 3.84 (s, 2H), 4.16 (s, 3H), 4.28 (s, 3H), 4.36 (s, 2H), 4.52 (d, *J* = 6.0 Hz, 4H), 4.57 (d, *J* = 6.0 Hz, 4H), 4.98 (br, 4H), 7.40–7.45 (m, 4H), 7.69 (s, 1H), 7.72 (s, 1H), 7.74 (s, 2H), 7.90 (s, 2H), 8.52 (s, 1H), 8.58 (s, 1H); MALDI-MS obsd 1391.0250, ESI-MS obsd 1389.7320, calcd

1389.7386 [$(M + H)^+$, M = $C_{78}H_{100}N_8O_{15}$]; λ_{abs} (CH_2Cl_2) 375, 525, 741 nm.

2,12-Bis[3,5-bis(*tert*-butoxycarbonamidomethyl)phenyl]-3-methoxycarbonyl-5-methoxy-15^2-*N*-(3-*tert*-butoxycarbonyl)propyl-8,8,18,18-tetramethylbacteriochlorin-13,15-dicarbodiimide (B18). Following a reported procedure,[3] a mixture of **B15** (15.0 mg, 11.9 μmol), $Pd(PPh_3)_4$ (13.6 mg, 11.9 μmol), and Cs_2CO_3 (15.6 mg, 47.6 μmol) and **6** (9.20 mg, 47.6 μmol) was dried under high vacuum in a Schlenk flask for 1 h. The flask was then filled with CO, and toluene (1.20 mL) (bubbled with argon and CO, each for 30 min) was added. The reaction mixture was then stirred at 80 °C for 16 h under a CO atmosphere. The reaction mixture was cooled to room temperature and washed with saturated aqueous $NaHCO_3$ and water. The organic layer was dried (Na_2SO_4), concentrated to dryness and chromatographed [silica, CH_2Cl_2/ethyl acetate/CH_3OH (200:12:1)]. The resulting solid was washed with diethyl ether to afford a red solid (3.8 mg, 25%): ^{1}H NMR δ –0.55 (s, 1H), –0.14 (s, 1H), 1.43 (s, 9H), 1.48 (s, 36H), 1.81 (s, 12H), 2.21 (m, 2H), 2.49 (t, *J* = 7.5 Hz, 2H), 4.14 (s, 3H), 4.25 (s, 3H), 4.44 (t, *J* = 7.5 Hz, 2H), 4.57 (s, 2H), 4.59 (s, 6H), 4.60 (s, 2H), 4.70 (s, 2H), 5.05 (s, 2H), 5.11 (s, 2H), 7.48 (s, 1H), 7.51 (s, 1H), 7.84 (s, 2H), 7.87 (s, 2H), 8.41 (s, 1H), 8.52 (s, 1H); MALDI-MS obsd 1337.92; ESI-MS obsd 1338.6928, calcd 1338.7026 [$(M + H)^+$, M = $C_{73}H_{95}N_9O_{15}$]; λ_{abs} (CH_2Cl_2) 376, 562, 810 nm.

(IV) Flow cytometry measurements

(A) Instrumentation and software. Samples were analyzed at the University of North Carolina Core Flow Cytometry Facility on a 19-parameter LSR-II SORP flow

cytometer (BD Biosciences, San Joe, CA) equipped with seven lasers (355, 405, 488, 532, 561, 594, and 633 nm) using FACSDiva 8.0 acquisition software. Data were collected using the 100 mW 355 nm laser. Post-experimental analysis was performed with FlowJo software (version 10.0.8, FlowJo, LLC, Ashland, OR).

(B) Materials. Simply Cellular™ anti-mouse for violet laser compensation standard beads (Bangs Laboratories, Fishers, IN) were used for all flow cytometry experiments. Antibody used was Protein A-purified mouse IgG (MU-003-C, ImmunoReagents, Raleigh, NC).

(C) Bioconjugation to form B2–Ab. Prior to bioconjugation, dialysis was used to exchange antibodies into 50 mM borate buffer (pH 8.5). Mouse IgG (0.5 μg) was added directly to 0.1 mg of the bacteriochlorin **B2-NHS** to achieve an 18-fold ratio of fluorophore to protein in a final reaction volume of 62 μL. This reaction solution was gently rotated in a microcentrifuge tube protected from light for 5 h at ambient temperature and then dialyzed against phosphate buffered saline (PBS) with a 20 kD MWCO dialysis membrane for 2 h at room temperature and then overnight at 4 °C to remove unreacted materials. The bacteriochlorin–antibody bioconjugate was further purified by affinity purification using Pierce Protein A Agarose beads (Thermo Scientific, Rockford, IL) and the manufacturer's protocol for immunoprecipitation. The resulting bacteriochlorin–antibody bioconjugate, **B2–Ab**, exhibited a fluorophore/protein ratio of 2.5 as determined by absorption spectroscopy using a molar absorption coefficient for the bacteriochlorin ($\varepsilon_{726\ nm}$ = 120,000 $M^{-1}cm^{-1}$; $\varepsilon_{280\ nm}$ = 16,100 $M^{-1}cm^{-1}$) and for the antibody[51] ($\varepsilon_{280\ nm}$ = 210,000 $M^{-1}cm^{-1}$). The value for the bacteriochlorin was drawn from that for a similarly substituted bacteriochlorin analogue.[10]

(D) Staining of compensation beads. All preparations used PBS with 0.5% bovine serum albumin (BSA) as the buffer for all steps. For blanks (negative controls), 1 drop of the anti-mouse compensation bead solution was added to buffer and adjusted to a final volume of 250 μL. Blanks were treated by the following sequence of washes and centrifugation but without antibody addition, then resuspended in 1.0 mL buffer. For labeled antibodies, 1.0 mL volumes of bead solution were prepared from 4 drops of beads, then 50 μL was aliquoted per sample. For the experiment shown in Figure 4.4, 0.8 μg of **B2–Ab** was added to each aliquot, and each sample was mixed gently for 30 min at ambient temperature in the dark. Solutions were washed twice by addition of buffer (1 mL) to each tube, centrifugation at 3000 × g for 3 min, and removal of supernatant. Samples were resuspended in 1.0 mL of buffer for analysis.

(E) Experiment and data analysis. The **B2–Ab** was excited with the 355 nm laser and read in channel A with a 685 nm longpass filter and a 730/45 nm bandpass filter in place (both provided with the instrument). Compensation beads were identified on the basis of forward and side light scatter. Gating was applied to exclude events with both lower and higher scatter than single beads and all further data were analyzed using this gating. For all experiments, 5000 gated events were collected.

Supplimentary information

(I) Scale-up procedures

Several bacteriochlorins were prepared at somewhat larger scale than in the

procedures described in the main paper. Bacteriochlorin **B2** was prepared in a larger scale (~40 mg) starting from bacteriochlorin precursor **B10**. The Suzuki coupling reaction of **BC-Br**[3,13] (270 mg) with **3** afforded **B10** (465 mg, 90% yield, to be compared to 85% yield for the smaller scale synthesis). A portion of the sample of bacteriochlorin **B10** (200 mg) was consumed for the 15-bromination and 15-acylation reaction (Suzuki coupling) to afford bacteriochlorin **B12** (60 mg, 25% yield; to be compared to a 31% yield for the smaller scale synthesis). The subsequent deprotection (97%) and PEGylation (77%) were conducted to afford the target bacteriochlorin **B2** (~40 mg). **B4** was also prepared in a larger scale (20 mg). Summaries and comparisons of the smaller- and larger-scale synthesis for **B2** and **B4** are listed in Table 4.3.

Table 4.3. Summaries and comparisons for the smaller- and larger-scale synthesis of **B2** and **B4**.

Cmpd	Smaller scale			Larger scale		
	Purification[a]	Time	Total yield	Purification[a]	Time	Total yield
B2	Column chromatography (2 steps), solvent wash (2 steps)	5 d	22%[b]	Column chromatography (2 steps), solvent wash (2 steps)	7 d	17%[b]
B4	Column chromatography (3 steps), solvent wash (2 steps)	6 d	3%[c]	Column chromatography (3 steps), solvent wash (2 steps)	8 d	6%[c]

[a]The aqueous/organic wash is not included. [b]Calculated from four continuous reaction steps from the synthesis of **B10** to **B2**. [c]Calculated from four continuous

reaction steps from the synthesis of **B14** to **B4**.

15-[4-(3-Carboxyethyl)phenyl]-3,13-bis[3,5-bis(11-methoxy-3,6,9-trioxaundecyl–amidomethyl)phenyl]-5-methoxy-8,8,18,18-tetramethylbacteriochlorin (B2). A mixture of **B13** (25.0 mg, 30.5 μmol), Cs_2CO_3 (200 mg, 613 μmol) and **PEG$_4$-NHS** (410 mg, 1.23 mmol) in DMF (375 μL) was stirred under argon for 2.5 h. The reaction mixture was diluted with saturated aqueous $NaHCO_3$ (2.5 mL) and stirred for 4 h. The remaining reaction protocol, purification procedure and characterization data (ESI-MS data were not obtained) were essentially identical with those in the main paper to afford the title bacteriochlorin (40.0 mg, 77% yield).

2,12-Bis[3,5-bis(11-methoxy-3,6,9-trioxaundecylamidomethyl)phenyl]-15-(7-carboxy-1-heptyl)-3,13-dimethoxycarbonyl-5-methoxy-8,8,18,18-tetramethylbacteriochlorin (B4). A solution of **B16** (17.0 mg, 13.0 μmol) in CH_2Cl_2 (2.80 mL) was stirred under argon for 2 min, followed by addition of TFA (0.280 mL). After 1 h, the reaction mixture was diluted with $CHCl_3$ (~3 mL) and dried under vacuum to thoroughly remove the CH_2Cl_2 and TFA. This procedure ($CHCl_3$ addition – solvent removal) was repeated twice, whereupon the mixture was dried under vacuum. Tributylamine (20 μL) was added to the solid residue, and the resulting suspension was sonicated for 3 min. A mixture of THF and hexanes (1:2) was then added, and the resulting suspension was sonicated (5 min) and centrifuged. The supernatant was discarded to afford a greenish solid. A mixture of the resulting bacteriochlorin (11.8 mg, 13.0 μmol), Cs_2CO_3 (20.0 mg, 64.7 μmol, 5 equiv)

and **PEG_4-NHS** (134 mg, 0.410 mmol, 34 equiv) in DMF (2.8 mL) was stirred under argon for 2 h. The remaining reaction protocol, purification procedure and characterization data (ESI-MS data were not obtained) were essentially identical with those in the main paper to afford the title bacteriochlorin (20.0 mg, 86% yield).

15-[4-(3-*tert*-Butoxycarbonylethyl)phenyl]-3,13-bis[3,5-bis(*tert*-butoxycarbonamido–methyl)phenyl]-5-methoxy-8,8,18,18-tetramethylbacteriochlorin (B12). A solution of **B10** (200 mg, 187 μmol) in THF (375 mL) was treated with NBS (40.0 mg, 224 μmol) in THF (2.25 mL) at room temperature for 1.5 h. The reaction mixture was diluted with CH_2Cl_2 and washed with saturated aqueous $NaHCO_3$. The organic layer was dried (Na_2SO_4) and concentrated to afford a red solid, which was transferred to a Schlenk flask. Samples of **4** (154 mg, 0.463 mmol), $Pd(PPh_3)_4$ (43.6 mg, 37.7 μmol), and Cs_2CO_3 (187 mg, 0.572 mmol) were placed in the Schlenk flask, and the mixture was dried and deaerated under high vacuum for 30 min. Toluene/DMF [9.5 mL (2:1), deaerated by bubbling with argon for 30 min] was added to the Schlenk flask under argon, and the resulting mixture was deaerated by three freeze-pump-thaw cycles. The remaining reaction protocol, purification procedure and characterization data (ESI-MS data were not obtained) were essentially identical with those in the main paper to afford the title bacteriochlorin (60.0 mg, 25% yield).

15-[4-(3-Carboxyethyl)phenyl]-3,13-bis[3,5-bis(aminomethyl)phenyl]-5-methoxy-8,8,18,18-tetramethylbacteriochlorin (B13). A solution of **B12** (50.0 mg, 39.2 μmol) in CH_2Cl_2 (2.35 mL) was stirred under argon for 2 min followed by the addition of TFA (1.51 mL). After 1 h, the reaction mixture was diluted with $CHCl_3$ and dried under an argon flow.

Tributylamine (642 μL, 2.70 mol) was added to the solid residue, and the mixture was sonicated for 3 min. The remaining reaction protocol, purification procedure and characterization data (ESI-MS data were not obtained) were essentially identical with those in the main paper to afford the title bacteriochlorin (31.0 mg, 97% yield).

3,13-Dimethoxycarbonyl-2,12-bis[3,5-bis(*tert*-butoxycarbonamidomethyl)phenyl-5-methoxy-8,8,18,18-tetramethylbacteriochlorin (B14). A mixture of **BC-Br^{3,13}Es^{3,13}** (298 mg, 443 μmol), **3** (450 mg, 964 μmol), $Pd(PPh_3)_4$ (306 mg, 265 μmol), Cs_2CO_3 (432 mg, 1.33 mmol) and toluene/DMF [45 mL (2:1), deaerated by bubbling with argon for 1 h] was added to a Schlenk flask and deaerated by three freeze-pump-thaw cycles. The remaining reaction protocol, and purification procedure and characterization data (ESI-MS were not obtained) were essentially identical with those in the main paper to afford the title bacteriochlorin (326 mg, 62% yield).

15-Bromo-3,13-dimethoxycarbonyl-2,12-bis[3,5-bis(*tert*-butoxycarbonamidomethyl)–phenyl-5-methoxy-8,8,18,18-tetramethylbacteriochlorin (B15). A solution of **B14** (326 mg, 275 μmol) in THF (63.0 mL) was treated with NBS (54.0 mg, 303 μmol) in THF (3.00 mL) at room temperature under argon for 40 min. The remaining reaction protocol, purification procedure and characterization data (ESI-MS data were not obtained) were essentially identical with those in the main paper to afford the title bacteriochlorin (250 mg, 72% yield).

15-(6-Carboxyhex-1-ynyl)-3,13-dimethoxycarbonyl-2,12-bis[3,5-bis(*tert*-butoxycar–bonamidomethyl)phenyl]-5-methoxy-8,8,18,18-tetramethylbacteriochlorin

(B16). A mixture of **B15** (250 mg, 198 μmol), $Pd_2(dba)_3$ (75.0 mg, 90.0 μmol, 0.45 equiv) and P(*o*-tol)$_3$ (150 mg, 475 μmol, 2.4 equiv) was dried under high vacuum in a Schlenk flask for 1 h. Toluene/DMF [19.5 mL (2:1), deaerated by bubbling with argon for 30 min] was added to the Schlenk flask under argon, and the resulting mixture was deaerated by three freeze-pump-thaw cycles. 6-Heptynoic acid (**5**, 250 μL, 2.00 mmol, 10 equiv) was added after the second freeze-pump-thaw cycle. The remaining reaction protocol, purification procedure and characterization data (ESI-MS data were not obtained) were essentially identical with those in the main paper to afford the title bacteriochlorin (45.0 mg, 17% yield). A mixture of debrominated bacteriochlorin **B14** and starting bacteriochlorin **B15** (1:1 determined by ^{1}H NMR spectroscopy, ~130 mg) was recovered after chromatography.

(II) Exploratory syntheses towards PEGylated bacteriochlorins

Several other target bacteriochlorins were also designed with expectation to tune the wavelength or to explore complementary synthetic methodologies. Three target compounds shown in Chart 4.4 were attempted. None of these target compounds was obtained due to synthetic difficulties encountered with the intermediates.

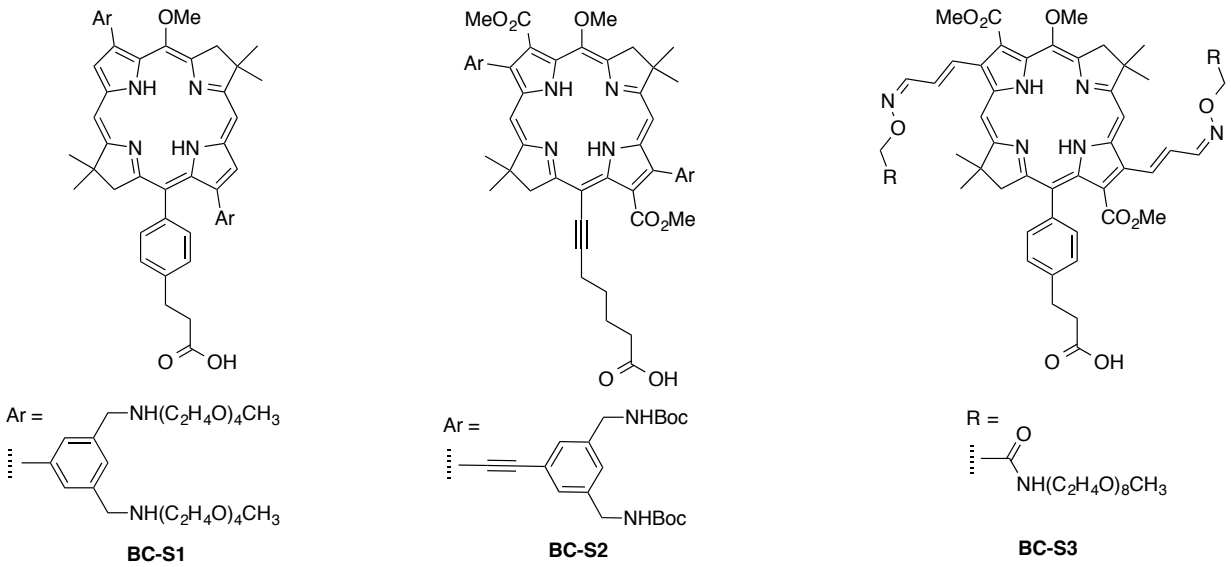

Chart 4.4. Attempted target bacteriochlorins.

Bacteriochlorin **BC-S1** was designed with expectation of a Q_y absorption band at ~730 nm. The Suzuki coupling reaction of **BC-Br**[3,13] with compound **S1**[11] failed to afford the tetraformylbacteriochlorin **BC-S4** (Scheme 4.5). This was a surprise, since a similar Suzuki coupling reaction with 15-bromo-2,12-bis(4-methylphenyl)bacteriochlorin using the same coupling partner successfully afforded the corresponding 15-(3,5-diformyl)-2,12-bis (4-

methylphenyl)bacteriochlorin in 81% yield.[11] This synthesis failure may stem from a difference in reactivity of the bacteriochlorin *meso* (15-) and β (3- and 13-) positions.[11]

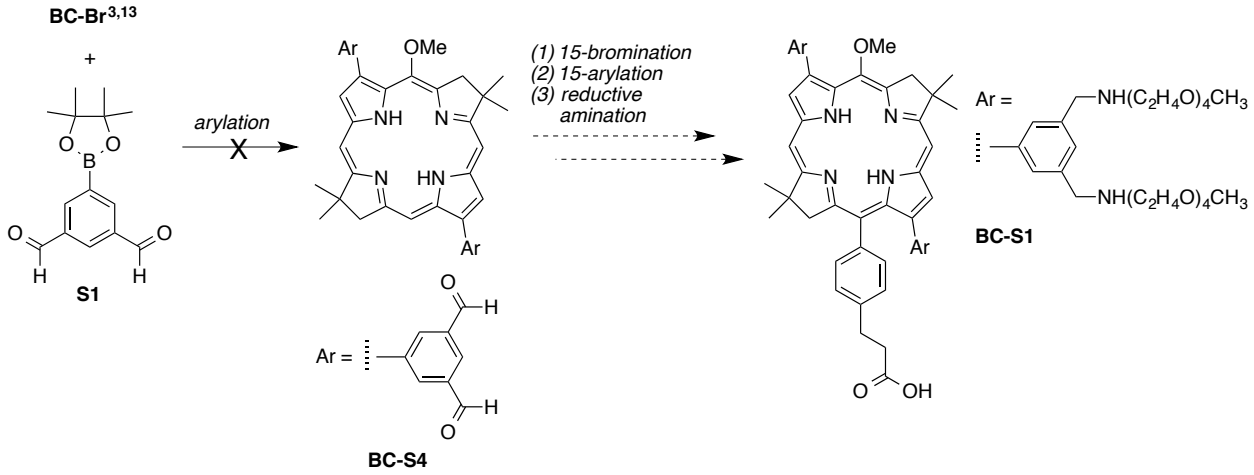

Scheme 4.5. Attempted synthesis of a PEGylated bacteriochlorin.

Previous studies revealed that attachment of 3,13-diethynyl groups shifted the Q_y absorption band of the bacteriochlorin to 749 nm, to be compared with 729 nm for the parent 3,13-dibromobacteriochlorin.[37] In a separate study,[11] a bathochromic shift of 18 nm was achieved by incorporating an ethynyl group at the 15-position of a 2,12-di-*p*-tolyl-5-methoxybacteriochlorin. Accordingly, incorporation of three ethynyl groups (2-, 12-, and 15-positions) with a 3,13-dicarboethoxybacteriochlorin was expected to cause a bathochomic shift of the Q_y band from 749 nm to ~795 nm.

Treatment of Boc-protected 3,5-diamino-1-bromobenzene **S2** with trimethylsilylacetylene (**S3**) under Pd-catalysis conditions afforded **S4** in 63% yield (Scheme 4.6).[53] The resulting compound **S4** was subjected to trimethylsilyl (TMS) group removal by

potassium carbonate in a mixed solvent of methanol and dichloromethane[54] to give the Sonogashira coupling partner **S5** in 67% yield. The use of triisopropylsilylacetylene (**S6**) instead of trimethylsilylacetylene (**S3**) failed to afford the desired product **S7** under various conditions. All conditions examined for both routes are summarized in Table 4.4.

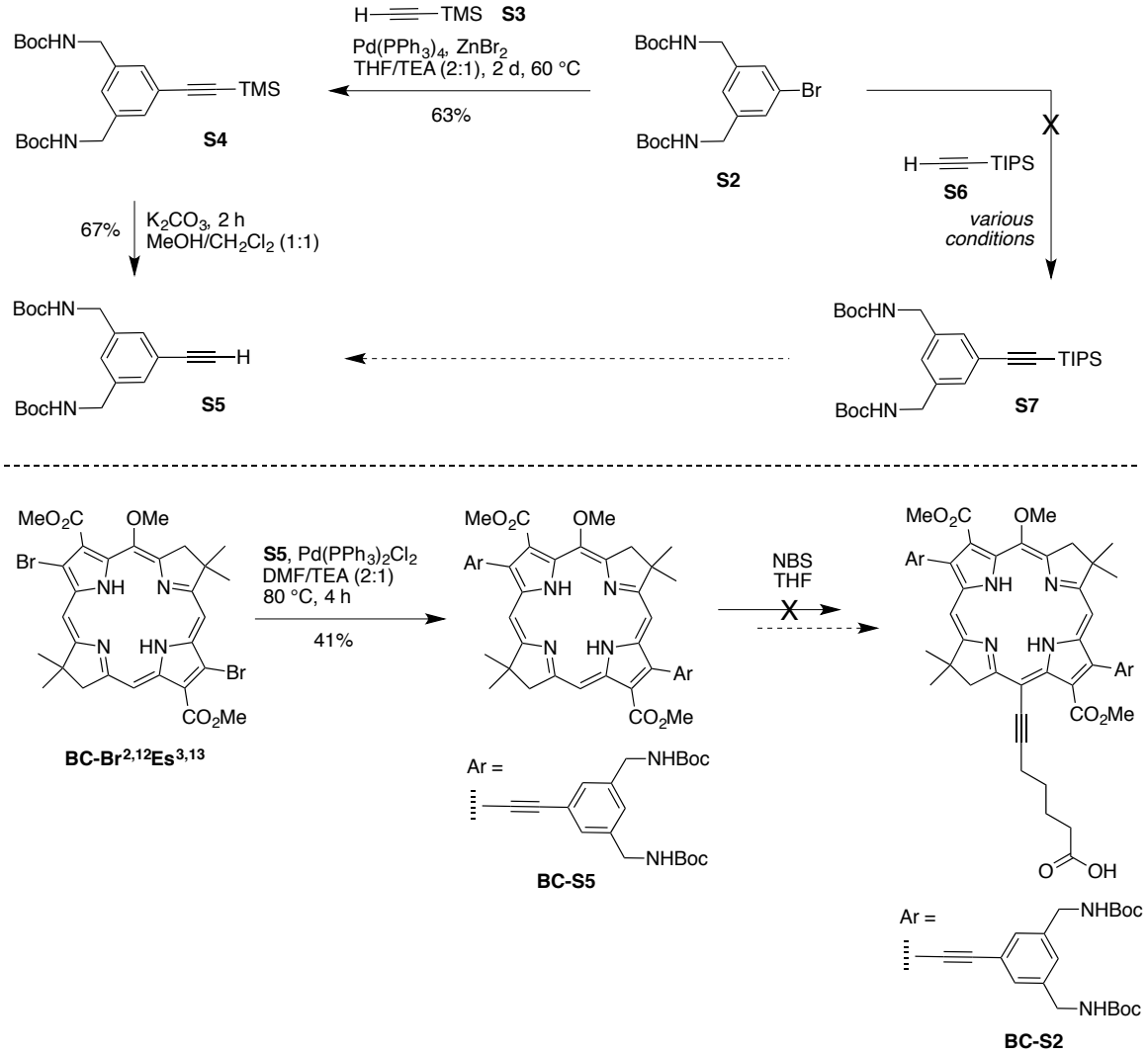

Scheme 4.6. Attempted synthesis of a PEGylated bacteriochlorin.

Table 4.4. Reaction conditions examined for the Sonogashira reaction.

Entry	Reaction conditions[a,b]	Observed	Detected by
1	Pyridine, $Pd(PPh_3)_2Cl_2$ (0.01 eq), **S6** (2 eq), CuI (0.2 eq), 80 °C, 16 h	unknown	^{1}H NMR
2	THF/TEA (3:2), $Pd(PPh_3)_2Cl_2$ (0.05 eq), **S6** (3 eq), CuI (0.4 eq), 80 °C, 16 h	unknown	^{1}H NMR
3	Pyridine, $Pd(PPh_3)_2Cl_2$ (0.05 eq), **S3** (3 eq), CuI (0.4 eq), 80 °C, 36 h	unknown	^{1}H NMR
4	THF/*i*-Pr_3N (3:2), $Pd(PPh_3)_2Cl_2$ (0.05 eq), **S3** (3 eq), CuI (0.4 eq), 80 °C, 36 h	unknown	^{1}H NMR
5	DMF/TEA (3:2), $Pd(PPh_3)_2Cl_2$ (0.05 eq), **S3** (3 eq), CuI (0.4 eq), 80 °C, 24 h	unknown	^{1}H NMR
6	THF/TEA (2:1), $Pd(PPh_3)_4$ (0.03 eq), **S3** (3 eq), $ZnBr_2$ (0.67 eq), 60 °C, 2 d	product **S4**	^{1}H NMR, ^{13}C NMR, ESI-MS

[a]Concentrations of **S2** are 0.40 M for entry 1, 0.24 M for entries 2–5, and 0.30 M for entry 6. [b]All equivalents in the brackets are relative to compound **S2**.

Sonogashira coupling reaction of **BC-Br**[2,12]**Es**[3,13] with coupling partner **S5** under copper-free Sonogashira conditions[11,35] gave Boc-protected bacteriochlorin **BC-S5** in 41% yield (Scheme S2). Treatment of bacteriochlorin **BC-S5** with NBS, however, failed to give the 15-brominated bacteriochlorin under various neutral and basic conditions, with the starting bacteriochlorin **BC-S5** unreacted or decomposed (Table 4.5).

Table 4.5. Reaction conditions for 15-bromination.

Entry	Reaction condition[a]	Observation[b]
1	NBS (1.0 eq), THF, 40 min, rt	SM[c]
2	NBS (2.0 eq), THF, 2 h, rt	SM[c]
3	NBS (3.0 eq), THF, 20 min, rt	SM[c]
4	NBS (6.0 eq), THF, 10 min, rt	decomposed
5	NBS (1.0 eq), CH_3CN, 16 h, rt	SM[c]
6	NBS (1.1 eq), CH_2Cl_2, pyridine (150 eq), 50 min, rt	SM[c]

[a]The concentration of **BC-S5** in THF was 4 mM for entries 1–5 and 5.5 mM for entry 6. A stock solution of NBS (0.1 M in THF) was used for all entries. [b]Confirmed by MALDI-MS and absorption spectroscopy. [c]Starting bacteriochlorin **BC-S5** was detected.

Bacteriochlorin **BC-S3** bearing an extended π-electron conjugation was designed to tune the wavelength to ~800 nm. The PEG unit was incorporated at the final step via Schiff's base formation. This route entailed the preparation of a PEGylated aminooxy compound **S11** as described below (Scheme 4.7): (i) EDC-mediated coupling reaction of a Boc-protected aminooxy carboxylic acid (**S8**) with PEG_8-amine **S9** to afford compound **S10** in 71% yield, and (ii) cleavage of the Boc group to give **S11** in 69% yield. Both **S10** and **S11** were used directly for the next step without column chromatography purification.

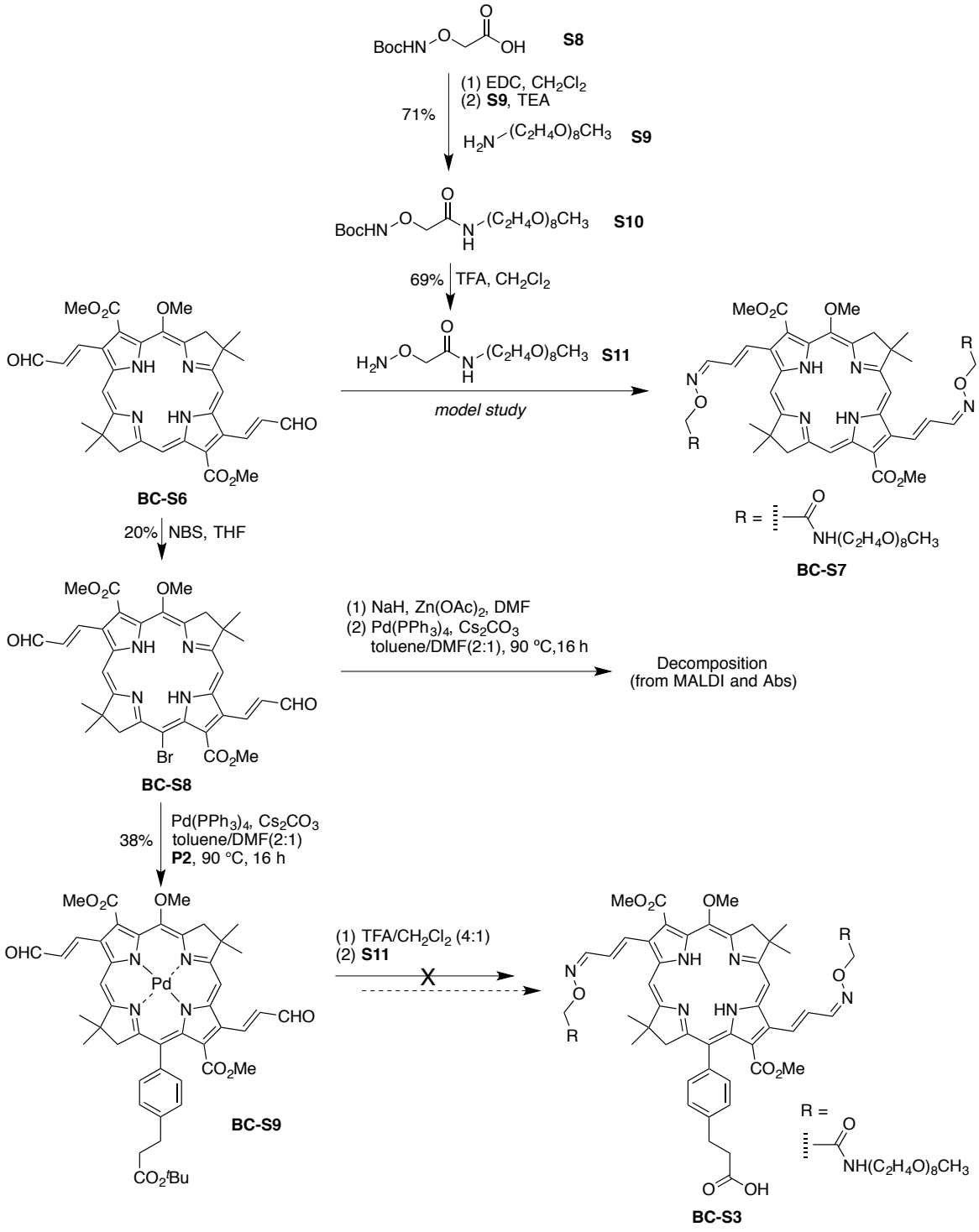

Scheme 4.7. Synthesis of a PEGylated bacteriochlorin.

A model study of the reactivity of the 3-oxopropenyl substituent toward the aminooxy group was examined with known bacteriochlorin **BC-S6**[55] and **S11**. The resulting mixture consisted of the starting bacteriochlorin **BC-S6**, mono-oxime (structure not shown) and di-oxime product **BC-S7** (Scheme 4.7 and Table 4.6). Variation of the reaction conditions did not improve the product yield (Table 4.6). Silica column chromatography was not effective in separating the three components, either. A second problem for this route was the unexpected Pd-insertion during the Suzuki coupling reaction at the bacteriochlorin 15-position for the introduction of a bioconjugatable tether. The Pd-metalated bacteriochlorin is undesirable because of a short-lived fluorescence lifetime, precluding any further photophysical studies or applications. Treatment with 80% TFA in dichloromethane was not successful in removing the chelated palladium. By contrast with the Pd-metalated bacteriochlorin, zinc bacteriochlorins typically exhibit satisfactory fluorescence properties. Accordingly, the bacteriochlorin was subjected to zinc metalation, following by Suzuki coupling at the 15-position; however, the bacteriochlorin decomposed during the Suzuki coupling step as determined by MALDI-MS and absorption spectroscopy. In short, derivatization of the 3-oxopropenyl substituent was not achieved.

Table 4.6. Reaction conditions for oxime formation.[a]

Entry	Catalyst	Solvent[c]	Temp.	Results[d]
1	aniline (100 eq)	CH_2Cl_2/DMSO/NH_4OAc = 2:1:0.2	rt	1:1:1
2	aniline (500 eq)	CH_2Cl_2	rt to 60 °C	1:2:3

Table 4.6. Continued.

3	N/A	CH_2Cl_2/C_2H_5OH = 1:1	80 °C	1:1:1
4[b]	N/A	NH_4OAc/CH_2Cl_2 = 1:1	rt	1:2:3

[a]10 mM of bacteriochlorin **BC-S6** and ~20 equiv of **S11**. [b]Starting bacteriochlorin is the product mixture from entry 2. [c]NH_4OAc buffer: pH 4.5, 100 mM. [d]**BC-S6**/mono-oxime/**BC-S7**.

Bacteriochlorin **BC-S11** was initially designed as an intermediate for elaboration to a water-soluble bioconjugatable bacteriochlorin (Scheme 4.8). The Suzuki coupling reaction of dibromobacteriochlorin **BC-S10**[38] and **S12** proceeded smoothly. The position of the Q_y absorption band of **BC-S11** (742 nm) was quite close to several other bacteriochlorins,[38] however, so further exploration was not pursued.

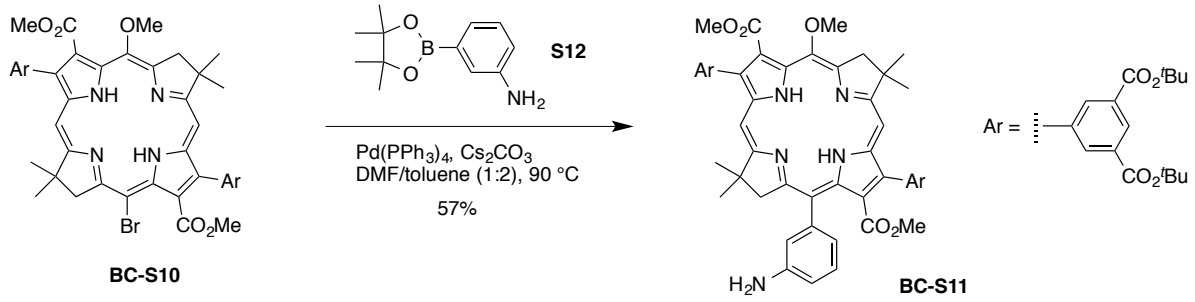

Scheme 4.8. Synthesis of a versatile bacteriochlorin building block.

Bacteriochlorin **BC-S13** was designed to prepare a water-soluble bacteriochlorin by quaternization of two primary amines (Scheme 4.9). The Sonogashira coupling reaction of dibromobacteriochlorin **BC-S12**[12] and **S13** proceeded smoothly. However, studies in parallel revealed that even four ammonium units on a bacteriochlorin did not afford the desirable

water-solubility.[15]

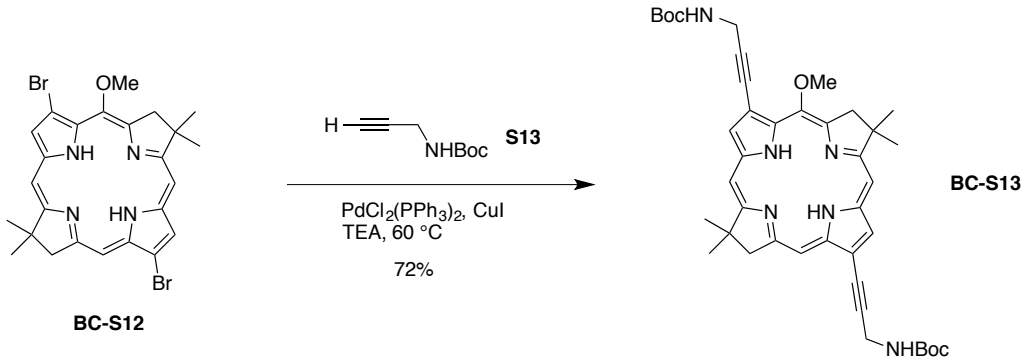

Scheme 4.9. Synthesis of a versatile bacteriochlorin building block.

Non-commercial compounds. Compounds **S1**,[11] **S2**,[56] **BC-S6**,[55] **BC-S10**,[38] and **BC-S12**[12] were prepared as described in the literature.

***tert*-Butyl 6-heptynoate.** A mixture of 6-heptynoic acid (**5**, 1.0 g, 7.9 mmol), di-*tert*-butyl dicarbonate (2.3 g, 10 mmol) and $MgCl_2$ (75 mg, 0.79 mmol) in *tert*-butyl alcohol (4.0 mL) was stirred under argon for 16 h. The crude reaction mixture was diluted with water and extracted with ethyl acetate. The organic extract was dried (Na_2SO_4), concentrated and chromatographed [silica, hexanes/ethyl acetate (24:1)] to afford a viscous colorless liquid (0.98 g, 68%): ^{1}H NMR (400 MHz, $CDCl_3$) δ 1.48 (s, 9H), 1.50–1.59 (m, 2H), 1.67–1.74 (m, 2H), 1.95–1.96 (m, 1H), 2.19–2.26 (m, 4H); ^{13}C NMR (100 MHz, $CDCl_3$) δ 18.4, 24.4, 28.1, 28.3, 35.2, 68.7, 80.3, 84.3, 173.0; ESI-MS obsd 205.1199, calcd 205.1196 [$(M + Na)^+$, M = $C_{11}H_{18}O_2$].

2-[3,5-Bis(*tert*-butoxycarbonamidomethyl)phenyl]-1-trimethylsilylacetylene (S4).

Following a reported procedure,[53] a mixture of **S2** (1.0 g, 2.4 mmol), $Pd(PPh_3)_4$ (80 mg, 0.07 mmol, 0.03 equiv) and $ZnBr_2$ (0.40 g, 1.8 mmol, 0.67 equiv) was dried and deaerated under high vacuum for 30 min in a Schlenk flask. A mixture of THF/triethylamine [12 mL (2:1), bubbled with argon for 30 min] was added, and the resulting mixture was deaerated by two freeze-pump-thaw cycles. Trimethylsilylacetylene (**S3**, 1.0 mL) was added, and the reaction mixture was subjected to a third freeze-pump-thaw cycle. The reaction mixture was stirred at 60 °C for 2 days. The resulting mixture was allowed to cool to room temperature, washed with brine and water, and dried over Na_2SO_4. After removal of the solvent under vacuum, hexanes (10 mL) was added. The resulting suspension was sonicated (2 min) and centrifuged. The supernatant was discarded to afford a brown solid (0.70 g, 63%): mp 169–170 °C; ^{1}H NMR (400 MHz, $CDCl_3$) δ 0.24 (s, 9H), 1.46 (s, 18H), 4.28 (s, 4H), 4.84 (s, 2H), 7.16 (s, 1H), 7.30 (s, 2H); ^{13}C NMR (100 MHz, $CDCl_3$) δ 28.5, 44.2, 80.0, 95.0, 104.5, 124.0, 127.1, 130.2, 140.2, 156.3; ESI-MS obsd 455.2335, calcd 455.2337 [$(M + Na)^+$, M = $C_{23}H_{36}N_2O_4Si$].

[3,5-Bis(*tert*-butoxycarbonamidomethyl)phenyl]acetylene (S5). Following a reported procedure,[54] a mixture of **S4** (0.66 g, 1.5 mmol) and K_2CO_3 (0.50 g, 3.6 mmol, 2.4 equiv) in MeOH/CH_2Cl_2 (6.6 mL, 1:1) was stirred at room temperature for 2 h. Water was added to the reaction mixture, and the resulting solution was extracted with CH_2Cl_2. The combined extract was washed with water, dried (Na_2SO_4), concentrated under vacuum, and chromatographed [silica, CH_2Cl_2/ethyl acetate (10:1 to 5:1)] to yield a pale white solid (0.37 g, 67%): mp 132–133 °C; ^{1}H NMR (400 MHz, $CDCl_3$) δ 1.45 (s, 18H), 3.05 (s, 1H), 4.26 (d, J = 5.6 Hz, 4H), 4.92 (s, 2H), 7.16 (s, 1H), 7.29 (s, 2H); ^{13}C NMR (100 MHz, $CDCl_3$) δ 29.0,

44.2, 79.2, 80.0, 83.8, 123.0, 127.2, 130.2, 140.3, 156.3; ESI-MS obsd 383.1939, calcd 383.1941 [$(M + Na)^+$, M = $C_{20}H_{28}N_2O_4$].

2-*tert*-Butoxycarbonylaminooxy-*N*-(3,6,9,12,15,18,21,24-octaoxahexacosanyl)acet–amide (S10). A mixture of carboxylic acid **5** (287 mg, 1.50 mmol) and EDC (288 mg, 1.50 mmol) in CH_2Cl_2 (3.00 mL) was stirred for 5 min, followed by addition of amine **S9** (575 mg, 1.5 mmol) and TEA (209 μL, 1.50 mmol). The reaction mixture was stirred at room temperature for 16 h. The reaction mixture was diluted with CH_2Cl_2 and washed one time with saturated $NaHCO_3$ solution and then with 2 N HCl solution. The organic phase was separated and dried ($MgSO_4$) to afford a colorless oil (595 mg, 71%): ^{1}H NMR (300 MHz, $CDCl_3$) δ 1.48 (s, 9H), 3.38 (s, 3H), 3.50–3.66 (m, 32H), 4.33 (s, 2H), 7.92 (br, 1H), 8.32 (s, 1H); ^{13}C NMR (75 MHz, $CDCl_3$) δ 28.4, 39.1, 59.2, 69.7, 70.2, 70.6, 70.69, 70.74, 72.1, 76.0, 82.5, 157.7, 169.3; ESI-MS obsd 557.3272, calcd 557.3280 [$(M + H)^+$, M = $C_{24}H_{48}N_2O_{12}$].

2-Aminooxy-*N*-(3,6,9,12,15,18,21,24-octaoxahexacosanyl)acetamide (S11). A sample of **S10** (162 mg, 0.290 mmol) in CH_2Cl_2 (1.00 mL) was stirred under argon for 2 min, followed by the addition of TFA (1.00 mL). After 1 h, the solvent was removed with a stream of argon, and the reaction residue was washed with saturated aqueous $NaHCO_3$. The organic layer was separated, dried (Na_2SO_4) and concentrated to afford a colorless oil (92.0 mg, 69%): ^{1}H NMR (300 MHz, $CDCl_3$, the two amine protons were not observed) δ 3.38 (s, 3H), 3.51–3.66 (m, 31H), 4.14 (s, 2H), 5.95 (s, 1H), 6.99 (br, 1H); ^{13}C NMR (75 MHz, $CDCl_3$) δ 38.8, 59.3, 69.9, 70.2, 70.5, 70.8, 72.2, 75.2, 76.3, 170.4; ESI-MS obsd 457.2756,

calcd 457.2756 [$(M + H)^+$, M = $C_{19}H_{40}N_2O_{10}$].

3,13-Dimethoxycarbonyl-2,12-bis[2-(3,5-bis(*tert*-butoxycarbonamidomethyl)phenyl)–ethynyl]-5-methoxy-8,8,18,18-tetramethylbacteriochlorin (BC-S5). Following a reported procedure,[35] a mixture of **BC-Br^{2,12}Es^{3,13}** (4.0 mg, 3.2 μmol), $Pd(PPh_3)_2Cl_2$ (1.0 mg, 1.5 μmol, 0.20 equiv) and **S5** (8.0 mg, 24 μmol, 4.0 equiv) was dried and deaerated under high vacuum in a Schlenk flask for 1 h. DMF (0.80 mL) and triethylamine (0.40 mL) (bubbled with argon for 1 h for each) were added, and the resulting mixture was deaerated by three freeze-pump-thaw cycles. The reaction mixture was stirred at 80 °C for 4 h. The reaction mixture was allowed to cool to room temperature and then washed with brine and water. The organic layer was separated, dried (Na_2SO_4), concentrated to dryness and chromatographed [silica, CH_2Cl_2/ethyl acetate (5:1 to 2:1)] to afford a red solid (3.0 mg, 41%): ^{1}H NMR (300 MHz, $CDCl_3$) δ −1.18 (s, 1H), −0.89 (s, 1H), 1.52 (s, 36H), 1.95 (s, 6H), 1.97 (s, 6H), 4.25 (s, 3H), 4.32−4.34 (m, 9H), 4.45 (s, 8H), 5.04 (s, 4H), 7.31 (s, 2H), 7.65 (s, 2H), 7.70 (s, 2H), 8.77 (s, 1H), 8.92 (s, 1H), 9.55 (s, 1H) ; ^{13}C NMR (100 MHz, $CDCl_3$) δ 28.7, 31.0, 31.2, 44.6, 46.0, 46.3, 47.9, 51.6, 52.4, 53.5, 64.6, 80.0, 82.9, 85.5, 95.8, 97.5, 98.9, 99.2, 101.0, 115.5, 118.0, 120.7, 124.0, 124.5, 127.0, 127.2, 128.8, 130.0, 135.7, 135.7, 135.9, 137.2, 140.3, 156.2, 157.9, 162.8, 165.8, 167.8, 170.6, 173; MALDI-MS obsd 1234.2789; ESI-MS obsd 1233.6212, calcd 1233.6231 [$(M + H)^+$, M = $C_{69}H_{84}N_8O_{13}$]; λ_{abs} (CH_2Cl_2) 383, 553, 791 nm.

15-Bromo-2,12-bis(3-oxopropenyl)-3,13-dimethoxycarbonyl-5-methoxy-8,8,18,18–tetramethylbacteriochlorin (BC-S8). Following a standard procedure,[11] a solution of **BC-S6** (5.8 mg, 9.3 μmol) in dry THF (3.1 mL) was treated dropwise (10 min)

with a solution of NBS (11 mg, 6.0 equiv) in dry THF (0.56 mL), and the resulting mixture was stirred at room temperature under argon for 1 h. The reaction mixture was diluted with CH_2Cl_2 and washed with saturated aqueous $NaHCO_3$. The organic layer was separated, dried (Na_2SO_4) and concentrated. Column chromatography [silica, CH_2Cl_2/ethyl acetate (50:1 to 25:1)] afforded a red solid (1.3 mg, 20%): ^{1}H NMR (300 MHz, $CDCl_3$) δ –0.83 (s, 1H), –0.58 (s, 1H), 1.92 (s, 6H), 1.93 (s, 6H), 4.21 (s, 3H), 4.28 (s, 3H), 4.29 (s, 2H), 4.31 (s, 3H), 4.36 (s, 2H), 7.19 (dd, *J* = 16.2, 7.5 Hz, 2H), 8.54 (s, 1H), 8.63 (s, 1H), 8.70 (d, *J* = 16.2 Hz, 2H), 10.07 (t, *J* = 7.5 Hz 2H); MALDI-MS obsd 702.2023, calcd 703.1762 [$(M + H)^+$, M = $C_{35}H_{35}BrN_4O_7$]; λ_{abs} (CH_2Cl_2) 345, 393, 787 nm.

15-[4-(3-*tert*-Butoxycarbonylethyl)phenyl]-2,12-bis(3-oxopropenyl)-3,13-dimethoxy–carbonyl-5-methoxy-8,8,18,18-tetramethylbacteriochlorin (BC-S9). Samples of **BC-S8** (6.0 mg, 8.5 μmol), $Pd(PPh_3)_4$ (3.9 mg, 3.4 μmol), Cs_2CO_3 (11 mg, 34 μmol) and **P2** (11 mg, 34 μmol) were placed in a Schlenk flask, and the resulting mixture was deaerated under high vacuum for 1 h. Toluene/DMF [0.8 mL (2:1), deaerated by bubbling with argon for 1 h] was added to the Schlenk flask under argon and deaerated by three freeze-pump-thaw cycles. The reaction mixture was stirred at 90 °C for 16 h. The reaction mixture was cooled to room temperature, concentrated to dryness, diluted with ethyl acetate and washed with saturated aqueous $NaHCO_3$. The organic layer was separated, dried (Na_2SO_4), concentrated and chromatographed [silica, CH_2Cl_2/ethyl acetate (50:1 to 25:1)] to provide a red solid (3.0 mg, 38%): MALDI-MS obsd 931.0782, calcd 933.2685 [$(M+H)^+$, M = $C_{48}H_{50}N_4O_9Pd$]; λ_{abs} (CH_2Cl_2) 339, 380, 561, 800 nm. ^{1}H NMR spectroscopy was tried, but

an informative spectrum was not obtained.

15-(3-Aminophenyl)-2,12-bis[3,5-bis(*tert*-butoxycarbonyl)phenyl]-3,13-dimethoxy–carbonyl-5-methoxy-8,8,18,18-tetramethylbacteriochlorin (BC-S11). Following a general procedure,[57] samples of **BC-S10** (9.2 mg, 8.0 μmol), Suzuki coupling partner **S12** (8.8 mg, 40 μmol), $Pd(PPh_3)_4$ (2.8 mg, 2.4 μmol), K_2CO_3 (13 mg, 96 μmol) and toluene/DMF [0.80 mL (2:1), deaerated by bubbling with argon for 45 min] were added to a Schlenk flask, whereupon the mixture was deaerated by three freeze-pump-thaw cycles. The reaction mixture was stirred at 90 °C for 20 h. The reaction mixture was cooled to room temperature, concentrated to dryness, diluted with CH_2Cl_2 and washed with saturated aqueous $NaHCO_3$. The organic layer was separated, dried (Na_2SO_4) and concentrated. Column chromatography [twice, silica, CH_2Cl_2/ethyl acetate (47:3)] afforded a red solid (5.5 mg, 62%): ^{1}H NMR ($CDCl_3$, 300 MHz) δ –1.40 (br, 1H), –1.09 (br, 1H), 1.64 (s, 18H), 1.66 (s, 18H), 1.74 (s, 3H), 1.77 (s, 3H), 1.83 (s, 3H), 1.85 (s, 3H), 3.52 (s, 3H), 3.86 (s, 2H), 4.20 (s, 3H), 4.30 (s, 3H), 4.37 (s, 2H), 6.93 (d, J = 2.4 Hz, 1H), 7.10 (s, 2H), 7.41 (t, J = 2.4 Hz, 1H), 8.50 (s, 1H), 8.60 (s, 1H), 8.75 (d, J = 1.8 Hz, 2H), 8.86 (s, 1H), 8.88 (s, 1H), 8.90 (d, J = 1.8 Hz, 2H), the two pyrrolic protons were not observed; MALDI-MS obsd 1161.8424; ESI-MS MS obsd 1060.5585, calcd 1060.5591 [$(M + H)^+$, M = $C_{67}H_{77}N_5O_{13}$]; λ_{abs} (CH_2Cl_2) 374, 527, 742 nm.

3,13-Bis[3-(*N*-*tert*-butoxycarbonyl)aminoprop-1-ynyl]-5-methoxy-8,8,18,18-tetra–methylbacteriochlorin (BC-S13). Following a general procedure,[37] samples of **BC-S12** (22 mg, 40 μmol), Sonogashira coupling partner **S13** (62 mg, 0.40 mmol), $PdCl_2(PPh_3)_2$

(5.6 mg, 8.0 μmol) and TEA (2.0 mL, deaerated by bubbling with argon for 45 min) were added to a Schlenk flask, whereupon the mixture was deaerated by three freeze-pump-thaw cycles. The reaction mixture was stirred at 60 °C for 18 h. The reaction mixture was cooled to room temperature, concentrated to dryness, diluted with CH_2Cl_2 and washed with saturated aqueous $NaHCO_3$. The organic layer was separated, dried (Na_2SO_4) and concentrated. Column chromatography [silica, CH_2Cl_2/TEA (99:1 to 49:1)] afforded a green solid (5.5 mg, 72%): ^{1}H NMR ($CDCl_3$, 300 MHz) δ –1.86 (br, 1H), –1.66 (br, 1H), 1.56 (s, 9H), 1.57 (s, 9H), 1.92 (s, 12H), 4.38–4.41 (m, 7H), 4.57 (br, 4H), 5.12 (br, 2H), 8.49 (s, 1H), 8.50 (s, 1H), 8.68 (d, J = 1.5 Hz, 1H), 8.70 (d, J = 1.5 Hz, 1H), 8.80 (s, 1H); ^{13}C NMR ($CDCl_3$, 100 MHz) δ 28.7, 31.0, 31.2, 45.7, 45.9, 51.9, 64.7, 78.3, 80.7, 89.6, 92.8, 96.5, 97.3, 97.6, 111.9, 116.5, 125.0, 125.8, 131.4, 134.3, 135.6, 135.9, 138.4, 154.8, 161.4, 170.0, 170.6; MALDI-MS obsd 708.1287; ESI-MS obsd 706.3841, calcd 706.3837 [M = $C_{61}H_{80}N_8O_9$]; λ_{abs} (CH_2Cl_2) 354, 365, 376, 518, 743 nm.

(III) Additional photophysics studies

A relatively low quantum yield of **B5** (0.017) was observed in neat water, compared with a value of 0.075 in DMSO. This diminution upon examination in aqueous solution was also observed with hydrophilic chlorins[58] and bacteriochlorins.[43] Herein, **B5** was examined in seven different solvents with distinct dielectric constants, and quantum yields were calculated using 2,12-di-*p*-tolyl-5-methoxybacteriolchlorin in toluene (Φ_f = 0.18) as the standard. The results are listed in Table 4.7. The highest Φ_f value (0.082) was obtained in toluene, which is the least polar solvent among those screened, while the lowest Φ_f (0.016)

was obtained in water.

Table 4.7. Solvent effects on the fluorescence properties of **B5**.

Solvent	Dielectric constant	Absorption		Emission		Φ_f
		λ_{max} (nm)	fwhm (nm)	λ_{max} (nm)	fwhm (nm)	
Toluene	2.4	811	33	820	30	0.082
CH_2Cl_2	8.9	810	35	821	30	0.054
CH_3OH	33	806	36	819	38	0.044
DMSO	47	810	34	821	34	0.075
H_2O	80	819	42	831	34	0.017
D_2O	80	819	43	832	36	0.025
Formamide	111	816	39	827	34	0.043

The absorption and emission spectra of **B9** in DMF are shown in Figure 4.6.

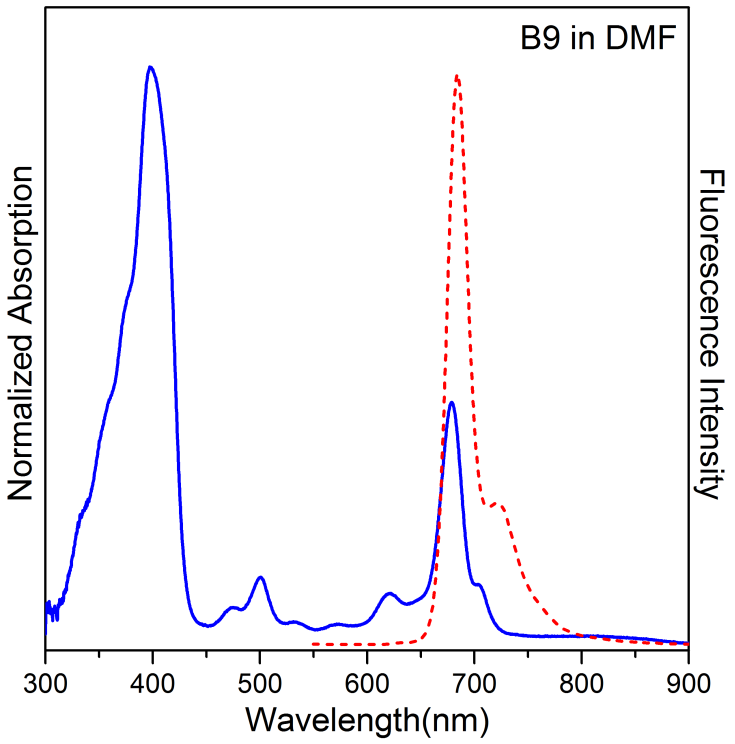

Figure 4.6. Absorption (solid) and fluorescence (dashed) spectra for **B9** in DMF. The fluorescence was obtained using excitation at the Soret maximum.

References

1 B. Robert, R. J. Cogdell and R. van Grondelle, in *Light-Harvesting Antennas in Photosynthesis*, ed. B. R. Green and W. W. Parsons, Kluwer Academic Publishers: Dordrecht, The Netherlands, 2003, Advances in Photosynthesis and Respiration, vol. 13, pp. 169−194.

2 J. B. Dawson, D. J. Barker, D. J. Ellis, E. Grassam, J. A. Cotterill, G. W. Fisher and J. W. Feather, *Phys. Med. Biol.*, 1980, **25**, 695–709.

3 P. Vairaprakash, E. Yang, T. Sahin, M. Taniguchi, M. Krayer, J. R. Diers, A. Wang, D. M. Niedzwiedzki, C. Kirmaier, J. S. Lindsey, D. F. Bocian and D. Holten, *J. Phys. Chem. B*, 2015, **119**, 4382–4395.

4 T. G. Minehan and Y. Kishi, *Angew. Chem. Int. Ed*., 1999, **38**, 923–925.

5 W. Wang and Y. Kishi, *Org. Lett.*, 1999, **1**, 1129–1132.

6 Y. Chen, G. Li and R. K. Pandey, *Curr. Org. Chem.*, 2004, **8**, 1105–1134.

7 M. Galezowski and D. T. Gryko, *Curr. Org. Chem.*, 2007, **11**, 1310–1338.

8 M. A. Grin, A. F. Mironov and A. A. Shtil, *Anti-Cancer Agents Med. Chem.*, 2008, **8**, 683–697.

9 C. Brückner, L. Samankumara and J. Ogikubo, In *Handbook of Porphyrin Science*, ed. K. M. Kadish, K. M. Smith and R. Guilard, World Scientific, Singapore, 2012, vol. 17, pp. 1–112.

10 H.-J. Kim and J. S. Lindsey, *J. Org. Chem.*, 2005, **70**, 5475–5486.

11 D. Fan, M. Taniguchi and J. S. Lindsey, *J. Org. Chem.*, 2007, **72**, 5350–5357.

12 M. Krayer, M. Ptaszek, H.-J. Kim, K. R. Meneely, D. Fan, K. Secor and J. S. Lindsey, *J. Org. Chem*., 2010, **75**, 1016–1039.

13 O. Mass and J. S. Lindsey, *J. Org. Chem.*, 2011, **76***,* 9478–9487.

14 H. Scheer, in *Chlorophylls and Bacteriochlorophylls. Biochemistry, Biophysics, Functions and Applications*, ed. B. Grimm, R. J. Porra, W. Rüdiger and H. Scheer, Springer: Dordrecht, The Netherlands, 2006, Advances in Photosynthesis and Respiration, vol. 25, pp. 1−26.

15 J. Jiang, E. Yang, K. R. Reddy, D. M. Niedzwiedzki, C. Kirmaier, D. F. Bocian, D. Holten and J. S. Lindsey, *New J. Chem.*, 2015, **39**, 5694–5714.

16 M. A. Harris, J. Jiang, D. M. Niedzwiedzki, J. Jiao, M. Taniguchi, C. Kirmaier, P. A. Loach, D. F. Bocian, J. S. Lindsey, D. Holten and P. S. Parkes-Loach, *Photosynth.*

Res., 2014, **121**, 35–48.

17 J. Jiang, K. R. Reddy, M. P. Pavan, E. Lubian, M. A. Harris, J. Jiao, D. M. Niedzwiedzki, C. Kirmaier, P. S. Parkes-Loach, P. A. Loach, D. F. Bocian, D. Holten, and J. S. Lindsey, *Photosynth. Res.*, 2014, **122**, 187–202.

18 Y.-Y. Huang, D. Luo and M. R. Hamblin, *Curr. Org. Chem*., 2015, **19**, 948–957.

19 R. Yin and M. R. Hamblin, *Curr. Med. Chem*., 2015, **22**, 2159–2185.

20 H. L. Kee, R. Nothdurft, C. Muthiah, J. R. Diers, D. Fan, M. Ptaszek, D. F. Bocian, J. S. Lindsey, J. P. Culver and D. Holten, *Photochem. Photobiol.*, 2008, **84**, 1061–1072.

21 H. L. Kee, J. R. Diers, M. Ptaszek, C. Muthiah, D. Fan, J. S. Lindsey, D. F. Bocian and D. Holten, *Photochem. Photobiol.*, 2009, **85**, 909–920.

22 M. Ptaszek, H. L. Kee, C. Muthiah, R. Nothdurft, W. Akers, S. Achilefu, J. P. Culver and D. Holten, *SPIE Proc.*, 2010, vol. 7576, 75760E.

23 V. M. Alexander, K. Sano, Z. Yu, T. Nakajima, P. Choyke, M. Ptaszek and H. Kobayashi, *Bioconjugate Chem.*, 2012, **23***,* 1671–1679.

24 Z. Yu and M. Ptaszek, *J. Org. Chem.*, 2013, **78**, 10678–10691.

25 T. Harada, K. Sano, K. Sato, R. Watanabe, Z. Yu, H. Hanaoka, T. Nakajima, P. L. Choyke, M. Ptaszek and H. Kobayashi, *Bioconjugate Chem.*, 2014, **25**, 362–369.

26 K. E. Borbas, P. Mroz, M. R. Hamblin and J. S. Lindsey, *Bioconjugate Chem*., 2006, **17**, 638–653.

27 P. K. Chattopadhyay, C.-M. Hogerkorp and M. Roederer, *Immunology*, 2008, **125**, 441–449.

28 P. K. Chattopadhyay and M. Roederer, *Methods*, 2012, **57**, 251–258.

29 S. C. Bendall, G. P. Nolan, M. Roederer and P. K. Chattopadhyay, *Trends Immunol.*, 2012, **33**, 323–332.

30 M. Liu, C.-Y. Chen, A. K. Mandal, V. Chandrashaker, R. B. Evans-Storms, J. B. Pitner, D. F. Bocian, D. Holten and J. S. Lindsey, *Chem. Sci.*, 2016.

31 J. Jiang, M. Taniguchi and J. S. Lindsey, *J. New J. Chem.*, 2015, **39**, 4534–4550.

32 J. M. Harris, in *Poly(ethylene glycol) Chemistry – Biotechnical and Biomedical Applications*, ed. J. M. Harris, Plenum Press: New York, 1992, pp. 1–14.

33 S. Zalipsky and J. M. Harris, in *Poly(ethylene glycol) Chemistry and Biological Applications*, ed. J. M. Harris and S. Zalipsky, American Chemical Society: Washington, DC, 1997, pp. 1–13.

34 M. Liu, Ph.D. Thesis, North Carolina State University, 2016, chapter 5, submitted.

35 Z. Yu and M. Ptaszek, *Org. Lett.*, 2012, **14***,* 3708–3711.

36 Z. Yu, C. Pancholi, G. V. Bhagavathy, H. S. Kang, J. K. Nguyen and M. Ptaszek, *J. Org. Chem.*, 2014, **79**, 7910–7925.

37 C. Ruzié, M. Krayer, T. Balasubramanian and J. S. Lindsey, *J. Org. Chem*., 2008, **73**, 5806–5820.

38 J. Jiang, C.-Y. Chen, N. Zhang, P. Vairaprakash and J. S. Lindsey, *New J. Chem,* 2015, **39**, 403–419.

39 C.-Y. Chen, E. Sun, D. Fan, M. Taniguchi, B. E. McDowell, E. Yang, J. R. Diers, D. F. Bocian, D. Holten and J. S. Lindsey, *Inorg. Chem.,* 2012, **51***,* 9443–9464.

40 J. M. Yuen, M. A. Harris, M. Liu, J. R. Diers, C. Kirmaier, D. F. Bocian, J. S. Lindsey and D. Holten, *Photochem. Photobiol.*, 2015, **91**, 331–342.

41 E. Yang, C. Kirmaier, M. Krayer, M. Taniguchi, H.-J. Kim, J. R. Diers, D. F. Bocian, J. S. Lindsey and D. Holten, *J. Phys. Chem. B*, 2011, **115**, 10801–10816.

42 J. B. Birks, in *Photophysics of Aromatic Molecules*, Wiley-Interscience, London, 1970, pp. 142–192.

43 J. Jiang, P. Vairaprakash, K. R. Reddy, T. Sahin, M. P. Pavan, E. Lubian and J. S. Lindsey, *Org. Biol. Chem.*, 2014, **12**, 86–103.

44 W. G. Telford, in *Recent Advances in Cytometry, Part A*: *Instrumentation, Methods*, 5th edition, ed. Z. Darzynkiewicz, E. Holden, A. Orfao, W. G. Telford, and D. Wlodkowic, *Methods Cell Biol.* vol. 102, special issue 5, part A, Elsevier Inc., Atlanta, GA, 2011, pp. 375–409.

45 R. Nguyen, S. Perfetto, Y. D. Mahnke, P. Chattopadhyay and M. Roederer, *Cytometry Part A*, 2013, **83A**, 306–315.

46 M. Ptaszek, in *Progress in Molecular Biology and Translational Science,* ed. M. C. Morris, Academic Press: Burlington, 2013, vol. 113, pp. 59–108.

47 X. Michalet, F. F. Pinaud, L. A. Bentolila, J. M. Tsay, S. Doose, J. J. Li, G. Sundaresan, A. M. Wu, S. S. Gambhir and S. Weiss, *Science*, 2005, **307**, 538–544.

48 P. K. Chattopadhyay, B. Gaylord, A. Palmer, N. Jiang, M. A. Raven, G. Lewis, M. A. Reuter, A. K. M. N. Rahman, D. A. Price, M. R. Betts and M. Roederer, *Cytometry Part A*, 2012, **81A**, 456–466.

49 W. G. Telford, *Cytometry Part A*, 2015, **87A**, 1127–1137.

50 N. Srinivasan, C. A. Haney, J. S. Lindsey, W. Zhang and B. T. Chait, *J. Porphyrins Phthalocyanines*, 1999, **3**, 283–291.

51 Tech Tip #6, Thermo Fisher Scientific, Inc., 2008.

52 N. Zhang, J. Jiang, M. Liu, M. Taniguchi, A. K. Mandal, R. B. Evans-Storm, J. B. Pitner, C. Kirmaier, D. F. Bocian, D. Holten and J. S. Lindsey, *Chem. Sci.*, 2016.

53 A. Florian, M. J. Mayoral, V. Stepanenko and G. Fernandez, *Chem. Eur. J.*, 2012, **18**, 14957–14961.

54 H. N. Nakayama, T. Morita and S. Kimura, *J. Physical Chemistry C*, 2010, **114**, 4669–4674.

55 E. Yang, N. Zhang, M. Krayer, M. Taniguchi, J. R. Diers, C. Kirmaier, J. S. Lindsey, D. F. Bocian and D. Holten, *Photochem. Photobiol*., 2015, **92**, 111–125.

56 B. Sookcharoenpinyo, E. Klein, Y. Ferrand, D. B. Walker, P. R. Brotherhood, C. Ke, M. P. Crump and A. P. Davis, *Angew. Chem. Int. Ed*., 2012, **51**, 4586–4590.

57 K. R. Reddy, J. Jiang, M. Krayer, M. A. Harris, J. W. Springer, E. Yang, J. Jiao, D. M. Niedzwiedzki, D. Pandithavidana, P. S. Parkes-Loach, C. Kirmaier, P. A. Loach, D. F. Bocian, D. Holten and J. S. Lindsey, *Chem. Sci.* 2013, **4**, 2036–2053.

58 K. E. Borbas, V. Chandrashaker, C. Muthiah, H. L. Kee, D. Holten and J. S. Lindsey, *J. Org. Chem*., 2008, **73**, 3145–3158.

CHAPTER 5

Synthesis of Oxobacteriochlorins

Preamble. This chapter is contributed by the following individuals. Masahiko Taniguchi and Chih-Yuan Chen: oxidation of a dibromobacteriochlorin.

Introduction

The red and near-infrared (NIR) spectral regions have been far less explored than the visible and ultraviolet regions owing chiefly to the availability of suitable chromophores. Nature captures light in the red and NIR regions through use of chlorophylls and bacteriochlorophylls, respectively. A longstanding objective in tetrapyrrole science has been to develop synthetic analogues of the natural chromophores that can be tailored at will for pursuit of diverse applications. A distinguishing feature of the routes to chlorins and bacteriochlorins that we have developed is the presence of a gem-dimethyl group in each reduced, pyrroline ring thereby stabilizing the macrocycle toward adventitious dehydrogenation. Such hydroporphyrins are displayed along with the natural macrocycles in Figure 5.1.

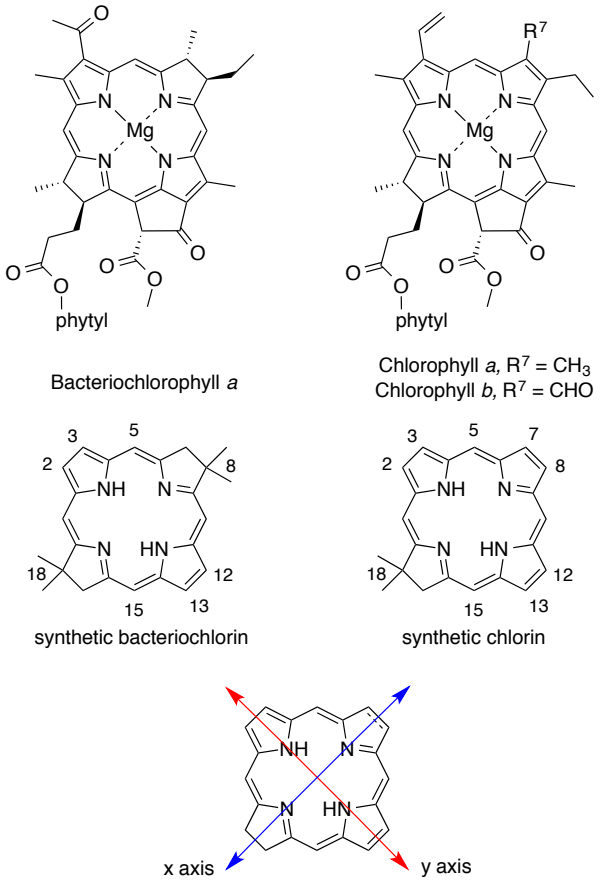

Figure 5.1. Natural hydroporphyrins (top), synthetic gem-dimethylhydroporphyrins (middle), and molecular axes (bottom).

We found that the position of the long-wavelength absorption (Q_y) band could be tuned by the placement of auxochromes at distinct sites about the perimeter of the macrocycle. In general, auxochromes located along the axis bisecting the two pyrrole rings (the y axis) result in a bathochromic shift versus that of the unsubstituted bacteriochlorin. The ability to control the position of the long-wavelength absorption band is of utmost importance, not only for the ability to capture light in a given spectral region but also because the band position defines the maximum energy of the first excited singlet state. The latter

places an upper limit on the energetics of photochemical processes emanating from the hydroporphyrin.

The Q_y absorption band positions are listed in Table 5.1 for a collection of benchmark (bacterio)chlorins (Chart 5.1). Notable trends are as follows: (1) Chlorins and bacteriochlorins encompass the spectral range of 602–715 nm and 695–888 nm, respectively. (2) Metalation of a chlorin causes a hypsochromic shift (entries 2 and 3) whereas metalation of a bacteriochlorin causes a bathochromic shift (entries 19 and 20). (3) In the bacteriochlorin series, the presence of a 5-methoxy group causes a hypsochromic shift (entries 12 and 13; 14 and 15; 17 and 18). (4) The presence of an oxo group in the pyrroline ring causes a significant hypsochromic shift for bacteriochlorins (entries 15, 11 and 10) but little or no spectral shift for chlorins (entries 1 and 2; 3 and 4). Additional photophysical trends concerning the effects of substituents have been described for the compounds shown in Table 5.1 and a large number of related macrocycles.[1–6]

Table 5.1. Long-wavelength absorption bands of (bacterio)chlorins.

Entry	Compound	Q_y band, nm	references
chlorins			
1	**ZnC-O**[17]	602	7,8
2	**ZnC**	603	9
3	**H_2C**	634	7,8
4	**H_2C-O**[17]	634	7,8

Table 5.1. Continued.

5	**H_2OP**	654	10
6	**H_2OP-M^{10}**	656	11
7	**H_2C-A^{3,13}M^{10}**	687	12,13
8	**H_2C-M^{10}I^{13,15}**	686	14
9	**H_2C-Es^{3}M^{10}I^{13,15}**	715	14
Bacteriochlorins			
10	**H_2BC-O^{7,17}T^{2,12}**	695	4
11	**H_2BC-O^{7}T^{2,12}**	709	4
12	**H_2BC-MeO^{5}**	709	15
13	**H_2BC**	713	16
14	**H_2BC-MeO^{5}T^{2,12}**	732	17
15	**H_2BC-T^{2,12}**	737	17
16	**H_2BC-A^{3,13}**	768	18
17	**H_2BC-Es^{3}MeO^{5}I^{13,15}**	798 (793)	19 (1)
18	**H_2BC-Es^{3}I^{13,15}**	823 (818)	19 (1)
19	**H_2BC- I^{3,5}I^{13,15}**	875	4
20	**ZnBC-I^{3,5}I^{13,15}**	888	4

Base macrocycles: C = chlorin; BC = bacteriochlorin; and OP = oxophorbine. Prefixes: H_2 = free base; and Zn = zinc chelate. Substituents: A = acetyl; Es = carboethoxy; I = *N*-benzylimide; M = mesityl; MeO = methoxy; O = O; and T = *p*-tolyl.

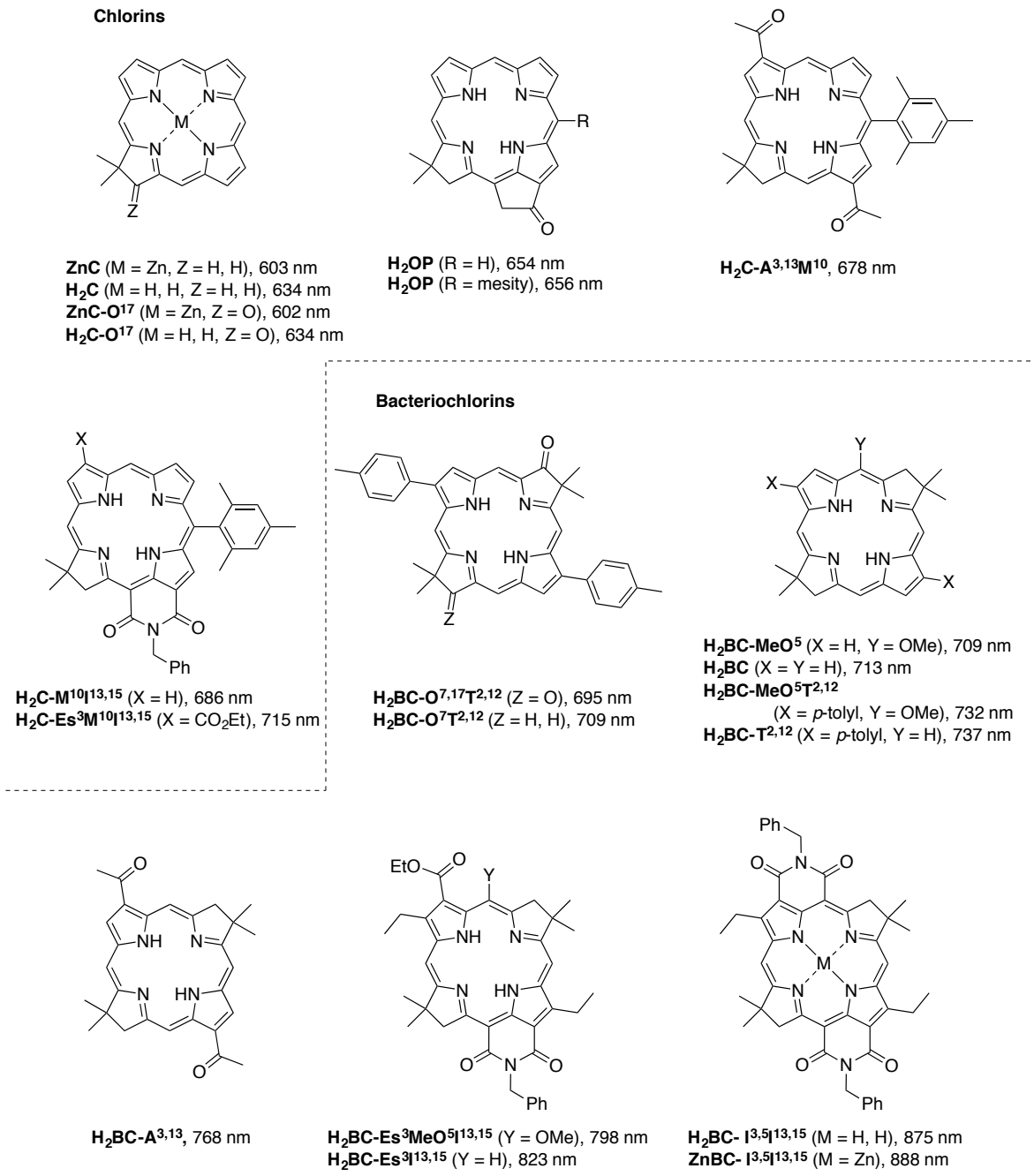

Chart 5.1. Diverse chlorins and bacteriochlorins.

The hypsochromic effect of the oxo group on the Q_y band of bacteriochlorins was

intriguing for several reasons. First, the absorption of the resulting structurally simple oxobacteriochlorins appears in the region accessed by elaborately functionalized chlorins, namely the chlorin–imides (e.g., **H_2C-Es^{3}M^{10}I^{13,15}-Bn**, entry 9, Table 5.1). The ability to access this spectral region merely by installation of an oxo group in the bacteriochlorin was very attractive. Second, dioxobacteriochlorins are known to occur naturally as the macrocycles known as tolyporphins.[20–26] About 12 tolyporphins are known, which generally contain the same core dioxobacteriochlorin macrocycle yet differ in the nature of the *C*-glycoside moiety. (Chart 5.2). The spectroscopic and photochemical properties of oxobacteriochlorins, which may bear on the native properties of tolyporphins, have been little explored. Third, in principle, the pyrroline oxo group could serve as a convenient (and little explored) site of further functionalization, with perhaps interesting features for such derivatives in wavelength tuning. For example, bacteriochlorophyll *b* contains an exocyclic ethylidene group in the pyrroline ring (Chart 5.2),[27] for which model compounds have not been prepared and examined spectroscopically.

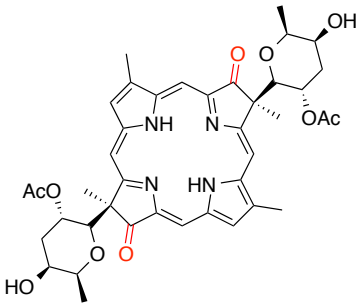

Tolyporphin A

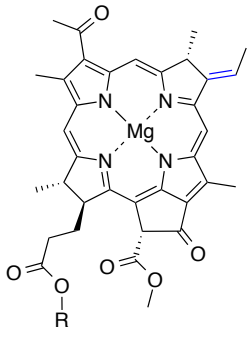

Bacteriochlorophyll *b*

Chart 5.2. Naturally occurring bacteriochlorins with exocyclic π-bonds in the pyrroline motif.

The traditional route for formation of oxobacteriochlorins has relied on treatment with OsO_4 followed by acid-mediated pinacol rearrangement. An example is shown in Scheme 5.1 for the reaction with octaethylporphyrin. Even with this symmetrical porphyrin, two dioxobacteriochlorins are produced. The complexity of the reaction mixture increases with less symmetric porphyrins due to differing selectivity for the particular pyrrole for oxidative cycloaddition with OsO_4 and the migration preferences of various alkyl groups.[28,29]

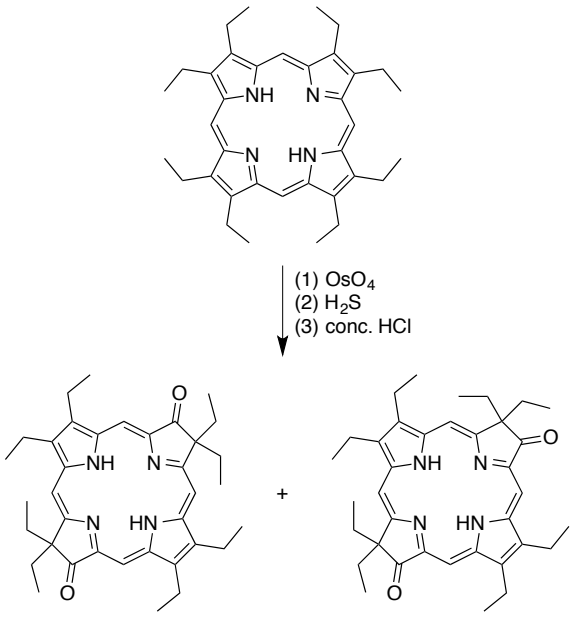

Scheme 5.1. Traditional route to oxobacteriochlorins

Rational routes for formation of oxobacteriochlorins have relied on preparation of a

gem-dialkylbacteriochlorin followed by oxidation of the methylene group of the pyrroline ring. Examples are displayed in Scheme 5.2. In example 1, Minehan and Kishi converted a dimethylbacteriochlorin to the corresponding dioxobacteriochlorin through use of CrO_3 and 3,5-dimethylpyrazole (DMP).[30] Minehan, Wang and Kishi extended this approach to gain access to tolyporphin A *O,O*-diacetate (example 2).[31,32] The same reagent (7 equiv) was used with a 2,12-di-*p*-tolylbacteriochlorin to form the dioxobacteriochlorin product **H_2BC-$O^{7,17}T^{2,12}$** (example 3).[4] Use of only 4 equivalents enabled preparation of the mono-oxobacteriochlorin **H_2BC-$O^7T^{2,12}$** (4.1 mg, 72% yield; not shown).[4]

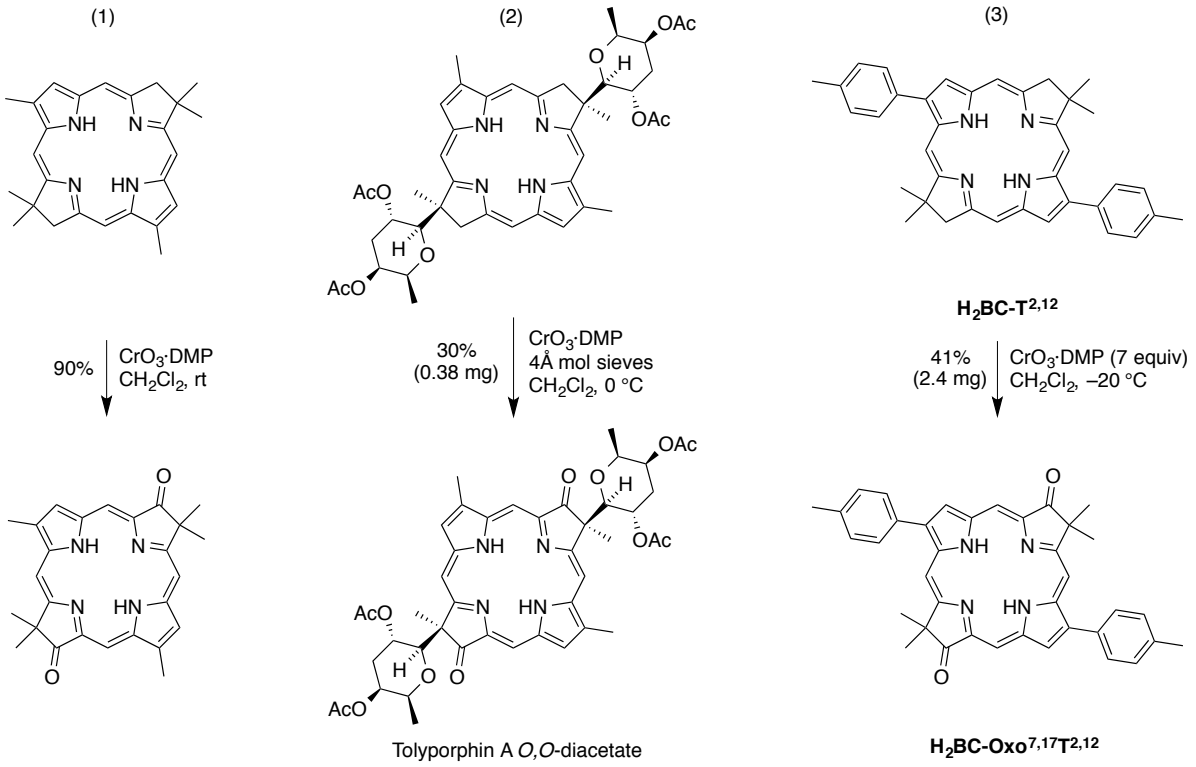

Scheme 5.2. Rational routes to oxobacteriochlorins

In this paper, we report the synthesis and characterization of several oxobacteriochlorins. The absorption spectra have been characterized to gain a deeper understanding of the energetic effects of the oxo group in the pyrroline motif. One bacteriochlorin has been elaborated to give a hydrophilic bioconjugatable bacteriochlorin.[6] Taken together, the work advances capabilities for tailoring the properties of bacteriochlorins by straightforward synthetic means.

Results and discussion

(I) Synthesis of oxobacteriochlorin

Treatment of the 3,13-dibromobacteriochlorin **H_2BC-Br^{3,13}** with a CH_2Cl_2 solution of CrO_3·DMP promptly yielded oxobacteriochlorins. On the other hand, the extremely hygroscopic nature of CrO_3 and the presence of a suspension made handling and quantitative usage quite awkward. Therefore, we set out to survey possible oxidizing agents and reaction conditions. It is noteworthy that Kishi and coworkers arrived at CrO_3·DMP following examination of a host of other oxidants, including Pt/O_2, DDQ, mcpba/dimethyl dioxirane, and benzoyl peroxide/O_2.[30] The similar oxidation of gem-dimethylchlorins to form oxochlorins also entailed a lengthy search to identify suitable reagents.[33]

Here, the well known oxidants for organic chemistry, PCC and PDC, were examined for use with 3,13-dibromobacteriochlorin **H_2BC-Br^{3,13}**. A variety of combinations of equivalents of PDC, bacteriochlorin concentration, and duration were examined. The best condition found was achieved by titration of a 2.1 equiv of PDC and expanding reaction time to 48 h. This condition was applied to a 15-mg batch of **H_2BC-Br^{3,13}**, whereupon following

chromatography the desired mono-oxobacteriochlorin **H_2BC-O^{7}Br^{3,13}** was obtained in 59% yield (Scheme 5.3).

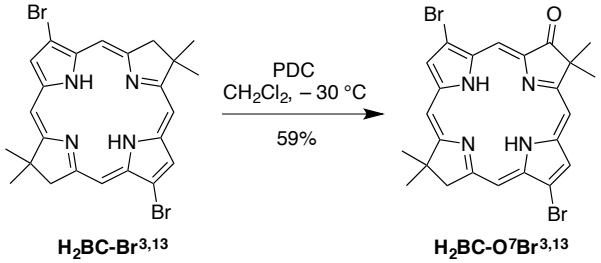

H_2BC-Br^{3,13} **H_2BC-O^{7}Br^{3,13}**

Scheme 5.3. Oxidation of a dibromobacteriochlorin with PDC.

The absorption spectra of several mono-oxo and di-oxo bacteriochlorins are shown in Figure 5.2. The spectra of mono-oxodibromobacteriochlorins **H_2BC-O^{7}Br^{3,13}** and **H_2BC-O^{7}T^{2,12}** are nearly identical with each other (top panel). Similarly, the spectra of dioxodibromobacteriochlorins **H_2BC-O^{7,17}Br^{3,13}** and **H_2BC-O^{7,17}T^{2,12}** are nearly identical with each other (bottom panel).

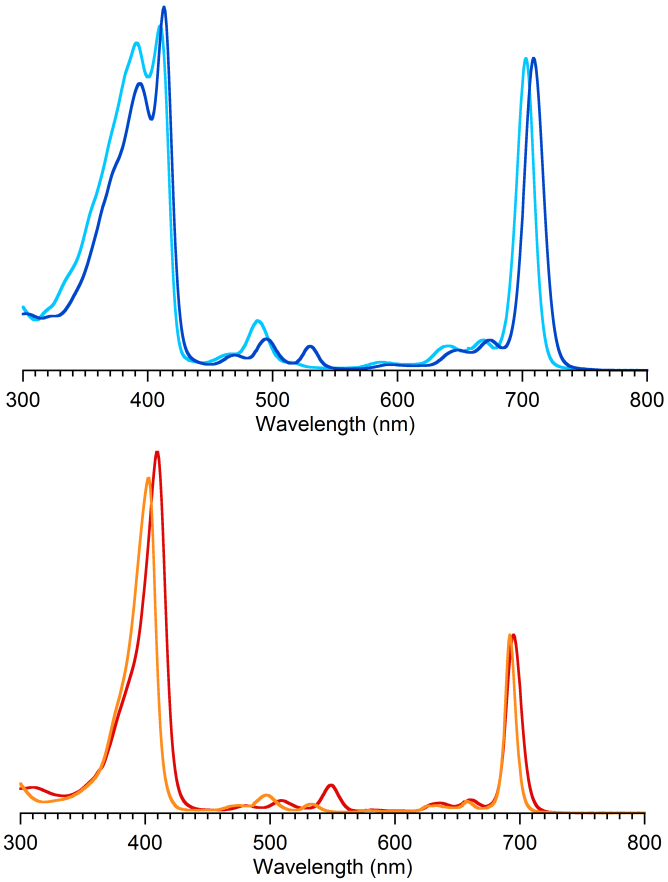

Figure 5.2. Absorption spectra at room temperature of $\mathbf{H_2BC\text{-}O^7T^{2,12}}$ (deep blue, toluene) and $\mathbf{H_2BC\text{-}O^7Br^{3,13}}$ (aqua, CH_2Cl_2) in the top panel, and $\mathbf{H_2BC\text{-}O^{7,17}T^{2,12}}$ (red, toluene) and $\mathbf{H_2BC\text{-}O^{7,17}Br^{3,13}}$ (orange, CH_2Cl_2) in the bottom panel.

(II) Oxobacteriochlorin without substituents.

The dibromooxobacteriochlorin $\mathbf{H_2BC\text{-}O^7Br^{3,13}}$ was treated to conditions for debromination (Scheme 5.4). Such conditions employ formic acid as the hydrogen-atom donor in the presence of the Pd(0) reagent $Pd(PPh_3)_4$ in hot triethylamine.[18,34,35] Thus, reaction of $\mathbf{H_2BC\text{-}O^7Br^{3,13}}$ under debromination conditions afforded the unsubstituted oxobacteriochlorin $\mathbf{H_2BC\text{-}O^7}$ in 47% yield. The fully unsubstituted bacteriochlorin, $\mathbf{H_2BC}$,

has been prepared in analogous fashion.[18]

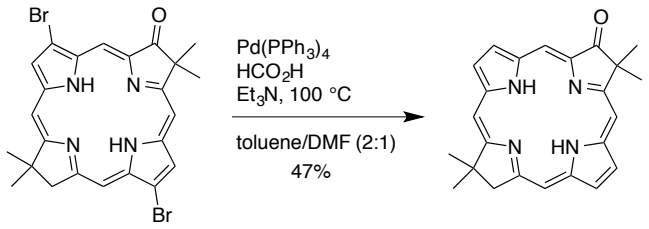

$H_2BC\text{-}O^7Br^{3,13}$ $H_2BC\text{-}O^7$

Scheme 5.4. Debromination to form the unsubstituted oxobacteriochlorin.

The absorption spectrum of the unsubstituted oxobacteriochlorin $\mathbf{H_2BC\text{-}O^7}$ is shown in Figure 5.3, along with that of the benchmark bacteriochlorin $\mathbf{H_2BC}$. The presence of the single oxo group causes a significant hypsochromic shift in the position of the Q_y band; conversely, the B-band manifold (comprised of B_x and B_y transitions) undergoes a bathochromic shift. In this regard, the trends in the spectral shifts resemble those of chlorophyll *b* related to chlorophyll *a*, where both the B and Q_y band shift toward each other due to the presence of the 7-formyl group (Figure 5.4). In both cases, an auxochrome along the x-axis causes the resulting inward movement of the B and Q_y bands.

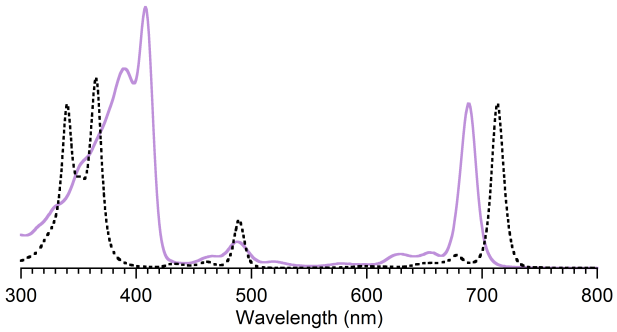

Figure 5.3. Absorption spectra at room temperature of **H_2BC** (dotted line, toluene) and **H_2BC-O**[7] (CH_2Cl_2).

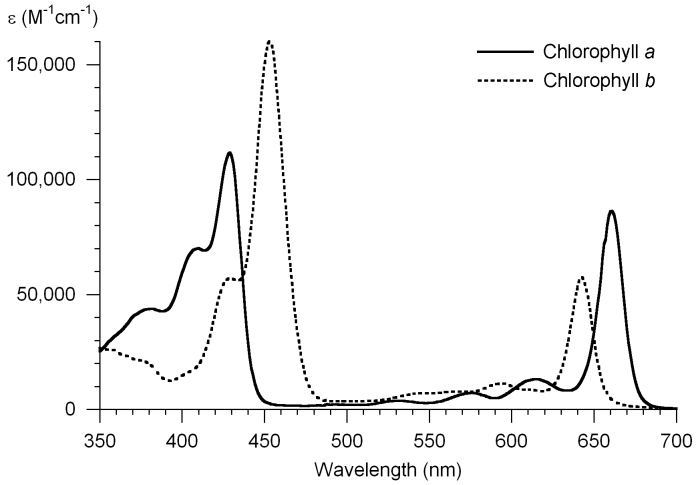

Figure 5.4. Absorption spectra in diethyl ether at room temperature of chlorophyll *a* (solid line) and chlorophyll *b* (dotted line). Adapted with permission from the American Chemical Society, reference 36, 2007.

(III) Application to a 5-methoxybacteriochlorin.

An oxobacteriochlorin building block was synthesized to shift the Q_y band hypsochromically into the red spectral region. Use of PDC afforded two oxobacteriochlorin

isomers but also resulted in extensive decomposition of the starting material. Upon use of the mild oxidizing reagent MnO_2, the conversion yield was 50% but no obvious decomposition was detected (Scheme 5.5). Three components were detected upon TLC analysis (Figure 5.5): unreacted starting material **H_2BC-MeO^{5}Br^{3,13}**, minor isomer **B6-b**, and major isomer **B6-a**. The two isomers exhibited distinct mobilities and also distinct colors. Upon column chromatographic separation of the mixture, starting material **H_2BC-MeO^{5}Br^{3,13}** was recovered, isomer **B6-a** was obtained in 54% yield, and isomer **B6-b** was isolated in 31% yield. The two isomers were easily separated via chromatography. Isomer **B6-a** was used in the preparation of a hydrophilic, bioconjugatable bacteriochlorin.[6]

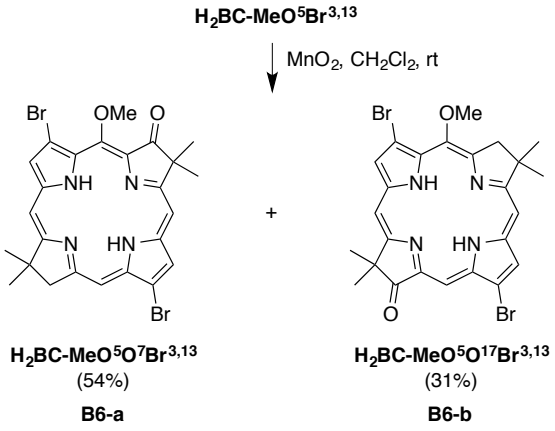

Scheme 5.5. Oxidation of a 5-methoxybacteriochlorin with MnO_2.

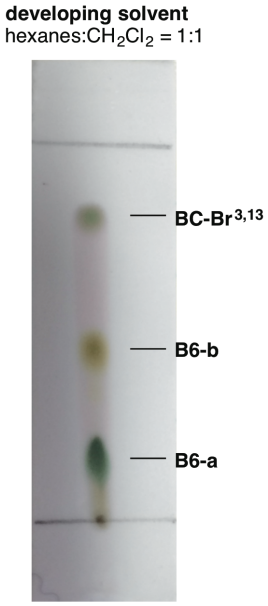

Figure 5.5. TLC plate of oxobacteriochlorin isomers.

The position of the oxo group in **B6-a** and **B6-b** was determined by analysis of 2D NOESY spectra (Figure 5.6). The NOE signal between the methylene group protons with the meso proton at the 15-position establishes the position of the oxo group in **6B-a** was located at 7-methylene site. On the other hand, the oxo group at 17-methylene site in **6B-b** was established with observation of NOE signal between the methylene group protons with the methoxy group protons at the 5-position. The observed selectivity for oxidation of the 7-methylene site, adjacent to the 5-methoxy group, versus that at the 17-position, is somewhat surprising. One interpretation is that the 7-methylene site is more susceptible to oxidation due to electronic stabilization of the putative incipient radical. A second interpretation is that the methoxy group provides some coordination of the incoming MnO_2 oxidant. The data are insufficient to provide any insight into these distinct possibilities. It warrants mention,

however, that reaction at the bromine sites can be quite affected by the neighboring 5-methoxy group. The Pd-mediated coupling reaction of **H_2BC-MeO^{5}Br^{3,13}** to install an ethynyl group (Sonogashira reaction)[37] or aryl group (Suzuki reaction)[38] proceeds selectively at the 13-position rather than the 3-position. The differential reactivity enables successive coupling reactions at both sites, and has been deftly exploited to create bacteriochlorin-containing arrays.[38,39] Thus, the regioselectivity for Pd-coupling at the pyrrole positions is quite different from that for oxidation at the pyrroline positions of the 5-methoxybacteriochlorin.

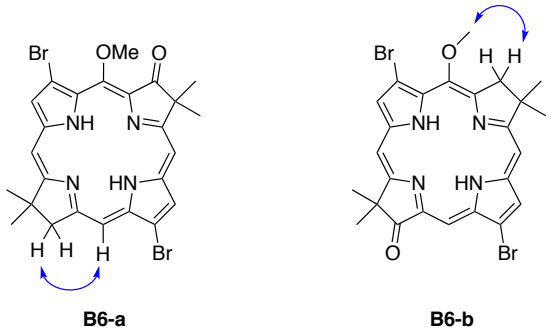

Figure 5.6. NOEs observed in oxobacteriochlorin isomers.

Experimental section

(I) General methods.

^{1}H NMR (300 MHz) and ^{13}C NMR (100 MHz) were collected at room temperature in $CDCl_3$ unless noted otherwise. Matrix-assisted laser-desorption mass spectrometry (MALDI-MS) was performed with the matrix 1,4-bis(5-phenyl-2-oxaxol-2-yl)benzene.[39] Electrospray ionization mass spectrometry (ESI-MS) data are reported for the

molecular ion. Silica gel (40 μm average particle size) was used for column chromatography. All solvents were reagent grade and were used as received unless noted otherwise. THF was freshly distilled from sodium/benzophenone ketyl. Sonication was carried out with a benchtop open-bath sonicator. Compounds **H_2BC-Br^{3,13}** (reference 18) and **H_2BC-MeO^{5}Br^{3,13}** (reference 41) were prepared following reported procedures.

(II) Synthesis.

3,13-Dibromo-8,8,18,18-tetramethyl-7-oxobacteriochlorin (H_2BC-O^{7}Br^{3,13}). A solution of **H_2BC-Br^{3,13}** (15.0 mg, 28.4 μmol) in freshly distilled CH_2Cl_2 (3 mL) at ≤ –30 °C (dry ice with EtOH/ethylene glycol = 1:1 bath)[42] was treated with PDC (22.1 mg, 58.7 μmol). The mixture was allowed to warm to room temperature. After 48 h, the reaction mixture was diluted with CH_2Cl_2 (~1 mL) and chromatographed [silica, CH_2Cl_2] to afford a green solid (9.1 mg, 59%): ^{1}H NMR δ –2.00 (brs, 1H), –1.90 (brs, 1H), 1.95 (s, 6H), 1.99 (s, 6H), 4.52 (s, 2H), 8.70 (s, 1H), 8.79 (s, 1H), 8.81 (d, J = 2.2 Hz, 1H), 8.97 (s, 1H), 8.99 (d, J = 2.1 Hz, 1H), 9.70 (s, 1H); ESI-MS obsd 541.0224, calcd 541.0233 [$(M + H)^+$, M = $C_{24}H_{22}Br_2N_4O$]; λ_{abs} (CH_2Cl_2) 391, 410, 488, 703 nm.

8,8,18,18-Tetramethyl-7-oxobacteriochlorin (H_2BC-O^7). Following a procedure for debromination of bacteriochlorins,[18] a mixture of **H_2BC-O^{7}Br^{3,13}** (10.8 mg, 19.9 μmol), $Pd(PPh_3)_4$ (29.5 mg, 25.5 μmol), formic acid (15 μL, 0.40 mmol), and TEA (55 μL, 0.40 mmol) was heated in toluene (20 mL) at 100 °C in a Schlenk flask. After 16 h, $Pd(PPh_3)_4$ (29.5 mg, 25.5 μmol), formic acid (15 μL, 0.40 mmol), and TEA (55 μL, 0.40 mmol) were

added. After 16 h, the reaction mixture was concentrated and chromatographed [silica, CH_2Cl_2] to afford a green solid (3.6 mg, 47%): ^{1}H NMR δ –2.18 (brs, 1H), –2.08 (brs, 1H), 1.97 (s, 6H), 2.01 (s, 6H), 4.53 (s, 2H), 8.81 (dd, *J* = 4.4, 2.0 Hz, 1H), 8.82 (s, 1H), 8.85 (dd, *J* = 4.7, 1.9 Hz, 1H), 8.89 (s, 1H), 8.91 (s, 1H), 8.97 (dd, *J* = 4.7, 1.8 Hz, 1H), 9.03 (dd, *J* = 4.4, 2.0 Hz, 1H), 9.64 (s, 1H); ESI-MS obsd 385.2019, calcd 385.2023 [$(M + H)^+$, M = $C_{24}H_{24}N_4O$]; λ_{abs} (CH_2Cl_2) 390, 408, 488, 688 nm.

3,13-Dibromo-5-methoxy-8,8,18,18-tetramethyl-7-oxobacteriochlorin (H_2BC-MeO^{5}O^{7}Br^{3,13} = B6-a). A solution of **H_2BC-MeO^{5}Br^{3,13}** (100. mg, 0.179 mmol) in CH_2Cl_2 (6 mL) was treated with MnO_2 (300. mg, 3.45 mmol) at room temperature. After 48 h, the reaction mixture was filtered through a Celite pad, and the pad was rinsed with CH_2Cl_2. The filtrate was concentrated and chromatographed. Starting material **H_2BC-MeO^{5}Br^{3,13}** was recovered (50. mg). The minor isomer **B6-b** (16 mg, 31%) was isolated first, followed by the major isomer **B6-a** (28 mg, 54%). Data for **B6-a**: ^{1}H NMR (400 MHz) δ –1.00 (s, 1H), –0.97 (s, 1H), 1.87 (s, 6H), 1.89 (s, 6H), 4.32 (s, 2H), 4.49 (s, 3H), 8.40 (s, 1H), 8.48 (s, 1H), 8.59 (s, 1H), 8.60 (d, *J* = 2.8 Hz, 1H), 8.80 (d, *J* = 2.4 Hz, 1H); ^{13}C NMR δ 23.6, 31.3, 45.3, 51.8, 52.5, 66.5, 96.2, 96.9, 98.0, 110.1, 115.8, 124.4, 125.3, 129.0, 135.8, 136.98, 137.08, 138.9, 141.8, 165.6, 166.2, 171.0, 206.6; ESI-MS obsd 571.0331, calcd 571.0339 [$(M + H)^+$, M = $C_{25}H_{24}Br_2N_4O_2$]; λ_{abs} (toluene) 396, 504, 692 nm.

Data for **3,13-dibromo-5-methoxy-8,8,18,18-tetramethyl-17-oxobacteriochlorin (H$_2$BC-MeO^{5}O^{17}Br^{3,13} = B6-b)**: ^{1}H NMR (400 MHz, $CDCl_3$) δ –2.45 (s, 1H), –2.09 (s, 1H), 1.95 (s, 6H), 1.98 (s, 6H), 4.39 (s, 3H), 4.53 (s, 2H), 8.75 (s, 1H), 8.83 (s, 1H), 8.85 (d, *J* =

2.0 Hz, 1H), 9.02 (d, J = 2.8 Hz, 1H), 9.63 (s, 1H); ^{13}C NMR δ 23.7, 31.3, 45.6, 48.6, 50.0, 65.1, 96.4, 97.2, 98.1, 109.1, 115.1, 124.1, 129.3, 130.1, 132.4, 135.1, 135.2, 136.0, 145.0, 160.5, 165.2, 171.3, 209.4; ESI-MS obsd 571.0331, calcd 571.0339 [$(M + H)^+$, M = $C_{25}H_{24}Br_2N_4O_2$]; λ_{abs} (toluene) 386, 412, 494, 524, 706 nm.

Acknowledgment

This work was supported by a grant from the Chemical Sciences, Geosciences and Biosciences Division, Office of Basic Energy Sciences, of the U. S. Department of Energy (DE-FG02-05ER15651). Mass spectra were obtained at the Mass Spectrometry Laboratory for Biotechnology at North Carolina State University. Partial funding for the facility was obtained from the North Carolina Biotechnology Center and the National Science Foundation.

References

1 Yang, E.; Kirmaier, C.; Krayer, M.; Taniguchi, M.; Kim, H.-J.; Diers, J. R.; Bocian, D. F.; Lindsey, J. S.; Holten, D. *J. Phys. Chem. B* **2011**, *115*, 10801–10816.

2 Chen, C.-Y.; Sun, E.; Fan, D.; Taniguchi, M.; McDowell, B. E.; Yang, E.; Diers, J. R.; Bocian, D. F.; Holten, D.; Lindsey, J. S. *Inorg. Chem.* **2012**, *51,* 9443–9464.

3 Yang, E.; Ruzié, C.; Krayer, M.; Diers, J. R.; Niedzwiedzki, D. M.; Lindsey, J. S.; Bocian, D. F.; Holten, D. *Photochem. Photobiol.* **2013**, *89*, 586–604.

4 Vairaprakash, P.; Yang, E.; Sahin, T.; Taniguchi, M.; Krayer, M.; Diers, J. R.; Wang, A.; Niedzwiedzki, D. M.; Kirmaier, C.; Lindsey, J. S.; Bocian, D. F.; Holten, D. *J.*

Phys. Chem. B **2015***, 119*, 4382–4395.

5 Yang, E.; Zhang, N.; Krayer, M.; Taniguchi, M.; Diers, J. R.; Kirmaier, C.; Lindsey, J. S.; Bocian, D. F.; Holten, D. *Photochem. Photobiol.* **2015**, *92*, 111–125.

6 Zhang, N.; Jiang, J.; Liu, M.; Taniguchi, M.; Mandal, A. K.; Storm-Evans, R. B.; Pitner, B. J.; Bocian, D. F.; Holten, D.; Lindsey, J. S. *Chem. Sci.* **2016**, *submitted*.

7 Taniguchi, M.; Ptaszek, M.; McDowell, B. E.; Lindsey, J. S. *Tetrahedron* **2007**, *63*, 3840–3849.

8 Taniguchi, M.; Ptaszek, M.; McDowell, B. E.; Boyle, P. D.; Lindsey, J. S. *Tetrahedron* **2007**, *63*, 3850–3863.

9 Laha, J. K.; Muthiah, C.; Taniguchi, M.; McDowell, B. E.; Ptaszek, M.; Lindsey, J. S. *J. Org. Chem.* **2006**, *71*, 4092–4102. *Additions and Corrections:* Laha, J. K.; Muthiah, C.; Taniguchi, M.; McDowell, B. E.; Ptaszek, M.; Lindsey, J. S. *J. Org. Chem.* **2009**, *74*, 5122.

10 Mass, O.; Taniguchi, M.; Ptaszek, M.; Springer, J. W.; Faries, K. M.; Diers, J. R.; Bocian, D. F.; Holten, D.; Lindsey, J. S. *New J. Chem*. **2011**, *35*, 76–88.

11 Ptaszek, M.; Lahaye, D.; Krayer, M.; Muthiah, C.; Lindsey, J. S. *J. Org. Chem*. **2010**, *75*, 1659–1673.

12 Kee, H. L.; Kirmaier, C.; Tang, Q.; Diers, J. R.; Muthiah, C.; Taniguchi, M.; Laha, J. K.; Ptaszek, M.; Lindsey, J. S.; Bocian, D. F.; Holten, D. *Photochem. Photobiol*. **2007**, *83*, 1110–1124.

13 Kee, H. L.; Kirmaier, C.; Tang, Q.; Diers, J. R.; Muthiah, C.; Taniguchi, M.; Laha, J. K.; Ptaszek, M.; Lindsey, J. S.; Bocian, D. F.; Holten, D. *Photochem. Photobiol*. **2007**, *83*, 1125–1143.

14 Ptaszek, M.; Lahaye, D.; Krayer, M.; Muthiah, C.; Lindsey, J. S. *J. Org. Chem.* **2010**, *75*, 1659–1673.

15 Krayer, M.; Ptaszek, M.; Kim, H.-J.; Meneely, K. R.; Fan, D.; Secor, K.; Lindsey, J. S. *J. Org. Chem*. **2010**, *75*, 1016–1039.

16 Taniguchi, M.; Cramer, D. L.; Bhise, A. D.; Kee, H. L.; Bocian, D. F.; Holten, D.; Lindsey, J. S. *New J. Chem.* **2008**, *32*, 947–958.

17 Kim, H.-J.; Lindsey, J. S. *J. Org. Chem.* **2005**, *70*, 5475–5486.

18 Taniguchi, M.; Cramer, D. L.; Bhise, A. D.; Kee, oH. L.; Bocian, D. F.; Holten, D.; Lindsey, J. S. *New J. Chem.* **2008**, *32*, 947–958.

19 Krayer, M.; Yang, E.; Diers, J. R.; Bocian, D. F.; Holten, D.; Lindsey, J. S. *New J. Chem*. **2011**, *35*, 587–601.

20 Prinsep, M. R.; Caplan, F. R.; Moore, R. E.; Patterson, G. M. L.; Smith, C. D. *J. Am. Chem. Soc.* **1992**, *114*, 385–387.

21 Smith, C. D.; Prinsep, M. R.; Caplan, F. R.; Moore, R. E.; Patterson, G. M. L. *Oncol. Res.* **1994**, *6*, 211–218.

22 Prinsep, M. R.; Patterson, G. M. L.; Larsen, L. K.; Smith, C. D. *Tetrahedron* **1995**, *51*, 10523–10530.

23 Morliere, P.; Maziere, J.-C.; Santus, R.; Smith, C. D.; Prinsep, M. R.; Stobbe, C. C.; Fenning, M. C.; Golberg, J. L.; Chapman, J. D. *Cancer Res.* **1998**, *58*, 3571–3578.

24 Prinsep, M. R.; Patterson, G. M. L.; Larsen, L. K.; Smith, C. D. *J. Nat. Prod.* **1998**, *61*, 1133–1136.

25 Minehan, T. G.; Cook-Blumberg, L.; Kishi, Y.; Prinsep, M. R.; Moore, R. E. *Angew. Chem. Int. Ed.* **1999**, *38*, 926–928.

26 Prinsep, M. R.; Puddick, J. *Phytochem. Anal.* **2011**, *22*, 285–290.

27 H. Scheer, in *Chlorophylls and Bacteriochlorophylls. Biochemistry, Biophysics, Functions and Applications*, ed. B. Grimm, R. J. Porra, W. Rüdiger and H. Scheer, Springer: Dordrecht, The Netherlands, 2006, Advances in Photosynthesis and Respiration, vol. 25, pp. 1−26.

28 Taniguchi, M.; Lindsey, J. S. *Chem. Rev.* **2016**, *116*, *submitted 11/28/2015.*

29 C. Brückner, L. Samankumara and J. Ogikubo, in *Handbook of Porphyrin Science*, ed. K. M. Kadish, K. M. Smith and R. Guilard, World Scientific, Singapore, 2012, Vol. 17, pp. 1–112.

30 Minehan, T. G.; Kishi, Y. *Tetrahedron Lett.* **1997**, *38*, 6811–6814.

31 Minehan, T. G.; Kishi, Y. Total Synthesis and the Proposed Structure of (+)-Tolyporphin A *O,O*-Diacetate. *Angew. Chem. Int. Ed.* **1999**, *38*, 923–925.

32 Wang, W.; Kishi, Y. *Org. Lett.* **1999**, *1*, 1129–1132.

33 Taniguchi, M.; Kim, H.-J.; Ra, D.; Schwartz, J. K.; Kirmaier, C.; Hindin, E.; Diers, J. R.; Prathapan, S.; Bocian, D. F.; Holten, D.; Lindsey, J. S. *J. Org. Chem.* **2002**, *67*, 7329–7342.

34 A. K. Sahoo, Y. Nakamura, N. Aratani, K. S. Kim, S. B. Noh, H. Shinokubo, D. Kim and A. Osuka, *Org. Lett.,* 2006, **8**, 4141–4144.

35 A. Kato, R. D. Hartnell, M. Yamashita, H. Miyasaka, K.-i. Sugiura and D. P. Arnold, *J. Porphyrins Phthalocyanines,* 2004, **8**, 1222–1227.

36 Muthiah, C.; Ptaszek, M.; Nguyen, T. M.; Flack, K. M.; Lindsey, J. S. *J. Org. Chem*. **2007**, *72*, 7736–7749.

37 Z. Yu and M. Ptaszek, *Org. Lett.*, 2012, **14***,* 3708–3711.

38 Z. Yu and M. Ptaszek, *J. Org. Chem.*, 2013, **78**, 10678–10691.

39 Z. Yu, C. Pancholi, G. V. Bhagavathy, H. S. Kang, J. K. Nguyen and M. Ptaszek, *J. Org. Chem.*, 2014, **79**, 7910–7925.

40 Srinivasan, N.; Haney, C. A.; Lindsey, J. S.; Zhang, W.; Chait, B. T. *J. Porphyrins Phthalocyanines* **1999**, *3*, 283–291.

41 Krayer, M.; Ptaszek, M.; Kim, H.-J.; Meneely, K. R.; Fan, D.; Secor, K.; Lindsey, J. S. J. Org. Chem. 2010, 75, 1016–1039.

42 Lee, D. W.; Jensen C. M. J. *Chem. Educ.* **2000**, *77*(5), 629.